Studies on the Roles of Endocytic Pathways in Drug Delivery and Resistance in Leukaemia Cells

Saly Al-Taei
BSc (Hons)

A thesis submitted in accordance with conditions governing candidates for the degree of Philosophiae doctor

Welsh school of Pharmacy
Cardiff University
United Kingdom

ProQuest LLC
789 East Eisenhower Parkway
P.O. Box 1346
Ann Arbor, MI 48106-1346

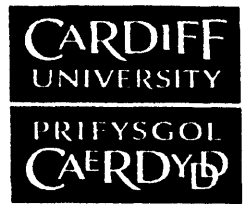

BINDING SERVICES
Tel +44 (0)29 2087 4949
Fax +44 (0)29 20371921
e-mail bindery@cardiff.ac.uk

For my family……

Acknowledgements

I would like to thank my supervisor Dr. Arwyn Jones for his guidance. I would also like to thank Prof. Ruth Duncan for all her help and valuable advice regarding my PhD and this thesis manuscript. A special thanks also to Dr. Janette Davidge for her continued support in so many ways, both on life and laboratory matters. Cardiff University is also gratefully acknowledged for their financial support during this PhD.

Throughout my PhD I have had the pleasure of meeting the most wonderful people at the Centre for Polymer Therapeutics who will always be close to my heart. Special thanks goes to Dr. Phillip Seib, Dr. Myrto Lee, Dr. Maria Manunta and Dr. Maria Vicent for advising me on various aspects of my work. Special thanks also goes to Tom Kean for his tireless help with all things technical and without whom I would have resorted to hand writing my thesis. I would also like to thank Michelle Lazenby, Dr. Vivian Diamanti, Lucile Dieudonne, Francesca Greco and Helena Guilbert for being good friends and whose antics never fail to cheer me up. A very big thanks goes to Karen Phelps, firstly for the music CD that got me through those endless nights of writing and secondly for all our lovely chats during all hours about everything and anything. Many thanks also to Dr. Ka-Wai Wan and Zeena Khayat for all their encouragement and wise words. Last but by no means least, I would like to thank Neal Penning for just being himself and ensuring that there is never a dull moment in the lab. He has helped to make my final year a very memorable one for all the right reasons.

Finally, my deepest thanks goes to my family for their support and especially my little sister and brother, who never fail to cheer me up. I really couldn't thank my husband enough for all his patience throughout these years. He has given me strength and confidence and without him this never would have been possible.

Abstract

Multidrug resistance (MDR) presents a major obstacle for therapeutic approaches to combating haematological malignancies such as acute and chronic myeloid leukaemias (AML and CML). However, there is no concensus in the literature on the mechanisms by which these leukaemic cancer cells reduce the amount of therapeutic agent reaching their intended target. The first part of this study aimed to elucidate the resistance mechanisms operating within human cell models of AML (KG1a; which constitutively overexpress the drug transporter P-glycoprotein (P-gp) and CML (K562; which lacks the expression of P-gp).

This study revealed similarities and major differences in their sequestration profiles. Two inherent resistance mechanisms were identified in KG1a cells; P-gp mediated drug exclusion and differential drug sequestration within lysosomes, which was independent of P-gp. Drug sequestration was also identified within a compartment sensitive to verapamil and cyclosporin A, implicating P-gp in drug sequestration. These differences in drug sequestration were charge dependent as revealed with cationic and zwitterionic compounds. In K562 cells, drug sequestration was identified in lysosomes but also in the Golgi compartment.

This study then focused on protein transduction domains (PTD), such as the HIV-Tat and octaarginine, which have shown great promise as vectors for drug delivery and have demonstrated abilities to bypass drug transporters thereby increasing drug efficacy. However their mechanism of entry and eventual cellular fate is much debated in the literature. KG1a and K562 cells were found to be good models for studying the cellular dynamics of fluorescently conjugated PTD as their suspension status minimised background fluorescence resulting from non-specific binding of fluorescent peptides to tissue culture plastic. Immunofluorescence microscopy and flow cytometry implicates a predominantly endocytic mechanism of uptake for these peptides and their final cellular distribution is indicative of late endosomes and lysosomes. Their cellular dynamics suggests they may be able to bypass conventional MDR processes, making them ideal for the circumvention of both transporter mediated drug exclusion and drug sequestration.

Index

List of Figures

Chapter 1

Chapter 2

Figure 2.2. Photograph of the cell cracker showing (A) separate components of the cell cracker and (B) when the cell cracker is assembled with the syringes inserted.

Figure 2.3. Photographs of the experimental set up used for immunofluorescence microscopy. (A) Hendley multi-well slides. (B) Washing procedure on a magnetic stirring block with the arrow pointing to the magnetic bar. (C) Humidified box used for antibody incubations.

Figure 2.4. Plasmid map of the rat mdr1b-enhanced green fluorescence protein vector.

Chapter 3

Figure 3.1. Schematic representation of the membrane topology of P-glycoprotein (Loo & Clarke, 1995), showing the antibody recognition sites.

Figure 3.2. Optimisation of electrophoretic protein transfer. Broad range molecular weight markers were subjected to SDS-PAGE then electrophoretic transfer using three different transfer buffers (A, B and C). The gels were then stained with Coomassie Brilliant blue to assess the transfer efficiency. Protein standards are indicated on the left hand side.

Figure 3.3. Characterisation of P-gp antibodies. Cell lysates (A and B) and a membrane preparation were prepared from KG1a cells and subjected to immunoblotting with (A) C219 (80 μg), (B) JSB-1 (25 μg) and (C) F4 (300 μg).

Figure 3.4. Optimisation of P-gp immunoprecipitation. A cell lysate was isolated from KG1a cells and subjected to immunoprecipitation using varying quantities of F4 antibody to precipitate P-gp. The gel was loaded with either 30 μg of lysate (lane 1) or imunoprecipitates obtained using 0.5, 1, 3, 5 and 10 μl of F4 antibody incubated with protein-G agarose beads (lanes 2-6 respectively). P-gp was then probed with the C219 antibody.

Figure 3.5. P-gp detection during immunoprecipitation. KG1a membrane preparation was isolated and 80 μg was loaded onto the gel (lane 1). Then 1 mg was subjected to immunoprecipitation. Following the preclearing, proteins were dissociated from the beads (lane 2) and after immunoprecipitation 5, 20 and 50 μl of the immunoprecipitate was loaded onto the gel (lanes 3-5 respectively). The blot was probed with C219 antibody.

Figure 3.6. Localisation of P-gp in both detergent soluble and insoluble membrane domains. (A) P-gp was immunoprecipitated from a detergent soluble (lane 1) and insoluble (lane 2) fraction with the F4 antibody and subsequently probed with C219. (B) A membrane preparation (25 μg) was blotted with an anti-caveolin-1 antibody.

Figure 3.7. Immunoprecipitation of P-gp from a cell lysate, whole cell lysate and membrane fraction. (A) Cell lysate, (B) whole cell lysate and (C) membrane preparations were isolated and P-gp was immunoprecipitated from each fraction using F4 antibody and then immunodetected with C219.

Figure 3.8. Cellular localisation of P-gp in KG1a cells. KG1a cells were fixed and immunolabelled for P-gp with F4 antibody. An enlarged cell is shown in the bottom left hand corner with an arrow showing the dense labelling of P-gp.

Figure 3.9. Effects of wortmannin on P-gp distribution in KG1a cells. The distribution of EEA-1 in the absence (A) or presence (B) of 150 nM wortmannin was determined by preincubating cells for 1 h with wortmannin prior to fixing and immunolabelling for EEA-1. The effect of wortmannin on Tf distribution was determined by internalising Tf for 1 h before incubating with either the diluent DMSO (C) or wortmannin (D). Cells were then treated with wortmannin as for EEA-1 with either DMSO (E) or wortmannin (F). Representative cells are shown in each case. Arrowheads indicate wortmannin induced structures. Scale bar= 10 μm.

Figure 3.10. Immnuoprecipitation of ubiquitinated P-gp. (A) P-gp was immunoprecipitated (IP) from a membrane fraction using F4 antibody and the immunoprecipitate was subjected to Western blotting and probed with either C219 (lane 1) or an anti-ubiquitin antibody (Ub; lane 2). (B) Immunoprecipitation from a membrane fraction was performed either in the presence (lane 1) or absence (lane 2) of F4 antibody. Samples were then probed with an anti-ubiquitin antibody.

Figure 3.11. Effects of K^+ depletion on P-gp ubiquitination. Cells were either subjected to K^+ depletion (lane 2) or the appropriate control (lane 1). P-gp was then immunoprecipitated and probed for ubiquitin. The experiment was repeated twice (A and B).

Figure 3.12. Effects of cellular cytosol acidification on P-gp ubiquitination. Cells were treated with ammonium chloride (lane 2) or the appropriate control (lane 1) and then subjected to immunoprecipitation for P-gp then probed for ubiquitin.

Chapter 4

Figure 4.1. Chemical structures of (A) verapamil and (B) cyclosporin A.

Figure 4.2. Chemical structures of (A) daunorubicin and (B) sulforhodamine 101.

Figure 4.3. Cellular distribution of DNR in KG1a and K562 cells. KG1a (A) and K562 (B) cells were incubated with 2 μg/ml DNR for 1 h at 37 °C, then analysed by epifluorescence microscopy. Arrowheads indicate DNR positive structures. Scale bar= 10 μm.

Figure 4.4. Functionality of intracellular P-gp in KG1a cells. KG1a (A-D) and K562 (E-H) cells were either incubated with DNR in the presence of PBS (A and E) or methanol (C and G) as controls for verapamil and cyclosporin A respectively or were treated with 10 μg/ml verapamil (B and F) or 6 μg/ml cyclosporin A (C

and G). Arrowheads indicate the vesicular DNR structures in KG1a cells in both treated and untreated cells. Scale bar= 10 μm.

Figure 4.5. Distribution of cellular markers in KG1a and K562 cells. Cells were subjected to immunofluorescence labelling for EEA-1 (A and B), TGN46 (C and D) and LAMPII (E and F) as described in materials and methods. Txr-Dex (1 mg/ml) was internalised for 2 h then chased into lysosomes for 4 h at 37 °C (G and H). Dextran loaded cells were analysed by confocal microscopy. Scale bar= 10 μm.

Figure 4.6. Effects of nigericin and bafilomycin A1 on DNR distribution. KG1a (A-D) and K562 (E-H) cells were either incubated with DNR in the presence of ethanol (A, E, C and G) as controls for nigericin and bafilomycin A1 or were treated with 10 μM nigericin (B and F) or 30 nM bafilomycin A1 (C and G). Scale bar= 10 μm.

Figure 4.7. Colocalisation studies between DNR and TxR-Dex in KG1a and K562 cells. KG1a (A-C) and K562 cells (D-F) cells were incubated with 1 mg/ml TxR-Dex for 2 h followed by a 4 h chase into lysosomes (A and D). DNR (2 μg/ml) was incubated with cells in the final 1 h of incubation (B and E). Cells were washed and analysed by confocal microscopy. DNR and TxR-Dex images were overlapped to assess colocalisation (C and F). Arrowheads indicate the colocalised structures in both cell lines. Scale bar= 10 μm.

Figure 4.8. Effect of wortmannin on DNR distribution. KG1a cells were immunolabelled for P-gp either in the absence (A) or presence (B) of 150 nM wortmannin. DNR (2 μg/ml) was incubated with KG1a cells either in the absence (C) or presence (D) of wortmannin. Arrowheads indicate the wortmannin induced structures. Scale bar= 10 μm.

Figure 4.9. SR101 distribution in KG1a and K562 cells. KG1a (A and B) and K562 (c and D) cells were incubated with 5 μM SR101 for 1 h at 37 °C, washed and either analysed immediately (A and C) or incubated for a further 1 h in the

absence of SR101 (B and D). Arrowheads indicate compartmentalisation of the drug. Scale bar= 10 μm.

Figure 4.10. Effects of verapamil and cyclosporin A on SR101 distribution in KG1a cells. KG1a cells were incubated with 5 μM SR101 with either PBS (A) or methanol (C) as control for verapamil and cyclosporin A respectively, or were treated with 10 μg/ml verapamil (B) or 6 μg/ml cyclosporin A (D). Scale bar= 10 μm.

Figure 4.11. Effects of brefeldin A on SR101 distribution in K562 cells. K562 cells were immunolabelled for TGN46 either in the absence (A) or presence (B) of 5 μg/ml brefeldin A. SR101 was incubated with K562 cells either in the absence (C) or presence (D) of brefeldin A as described in materials and methods. Arrowheads indicate the differences in TGN46 and SR101 labelling following treatment with brefeldin A. Scale bar= 10 μm.

Figure 4.12. Characterisation of the rat mdr1b-EGFP plasmid. (A) plasmid map showing te restriction sites surrounding mdr1b-EGFP. (B) Rat mdr1b-EGFP plasmid was either left uncut (lane 1) or treated with the restriction enzymes NotI (lane 2), EcoRI (lane 3), BamHI (lane 4) and NotI and EcoRI in a double digest (lane 5). All samples were run on a 0.6 % agarose gel and photographed on a polaroid gel imaging system. Markers are indicated on the left hand side of the gel.

Figure 4.13. Electroporation of KG1a and K562 cells with the rat mdr1b-EGFP. KG1a (A) and K562 (B) cells were subjected to electroporation with 5 μg mdr1b-EGFP plasmid. Cells were analysed 36 h following transfection. Scale bar= 10 μm.

Figure 4.14. Fugene 6 transfection of K562 cells with rat mdr1b-EGFP. K562 cells were transfected using Fugene 6 with either 1 μg mdr1b-EGFP plasmid (A) or 1 μg EGFP plasmid (B). Cells were analysed 36 h following transfection. Scale bar= 10 μm.

Figure 4.15. Fugene 6 transfection of Hela cells with rat mdr1b-EGFP. Hela cells were subjected to Fugene 6 transfection with 1 μg mdr1b-EGFP plasmid (A). After 24 h, DNR (2 μg/ml) was incubated with transfected cells for 1 h (B). The mdr1b-EGFP and DNR images were then overlayed (C). Arrowhead indicates the bleed through of fluorescence from DNR into the green channel and the asterisk highlights the transfected cells which lack DNR accumulation. Scale bar= 10 μm.

Chapter 5

Figure 5.1. Distribution of alexa-488 Tat and TxR-R_8 in KG1a and K562 cells. KG1a (A and B) and K562 (C and D) cells were incubated with alexa-488-Tat (A and C) or TxR-R_8 (B and D) for 1 h at 37 °C. Arrowheads indicate the peptide labelled structures. Scale bar= 10 μm.

Figure 5.2. Time dependent uptake of alexa-488 Tat and –R_8 in KG1a and K562 cells. KG1a (A) and K562 (B) cells were incubated with alexa-488 Tat (squares) and –R_8 (circles) for 2 h at 37 °C. Cells were washed with trypsin and heparin then analysed by FACS. Each point is the mean ±SD of three experiments. For each point, the mean fluorescence intensity of cells alone was substracted from the fluorescence of cells incubated with the peptide.

Figure 5.3. Temperature dependent uptake of alexa-488 Tat and –R_8 in KG1a and K562 cells. KG1a (A-D) and K562 cells (E-H) were incubated for 5 min (A, C, E and G) or 60 min (E, D, F and H) with Tat (A, B, E and F) or R_8 (C, D, G and H) at either 4 °C (grey line) or 37 °C (black line). Background fluorescence was indicated by the dotted line.

Figure 5.4. Temperature effects the distribution of alexa-488 Tat and TxR-R_8 in KG1a and K562 cells. KG1a (A-F) and K562 (G-L) were incuabted for 1 h with either alexa-488 Tat (A-C and G-I) or TxR-R_8 (D-F and J-L) for 1 h at either 4 (A, D, G and J), 16 (B, E, H and K) or 37 °C (C, F, I and L).

Figure 5.5. Sensitivity of alexa-488 Tat and $-R_8$ uptake to endocytosis modulators. The effects of 10 μM EIPA, 10 μM nocodazole, 150 nM wortmannin and 50 μM cytochalasin D on the accumulation of alexa-488 Tat (A) and R_8 (B) was determined by FACS analysis as described in materials and methods. Each bar is the mean±SD of five experiments. For each point, the mean fluorescence intensity of untreated cells was subtracted from fluorescence obtained with the peptide. Statistical analysis was performed by ANOVA followed by Dunnettes post test, * $p<0.05$ and ** $p<0.01$.

Figure 5.6. Effect of wortmannin on alexa-488 Tat and TxR-R_8 distribution in KG1a and K562 cells. KG1a (A-F) and K562 (G-L) cells were incubated either with 3 μM TxR-R_8 (A-C), 3 μM alexa-488 Tat (D-F and J-L) or 1 μM alexa-488 R_8 (G-I) in the absence or presence of 150 nM wortmannin as detailed above. Phase contrast pictures were taken of wortmannin treated KG1a (C and F) and K562 (I and L) cells to reveal the confines of the cell. Arrowheads indicate the wortmannin induced structures in KG1a cells. Scale bar= 10 μm.

List of Tables

Chapter 1

List of Abbreviations

Abelson Murine Leukaemia Oncogene	Abl
Acute Myeloid Leukaemia	AML
Adenosine Triphosphate	ATP
Adenosine Triphosphatase	ATPase
ATP-Binding Cassette	ABC
Ammonium Chloride	NH_4Cl
Ammonium Persulphate	APS
Blood Brain Barrier	BBB
Bovine Serum Albumin	BSA
Breakpoint Cluster Region	Bcr
Breast Cancer Resistance Protein	BCRP
Calcium Chloride	$CaCl_2$
Chronic Myeloid Leukaemia	CML
Cystic Fibrosis Transmembrane Conductance Regulator	CFTR
Daunorubicin	DNR
Deoxyribonucleic Acid	DNA
Dimethyl Sulphoxide	DMSO
Distilled Water	dH_2O
Dithiothreitol	DTT
Early Endosomes	EE
Early Endosomal Antigen-1	EEA-1
Enhanced Chemiluminescence	ECL
Enhanced Green Fluorescent Protein	EGFP
Epidermal Growth Factor Receptor	EGFR
Ethylenediaminetetra-Acetic Acid	EDTA
Ethyleneglycol-bis[β-aminoethylether]N, N, N, N'-tetraacetic acid	EGTA
Ethylisopropylamiloride	EIPA

Fluorescence Assisted Cell Sorting	FACS
9-Fluorenylmethylcarbonyl	F-moc
Foetal Bovine Serum	FBS
Glycosyl-Phosphatidyl Inositol	GPI
Green Fluorescent Protein	GFP
High Performance Liquid Chromatography	HPLC
Hydrochloric Acid	HCl
Inhibitory concentration for 50% of cells	IC_{50}
Late Endosomes	LE
Lauria-Bertani	LB
Lung Resistance Protein	LRP
Lysosome Associated Membrane Protein	LAMP
Magnesium Chloride	$MgCl_2$
Matrix-Assisted Laser Desorption Ionisation Time of Flight	MALDI-TOF
Messenger Ribonucleic Acid	mRNA
Mdr1b-Enhanced Green Fluorescent Protein	mdr1b-EGFP
Multidrug Resistance	MDR
Multidrug Resistance Associated- Protein	MRP
N-[2-hydroxyethyl]piperazine-N'-[2-ethanesulfonic acid]	HEPES
N, N, N, N'-tetramethylethylenediamine	TEMED
Octamer of Arginines	R_8
One Way Analysis of Variance	ANOVA
P-glycoprotein	P-gp
Phosphate Buffered Saline	PBS

Post nuclear supernatant	PNS
Potassium Chloride	KCl
Protein Transduction Domains	PTD
Radioimmunoprecipitation assay	RIPA
Recycling Endosome	RE
Sodium Hydroxide	NaOH
Sodium Chloride	NaCl
Sodium Dodecyl Sulphate	SDS
SDS-Polyacrylamide gel electrophoresis	SDS-PAGE
Standard Deviation	SD
Texas-Red Dextran	TxR-Dex
Texas-Red Transferrin	TxR-Tf
Transferrin	Tf
Transferrin receptor	TfR
Transactivator of Transcription	Tat
Trans-Golgi Network	TGN
Transporter of Antigenic Peptides	TAP
Tris(hydroxymethyl)aminomethane	Tris
Tris-Borate-EDTA	TBE

Amino Acid Abbreviations

Alanine	A
Cysteine	C
Phenylalanine	F
Glycine	G
Histidine	H
Isoleucine	I
Lysine	K
Leucine	L

Methionine	M
Asparagine	N
Proline	P
Glutamine	Q
Arginine	R
Serine	S
Threonine	T
Valine	V
Tryptophan	W
Tyrosine	Y

Chapter 1:

General Introduction

1.1 Introduction

MDR is associated with the failure of numerous therapeutic strategies against a diverse range of diseases, including haematological malignancies. Consequently, the co-administration of a resistance modulator with current therapeutic regimes would undoubtedly be of great clinical benefit for such diseases. However, although much effort has been devoted to the development of effective resistance modulators, these have had limited clinical efficacy. Such inadequacies, coupled to a poor understanding of resistance mechanisms implicated in these disease states, dictates the high mortality rate associated with such diseases.

This study aims to investigate and subsequently clarify the resistance mechanisms operating within two human cell line models of myeloid leukaemias, KG1a and K562, which have generated much conflicting observations with respect to the nature of their resistance. This may help to explain why the treatment of these leukaemias remains problematic and highlights the clinical importance of this study. This study also extends to evaluating novel concepts for the circumvention of MDR in our cell line models.

1.2 Endocytosis

The word 'endocytosis' is a broad term encompassing a diverse range of processes adopted by cells to internalise molecules either from the extracellular space or the plasma membrane. Endocytosis plays a critical role in diverse cellular processes such as growth and development, immunity, neurotransmission, cellular communication, signal transduction and homeostasis (reviewed in Conner & Schmid, 2003). The process of endocytosis begins on the cell surface where molecules are endocytosed via distinct pathways. These are then trafficked within one of several endocytic pathways, which ultimately determines their intracellular fate. The process of endocytosis and intracellular trafficking is described below.

1.2.1 Cellular Internalisation and Trafficking

There are several mechanisms of cellular internalisation (reviewed in Johannes & Lamaze, 2002). These are described below and illustrated in Figure 1.1.

Clathrin-Dependent Endocytosis

Clathrin-mediated endocytosis has received the most attention due to its importance in receptor mediated internalisation of external ligands. It is the principal mode of internalisation of cell surface receptors such as the transferrin (Tf) receptor (TfR) and epidermal growth factor receptor (EGFR; Harding et al., 1983; Huang et al., 2004). Proteins destined for clathrin-mediated endocytosis often contain amino acid sequences in their cytoplasmic domains which help to localise the protein within clathrin-coated pits. These motifs include the tyrosine and dileucine motifs and acidic cluster sequence (Ohno et al., 1995; Mauxion et al., 1996; Dietrich et al., 1997). They are recognised by adaptor complexes, which interact with clathrin and drive clathrin coat formation. The coated pit is then constricted and excised from the plasma membrane. Once internalised, a clathrin-coated vesicle sheds its coat to enable fusion with early endocytic compartments (Figure 1.1A; reviewed in Schmid, 1997 and Conner & Schmid, 2003).

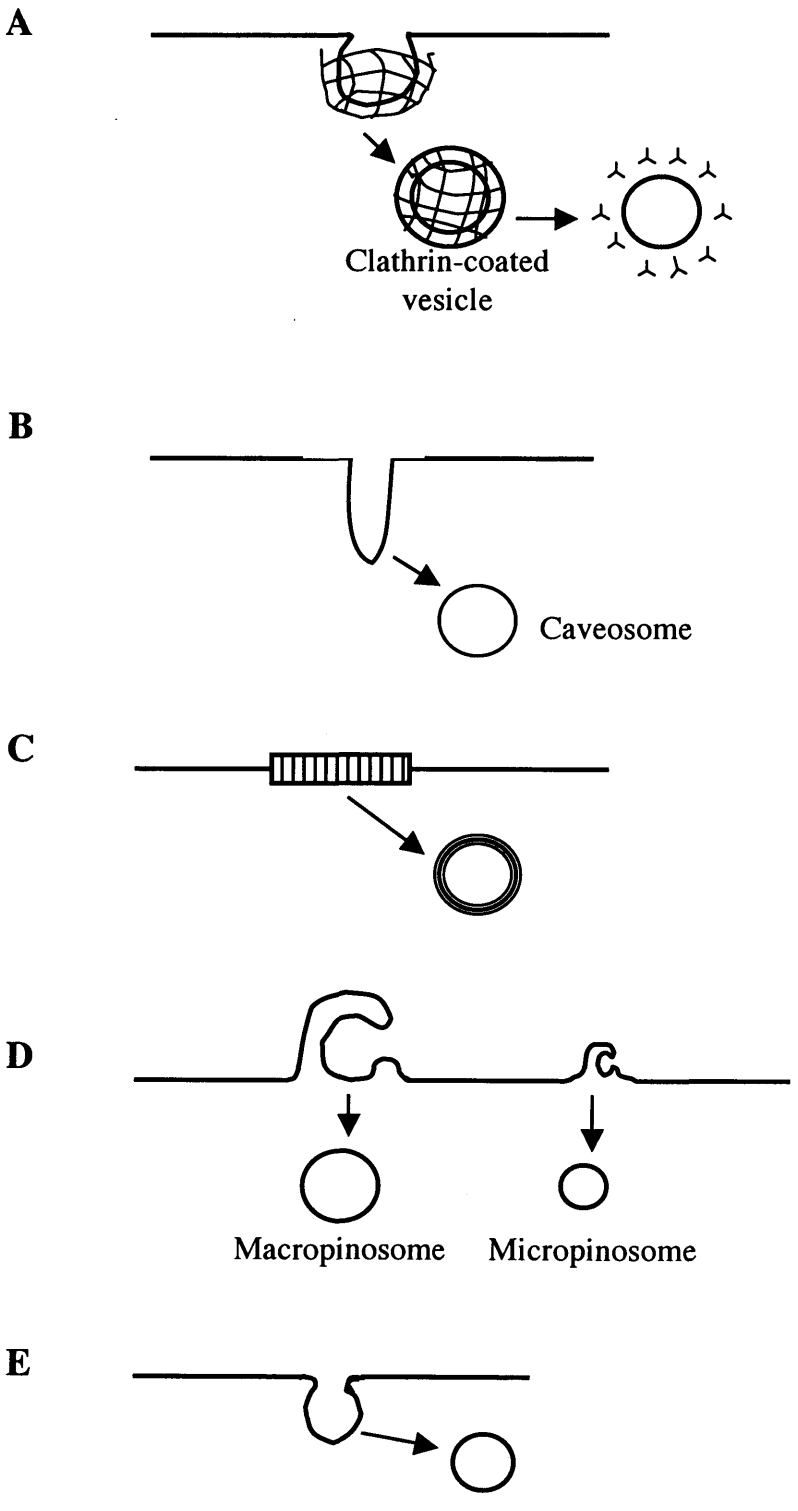

Figure 1.1. Mechanisms of cellular endocytosis; (A) Clathrin-mediated endocytosis. (B) Caveolae-dependent endocytosis (Potocytosis). (C) Lipid raft-dependent endocytosis. (D) Pinocytosis. (E) Clathrin- and caveolae- independent endocytosis.

Caveolae-Mediated Endocytosis (Potocytosis)

Caveolae are flask shaped, non-coated plasma membrane invaginations, characterised by their association with cholesterol-binding proteins called caveolins and are utilised as endocytic platforms. These function to create and maintain caveolae structures (Rothberg et al., 1992) and they internalise material into endocytic structures called caveosomes (Figure 1.1B). Biochemically, caveolae can be isolated as detergent resistant membranes enriched in cholesterol and glycosphingolipids (Simons & Toomre, 2000). Proteins that utilise caveolae as endocytic platforms exhibit a much slower rate of uptake when compared to clathrin dependent endocytosis, owing to the high cholesterol content of these structures (Mayor et al., 1998). Caveolae have been implicated in the uptake of glycosylphosphatidyl inositol (GPI)-anchored proteins and extracellular ligands such as folic acid (reviewed in Pelkmans & Helenius, 2002).

Lipid Raft-Mediated Endocytosis

Lipid rafts or 'membrane microdomains' display the same lipid composition of caveolae but are organised as distinct structures which diffuse freely at the cell surface and can compartmentalise distinct molecules (Figure 1.1C; Sowa et al., 2001). They also lack the caveolar protein caveolin-1. They can act as internalisation platforms and may have a role in endosomal sorting (Ikonen, 2001). GPI-anchored proteins appear to have a high affinity for lipid rafts (Legler et al., 2005).

Pinocytosis

Membrane internalisation frequently leads to the formation of vesicular structures called micropinosomes. This process of pinocytosis has been restricted to the intracellular delivery of solutes, nutrients and the recycling of membranes. It is also known as fluid phase endocytosis. Membrane ruffling can also lead to the formation of large pinocytic structures called macropinosomes. Macropinocytosis is driven by the actin dependent membrane protrusions or ruffles, which then fuse with the plasma membrane (Figure 1.1D). Macropinocytosis may either be constitutive or stimulated by growth factors such as epidermal growth factor and

fulfils diverse functions such as cell migration and immune surveillence (Mellman & Steinman, 2001; Ridley, 2001).

Clathrin and Caveolae-Independent Endocytosis

A constitutive cellular internalisation mechanism that does not utilise clathrin or caveolae and is distinct from pinocytosis, was also identified (Figure 1.1E; Puri et al., 2001). This is used by the interleukin-2 receptor in lymphocytes, which is rapidly internalised by a clathrin-independent pathway in cells that are devoid of caveolae (Subtil et al., 1994). Very little is known about the exact nature of this pathway, although it appears to be very similar to lipid raft mediated endocytosis. Several markers for lipid rafts such as GPI-anchored proteins were shown to be endocytosed to the Golgi possibly via this pathway (Nichols et al., 2001).

Downstream of the Plasma Membrane

Following cellular internalisation, endocytosed molecules are then sorted via different endocytic pathways, which are illustrated in Figure 1.2. Endocytosed material is typically delivered to early endosomes (EE), the first sorting station in the endocytic pathway, which are also referred to as sorting endosomes. Clathrin coated vesicles are primarily uncoated to allow fusion with EE (Cremona, 2001). In contrast, material internalised via caveolae (into caveosomes) has been shown to either fuse with EE (Pelkmans et al., 2004), to be delivered to the Golgi (Nichols et al., 2001; Nichols, 2002) or to the endoplasmic reticulum (Pelkmans et al., 2001).

The acidic environment of EE (pH6.4-6.6) is utilised to dissociate many ligands from their receptors or the dissociation of iron from Tf (Ciechanover et al., 1983). Internalised material then departs from the EE and can follow one of four routes. The first one leads to late endosomes (LE) and is required for nutrient uptake and receptor down regulation. The second route allows the recycling of receptors such as the TfR from the EE back to the plasma membrane. This can occur via two routes, direct or fast recycling from EE to the plasma membrane and indirect or slow recycling which occurs via recycling endosomes (RE). However, in addition to these well characterised routes, the existence of another pathway

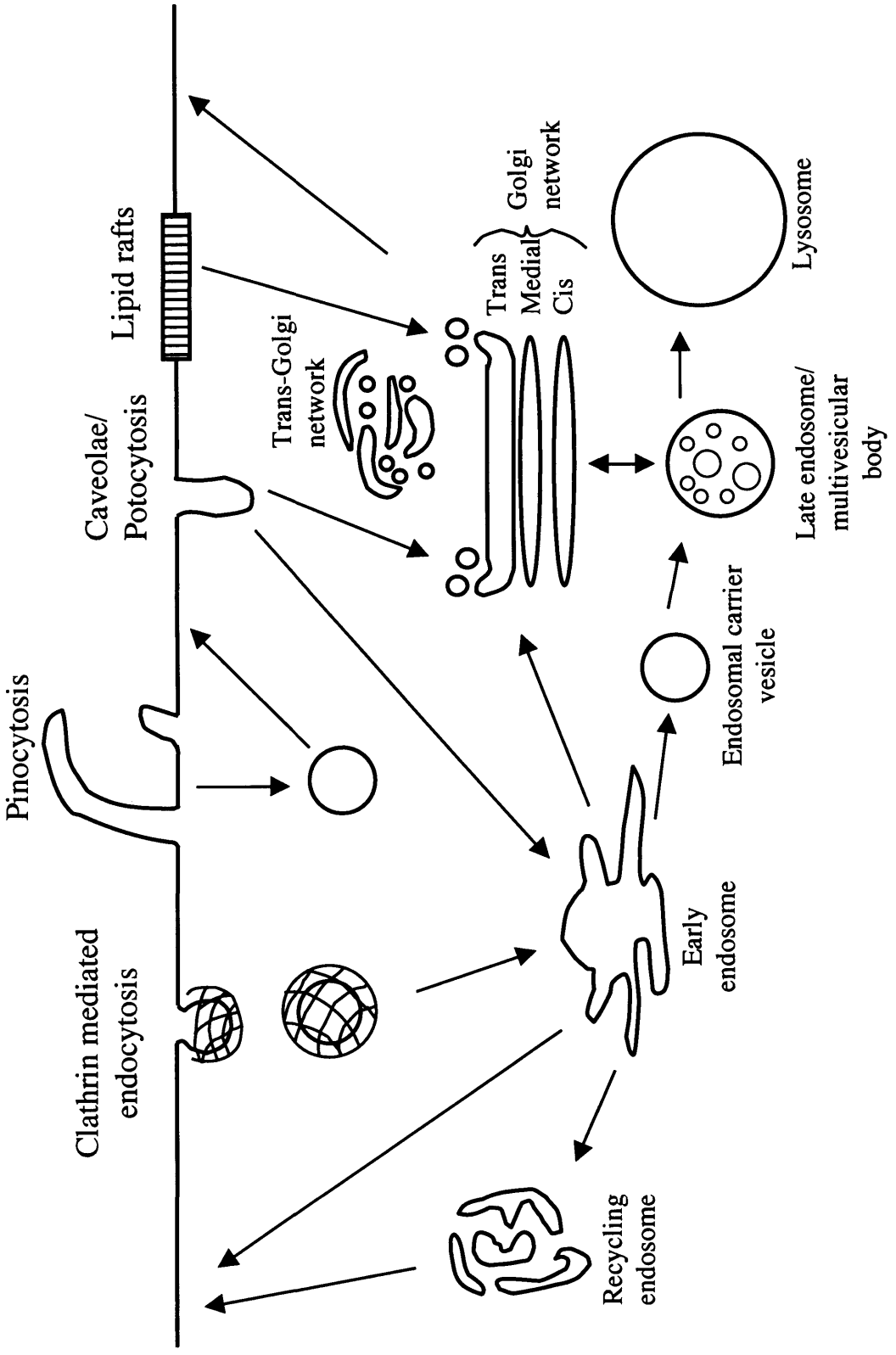

Figure 1.2. Schematic representation of the endocytic pathways in the cell.

from EE to the Golgi also exists and has been associated with lipid raft mediated endocytosis (Falguieres et al., 2001). This is utilised by a number of cellular proteins such as TGN46 and pathogen toxins such as the Shiga toxin (Mallard et al., 1998).

Although signals have been identified that lead to lysosomal targeting and degradation, recycling is thought to occur by default as a bulk flow process (Mayor et al., 1993). As lipid raft components are abundant in RE (Gagescu et al., 2000), they may contribute to protein recycling. Indeed, GPI anchored proteins that preferentially partition into lipid rafts follow the same route as the rafts themselves (Mayor et al., 1998). Studies on the TfR, which is a well characterised recycling receptor, failed to identify a recycling signal (Rutledge et al., 1991). A study by Zaliauskiene and co-workers, demonstrated that insertion of polar residues TGT into the transmembrane domain of wild type TfR promotes receptor downregulation (Zaliauskiene et al., 2000). Receptors that are efficiently downregulated are known to contain these residues whereas recycling receptors lack these residues, suggesting that trafficking domains may also be located within the membrane bilayer.

Transport from EE to LE involves intermediate organelles termed endosomal carrier vesicles (Gruenberg et al., 1989). These and LE are comprised of two morphologically visible membrane domains, internal invaginations and a limiting membrane and are also known as multi-vesicular bodies. The internal membrane is thought to contain material destined for degradation as it accumulates receptors destined for down-regulation such as EGFR (Futter et al., 1996). The limiting membrane is thought to accumulate proteins destined for the *trans*-Golgi network (TGN), bypassing degradation and so trafficking from LE to the TGN functions as a salvage pathway (Green & Kelly, 1992). However, an exception to this rule is the mannose-6-phosphate receptor, which segregates into the internal membrane despite being transported between LE and the TGN (Griffiths et al., 1988).

Multi-vesicular bodies carrying proteins for degradation, deliver their contents to lysosomes. The lysosomes contain a cocktail of hydrolytic enzymes and are regarded as the terminal degradation compartment of the endocytic pathway. LE are thought to fuse with lysosomes forming a hybrid organelle (Luzio et al., 2000; Piper & Luzio, 2001). Lysosomes then bud off and are re-used (Pryor et al., 2000).

1.2.2. Proteins that Define Intracellular Structures

Knowledge of the distribution of intracellular endocytic markers is useful in cell biology and drug delivery studies to identify the distribution and intracellular fate of molecules such as therapeutic agents or proteins. A number of cellular markers were used in this study to outline the distribution of intracellular compartments, of predominantly the endocytic pathway within the chosen cell lines. These are highlighted in Figure 1.3.

Early endosomal antigen-1 (EEA-1) is required for homotypic fusion of EE. It resides in the cytosol and on EE membranes and is a common marker for this organelle (Sheff et al., 2002). It most likely tethers endosomes together by forming homodimeric complexes through its coiled coil domain (Christoforidis et al., 1999). EEA-1 localises to endosome membranes through its amino-terminal phosphatidyl inositol-3-phosphate binding zinc finger FYVE domain (Stenmark et al., 1996). TGN46 is a transmembrane protein that recycles between the cell surface and the TGN and at steady-state distribution, most of the protein is located to the TGN (Prescott et al., 1997; Ghosh et al., 1998). However to date, no function has been identified for this protein. The lysosomal membrane contains several highly *N*-glycosylated membrane proteins, designated the lysosome associated membrane proteins (LAMP). There are two subtypes, LAMPI and II, and although their functions are similar, LAMPII is more specialised and acts as a receptor for the selective degradation of cytosolic proteins within lysosomes, a process known as chaperone-mediated autophagy (Cuervo & Dice, 1996). They are synthesised in the Golgi, sorted in the TGN and then delivered to LE/lysosomes either directly or indirectly via the cell surface (Niwa et al., 2003).

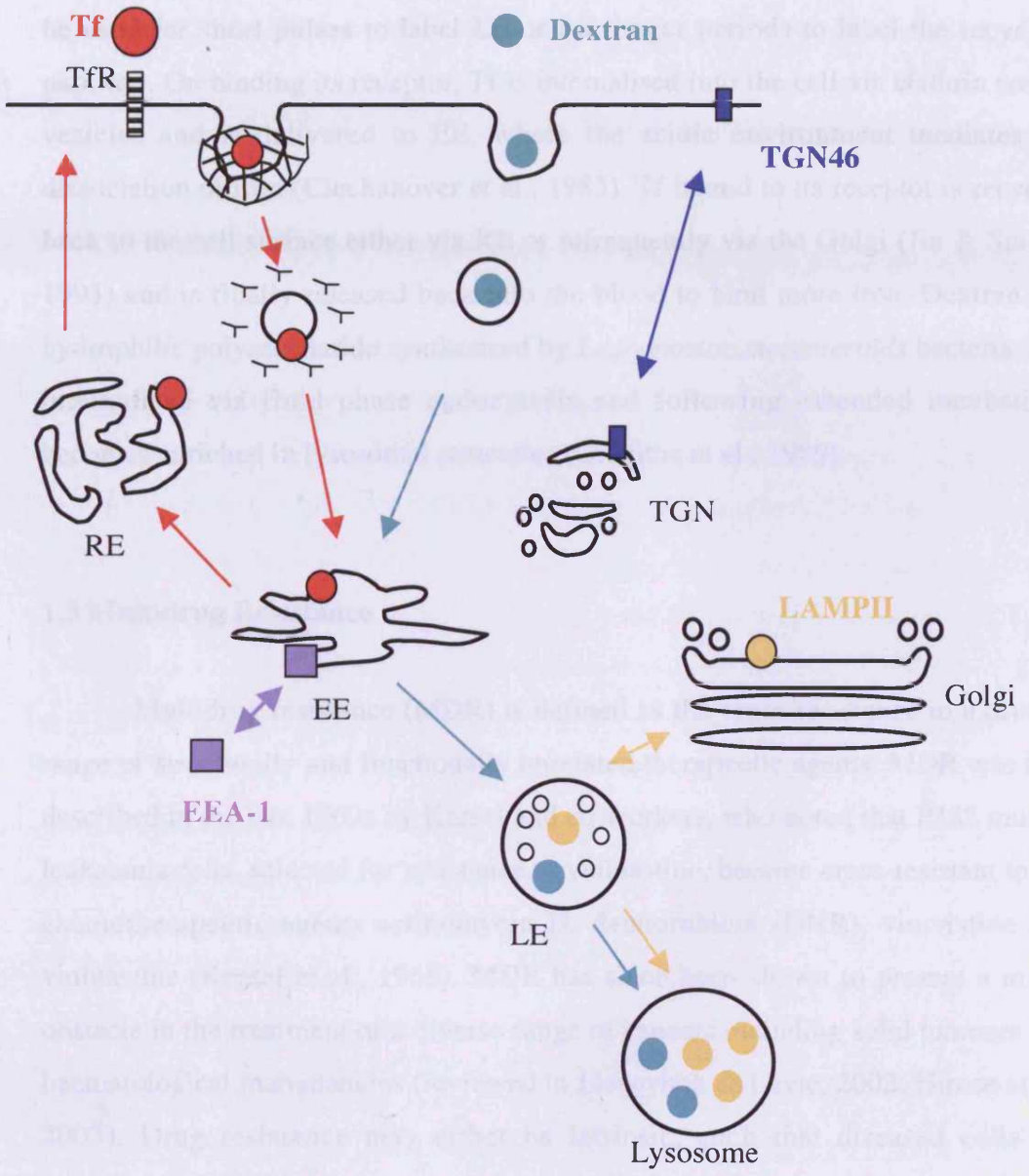

Figure 1.3. Localisation of cellular markers used to define endocytic organelles.

As well as endogenous cellular markers such as those named above, fluorescently conjugated internalised ligands are also commonly used to label endocytic structures. Fluorescently labelled Tf, the serum iron binding protein, can be used for short pulses to label EE or for longer periods to label the recycling pathway. On binding its receptor, Tf is internalised into the cell via clathrin coated vesicles and is delivered to EE, where the acidic environment mediates the dissociation of iron (Ciechanover et al., 1983). Tf bound to its receptor is recycled back to the cell surface either via RE or infrequently via the Golgi (Jin & Snider, 1993) and is finally released back into the blood to bind more iron. Dextran is a hydrophilic polysaccharide synthesised by *Leuconostoc mesenteroids* bacteria. It is internalised via fluid phase endocytosis and following extended incubations becomes enriched in lysosomal structures (Griffiths et al., 1989).

1.3 Multidrug Resistance

Multidrug resistance (MDR) is defined as the cross-resistance to a diverse range of structurally and functionally unrelated therapeutic agents. MDR was first described in the late 1960s by Kessel and co-workers, who noted that P388 murine leukaemia cells, selected for resistance to vinblastine, became cross-resistant to the chemotherapeutic agents actinomycin D, daunorubicin (DNR), vincristine and vinblastine (Kessel et al., 1968). MDR has since been shown to present a major obstacle in the treatment of a diverse range of cancers including solid tumours and haematological malignancies (reviewed in Liscovitch & Lavie, 2002; Hirose et al., 2003). Drug resistance may either be intrinsic, such that diseased cells are inherently resistant in the absence of prior drug treatment, or acquired, where drug resistance is a consequence of therapeutic intervention. The main mechanisms of resistance in eukaryotic cells are described below.

1.3.1 Drug Transporters

Initial studies by Dano (1973) had demonstrated the possibility that an active energy-requiring drug efflux pump in resistant Ehrlich ascites tumour cells may be responsible for decreased drug levels. The adenosine triphosphate (ATP)-

binding cassette (ABC) family of transporters were then identified as major implicators in MDR and this family boasts 48 transporters including MDR1 or P-glycoprotein (P-gp; described in detail in 1.4), multidrug resistance-associated protein (MRP) and breast cancer resistance protein (BCRP; reviewed in Dean et al., 2001). As well as the ABC transporters, the major vault ribonucleoprotein, lung resistance protein (LRP), is also strongly implicated in MDR (Izquierdo et al., 1996a).

Three years after the initial discovery of an active drug efflux mechanism, Juliano and Ling identified P-gp as a drug transporter expressed on the surface of resistant Chinese hamster ovary cells (Juliano & Ling, 1976). For more than 10 years after the discovery of P-gp, this was thought to be the only protein capable of conferring MDR. However, it was subsequently shown that at least one other transporter, a 190kDa transmembrane glycoprotein termed MRP, also conferred MDR (Cole et al., 1992; Zaman et al., 1994). It shares many substrates with P-gp, conferring resistance to the chemotherapeutic agents doxorubicin, DNR, epirubicin, etoposide, actinomycin D, colchicine, vincristine and vinblastine (Cole et al., 1994; Breuninger et al., 1995). MRP also transports glutathione-, glucoronate- and sulphate- conjugates of chemotherapeutic agents such as anthracyclines, vinca alkaloids and etoposide (Homolya et al., 2003) and therefore works synergistically with drug detoxification systems in the cell. MRP mediated resistance has been associated with oesophageal and gastrointestinal cancers (Takebayashi et al., 1998).

BCRP is a more recent addition to the ABC transporter family. It was discovered by Doyle and co-workers who identified it as the transporter of mitoxantrone, a drug that is a poor substrate for P-gp and MRP (Doyle et al., 1998). It also confers resistance to camptothecins (Brangi et al., 1999) and has been implicated in treatment failure for lung cancer (Yoh et al., 2004).

LRP is a 110kDa protein discovered in 1993 (Scheper et al., 1993) and is often associated with cytoplasmic and nuclear compartments, consistent with its role in drug redistribution and sequestration (Meschini et al., 2002). LRP is

implicated in resistance to doxorubicin, vincristine, etoposide, gramicidin D and paclitaxel (Kitazono et al., 1999). Overexpression of LRP is associated with a poor response to chemotherapy in ovarian cancer and acute myeloid leukaemia (AML; List et al., 1996).

Many more ABC transporters are implicated in drug resistance, although these have received comparatively little attention. This includes the transporter of antigenic peptides (TAP) which is a heterodimer of TAP1 and TAP2 genes (Neefjes et al., 1993). and confers resistance to etoposide, vincristine and doxorubicin (Izquierdo et al., 1996b). Sister of P-gp, which is expressed in high levels in liver cells, was shown in transfection experiments to confer low-level resistance to paclitaxel (Childs et al., 1998). The anthracycline resistance-associated protein has been shown to be overexpressed in the drug resistant leukaemia cell line CCRF-CEM (Longhurst et al., 1996). ABCA2 is overexpressed intracellularly in endosomal vesicles in some resistant cells (Laing et al., 1998) and has been shown to confer resistance to mitoxantrone in a small cell lung cancer cell line (Boonstra et al., 2004).

1.3.2 Drug Sequestration

A much-disputed mechanism of drug resistance involves the entrapment of drugs within intracellular structures away from their site of action by a process known as drug sequestration. This is often associated with the expression of drug transporters. P-gp resident on Golgi membranes, as well as on cytoplasmic vesicles derived from them, is active in drug sequestration (Willingham et al., 1987; Arancia et al., 2001). MRP has been shown to sequester doxorubicin in a perinuclear compartment in NIH/3T3 cells (Breuninger et al., 1995) and LRP has also been implicated in doxorubicin sequestration in A549 cells (Meschini et al., 2002).

Drug sequestration may also be driven by pH gradients that exist between the cell cytoplasm and subcellular compartments as shown in Figure 1.4A. The cytoplasm of the cell is typically pH7.2-7.3, whilst the early endosomal and Golgi pH is approximately 6.0-6.6. The LE are more acidic, with a pH of approximately

5.3. The most acidic organelles in the cell are the lysosomes with a pH of 4.5-5.5. The steady-state organelle pH is regulated by the concerted efforts of proton pumps and ions channels (reviewed in Weisz, 2003); these are illustrated in Figure 1.4B. A proton pump, known as the vacuolar H^+-ATPase, maintains an acidic endosomal pH and its expression is often upregulated in MDR cells (Murakami et al., 2001). Activity of this proton pump is inhibited by excess positive charge and so passive anion flow through a chloride channel and proton leakage from the organelle help to neutralise this potential, allowing acidification to continue (Glickman et al., 1983; Schapiro & Grinstein, 2000). In early endocytic organelles, the Na^+-K^+ATPase contributes to the maintenance of a positive membrane potential, thereby reducing the activity of the vacuolar H^+-ATPase. This inhibition of acidification is restricted to early endocytic compartments, consitent with their higher pH relative to LE and lysosomes (Cain et al., 1989).

Drug sequestration within acidic organelles limits the efficacy of some weakly basic drugs. One such example is the anthracycline DNR which in its neutral form is relatively membrane-permeable thus on encountering the acidic environment of endosomes or lysosomes, it becomes protonated rendering the DNR membrane-impermeable. Consequently DNR is entrapped within these compartments, a process known as 'acid trapping'.

Drug containing acidic vesicles could therefore be transported towards the cell surface where the drug may be secreted into the extracellular space by the process of exocytosis (Seidel et al., 1995). Indeed, enhanced endocytosis and exocytosis have been described for drug resistant cell lines. Ehrlich ascites tumor cells have a two-fold higher membrane turnover than parental cell lines, resulting in cells that recirculate a membrane area corresponding to the entire plasma membrane every hour (Sehested et al., 1987). Further evidence for the exocytosis of drugs from acidic vesicles is provided by the observation that MDR cell lines have increased secretion of lysosomal enzymes (Warren et al., 1991, 1995). An increase in lysosomal enzymes in the extracellular space in drug resistant cells possibly suggests that vesicles are themselves transported for exocytosis onto the

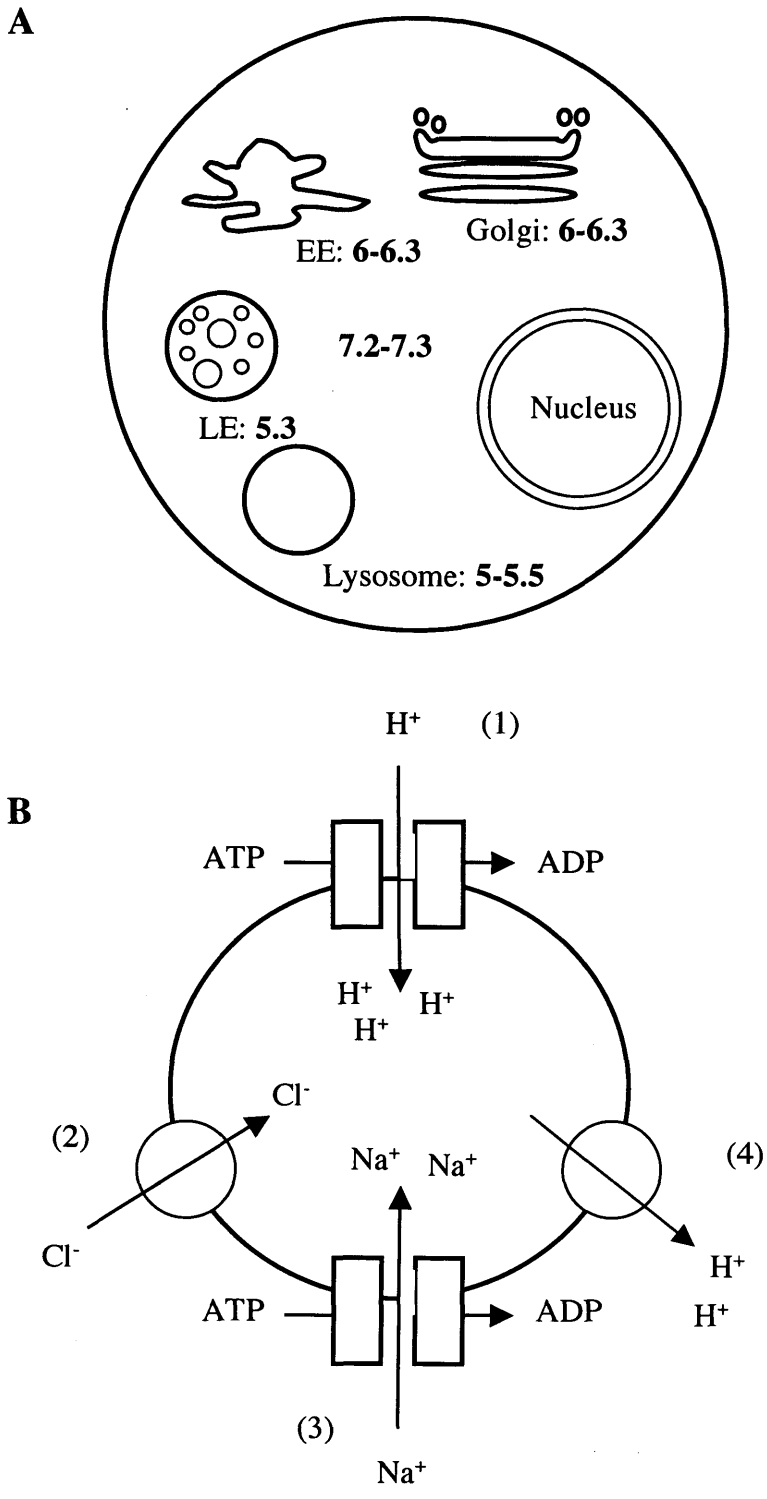

Figure 1.4. (A) Luminal pH of cellular organelles. (B) Illustration of the main mechanisms involved in the regulation of endosomal pH; (1) Vacuolar H^+-ATPase, (2) Cl^- channel, (3) Na^+K^+ -ATPase and (4) H^+ leakage.

cell surface (Ouar et al., 2003). Some weak base drugs may also be sequestered within the mitochondrial compartment, a process that is driven by the negative membrane potential associated with these organelles (Duvvuri et al., 2004). The mitochondrial environment is more alkaline and negative than the cytosol (Rottenberg, 1979). This may result in the preferential accumulation of cationic molecules in mitochondria (Smith et al., 2003).

1.3.3 Drug Detoxification

The cell glutathione system is a critical component for the detoxification of cytotoxics in the cell. Glutathione can interact via its thiol group with the reactive site of the drug, resulting in conjugation of the drug to glutathione, a process catalysed by glutathione S-transferases. The conjugate is less active and more water soluble, and it is excluded from the cell via the participation of transporter proteins such as MRP (reviewed in Townsend & Tew, 2003). Increased levels of glutathione have been found in cells resistant to alkylating agents (Colvin et al., 1993).

CYP3A is the primary cytochrome P450 subfamily responsible for phase I metabolism of drugs. It has very wide substrate specificity, encompassing a wide variety of therapeutic agents (Li et al., 1995). Many cancer chemotherapeutic agents, such as the epipodophyllotoxins and vinca alkaloids, are substrates for CYP3A (Zhou-Pan et al., 1993; Relling et al., 1994).

The synthesis of metallothionein has been proposed as a possible mechanism for the intracellular inactivation of metal-containing therapeutic agents and is implicated in resistance to cisplatin, chlorambucil and doxorubicin (Kelley et al., 1988).

1.3.4 Alteration of Drug Targets

Alteration of the drug target or enhancement of target repair constitutes another mechanism of resistance. Some anti-cancer agents are inhibitors of the nuclear enzymes, deoxy-ribonucleic acid (DNA) topoisomerases that catalyse the concerted breaking and rejoining of DNA strands. Two major topoisomerases,

topoisomerase I and II, have been identified which induce transient single and double strand breaks respectively (Liu et al., 1980). Several anti-cancer drugs such as the anthracyclines, stabilise the DNA-topoisomerase complex, which is normally easily dissociated. In some MDR cell lines a reduction in the activity of topoisomerase II is evident (Matsuo et al., 1990). A reduction in mRNA levels and gene mutations can also occur where reduced enzyme synthesis occurs following gene transcription. This type of resistance is associated with the chemotherapeutic agents doxorubicin, DNR, mitoxantrone and etoposide (Tan et al., 1989).

Anticancer drugs typically induce apoptosis and so one mechanism of resistance is the inability of cells to undergo apoptosis. The p53 tumour suppression gene has a key role in controlling apoptosis and its activation in response to cell injury results in cell cycle arrest or apoptosis. Alterations impairing p53 function are commonly found in tumours which results in the inability of cells to undergo apoptosis (Lowe et al., 1993). P53 also regulates the expression of a downstream protein, bcl-2, which serves to protect the cell from apoptotic stimuli (Miyashita et al., 1994). Bcl-2 expression confers resistance to drugs such as doxorubicin, taxol, camptothecin, mitoxantrone and cisplatin (reviewed in Reed, 1995). An alteration in cellular levels of ceramide, a mediator of apoptosis, has been shown in MCF-7 breast cancer cells and alters the apoptotic ability of cells (Liu et al., 1999).

1.4 Cell Biology of P-glycoprotein and its Role in Multidrug Resistance

P-gp is encoded by a multigene family known as mdr (Chin et al., 1989). Humans express class I and III isoforms of P-gp (termed MDR1 and MDR3 respectively). MDR1 is typically associated with drug efflux but has also been shown to have physiological roles not linked to MDR (reviewed in Johnstone et al., 2000). MDR3 was thought to function primarily as a phosphatidylcholine flippase, responsible for export of this phospholipid into the bile (Smit et al., 1993; Ruetz & Gros, 1994). However, it is now appreciated that MDR3 is also capable of transporting drugs (Smith et al., 2000). Generally, MDR1 corresponds to P-gp and this terminology will be used throughout this thesis.

The DNA sequence of P-gp reveals that the protein comprises of 1280 amino acids expressed as a single polypeptide chain containing two homologous portions of equal length (Gros et al., 1986). The membrane organisation of P-gp is illustrated in Figure 1.5 and shows that the protein comprises of two homologous halves, each consisting of one integral membrane domain containing six transmembrane domains and one nucleotide binding domain (Higgins et al., 1997). The two halves of the protein are separated by a linker region which is phosphorylated at several sites by protein kinase C (Chambers et al., 1993). There are multiple glycosylation sites on the first extracellular loop and variation in the glycosylation status and *N*-linked carbohydrate heterogeneity gives rise to P-glcoproteins of diverse molecular weights (Greenberger et al., 1987).

1.4.1 Mechanisms of P-glycoprotein Mediated Drug Efflux

Hundreds of compounds have now been identified as P-gp substrates, some of these are listed in Table 1.1. This list reflects P-gps promiscuity and also illustrates how widespread the MDR phenomenon can be. However, specific rules governing the relationship between molecular structures and P-gp substrate recognition are yet to materialise. Several models have however been proposed in attempts to explain the diversity of P-gp substrates. One model is based on the knowledge that most P-gp substrates contain an aromatic ring capable of binding aromatic amino acid residues. P-gp has a high content of aromatic amino acid residues within its transmembrane domains compared to other ABC transporters and these residues are highly conserved between species. Pawagi and co-workers proposed that P-gp substrates may encounter a channel lined by aromatic residues or drugs may bind external aromatic side chains between the transmembrane domains and the surrounding lipid environment (Pawagi et al., 1994). This model accommodates the diverse substrate size, shape and structure of P-gp substrates.

Despite this promiscuity, P-gp still displays obvious structural preferences. Agents such as camptothecin which are sparingly water soluble are not P-gp substrates indicating that hydrophilicity is required for recognition of substrates

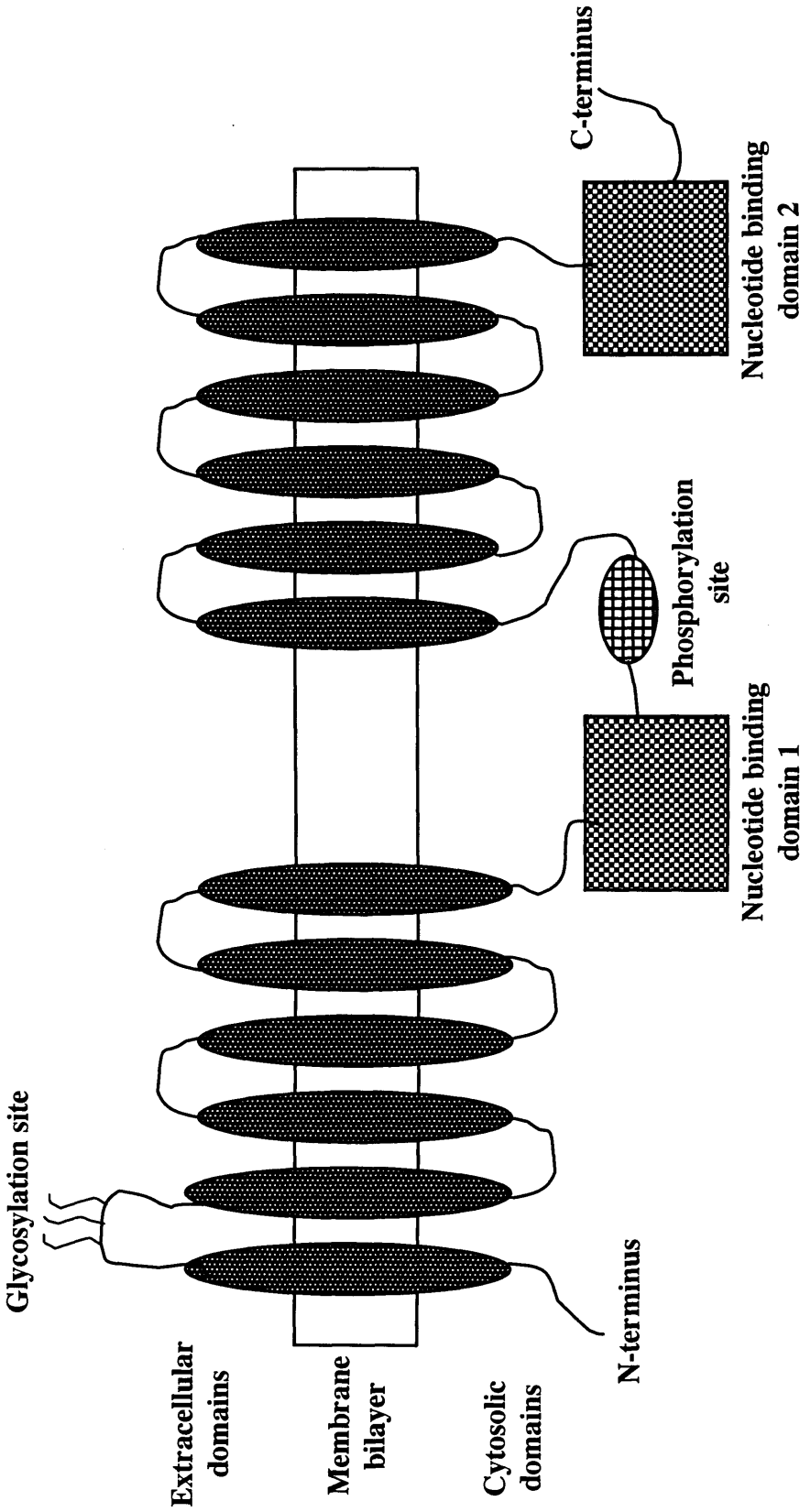

Figure 1.5. Membrane domain organisation of P-glycoprotein (adapted from Higgins et al., 1997).

Table 1.1. Substrates of P-glycoprotein.

Substrate	Reference
Anticancer Agents	
Doxorubicin, daunorubicin, docetaxel, mitomycin c, mitoxantrone, paclitaxel, teniposide, topotecan and vinblastine	(Wils et al., 1994; Relling, 1996; Sparreboom et al., 1997; Hoki et al., 1997; Wielinga et al., 2000)
Calcium channel Blockers	
Mibefridil and verapamil	(Wandel et al., 2000; Pauli-Magnus et al., 2000)
Immunosuppressants	
Cyclosporin A	(Saeki et al., 1993)
Antibiotics	
Erythromycin and sparfloxacin	(Schuetz et al., 1998; de Lange et al., 2000)
Cardiac Drugs	
Digitoxin and digoxin	(Pauli-Magnus et al., 2001; Schinkel et al., 1995)
HIV Protease Inhibitors	
Indinavir, suquinavir and ritonavir	(Lee et al., 1998)
H_1 and H_2 antagonists	
Cimetidine and ranitidine	(Collett et al., 1999)
Anti-emetics	
Domperidon and ondansetron	(Schinkel et al., 1996)
Lipid Lowering Agents	
Atorvastatine	(Wu et al., 2000)

By P-gp (Chen et al., 1991). Positively charged agents are recognised better than their neutral counterparts (Lampidis et al., 1997), for example zwitterionic rhodamine analogues were not recognised by P-gp expressing cells as efficiently as their positively charged analogues were (Lampidis et al., 1989). The drug efflux rate of P-gp appears to increase with increasing lipophilicity of the drug, presumably to compensate for increased membrane diffusion (Mulder et al., 1995). However, one study has shown that methotrexate, a hydrophobic negatively charged drug, is thought to be unaffected by P-gp expression due to its high influx rate. In cells where the influx rate of methotrexate is low, the cells can be made methotrexate resistant by introducing P-gp via recombinant retroviral infection (de Graaf et al., 1996).

Several hypothesis have been proposed to explain the actual efflux mechanism utilised by P-gp. When the amino acid sequence of P-gp was determined, structural and functional analogies were made with bacterial ABC transporters (Chen et al., 1986; Gerlach et al., 1986; Gros et al., 1986). This homology has supported the role of P-glycoprotein as an energy-dependent drug efflux pump. A model has been proposed in which drugs bind directly to P-gp and are actively effluxed via a channel formed by the molecules multiple transmembrane domains using energy derived from ATP hydrolysis (Chen et al., 1986). However, the observation that an increase in efflux in MDR cells is also accompanied by a decrease in influx, led to the proposal of the 'hydrophobic vacuum cleaner' model by Raviv and co-workers (Raviv et al., 1990). The model dictates that P-gp removes drugs directly from the lipid bilayer of the plasma membrane. In support of this model, Higgins and Gottesman postulated that P-gp encounters xenobiotics in the inner leaflet of the plasma membrane, flipping them to the outer leaflet where they diffuse out of the cell and so P-gp acts as a drug 'flippase' (Higgins & Gottesman, 1992). This is supported by the fact that P-gp displays phospholipid flippase activity (van Helvoort et al., 1996; Romsicki & Sharom, 2001).

There is an alteration in membrane lipid composition in MDR cells, with notable increases in cholesterol and glycosphingolipids, both major constituents of

caveolae and lipid rafts (Lavie & Liscovitch, 2000). The upregulation of these lipids utilises the cholesterol efflux pathway, which delivers cholesterol to the plasma membrane. This pathway is also implicated in carrying cytotoxic drugs on the same platform that delivers cholesterol and sphingolipids (Liscovitch & Lavie, 2000). A highly active cholesterol efflux pathway would facilitate drug transport by accelerating the transport of drugs from intracellular membranes to the plasma membrane against a steep concentration gradient and by delivering drug binding rafts directly to plasma membrane cholesterol-rich domains, where P-gp preferentially localises (Demeule et al., 2000). The drugs are then excluded from the plasma membrane by drug transporters such as P-gp.

Aside from its drug efflux function, P-gp has also been postulated to have a variety of indirect effects in mediating drug resistance. P-gp has been shown to protect cells against caspase dependent apoptosis (Johnstone et al., 1999) and one possible reason for this is that most apoptotic pathways are sensitive to ATP (Eguchi et al., 1997), raising the possibility that P-gp affects apoptosis by altering intracellular ATP levels. Indeed, P-gp has been shown to function as an ATP channel, releasing ATP from the cell (Abraham et al., 1993). The alkalinisation of intracellular pH, possibly mediated by P-gp, is another possible mechanism for reduced apoptosis. It has been shown that apoptosis is preceded by intracellular acidification (Gottlieb et al., 1996) and the induction of apoptotic events such as DNA laddering can be inhibited by cellular alkalinisation (Robinson et al., 1997). Therefore P-gp mediated alteration of intracellular pH places the cell in a state of caspase inactivity. It has been hypothesized that P-gp may also exert its antiapoptotic effects by reducing the pool of plasma membrane sphingomyelin that can be hydrolysed by sphingomyelinase to ceramide (Bezombes et al., 1998).

Roepe and co-workers have proposed the altered partitioning model which proposes that P-gp overexpression leads to an alteration of electrical membrane potential and increased intracellular pH (Thiebaut et al., 1990; Roepe, 1995; Hoffman & Roepe, 1997). This increased intracellular pH serves to prevent target binding and reduces drug accumulation (Simon et al., 1994).

1.4.2 Distribution and Cellular Localisation of P-glycoprotein

P-gp was initially identified on the plasma membrane of MDR CHO cells (Julianio & Ling, 1976) and its expression on the cell surface is consistent with the MDR phenotype in many cells (Kartner et al., 1983; Willingham et al., 1987). Further studies revealed that P-gp is also naturally expressed at the apical plasma membrane domain of several cells in normal tissues. In the liver, P-gp was localised to the canalicular membrane of hepatocytes where it functions in the secretion of bile (Kipp et al., 2001). It has also been located in the small intestine on the brush border membrane of enterocytes, where it limits the absorption of drugs from the gut (Hunter et al., 1993). In the kidney, P-gp is found on the brush border membrane of proximal tubule epithelium where it is expected to participate in the excretion of xenobiotics (Tsuruoka et al., 2001). In the blood brain barrier (BBB), P-gp is localised to the apical membrane of capillary endothelial cells where it functions in the exclusion of xenobiotics (Jette et al., 1995a). P-gp is also found on the basolateral side of human broncho-tracheal epithelial cells, Calu-3 (Florea et al., 2001).

Functional P-gp has also been identified in intracellular compartments such as the Golgi in several MDR cell lines including MCF-7, CEM, KB-C4 and U-2 OS cells (Willingham et al., 1987; Molinari et al., 1994, 1998). Other studies reported the presence of P-gp on nuclear membranes and the nuclear matrix (Baldini et al., 1995; Calcabrini et al., 2000). In P-gp transfected Hela cells, the lysosomal localisation of P-gp was shown and was proposed to mediate drug sequestration of doxorubicin (Rajagopal & Simon, 2003). P-gp has also been detected in the culture media of cancer cells and in the extracellular fluids of cancer patients, although the functional significance of this is yet to be determined (Chu et al., 1994). Despite several reports of a significant fraction of cellular P-gp being interior of the plasma membrane, few studies have investigated a functional role for intracellular P-gp and whether it contributes in any way to MDR. This is the focus of a number of experiments described in this study.

1.5 Circumvention of P-glycoprotein Mediated Drug Resistance

Owing to the role of P-gp in mediating MDR, a great deal of effort has been devoted to the inhibition of P-gp activity. In 1981, Tsuruo and co-workers demonstrated the *in vitro* MDR reversal effect of the calcium channel blocker verapamil (Tsuruo et al., 1981). Numerous compounds have since been identified that are capable of reversing MDR *in vitro* and such compounds have been classified as either first, second or third generation inhibitors (Table 1.2). The first generation of P-gp inhibitors were drugs already in clinical use and include calcium channel blockers (Tsuruo et al., 1983), calmodulin antagonists (Akiyama et al., 1986), immunosuppressants (Twentyman, 1988) and hormones (Bekaii-Saab et al., 2004). However in the clinic they often show severe toxic effects at doses required to effectively block P-gp function, before the reversal of MDR is achieved. For example cyclosporin A caused significant renal toxicity and hypertension, in addition to being highly immunosuppressive (Yahanda et al., 1992). This led to the development of non-toxic second generation modulators which are often stereoisomers or structural analogues of first generation agents. They include the non-immunosuppressive cyclosporin analogue PSC 833 (Boesch et al., 1991) and less cardiotoxic analogues of verapamil such as dexverapamil, emopamil and gallopamil (Pirker et al., 1989, 1990). Third generation modulators have been designed using structure-activity relationships and combinatorial chemistry approaches. These agents have far superior potency and exhibit effective reversing concentrations in the nanomolar range. An example is cyclopropyldibenzosuberane LY 335979 which displays a ten-fold increased potency compared to cyclosporin A (Dantzig et al., 1996). Others, such as GF120918 have superior potency against different drug transporters (P-gp and BCRP), a property that would undoubtedly prove valuable in a clinical setting (Kruijtzer et al., 2002).

Certain anti-P-gp antibodies block conformational changes required for drug transport function. The first such anti-P-gp monoclonal antibody, MRK16, was developed by Hamada and Tsuruo (Hamada & Tsuruo, 1986) and was shown to inhibit ATP-dependent drug exclusion and modulate P-gp mediated resistance (Mikisch et al., 1992). Another anti-P-gp monoclonal antibody capable of

modulating drug resistance is UIC2 (Mechetner & Roninson, 1992). Immunotoxins comprising a cytotoxic agent conjugated to an antibody may also be potentially valuable. Fitzgerald and co-workers conjugated Pseudomonas endotoxin to the MRK16 antibody and found that this immunotoxin specifically killed KB cervix carcinoma cells with acquired drug resistance, while sensitive KB cells were unaffected (Fitzgerald et al., 1987).

The use of antisense oligonucleotides and ribozymes against the MDR-1 gene has been shown to reverse P-gp mediated resistance (Bertram et al., 1995). Antisense oligonucleotides hybridise to messenger ribonucleic acid (mRNA), engaging the RNAse H endonuclease which cleaves and thus destroys the mRNA strand. The antisense oligonucleotide is then released intact to hybridise to another mRNA. The use of antisense oligonucleotides has proved effective in circumvention of P-gp mediated resistance *in vitro* in studies on MDR K562, MCF-7 and LoVo cells (Vasanthakumar & Ahmed, 1989; Jaroszewski et al., 1990; Rivoltini et al., 1990). Ribozymes are RNA molecules with enzymatic activity that form complexes with RNA and catalyse the hydrolysis of phosphodiester bonds, which cause RNA strand cleavage. These have also proved effective in circumventing P-gp mediated resistance (Kiehntopf et al., 1994).

1.6 Multidrug Resistance in Leukaemia

Haematopoiesis, which refers to the formation or differentiation and maturation of blood cells, initiates in the bone marrow and then proceeds in the blood. A schematic of haematopoiesis is shown in Figure 1.6 and reveals the ability of a pluripotent stem cell to differentiate into a variety of different blood cell types. Leukaemia can originate from an expansion in a subset of one of these cell lines at any stage during haematopoiesis. The treatment of some leukaemias is severely hampered by MDR and leukaemias originating from more mature cells, have a better prognosis than those associated with immature cells. This is due to high levels of P-gp expressed notably by early haematopoietic stem cells. Two malignancies whose therapy is hampered by MDR are AML and chronic myeloid

Table 1.2. Pharmacological modulators of P-glycoprotein.

Modulator	Reference
First Generation Inhibitors	
Calcium Channel Blockers	
Verapamil, Nifedipine, Nicardipine,	(Tsuruo et al., 1981, 1983; Schuurhuis, 1987;
Bepridil and Pentoxifylline	Breier et al., 1994)
Immunosuppressants	
Cyclosporin A	(Twentyman, 1988)
Calmodulin Antagonists	
Trifluorperazine, Chlorpromazine,	(Akiyama et al., 1986; Ford et al., 1989)
Prochlorperazine, Clopenthixol and Thioridazine	
Hormones	
Tamoxifen, Toremifene and Progesterone	(Bekaii-Saab et al., 2004; Qian & Beck, 1990; Mubashar et al., 2004)
Second Generation Inhibitors	
Cyclosporin Analogue	
PSC833	(Boesch et al., 1991)
Verapamil Analogues	
Dexverapamil, Emopamil and Gallopamil	(Wilson et al., 1995; Pirker et al., 1989, 1990)

Table 1.2. Pharmacological modulators of P-glycoprotein (continued).

Modulator	Reference
Anti-P-gp Antibodies	
MRK-16 & UIC2	(Mikisch et al., 1992; Mechetner & Roninson, 1992)
Antisense MDR1 oligonucleotides	(Bertram et al., 1995)
Third Generation Inhibitors	
LY335979	(Dantzig et al., 1996)
GF120918	(Hyafil et al., 1993)
XR9051	(Dale et al., 1998)
OC144-093	(Newman et al., 2000)

leukaemia (CML) and studies on these leukaemias utilise the cell line models KG1a and K562 respectively. Their status during haematopoiesis is indicated on Figure 1.6 and further details about their characteristics relating to MDR are given in section 1.7.

1.6.1 Acute Myeloid Leukaemia

AML is a heterogeneous leukaemia characterised by the blockage of myeloid differentiation at different stages of haematopoiesis giving rise to distinct AML subtypes (AML-M0 to AML-M5; Bennett et al., 1985). Approximately 2000 new cases of AML are diagnosed each year in the UK and the condition is most prevelant in adult (>40 years of age) males. Approximately 15-30 % of AML patients are intrinsically resistant to chemotherapy and 60-80 % of patients who achieve complete remission will inevitably relapse and succumb to their disease (Paietta, 1997). Treatment regimens for AML typically utilise cytosine arabinoside and DNR, a regimen that has been unaltered for almost 20 years despite clinical trials that have substituted DNR for another anthracycline idarubicin and the addition of other cytotoxic drugs such as etoposide (Stone et al., 2004). However, in relapsed or refractory AML, antibody-targeted chemotherapy is a promising new alternative. Gemtuzumab ozogamicin or Mylotarg consists of an anti-CD33 antibody which is coupled to the cytotoxic agent calichaemicin (Hamann et al., 2002) and has shown a 30 % overall response rate in relapsed AML patients. CD33 is a glycoprotein expressed during myeloid differentiation (so it is absent in AML-M0) and is found in 90 % of AML patients (Dinndorf et al., 1986), thus targeting CD33 helps diminish toxic side effects.

The MDR phenotype has been suspected as a major mechanism of therapy failure in this disease and the majority of patients are intrinsically resistant to chemotherapy at initial diagnosis before chemotherapeutic exposure. Intrinsic resistance frequently results from expression of P-gp, which is inversely associated with clinical outcome (Marie et al., 1991). One study has reported that 58 % of AML patients are intrinsically resistant to therapy and this has been associated with the expression, on leukaemia cells, of the differentiation marker CD34; this is

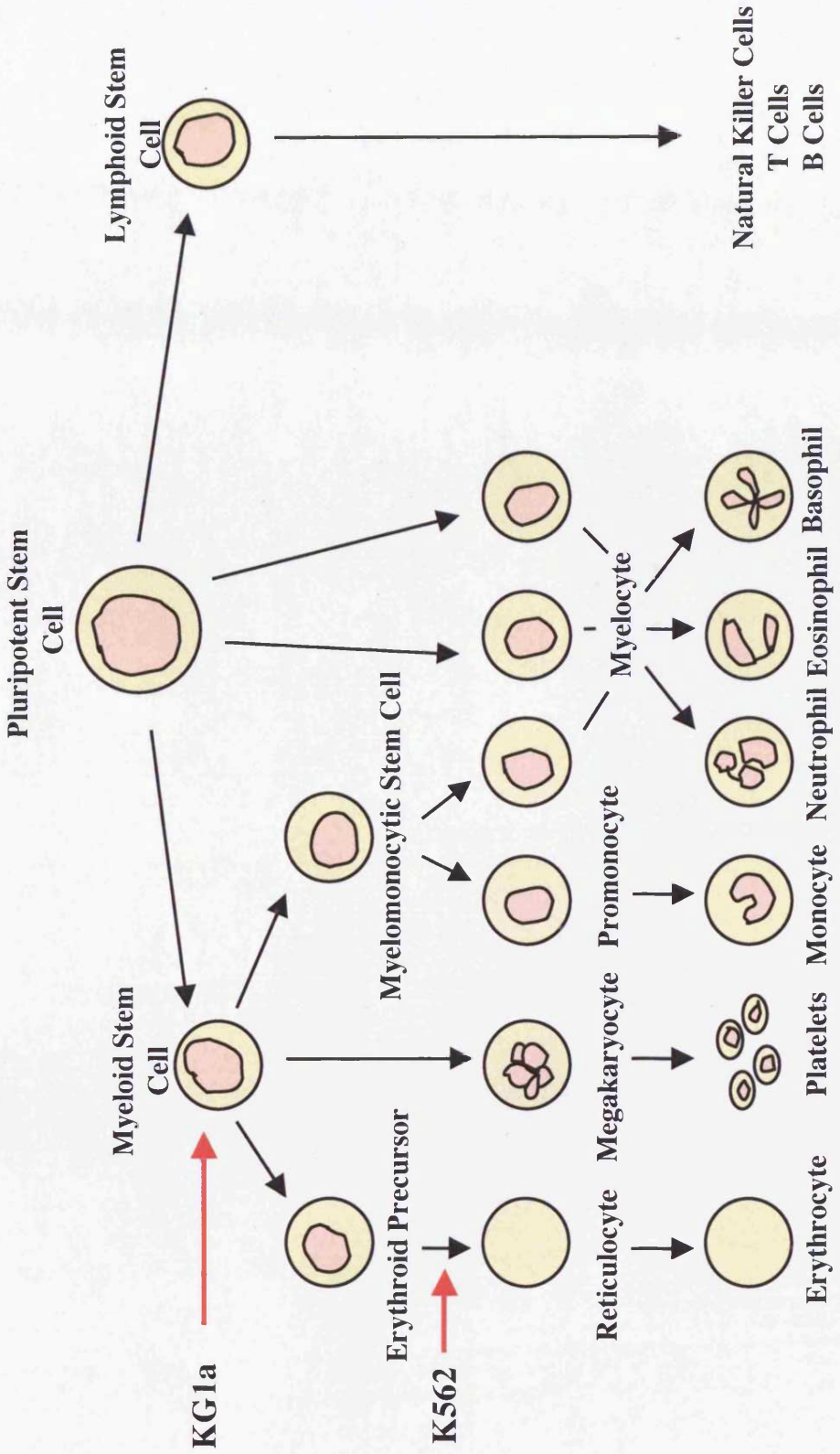

Figure 1.6. Haematopiesis of stem cells into mature blood cells. The position of KG1a and K562 cells used in this study is indicated (red arrows).

present on early progenitor cells and is associated with P-gp overexpression (te Boekhorst et al., 1993).

There is great confusion regarding the significance of P-gp and other mechanisms of resistance in the failure to treat AML and methodological inconsistencies have been proposed to contribute to this (Leith, 1998). Different subtypes of AML, stage of the disease and the patients age, all yield different MDR phenotypes. AML cells have a higher threshold for apoptosis due to overexpression of Bcl-2 (Campos et al., 1993) and a loss of p53 activity (Prokocimer & Rotter, 1994). MRP expression has been shown to confer clinical resistance in AML (Hunault et al., 1997; Legrand et al., 1999), however, other studies do not see a correlation between MRP expression and MDR (Filipits et al., 1997a; Leith et al., 1999). The clinical significance of LRP expression in AML is also unclear but a study by Filipits and co-workers found that 35% of AML samples expressed LRP and this expression was strongly associated with clinical response and overall survival (Filipits et al., 1998). In contrast, another study found that LRP did not influence clinical outcome (Borg et al., 2000). BCRP was also shown to be upregulated in AML cells and is functional in drug efflux (Sargent et al., 2001; van den Heuvel-Eibrink et al., 2002). P-gp has also been shown to confer antiapoptotic properties to primary AML cells by modulating the sphingomyelin-ceramide pathway (Pallis & Russell, 2000).

Several clinical trials testing modulators of P-gp have been conducted in patients with AML. At present, cyclosporin A and PSC 833 (which is currently in phase III clinical trials) are the most promising compounds for clinical drug modulation. A large study with cyclosporin A and PSC833 in AML patients refractory to therapy, showed an improved relapse-free and overall survival for patients receiving these modulators (Advani et al., 1999; Dorr et al., 2001; List et al., 2001). In contrast to the suggested benefits of P-gp modulators in these studies, other studies have shown no real effect of P-gp modulation on patient survival (Solary et al., 1996; Lin Yin et al., 2001; Baer et al., 2002). However, any therapeutic strategy used to circumvent MDR, needs to address the contribution of multiple mechanisms of drug resistance. The importance of this was demonstrated

in one study where treatment with cyclosporin A resulted in the relapse of some patients with drug resistant AML, irrespective of P-gp (List et al., 1993).

1.6.2 Chronic Myeloid Leukaemia

CML is a myeloproliferative disease of the pluripotent haemopoietic stem cell (Faderl et al., 1999). The disease progresses from a chronic phase through an accelerated phase and to a blast phase, where AML or acute lymphocytic leukaemia may cause mortality (Gale & Canaani, 1984). There are less than 1000 cases in the UK each year and is again more prevelant in adult males. CML is predominantly characterised by the Philadelphia chromosome, arising from the reciprocal chromosome translocation, (9;22)(q34;q11), and is characterised molecularly via fusion of parts of the Abelson murine leukaemia oncogene (Abl) gene (9q34) with parts of the breakpoint cluster region (Bcr) gene (22q11), generating an abnormal Bcr-abl fusion gene which marks the onset of CML (Rowley, 1973). This also contributes to resistance of CML to apoptotic stimuli (McGahon et al., 1994). In general, more than 85% of patients diagnosed with CML are found to have the Philadelphia chromosome.

The chronic phase of CML may be controlled by combination of interferon-α with cytotoxic drugs, such as hydroxyurea, cytarabine, busulphan and homoharringtonine, but survival is extremely short after the onset of blast crisis (Sawyers, 1999). Stem cell transplantation is also employed early in the disease (reviewed in Bhatia et al., 1997). The blast crisis of CML is refractory to most forms of chemotherapy. Imatinib mesylate, a 2-phenylaminopyrimidine derivative, has been recently introduced in the treatment of CML where it acts through the selective inhibition of kinase activity of the Bcr-abl protein (Druker et al., 2001; Savage & Antman, 2002). It has been shown to induce sustained remissions in 30% of patients in blast crisis (Sawyers et al., 2002), although it does not have long term efficacy in patients in the acute phase of the disease (Goldman, 2000). Recent reports have also shown that resistance develops on prolonged exposure to the drug, with increased expression of the target protein (Weisberg & Griffin, 2000) and P-gp-mediated efflux being implicated (Illmer et al., 2004).

While the main mechanism of drug resistance appears to be transporter-mediated in acute myeloid leukaemia, chronic myeloid leukaemia appears to rely mainly on antiapoptotic mechanisms. The anti-apoptotic activity of Bcr-abl not only contributes to the development of CML but also to the resistance of CML cells to apoptotic stimuli (McGahon et al., 1994) and has been shown to inhibit caspase-dependent apoptosis (Amarante-Mendes et al., 1998). Loss of function of p53 has been associated with suppression of apoptosis and progression into blast crisis (Stuppia et al., 1997). An energy dependent drug exclusion mechanism that is independent of P-gp and MRP was also reported in some patients at initial diagnosis and prior to drug treatment (Carter et al., 2001). Whilst P-gp activity is not definitively associated with chronic and accelerated phases of drug resistance (Stavrovskaya et al., 1998; Giles et al., 1999), reports have shown that approximately 70 % of pateints in blast crisis express functional P-gp (Kuwazuru et al., 1990; Herweijer et al., 1990). However, one study has shown that the addition of cyclosporin A to treatment regimen yields no therapeutic benefit to CML patients (List et al., 2002). This study is contradicted by in vitro models of drug resistant CML (Illmer et al., 2004) and also by an *ex vivo* study showing that DNR accumulation could be increased in CML cells by addition of verapamil and cyclosporin A (Herweijer et al., 1990).

1.7 Cell Models of Leukaemia

Ideally in vitro studies on AML and CML should utilise primary AML and CML cells. However, primary cells have a very short lifespan, may not be readily available and need to be sorted from a mixture of blood cells. Instead, commercially available human cell line models of AML and CML are commonly used. In this study, KG1a and K562 cell lines were used as representative models of AML and CML respectively. Their position within the stem cell differentiation pathway was indicated in Figure 1.6. They were also selected due to other features relating to P-gp expression and these are described below.

1.7.1 KG1a

KG1a cells originated from a patient with the M0 subtype of AML. They are a variant subline of human KG-1 cells that originated when the original myelomonocytic KG-1 cells were cultured in two separate laboratories under identical conditions and the cells from one laboratory expressed morphological differences from the parent cell line. This variant was designated KG1a and was characterised as immature and undifferentiated (Koeffler et al., 1980) and later identified as a myeloid stem cell line. An unusual feature of KG1a cells is their inability to differentiate when treated with chemicals such as dimethyl sulphoxide (DMSO) and phorbol esters which are typically known to trigger differentiation of other leukemic cells (Koeffler et al., 1980). As myeloid progenitors, they express high levels of the differentiation marker CD34 that is expressed on pluripotent stem cells and more differentiated progenitors. CD34 is often used as a marker for P-gp expression and drug resistance in leukaemia (Campos et al., 1992). The cells were chosen for this study as they contain intrinsically high levels of functional P-gp but interestingly, the majority of this protein is localised away from the plasma membrane (Ferrao et al., 2001).

Ferrao and co-workers suggest that intracellular P-gp contributes to drug sequestration of DNR within cytoplasmic vesicles (Ferrao et al., 2001). In complete contrast, Lautier and co-workers have shown that KG1a cells sequester DNR within vesicles associated with the Golgi via an energy dependent mechanism, independent of P-gp (Lautier et al., 1997). KG1a cells are thought to lack MRP expression (Fardel et al., 1998) and there are no reports supporting the presence of other drug transporters such as LRP or BCRP. KG1a resistance to mitoxantrone has been associated with apoptotic defects (Bailly et al., 1997), and this was correlated to P-gp expression as sensitivity can be restored by P-gp inhibitor PSC833 (Bezombes et al., 1998). They are also resistant to various apoptotic stimuli such as ceramide induced apoptosis (Turzanski et al., 2005) and caspase-mediated apoptosis, resulting from Fas transduction of apoptotic signals (de Thornel et al., 2001).

1.7.2 K562

K562 is an erythroleukaemic cell line derived from a patient with chronic

myeloid leukemia in terminal blast crisis (Lozzio & Lozzio, 1975). These cells were initially identified as a chronic myeloid leukaemia but were later determined to be an erythroleukaemia, probably arrested at early stages of erythroid differentiation (Andersson et al., 1979a). They are also used as a model for early development of erythrocytes from stem cells as they undergo erythrocytic differentiation into haemoglobin-producing cells, some with erythrocyte-like morphology (Andersson et al., 1979b; Rutherford et al., 1979). As they have multipotential capacity, they can also differentiate into progenitors of the granulocytic and monocytic series (Lozzio et al., 1981; Sutherland et al., 1986).

Studies have shown that K562 cells express low or undetectable levels of P-gp and MRP (Fardel et al., 1998; Ferrao et al., 2001). However, they display DNR sequestration within a compartment described as dense and perinuclear in distribution (Ferrao et al., 2001). One study has identified this compartment as lysosomes, however, seuqestration occurs to the same degree in drug resistant and sensitive cells and so is not thought to contribute a great deal to drug resistance (Loetchutinat et al., 2001). Another study, in complete contrast, reported that drug sequestration does not occur in K562 cells (Gong et al., 2000). K562 cells are resistant to various apoptotic stimuli owing to the expression of the Bcr-abl fusion protein (McGahon et al., 1994), although sensitivity to apoptotic stimuli can be restored in K562 cells using Bcr-abl antisense oligonucleotides (Smetsers et al., 1994).

1.8 Drug Delivery via Protein Transduction Domains

Macromolecular therapies using agents such as peptides, proteins and nucleic acids are now being considered as replacements for small molecular drugs such as DNR. However, their size, polarity and net charge often render these agents impermeable to cellular membranes, thereby greatly reducing their bioavailability and clinical efficacy. There is therefore a great demand for molecules that enhance drug delivery into cells. The identification of short peptide sequences capable of translocating across cellular membranes, carrying cargo that

is 100 fold their own size, has gained much interest in drug delivery research. Several studies have revealed their ability to translocate DNA (Tung et al., 2002), peptide nucleic acids (Pooga et al., 1998a), antigenic peptides (Shibagaki & Udey, 2002), antisense oligonucleotides (Astriab-Fisher et al., 2002), full length proteins (Nagahara et al., 1998), nanoparticles (Lewin et al., 2000) and liposomes (Torchilin et al., 2001) into cells. Another important feature of these peptides is their proven ability to circumvent drug resistance in K562 cells (Mazel et al., 2001). These peptide sequences have been called protein transduction domains (PTD) or cell penetrating peptides. For the remainder of this study they will be referred to as PTD.

1.8.1 Mechanisms of Transduction Across the Cell Membrane

The first indication that proteins may contain sequences reponsible for their translocation across cell membranes came from the observation that living cells internalised an 86-amino acid fragment from the human immunodeficiency virus (HIV)-1 transactivator of transcription (Tat) protein (Green & Loewenstein, 1988). Some years later it was discovered that a 60-amino acid homeodomain of the Antennapedia protein of *Drosophila* was also able to translocate cell membranes (Joliot et al., 1991). Site directed mutagenesis of this domain led to the identification of a 16-amino acid PTD called penetratin (Derossi et al., 1994). Since this period, several other protein derived PTD have been discovered as shown in Table 1.3. These include the HIV-1 Tat peptide (Vives et al., 1997), chimeric peptides such as transportan (Pooga et al., 1998b) and synthetic peptides such as the polyarginine sequences (Futaki et al., 2001). These peptides can be divided into two classes, the first encompassing amphipathic helical peptides where lysine is the main contributor to the positive charge and the second class are the arginine rich peptides such as Tat.

Several models have been proposed to explain how these molecules traverse biological membranes and these are illustrated in figure 1.7. The inverted micelle model was proposed based on the interaction of penetratin with phospholipid membranes and proposes that the positive charge of the peptide initially interacts with the negative charge on the phospholipid membrane. Then

Table 1.3. Examples of protein transduction domains used for cellular delivery (Jarver & Langel, 2004).

Peptide	Sequence	Reference
Penetratin	RQIKIWFQNRRMKWKK	(Derossi et al., 1994)
Tat	YGRKKRRQRRR	(Vivès et al., 1997)
MAP	KLALKLALKALKAALKLA	(Oelhke et al., 1998)
Transportan	GWTLNSAGYLLGKINLKALAA-LAKKIL	(Pooga et al., 1998)
PVEC	LLIILRRRIRKQAHAHSK	(Elmquist et al., 2001)
pISL	RVIRVWFQNKRCKDKK	(Kilk et al., 2001)
Polyarginines	$R_{(4-16)}$	(Futaki et al., 2001)
Pep-1	KETWWETWWTEWSQPKKKRKV	(Morris et al., 2001)

via the interaction of the hydrophobic amino acid with the membrane creates an inverted micelle, the cavity of which accomodates the peptide, which is subsequently released into the cytosol (Figure 1.7A; Derossi et al., 1996). The carpet model was first presented as a model for translocation of antimicrobial peptides (Matsuzaki et al., 1999b) and has also been suggested as a possible model for PTDs. This model proposes that the peptide interacts ionically with the membrane and then rotates, inducing a disruption of the lipid packing and consequent permeabilisation of the membrane and entry of the peptide into the cell (Figure 1.7B). Another model is the pore formation model where pores form as a result of the bundles formed by amphipathic alpha helical peptides, when the outwardly facing hydrophobic residues interact with the lipid membrane and the inwardly facing hydrophilic surfaces form the pore. This route is also utilised by antimicrobial peptides, to weaken the bacterial membrane (Figure 1.7C; Gazit et al., 1994).

A common feature of these peptides is the high content of basic amino acids resulting in structures with a net positive charge. However, a study by Futaki and co-workers has showed that charge itself is not sufficient for translocation showing that an octamer of arginines (R_8) was successfully internalised whereas a polymer of sixteen arginines did not show any significant signs of translocation (Futaki et al., 2001). In the last three years endocytosis has become an increasingly important physiological parameter when considering the ability of PTD to enter cells (Vives, 2003). A number of studies now show a dramatic reduction in intracellular levels of PTD when endocytosis is inhibited and these are described in more detail later.

1.8.2 Clinical Applications of Protein Transduction Domains

Further development and characterisation of these peptides has led to the identification of potentially diverse clinical applications. For example, a study by Vocero-Akbani and co-workers demonstrated the potency of PTD Tat to selectively induce apoptosis in HIV-infected cells. They engineered caspase-3 pro-apoptotic Tat-fusion protein with the endogenous caspase cleavage sites modified and replaced by a 14-residue HIV cleavage site, thus leaving the complex

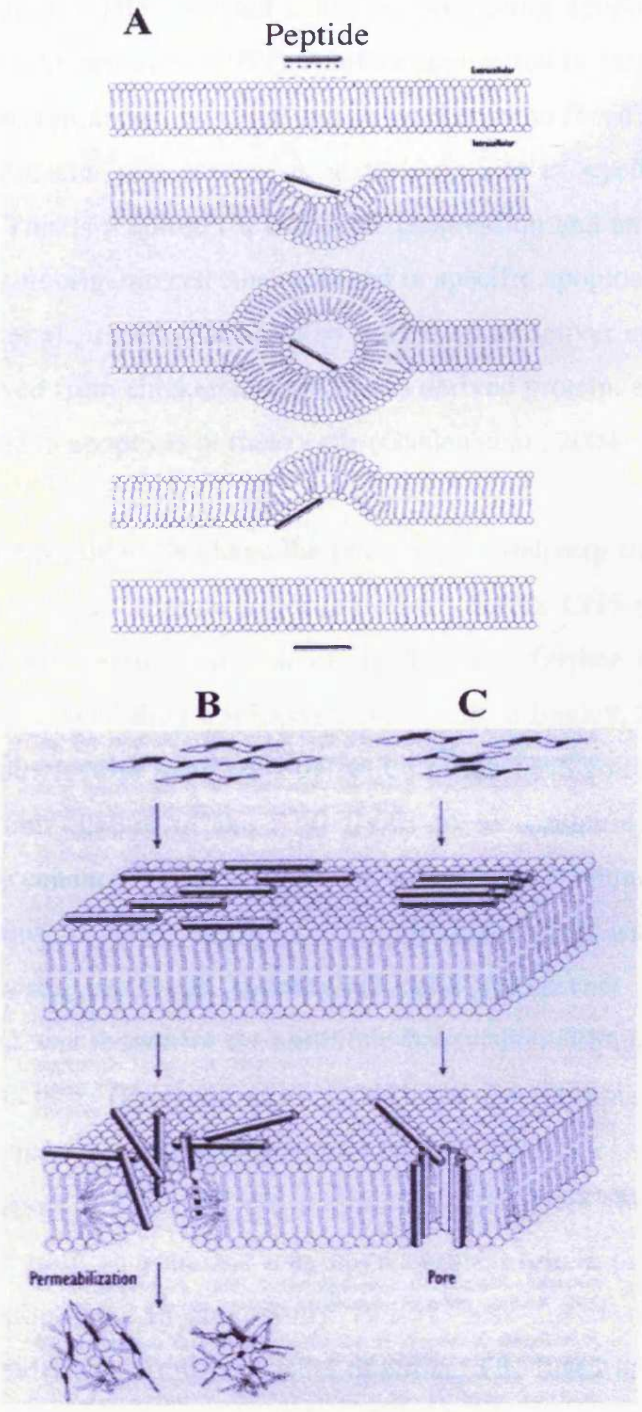

Figure 1.7. Schematic representation of (A) the inverted micelle, (B) carpet and (C) pore formation models proposed for peptide transduction domain internalisation (Lundberg & Langel, 2003).

inactivated in non-HIV-infected cells, but promoting apoptosis in HIV-infected cells (Vocero-Akbani et al., 1999). Another application is targeted chemotherapy, which was accomplished by Chen and co-workers who fused Tat and penetratin to a peptide domain that serves as a docking site of cyclin-dependent kinase complexes. This is required for cell cycle progression and applying the peptide to normal and tumorigenic cell lines resulted in specific apoptosis of the tumorigenic cells (Chen et al., 1999). Tat has also been used to deliver an apoptosis inducing protein derived from chicken anaemia virus derived protein, apoptotin, into cancer cells resulting in apoptosis of these cells (Guelen et al., 2004).

These peptides also have the potential for delivery through the BBB. The BBB poses a major obstacle for drug delivery to the CNS (reviewed in Begley, 2004a) and the barrier function of the BBB is further strengthened by the expression of several drug transporters (reviewed in Begley, 2004b). An extensive range of biomolecules have been delivered to the CNS following conjugation to PTD. The conjugation of the PTD SynB to doxorubicin has been shown to significantly enhance the brain uptake of doxorubicin without compromising BBB integrity (Rouselle et al., 2000). Interestingly this strategy was also able to bypass P-gp expressed on BBB endothelial cells (Mazel et al., 2001). Similar enhancement was shown for the antibiotic benzyl-penicillin used for the treatment of CNS infections (Rouselle et al., 2002) and for the uptake of the analgaesic enkephalin analogue, dalargin (Rouselle et al., 2003). Cao and co-workers utilised Tat to transport Bcl-xL, an anti-apoptotic molecule of the Bcl-2 family. It is expressed in adult neurons and may have a crucial role in protecting cells against neuronal apoptosis. In this study Bcl-xL was fused to Tat and injected intraperitoneally into a murine model of stroke. The fused protein demonstrated a decrease in cerebral infarction in a dose dependent manner (Cao et al., 2002).

1.9 Aims of this Thesis

The refractoriness of AML and CML to current therapeutic regimen, dictates the high mortality rate associated with these leukaemias. However, despite

much effort to unravel the nature of their resistance, these have only generated conflicting observations. Therefore there remains the need for the clarification of the resistance mechanisms operating within these leukaemias. The main study objectives were aimed at initially elucidating the mechanisms of resistance, then testing novel concepts for the circumvention of drug resistance in our human cell line models of AML and CML.

Chapter 3 aimed to identify the presence and trafficking of P-gp in KG1a cells as this knowledge could then be used to test whether an alteration in P-gp trafficking and distribution could modulate P-gp-mediated resistance. It was first necessary to optimise Western blotting and immunoprecipitation, taking into consideration the extensive cross-reactivity profiles of commercially available anti-P-gp antibodies. These techniques were then used not only to detect P-gp, but also to identify potential protein interactions that may give clues as to the trafficking and intracellular fate of this protein. A novel immunofluoresence protocol was fully optimised for assessing P-gp distribution and investigating the effects of various modulators of cellular trafficking on its distribution.

Chapter 4 aimed at elucidating the drug resistance mechanisms operating in KG1a and K562 cells utilising epifluorescence and confocal microscopy studies with the inherently fluorescent cytotoxic agent DNR. The cellular compartmentalisation of the drug and its sensitivity to known resistance modulators was assessed in order to identify possible resistance mechanisms. The possibility that P-gp-mediated resistance may be modulated by altering P-gp distribution and trafficking was also tested in this chapter.

Finally in chapter 5, the main focus was on determining the cellular uptake mechanisms and localisation of PTD in KG1a and K562 cells, as these peptides have demonstrated the potential to circumvent drug resistance in K562 cells (Mazel et al., 2001). Knowledge of their cellular uptake and intracellular fate would help to assess their suitability as resistance modulators in our cell line models of AML and CML.

Chapter 2:

Materials and Methods

2.1 Materials

General Chemicals

Phosphate buffered saline tablets (PBS), dithiothreitol (DTT), Triton X-100, tris (hydroxymethyl) aminomethane (Tris), sodium chloride (NaCl), potassium chloride (KCl), ammonium chloride (NH_4Cl), calcium chloride ($CaCl_2$), magnesium chloride ($MgCl_2$), ethylenediaminetetra-acetic acid (EDTA), ethyleneglycol-bis[β-aminoethylether]-N,N,N,N'-tetra acetic acid (EGTA), N-[2-Hydroxyethyl]piperazine-N'-[2-ethanesulfonic acid] (HEPES), sodium deoxycholate, bovine serum albumin (BSA), amiloride, sodium hydroxide (NaOH), phosphoric acid, brefeldin A, wortmannin, bafilomycin A1, nigericin, verapamil, cyclosporin A, cytochalasin D, ethylisopropylamiloride (EIPA), nocodazole, methyl-β-cyclodextrin, leupeptin, pepstatin A and aprotinin were purchased from Sigma (Dorset, UK). Glucose, ethanol, methanol, acetone, hydrochloric acid (HCl) and glycerol were purchased from Fisher Scientific Laboratories (Leicestershire, UK).

Antibodies

JSB-1 and C219 anti-P-gp antibodies were obtained from ID Labs (Glasgow, UK). F4 anti-P-gp antibody, goat anti-mouse and rabbit anti-goat horseradish peroxidase conjugated antibodies were from Sigma (Dorset, UK). Goat anti-EEA-1 antibody was from Santa Cruz Biotechnology (California, USA). Sheep anti-TGN46 and goat anti-ubiquitin antibodies were from Serotec Ltd (Oxford, UK). Mouse anti-LAMPII antibody was from Developmental Studies Hybridoma Bank (Iowa, USA). Alexa-fluor 594 conjugated goat anti-mouse, donkey anti-sheep and rabbit anti-goat were purchased from Molecular Probes (Leiden, Netherlands).

Tissue Culture

RPMI 1640 media containing L-glutamine and phenol red, foetal bovine serum (FBS) and trypan blue were obtained from Gibco BRL (Paisley, UK). Penicillin/streptomycin and DMSO were from Sigma (Dorset, UK). Acute myeloid leukaemia cells, KG1a, were purchased from ECACC (Wiltshire, UK). The

chronic myeloid leukaemia cell line, K562, were a kind gift from Dr. Paul Brennan (Cardiff University School of Medicine, Cardiff, UK).

Sodium Dodecyl Sulphate- Polyacrylamide Gel Electrophoresis (SDS-PAGE) and Western Blotting

Bis-acrylamide (40%), Tween® 20, ammonium persulphate (APS), Ponceau S and protein G-agarose were obtained from Sigma (Dorset, UK). Glycine was from ICN Biomedicals Inc. (Ohio, USA). Broad range molecular weight standards, N, N, N, N'-tetramethylethylenediamine (TEMED), β-mercaptoethanol, sodium dodecyl sulphate (SDS), bromophenol blue and Coomassie Brilliant blue G-250 were purchased from BioRad Laboratories (Hertfordshire, UK). Marvel dried milk powder was from Sainsburys. Nitrocellulose paper was purchsed from Schleicher & Schuell (Dassel, Germany). Enhanced chemiluminescence™ (ECL) Western blotting analysis system was from GE Healthcare (Buckinghamshire, UK). Developer and fixer solutions were purchased from Photosol Ltd (Essex, UK)

Fluorescence Microscopy

Paraformaldehyde was purchased from Fisher Scientific Laboratories (Leicestershire, UK). Microscope lens immersion oil was purchased from Leica Microsystems (Cambridge, UK). Texas-red Tf (TxR-Tf) and 10 kDa Texas-red dextran (TxR-Dex) were purchased from Molecular Probes (Leiden, Netherlands). DNR was purchased from Sigma (Dorset, UK). Alexa-fluor 488 Tat and Texas-red and alexa-fluor 488 R_8 peptides were supplied by Dr. Shiroh Futaki (Institute for Chemical Research, Kyoto University, Kyoto, Japan).

Plasmid Amplification and Transfection

E-coli DH5α, kanamycin, Maxiprep® kit and lipofectamine™ 2000 were purchased from Gibco BRL (Paisley, UK). Isopropanol was from Fisher Scientific Laboratories (Leicestershire, UK). Rat mdr1b-enhanced green fluorescent protein (mdr1b-EGFP) plasmid was a gift from Dr Irwin Arias (Tufts University School of Medicine, Boston, USA) and the EGFP vector was a gift from Paul Brennan (Cardiff University, School of Medicine, Cardiff, UK). Lauria-Bertani (LB) broth

was from Anachem Ltd (Bedfordshire, UK). LB agar was from Sigma (Dorset, UK). Fugene 6® was from Roche Diagnostics (Sussex, UK).

Agarose Gel Electrophoresis

Ethidium bromide and Tris-Borate-EDTA (TBE) buffer was from Sigma (Dorset, UK). Agarose was from Bioline (London, UK). DNA ladder (1 kb) was from Invitrogen (Paisley, UK). Restriction enzymes, EcoRI, BamHI and NotI, with their corresponding reaction buffers, were from Promega (Southampton, UK)

Flow Cytometry

Fluorescence assisted cell sorting (FACS) flow sheath fluid, FACS rinse and FACS clean were purchased from Becton Dickinson (Oxford, UK).

2.2 Equipment

General Lab Equipment

A varifuge 3.0 RS centrifuge was obtained from Heraeus Instruments (Germany). Optima™ LE-80K ultracentrifuge and Beckman type 50.4 Ti ultracentrifuge rotor was from Beckman Coulter (USA). Weighing scale Precisa 180A was purchased from Sartorius (Hanover, Germany). Eppendorf centrifuge 5417R was from Eppendorf (Hamburg, Germany). Sunrise absorbance reader was from Tecan (Austria). The cell cracker was from the European Molecular Biology Laboratories (Heidelberg, Germany).

Tissue Culture

Neubauer haemocytometer was obtained from Weber Scientific (Sussex, UK). BD plastipak syringes were from Becton Dickinson (Madrid, Spain). Ministart® 0.2 μm filters were from Sartorius (Hanover, Germany). Tissue culture flasks (25 cm^2, 75 cm^2 and 150 cm^2) with cantered necks and vented tops and freezing vials were from Corning, Fisher Scientific Laboratories (Leicestershire, UK). Serological pipettes were from Elkay (Hampshire, UK).

SDS-PAGE and Western Blotting

Mini PROTEAN II® gel electrophoresis tank with accessories and the Powerpac 300 were purchased from BioRad Laboratories (Hertfordshire, UK).

Fluorescence Microscopy

DRAM2 epifluorescent microscope was from Leica Microsystems (Cambridge, UK) and was equipped with a QImaging Retiga 1300 digital camera system from QImaging (Canada). Leica TCS SP2 AOBS confocal inverted DM IRE2 microscope system was from Leica Microsystems (Cambridge, UK). Multi-well slides were from C. A. Hendley Ltd (Essex, UK).

Plasmid Amplification and Transfection

Sanyo orbital incubator was purchased from Sanyo (USA). Horizon® horizontal agarose gel electrophoresis tank and the polaroid gel documenting system were from Gibco BRL (Paisley, UK). UV transilluminator was purchased from UVP (California, USA). Cary 1G UV spectrophotometer was obtained from Varian Inc (California, USA). Gene Pulser® II was purchased from BioRad Laboratories (Hertfordshire, UK).

Flow Cytometry

FACSCalibur® flow cytometer was purchased from Becton Dickinson (Oxford, UK).

2.3 Methods

2.3.1 Tissue Culture

2.3.1.1 Maintenance of Cells

Bright field images comparing the cell morphologies of KG1a and K562 cells are shown in Figure 2.1. KG1a and K562 cells were grown in RPMI 1640 media containing L-glutamine and supplemented with 10 % FBS, 100 U/ml penicillin and 100 μg/ml streptomycin. Cells were maintained in an atmosphere of 5 % CO_2 in a humidified CO_2 incubator. The passaging of cells was carried out in a

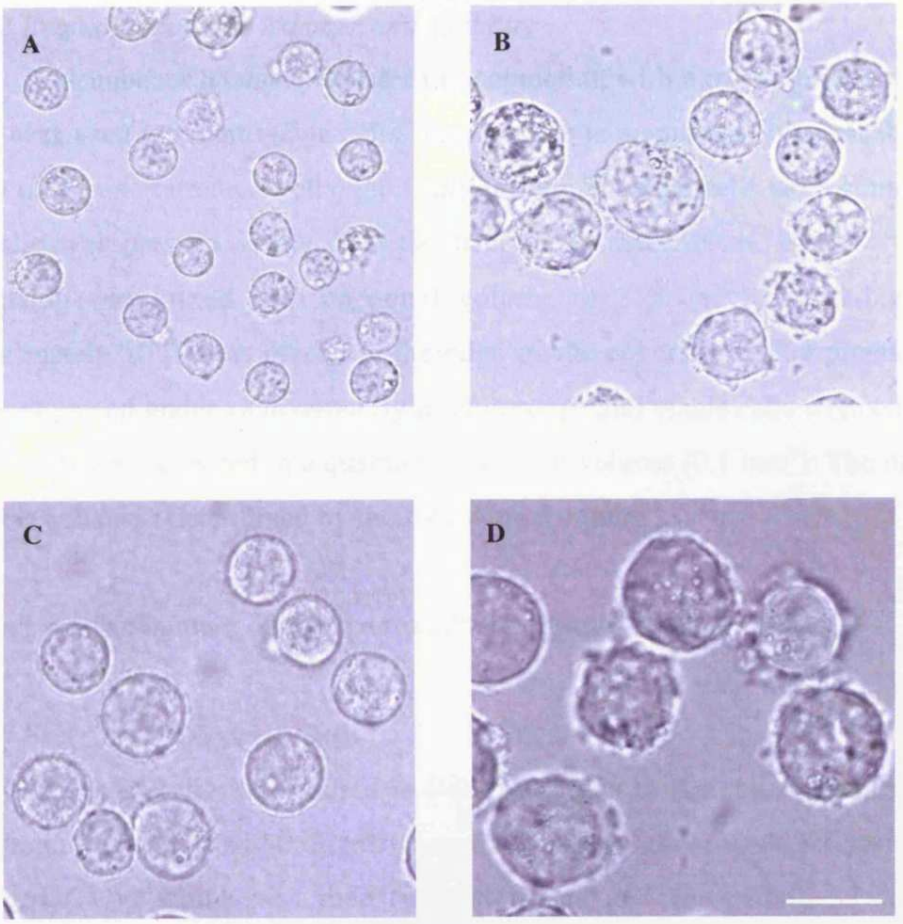

Figure 2.1. Phase contrast pictures of KG1a (A and C) and K562 (B and D) cells taken at x40 (A and B) and x63 (C and D) magnification. Scale bar= 10 μm.

class II laminar flow cabinet at a cell density of approximately 1 x 10^6 cells/ml. Typically, 8 ml of the cell suspension was transferred to a new 75 cm^2 flask and 12 ml of media warmed to 37 °C was then added to the cell suspension. Passage numbers were recorded after every cell passage and the maximum cell passage number used was 50.

2.3.1.2 Evaluation of Cell Number and Viability

A Neaubauer haemocytometer in conjunction with a trypan blue exclusion assay was used to count viable cells. Trypan blue is membrane-impermeable and so can only penetrate dead cells, thus only unstained viable cells were counted. A coverslip was pressed firmly onto the haemocytometer. Next, 20 µl of a cell suspension was mixed with an equal volume of 2 % (v/v) trypan blue and approximately 10 µl was placed at the edge of the coverslip with a pipette. The slide was placed under an inverted light microscope and viable cells were counted. Viable cells were counted in a quadrant of known volume (0.1 mm^3). The number of viable cells was determined by the following formula:

Cells/ml = mean number of cells per quadrant x dilution factor x 10^4.

2.3.1.3 Freezing and Storing Cells

Stocks of cells were stored in liquid nitrogen to maintain supplies when passage numbers reached 50. Freezing media consisted of 90 % FCS (v/v) and 10 % DMSO (v/v) which was then filter sterilised and warmed to 37 °C in a waterbath. Cells were counted, then centrifuged at 1000 g for 1 min. Following this, the supernatant was removed and cells resuspended in the appropriate volume of freezing media to yield a cell density of 1 x 10^6 viable cells/ml. Aliquots (1 ml) of cell suspension were then transferred to cryogenic vials. These were placed at –20 °C for 1 h and then at –80 °C overnight, before being transferred to liquid nitrogen for long-term storage.

2.3.1.4 Cell Recovery from Cell Banks

To recover cryogenically frozen cells, the vials were placed at room temperature for 2 min then into a 37 °C waterbath for approximately 5 min or until

the liquid had fully thawed. Cells were then transferred into a 25 ml universal sterilin and centrifuged at 1000 g for 1 min and the supernatant removed. Cells were resuspended in 5 ml of media and transferred to 25 cm^3 flasks. K562 cells were confluent after 3 days, whereas KG1a were confluent after 6 days, with the media being changed every 2 days. Once cells had reached a density of $1x10^6$ cells/ml, they were seeded into 75 cm^2 flasks.

2.3.2 Inhibition of Clathrin-Mediated Endocytosis

2.3.2.1 Potassium Depletion

KG1a cells (2 x 10^6) were washed twice in PBS and incubated in 2 ml serum free media at 30 °C for 30 min. Cells were then washed twice in ice cold K^+ free buffer A (0.14 M NaCl, 20 mM HEPES pH7.4, 1 mM $CaCl_2$, 1 mM $MgCl_2$, 1 g/L glucose and 0.1 % w/v BSA) and once in ice cold buffer B (Buffer A diluted 1:1 in dH_2O), before incubation in buffer B for 5 min at 30 °C. Cells were split into two aliquots; one was washed three times in ice cold buffer A and the other three times in ice cold buffer A supplemented with 10 mM KCl. Cells were then incubated with buffer A for 30 min at 30 °C, then finally washed three times in PBS.

2.3.2.2 Cellular Cytosol Acidification

KG1a cells (2 x 10^6) were washed twice in PBS then incubated in serum free media at 30 °C for 30 min, centrifuged and resuspended in serum free media supplemented with 20 mM NH_4Cl and incubated for a further 30 min at 30 °C. Cells were then washed once in ice cold amiloride buffer (0.14 M KCl, 20 mM HEPES pH7.0, 2 mM $CaCl_2$, 1 mM $MgCl_2$, 1 mM amiloride, 1 g/L glucose and 0.1 % w/v BSA). Finally cells were incubated in amiloride buffer for 5 min at 30 °C. In control experiments, the NH_4Cl was omitted. Following treatment, cells were washed three times in PBS.

2.3.3 Isolation of Cell Extracts for P-gp Analysis in KG1a Cells

2.3.3.1 Preparation of a Cell Lysate

All steps were performed at 4 °C. Cells (1 x 10^8) were centrifuged at 1000 g for 1 min. The resultant pellet was washed, by aspirating the media and

resuspending the pellet in PBS, before further centrifugation. This procedure was repeated once more and after the final wash, the cell pellet was resuspended in 1.5 times the pellet volume of lysis buffer (1 % Triton X-100, 20 mM Tris pH7.4, 150 mM NaCl and 5 mM EDTA) with 1 mM DTT and protease inhibitors, pepstatin A (1 μg/ml), aprotinin and leupeptin (2 μg/ml). The cells were incubated for 10min in lysis buffer then centrifuged at 13000 g for 10 min. The cell lysate was isolated as the supernatant whilst the pellet represents any Triton X-100 insoluble material and was discarded. In cell lysates prepared for immunoprecipitation, the DTT was omitted. To isolate a whole cell lysate, cells were lysed as described above with the omission of the final 13000 g centrifugation step.

2.3.3.2 Isolation of Membrane and Cytosol Fractions

All the following steps were performed at 4 °C. A cell pellet (4 x 10^8 cells) was washed as before then resuspended in 1.5 times the pellet volume of ice cold homogenisation buffer (0.1 M KCl, 85 mM sucrose, 20 mM HEPES pH7.4 and 20 μM EGTA), supplemented with 1 mM DTT (omitted for immunoprecipitation samples) and protease inhibitors. Cells were incubated in homogenisation buffer for 10 min before being passed six times through a cell cracker (previously cooled to 4 °C) using the 8.010∅ size ball bearing (Figure 2.2A and B), which leaves a 8 μm gap on either side of the ball. Cell breakage was visualised by mixing 5 μl of cell homogenate with an equal volume of trypan blue and subsequent visualisation using bright field microscopy. With six passages, approximately 80% cell breakage was typically observed. The cell homogenate was then centrifuged at 1600 g for 5 min. The supernatant, designated post-nuclear supernatant (PNS) was retained and the pellet bearing intact cells and nuclei was discarded. To isolate total membrane and cytosol fractions, the PNS was centrifuged at 100000 g for 30 min and then reconstituted in 100 μl homogenisation buffer.

2.3.3.3 Isolation of Detergent Soluble and Insoluble Fractions

Detergent soluble and insoluble material was isolated according to the method of Brown and Rose (1992). All steps were performed at 4 °C. Cells (1 x 10^8) were lysed with 1 ml of extraction buffer (25 mM HEPES pH7.5, 150 mM NaCl and 1 % Triton X-100) supplemented with protease inhibitors, for 20 min on

A

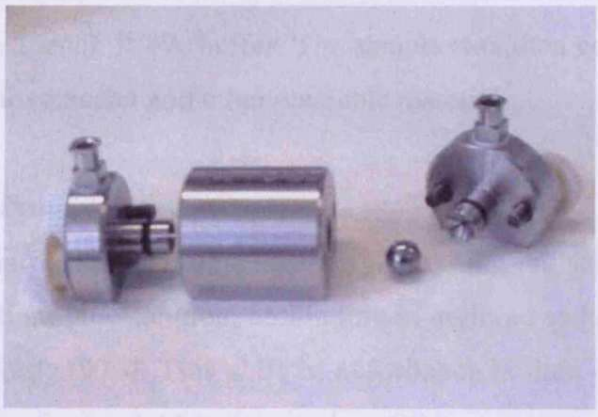

B

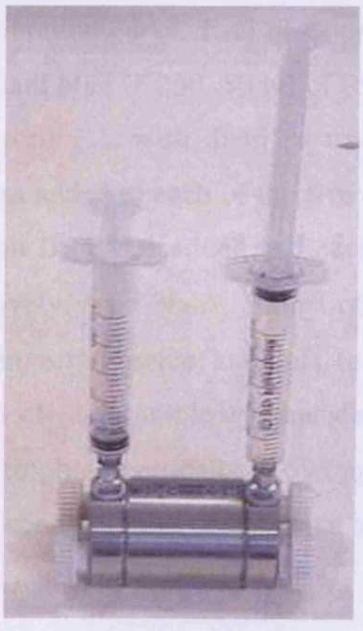

Figure 2.2. Photograph of the cell cracker showing (A) separate components of the cell cracker and (B) when the cell cracker is assembled with the syringes inserted.

ice, then centrifuged at 13000 g for 10 min. Detergent-soluble material (supernatant) was bought to 1x radioimmunoprecipitation assay (RIPA) buffer (50 mM Tris pH7.5, 150 mM NaCl, 1 % Triton X-100, 1 % sodium deoxycholate and 0.1 % SDS) by addition from a 5x stock. Detergent insoluble material (pellet) was vortexed for 4 h in the cold room in 800 µl of extraction buffer and 200 µl of five-fold concentrated stock RIPA buffer. The sample was then centrifuged at 1000 g for 3 min to remove nuclei and other insoluble material.

2.3.4 Bradford Protein Assay

The Bradford method depends on quantitating the shift of absorbance of Coomassie Brilliant blue solution, on binding to arginine and aromatic residues in proteins (Bradford, 1976). This shift in absorbance is then compared to that of varying amounts of a standard protein such as BSA.

To construct a calibration curve, 1 ml of Coomassie Brilliant blue solution (100 mg Coomassie Brilliant blue G-250, 50 ml of 95 % ethanol, 100 ml of 85 % phosphoric acid made up to 1 L with distilled water (dH_2O), filtered through Whatman filter paper), was added to each of the five eppendorf tubes. Then 5, 10, 15 and 20 µl of 0.5 mg/ml BSA was added and each was made up to 100 µl by addition of dH_2O respectively. As a blank, 100 µl of dH_2O was added instead of BSA. The tubes were inverted twice and left to stand for 2 min at room temperature. Then, 300 µl of each sample was transferred into a 96-well plate and the plates were read spectrophotometrically at 595 nm using a 96-well microtitre plate reader. The protein concentration of unknown samples was estimated using the BSA calibration curve.

2.3.5 Immunoprecipitation

Immunoprecipitation is a procedure for isolating specific proteins from a cell extract using an antibody conjugated to a stationary phase such as a bead. Proteins that react specifically with the antibody are removed from solution for further analysis. For this procedure, protein-G coated agarose beads were used. Protein G, isolated from type G Streptococci, binds IgG antibody subtype with high affinity. An antibody against the protein of interest is initially bound to

protein G coated agarose beads and the complex is then added to the cell extract. Following binding, the beads are isolated via centrifugation, and the antibody and isolated protein are dissociated. In this study, immunoprecipitation was used to purify P-gp from cell extracts and also to determine whether P-gp is ubiquitinated.

Once a cell extract was prepared and the protein concentration determined, 1 mg of the cell sample was diluted to a final volume of 800 µl with their respective buffers i.e. cell lysates were diluted in lysis buffer. Protein G-agarose beads were initially prepared by rehydration in excess dH_2O for 30 min at room temperature. Once rehydrated, the beads were centrifuged at 1000 g for 5 s and washed in excess wash buffer (0.1 % SDS w/v, 20 mM Tris pH8.0, 150 mM NaCl, 5 mM EDTA and 0.2 % BSA w/v). This step was repeated two times before equilibrating the beads in excess wash buffer for 20 min at room temperature. Then, 90 µl volume of beads were washed three times in the appropriate buffer i.e. lysis buffer. The sample was then added to the beads, in the absence of any antibody, and incubated for 1 h on a roller mixer at 4 °C. This process is termed clearing and minimises non-specific binding from proteins that have a natural affinity for the beads. Meanwhile 25 µl volumes of beads were washed as described previously. These beads were resuspended in 400 µl of the corresponding buffer and various amounts of the anti-P-gp antibody then incubated on a roller mixer at 4 °C for 2 h. In control experiments, to test the specificity of binding, the antibody was omitted. Once the antibody has bound, the beads were washed twice in the appropriate buffer to remove excess antibody. After clearing, the beads were centrifuged at 1000 g for 5 s and the cleared supernatant was utilised for subsequent immunoprecipitation after addition to the antibody bound protein G-agarose beads. The mixture was incubated for 3 h on a roller mixer in the cold room. Beads were then centrifuged at 1000 g for 5 s, washed once in the appropriate buffer, three times with the wash buffer and once with gel buffer (50 mM Tris pH8.0). To dissociate the antibody and P-gp from the beads, 40 µl of SDS sample buffer diluted from a 4x concentrated stock (1.936 g Tris pH6.8, 6.0 g SDS and 22 ml glycerol (made up to 45 ml with dH_2O), 1.2 ml of 0.5 % bromophenol blue and 1.13 g β-mercaptoethanol finally made up to 50 ml with dH_2O). DTT was added to a final concentration of 10 mM, and the sample was

heated at 95 °C for 5 min. The samples were then subjected to sodium dodecyl sulphate-polyacrylamide gel electrophoresis (SDS-PAGE) and Western blotting as described below.

2.3.6 Sodium Dodecyl Sulphate-Polyacrylamide Gel Electrophoresis

Electrophoresis is used to separate a complex mixture of proteins for further purification and to determine molecular size. In SDS-PAGE, the proteins are fully denatured with a reducing agent such as β-mercaptoethanol or DTT, then saturated with SDS. SDS disrupts non-covalent interactions and so unfolds polypeptide chains and coats the proteins thereby eliminating charge variability between polypeptides, giving them all the same charge:mass ratio and forcing them all into rod like shapes. The protein migrates through pores in the gel matrix. Pore size decreases with higher acrylamide concentrations and so a suitable porosity is selected to enable separation of the protein according to its molecular weight. SDS-PAGE was used to separate a complex mixture of proteins from cell extracts, in preparation for subsequent Western blotting.

The gel holding apparatus was cleaned thoroughly with methanol before assembly. The apparatus was tested for leaks using methanol prior to preparation of the gels. The separating gel (8 % acrylamide) was prepared in a universal container as follows:

Stock solution	*Amount added: 8 % seperating gel*
3 M Tris pH8.8	2.5 ml
40 % bis-acrylamide	4 ml
10 % SDS	200 µl
dH_2O	13.2 ml
10 % APS (freshly made)	150 µl
TEMED	15 µl

TEMED and APS are the polymerisation initiators. TEMED catalyses free radical production from the APS. The mixture was swirled gently and carefully introduced into the glass plate sandwich within the gel holder apparatus using a Pasteur pipette. DH_2O was immediately layered over the top of the gel to prevent dehydration of the mixture whilst setting. The gel was left to polymerise for 30 min.

Meanwhile the stacking gel was prepared as follows:

Stock solution	*Amount added: 4 % stacking*
1 M Tris pH6.8	1.3 ml
40 % bis-acrylamide	1 ml
10 % SDS	100 µl
dH_2O	7.6 ml
10 %APS	75 µl
TEMED	10 µl

The mixture was swirled gently and overlayed onto the polymerised separating gel after the dH_2O was discarded. A 10 well comb was positioned at the top of the stacking gel, which was left to polymerise for 30 min. After polymerisation, the comb was removed and the apparatus was immersed into a tank containing 1x running buffer diluted from a 5x concentrated stock (720 g glycine, 25 g SDS and 151.5 g Tris, made up to 5 L) and cooled to 4 °C. Protein samples were mixed with 1x SDS sample buffer (diluted from a 4x stock) and DTT at a final concentration of 10 mM, then heated at 95 °C for 5 min. Samples were then centrifuged at 1000 g for 5 s to ensure that all the sample could be loaded onto the gel. Broad range molecular weight markers (10 µl) were loaded onto the outermost wells.

The gels were run at 110 V for 1 h or until the sample was visible at the end of the gel. The glass plate was pulled apart and the gel was carefully placed into a container and rinsed with dH_2O. The gel was then subjected to Western blotting as described below.

2.3.7 Western Blotting

Western blotting is used to identify specific antigens recognised by antibodies. Following the electrophoretic separation of cell extracts by SDS-PAGE, the antigens are transferred to a nitrocellulose membrane via migration from the cathode to the anode. Transferred proteins are bound to the surface of the membrane, providing access for reaction with antibodies.

Initially the gel was equilibrated for 5 min in transfer buffer cooled to 4 °C. This prevents a change in gel size during transfer. The transfer cassette was placed into a container filled with enough transfer buffer to cover the cassette. The transfer sandwich was then assembled in order of sponge, filter paper, gel, nitrocellulose, filter paper and sponge. All components were equilibrated in transfer buffer for 15 min prior to assembly. When the nitrocellulose membrane was placed onto the gel, air bubbles were removed by gently rolling a glass rod over the surface of the nitrocellulose as air bubbles will obstruct the current flow and prevent protein transfer. The tank containing the electroblotting apparatus was filled with transfer buffer at 4 °C. The cassette was placed into the electroblotting apparatus with the nitrocellulose facing the anode and the gel facing the cathode. An ice unit was placed into the tank to cool down the transfer system to ensure efficient transfer. A magnetic stirrer was placed at the bottom of the tank to evenly disperse any heat generated during transfer. Proteins were transferred for 1 h at 350 mA. Following transfer, the nitrocellulose was removed and rinsed in dH_2O before immersion into Ponceau S to visualise transferred protein. The gel was also stained with Coomassie Brilliant blue (0.001 % Coomassie Brilliant blue w/v, 5 % acetic acid, 35 % methanol and 60 % dH_2O) to assess transfer efficiency. The nitrocellulose was subsequently washed with PBS to remove any traces of the stain, then placed into a container of blocking solution (5 % milk powder dissolved in PBS 0.1 % v/v Tween) and incubated on a rotator for 30 min to block non-

specific binding sites. The milk was then discarded and primary antibody, diluted in the blocking solution, was added and incubated on the shaker with gentle swirling for either 2 h at room temperature or overnight in the cold room. The primary antibodies used in this section are detailed below:

Primary antibody	Type	Dilution
C219 (anti-P-gp)	IgG2a mouse monoclonal	1:100
JSB-1 (anti-P-gp)	IgG1 mouse monoclonal	1:100
F4 (anti-P-gp)	IgG1 mouse monoclonal	1:500
Anti-ubiquitin	IgG goat polyclonal	1:500

Following the antibody incubation, the nitrocellulose was washed three times for 5 min (on the rotator) in PBS 0.1 % v/v Tween, then a further two 5 min washes in PBS alone. The appropriate secondary antibody, also diluted in blocking solution, was then incubated with the nitrocellulose paper for 1 h at room temperature on the rotator. The horseradish peroxidase conjugated secondary antibodies used in this section are detailed below:

Secondary antibody	Dilution
Goat anti-mouse	1:5000
Rabbit anti-goat	1:8000

The secondary antibody was washed also washed three times for 5 min in PBS 0.1 % v/v Tween, then twice in PBS alone.

2.3.8 Enhanced Chemiluminescence Detection of Transferred Proteins

The following procedure was carried out in a darkroom. First, 1 ml of each of the ECL reagents were mixed together, then added to the nitrocellulose paper and left on for 1 min. The nitrocellulose was gently shaken to remove excess reagents and placed inside a plastic bag and then into the developer cassette. A sheet of film was overlayed onto the nitrocellulose and the cassette was closed. The exposure time was typically between 30 to 60 min. The film was then removed and placed into developer solution for 3 min and then fixer solution for a further 3 min. The film was finally rinsed in dH_2O and left to dry.

2.3.9 Fluorescence Microscopy

Fluorescence microscopy was used extensively in this study to analyse the subcellular distribution of organelles, fluorescently conjugated probes and peptides and inherently fluorescent drugs. The two types of fluorescence used in this study are direct and indirect fluorescence. Direct fluorescence refers to the incubation of a fluorescent compound with cells and subsequent visualisation either with or without fixing. Indirect fluorescence refers to the immunodetection of proteins with a primary antibody against the protein of interest followed by a fluorescently conjugated secondary antibody. Immunofluorescence microscopy of these cells had not been previously performed in the laboratory and therefore a number of methods were initially investigated before final methods were developed and fully optimised. The excitation and emission wavelengths of all the fluorophores used in this study are detailed below:

Fluorophore	Excitation	Emission
Alexa-fluor 594	594	615
Alexa-fluor 488	494	519
TxR	596	615
EGFP	489	508

2.3.9.1 Indirect Fluorescence Microscopy

Indirect immunofluorescence was used to determine the intracellular localisation of P-gp and several cellular compartments in K562 and KG1a cells. All the primary and secondary antibodies used in this section are detailed below:

Primary antibody	Type	Dilution
Anti-EEA-1	Goat polyclonal	1:200
Anti-TGN46	Sheep polyclonal	1:750
Anti-LAMPII	Mouse monoclonal	1:200
F4 (anti-P-gp)	Mouse monoclonal	1:200

Secondary antibody	Fluorophore	Dilution
Goat anti-mouse	Alexa-594	1:400
Rabbit anti-goat	Alexa-594	1:400
Donkey anti-sheep	Alexa-594	1:400

Two different immunofluorescence protocols were characterised and their differences lies in the fact that some antibodies were found to be sensitive to Triton X-100. For immunofluorescence using anti-TGN46 or anti-EEA-1 antibodies, 1 x 10^6 cells were harvested and washed twice with PBS before fixing with PBS 2 % v/v PFA for 15 min at room temperature. Cells were washed twice in PBS by centrifugation at 1000 g for 1 min, followed by resuspension in excess PBS. After the final wash, cells were resuspended in 100 µl of PBS. To a single well on a Hendley multi-well slide (Figure 2.3A), 25 µl of cell suspension was added and left to settle for 5 s before excess liquid was aspirated. Cells were then left to dry onto the slide under an air hood for 2 min. These were permeabilised by addition of 30 µl of PBS 0.1 % v/v Triton X-100 for 10 min. The slides were then washed once in PBS for 2 min by transferring the slide into a container of PBS with a

magnetic stirrer to create a flow of PBS over the cells (Figure 2.3B). Non-specific binding sites were then blocked by the addition of 30 µl of blocking solution (PBS 10 % v/v FBS) to the well and incubating for 10 min at room temperature. The blocking solution was aspirated and replaced with primary antibody diluted in blocking solution. The primary antibody was incubated for 30 min at 37 °C in a humidified box (Figure 2.3C). To control for any non-specific binding of the secondary antibody, the primary antibody was omitted thus any fluorescence signal was non-specific and this could be compared with the signal obtained when both antibodies were used. Cells were then washed three times for 2 min in PBS 0.1 % v/v Triton X-100 followed by a single wash in PBS alone. The slide was removed and the spaces between the wells were dried before addition of the secondary antibody and a 30 min incubation at 37 °C as described for the primary antibody. The cells were then washed as described, dried and the wells filled with 5 µl of PBS. The slide was covered with a coverslip and sealed with nail polish. Slides were analysed by epifluorescence microscopy.

For immunolabelling experiments utilising anti-LAMPII or F4 anti-P-gp antibodies, a modified protocol was developed as neither of these antigens could be detected using the previous protocol. The cells were harvested, washed, fixed in PFA and dried onto the slide as before. Then they were rehydrated with 30 µl of PBS for 5 min. Cells were then post-fixed and permeabilised with acetone (at room temperature) for 30 s and blocked with blocking solution and immunolabelled as described above.

To test the effects of pharmacological agents acting on intracellular compartments and trafficking, the cells were pretreated for 30 min at 37 °C with the appropriate agent in serum supplemented media, before being washed and fixed in PFA and immunolabelled as described above. The cells were incubated with the diluent for each drug as a control.

2.3.9.2 Direct Fluorescence Microscopy

2.3.9.2.1 Incubation of Cells with Texas-Red Transferrin

Cells (2 x 10^6) were harvested, pelleted and washed twice in PBS

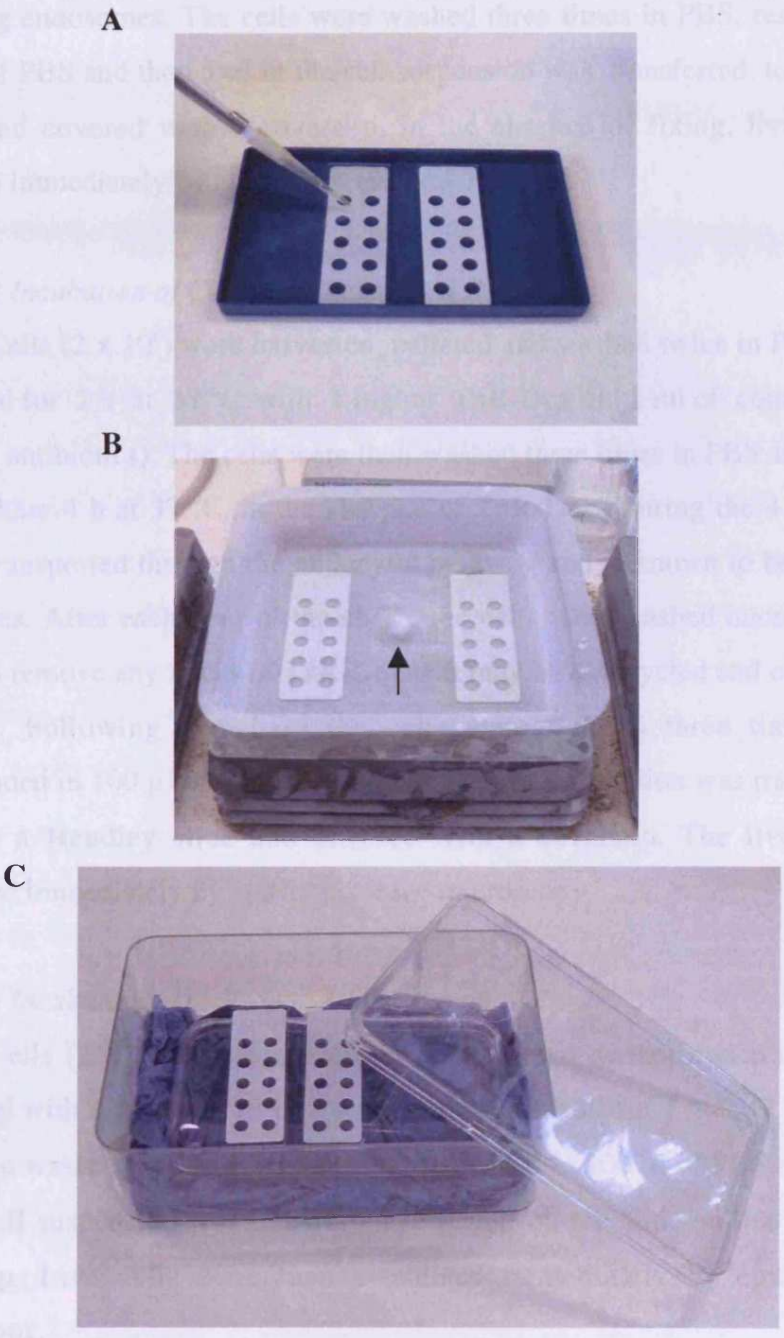

Figure 2.3. Photographs of the experimental set up used for immunofluorescence microscopy. (A) Hendley multi-well slides. (B) Washing procedure on a magnetic stirring block with the arrow pointing to the magnetic bar. (C) Humidified box used for antibody incubations.

and then incubated for 1 h at 37 °C with 25 ng/ml TxR-Tf in 2 ml of serum free media. In 1 h the TxR-Tf should label the entire Tf pathway, including early and recycling endosomes. The cells were washed three times in PBS, resuspended in 100 µl of PBS and then 5 µl of the cell suspension was transferred to a Hendley slide and covered with a coverslip. In the absence of fixing, live cells were analysed immediately by epifluorescence microscopy.

2.3.9.2.2 Incubation of Cells with Texas-Red Dextran

Cells (2 x 10^6) were harvested, pelleted and washed twice in PBS and then incubated for 2 h at 37 °C with 1 mg/ml TxR-Dex in 1 ml of complete media (without antibiotics). The cells were then washed three times in PBS and incubated for a further 4 h at 37 °C, in the absence of TxR-Dex. During the 4 h chase, the Dex is transported through the endocytic pathway and is known to be enriched in lysosomes. After each hour of the chase, the cells were washed once in complete media to remove any traces of TxR-Dex that may have recycled and could re-enter the cell. Following the chase the cells were washed three times in PBS, resuspended in 100 µl of PBS then 5 µl of the cell suspension was transferred to a well on a Hendley slide and covered with a coverslip. The live cells were visualised immediately by epifluorescence microscopy.

2.3.9.2.3 Incubation of Cells with Daunorubicin

Cells (2 x 10^6) were harvested, pelleted and washed twice in PBS, then incubated with 2 µg/ml DNR in 2 ml of complete media for 1 h at 37 °C. The cells were then washed three times in PBS, resuspended in 100 µl of PBS and then 5 µl of the cell suspension was transferred to a well on the slide and covered with a coverslip. Live cells were then visualised immediately by epifluorescence microscopy.

2.3.9.2.4 Colocalisation Studies of Daunorubicin with Texas-Red Dextran

Cells (2 x 10^6) were treated with TxR-Dex as described in section 2.3.9.2.2. During the final hour of incubation, 2 µg/ml DNR was added. Cells were washed three times in PBS then visualised live by dual labelling confocal microscopy.

2.3.9.2.5 Incubation of Cells with Sulforhodamine 101

Cells (2 x 10^6) were harvested, pelleted and washed twice in PBS, then incubated with 5 μM SR101 in 2 ml of complete media for 1 h at 37 °C. The cells were then washed three times in PBS and incubated for a further 1 h at 37 °C in complete media in the absence of SR101. The cells were then washed three times in PBS, resuspended in 100 μl of PBS and then 5 μl of the cell suspension was transferred to a well on the slide and covered with a coverslip. Live cells were then visualised immediately by epifluorescence microscopy.

2.3.9.2.6 Incubation of Cells with Alexa-488-Tat, -R_8 and Texas-Red-R_8

All the peptides used in this study were chemically synthesised by Dr. Shiroh Futaki (Institute for Chemical Research, Kyoto University, Kyoto, Japan). All the peptides were purified by high performance liquid chromatography (HPLC) and the molecular masses were confirmed by matrix-assisted laser desorption ionisation time of flight mass spectrometry (MALDI-TOF). TxR was attached to the amino-terminus of R_8 whilst the alexa-488 peptides contained the fluorophore at the carboxy-terminus.

The TxR-R_8 peptide chain was constructed by 9-fluorenylmethylcarbonyl (Fmoc)-solid-phase peptide synthesis on a Rink amide resin as previously reported (Futaki et al., 1997). After removal of the amino-terminus Fmoc group, the amino-terminus of the peptide resins were fluorescently labelled by the treatment with TxR-X succinimidyl ester mixed isomer. The fluorescently labelled peptide resins were then treated with trifluoroacetic acid-ethanedithiol (95:5) at 25 °C for 2 h to yield TxR-R_8-amide.

For synthesis of alexa labelled peptides, the peptide segments bearing extra cysteine or glycylcysteine residues at the carboxy-terminus of the arginine segments were prepared by Fmoc-solid phase peptide synthesis followed by treatment with trifluoroacetic acid-ethanedithiol and HPLC purification. Peptides were then treated with alexa-488 C_5 maleimide sodium salt and purified by HPLC.

The structures of the peptides synthesised are: alexa-488 Tat, NH_2-

GRKKRRQRRRPPQC (alexa-488)-amide; alexa-R_8, NH_2-$(R)_8$-GC (alexa-488)-amide. MALDI-TOF; alexa-488 Tat, 2521.1 and alexa-488 R_8 2126.81.

Cells (5 x 10^5) were harvested, pelleted and washed twice in PBS, then incubated in either 200 µl of 3 µM alexa-488 Tat or 1-3 µM alexa-488 or texas-red R_8 in complete media, for 1 h at either 4, 16 or 37 °C. The cells were then washed four times in PBS, resuspended in 50 µl of PBS and 5 µl transferred to a well on the slide and covered with a coverslip. The live cells were then analysed immediately by fluorescence microscopy.

The effect of various pharmacological agents on the uptake and distribution of internalised ligands were analysed by pretreating the cells for 15 min with the agent followed by simultaneous incubation with the agent and ligand for a further 1 h.

2.3.10 Amplification, isolation and characterisation of the Rat mdr1b-EGFP Plasmid

Rat mdr1b-EGFP plasmid was acquired as a gift from Dr. Irwin Arias (Boston, USA; Sai et al., 1999). The vector was created by subcloning rat mdr1b into the commercial parent vector pEGFP-N3 (BD Biosciences, Oxford, UK). The plasmid map is shown in Figure 2.4.

2.3.10.1 Amplification of the Plasmid

E. coli DH5α cells were recovered from –80 °C freezer and left to thaw on ice. Then, 200 µl of cells were transferred to a sterile, pre-chilled eppendorf tube and approximately 10 ng of rat mdr1b-EGFP DNA was added to the bacterial cells. The mixture was aspirated gently and left on ice for 30 min. The cells were then heat shocked to allow entry of the plasmid into the cells. This was achieved by transferring the eppendorf tube to a waterbath heated to 42 °C for 60 s. Cells were then transferred back to ice for 2 min. Sterile LB broth (800 µl), heated to 37 °C was added to the transformed cells which were then incubated for 45 min in a 37 °C waterbath. For the preparation of agar plates, 20 ml of warm LB agar, supplemented with 50 µg/ml kanamycin, was poured into a culture plate and left to

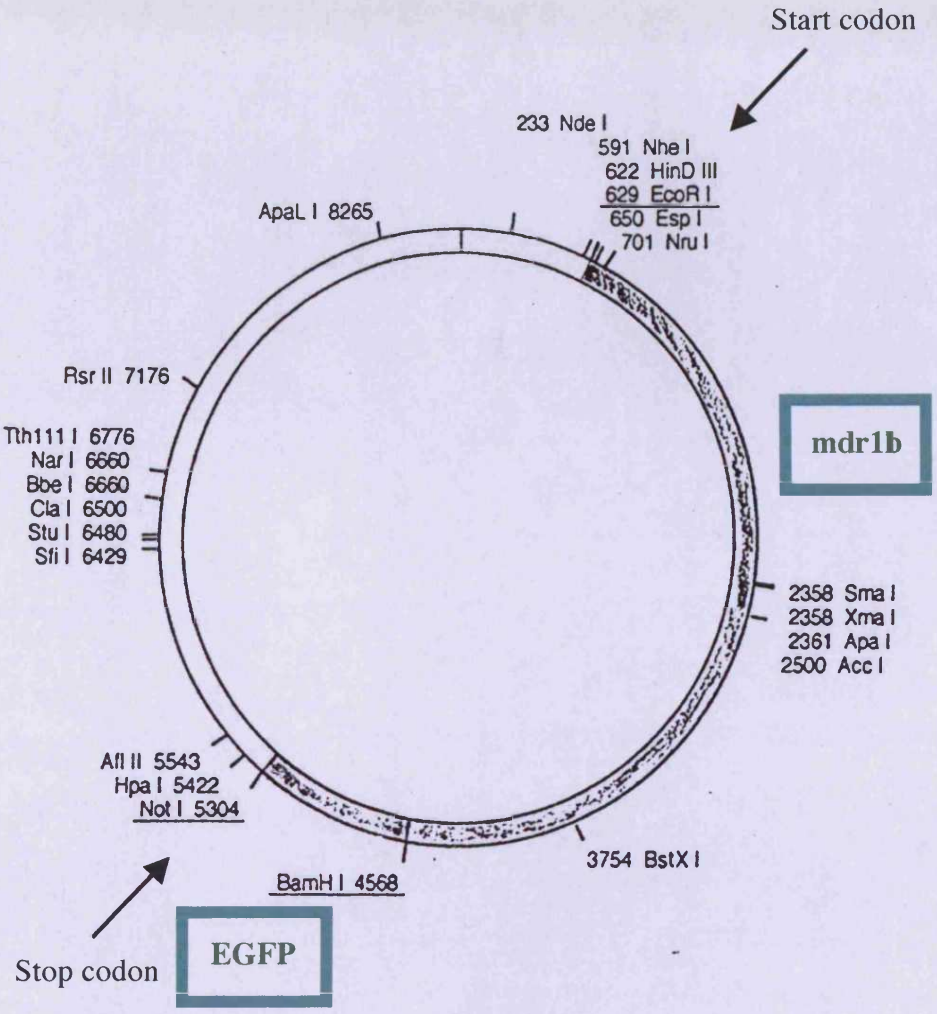

Figure 2.4. Plasmid map of the rat mdr1b-enhanced green fluorescence protein vector.

set. Aliquots of 5, 10, 50 and 100 µl of transformed cells were added to the plates, which were incubated overnight at 37 °C to allow for growth of bacterial colonies. Transformed cells, resistant to kanamycin were then utilised as follows.

A single colony was lifted from the plate using a sterile pipette tip and placed into a sterile 25 ml universal container containing 10 ml of LB broth supplemented with 50 µg/ml kanamycin. The bacteria were cultured at 37 °C in an orbital shaker at 200 rpm for 7 h. This culture was then used to inoculate a large 5 L flask containing 250 ml of sterile LB broth containing 50 µg/ml kanamycin. The flask was then incubated overnight at 37 °C in an orbital shaker at 200 rpm.

2.3.10.2 Isolation of the Plasmid

The plasmid was then extracted using a Maxiprep® kit according to the manufacturers instructions. A maxiprep column was initially equilibrated with 30 ml of equilibration buffer (E4) that was drained by gravity flow. The overnight culture was then pelleted at 6000 g for 15 min at 4 °C then the LB broth discarded and 10 ml of cell suspension buffer (E1) containing RNase A was used to resuspend the bacteria. Next, 10 ml of a cell lysis solution (E2) was added to the cell suspension then mixed gently by inverting the capped tube. The mixture was incubated at room temperature for 5 min. The lysis solution was neutralised by the addition of 10 ml neutralisation buffer (E3) and subsequent mixing by gentle inversion five times. The mixture was then centrifuged at 15000 g at room temperature for 10 min. The supernatant was loaded onto the equilibrated column and left to drain by gravity flow. The column was washed with 60 ml of wash buffer (E5), which was also drained by gravity flow. The flow-through was discarded. A 50 ml centrifuge tube was placed under the column and the DNA was eluted by adding 15 ml of elution buffer (E6). To the eluate, 10.5 ml of isopropanol was added, mixed and the mixture centrifuged at 15000 g for 30 min at 4 °C. The supernatant was then discarded and the DNA pellet washed with 5 ml of 70 % ethanol, followed by another centrifugation at 15000 g for 5 min at 4 °C. The supernatant was removed and the DNA pellet was air dried for 10 min. The final DNA pellet was finally resuspended in 500 µl of Tris-EDTA buffer (10 mM Tris pH8.0 and 1 mM EDTA).

The concentration of the purified plasmid DNA was assessed by measuring its optical density at 260 nm in a UV-visible spectrophotometer. The concentration was calculated as follows:

DNA concentration (μg/ml) = Absorbance x 50 x 50

2.3.10.3 Characterisation of the Plasmid

In order to ensure that the plasmid that has been isolated is intact and is the same plasmid that was initially used to transform the *E. coli* DH5α, it was essential to perform restriction digests. For this, specific restriction enzymes are used to cleave double stranded DNA at unique base pair sequences. The size of the fragments are then compared with a DNA ladder.

The plasmid was digested using a series of single and double digests using NotI, EcoRI and BamHI. To 1 μg of DNA, either 1 μl (for single digests) or 0.5 μl (for double digests) of restriction enzymes were added. Then 2 μl each of the appropriate reaction buffers and BSA was added from a 10x stock. The samples were made up to the same volume with water, gently mixed by pipetting and then incubated for 1 h at 37 °C. Following the reaction, gel buffer was added from a 10x stock (20 % Ficoll 400, 0.1 M Na_2EDTA pH8.0, 1 % SDS and 0.25 % bromophenol blue).

The samples were then subjected to agarose gel electrophoresis using a 0.6 % gel. Into 150 ml of TBE buffer (made up from 10x stock), 0.6 % of agarose was added and then heated in a microwave until the agarose fully dissolved. When the agarose solution cooled down to approximately 50 °C, 5 μl of ethidium bromide was added, the mixture was swirled and then poured into the cast. The comb was inserted into the gel immediately and the gel was left to set for 45 min. The gel was then placed into a tank filled with 1x TBE buffer. The samples were loaded into the wells with the outer wells containing 25 μl of 1kbase DNA ladder. The gel was run at 110 V until the samples reached the middle of the gel. The gel was then imaged and photographed on a polaroid gel documenting system.

2.3.11 Transfection of KG1a, K562 and Hela Cells

The purified rat mdr1b-EGFP plasmid was used to transfect KG1a, K562 and Hela cells. Owing to the refractory nature of these cells to transfection, several methods were tested and these are described below.

2.3.11.1 Lipofectamine ™ 2000-Mediated Transfection

A protocol was adapted from the manufacturers instructions. KG1a and K562 cells were seeded at 1 x 10^6/ml in serum supplemented media (without antibiotics) and 0.5 ml was transferred to a well in a 24 well plate. Various amounts of DNA (0.5-2.5 μg) were then diluted in 50 μl of serum free media. For each well, 2 μl of lipofectamine reagent was incubated with 50 μl of serum free media at room temperature for 5 min. DNA and Lipofectamine were then combined and incubated for 20 min at room temperature. The mixture was then added dropwise into the well and mixed by gently rocking the plate. The cells were placed in the tissue culture incubator for 6 h after which the cells were spun down and resuspended in fresh media. This was followed by a 36 h incubation under standard tissue culture conditions and subsequent analysis by epifluorescence microscopy.

2.3.11.2 Fugene 6™-Mediated Transfection

A protocol was adapted from the manufacturers instructions. KG1a and K562 cells were seeded at 3 x 10^5 cells in 1 ml serum supplemented media in a 12 well plate and grown overnight. In an eppendorf, 1 μg DNA and 3 μl of Fugene 6 reagent were added to 100 μl of serum free media and after gentle mixing, were incubated for 45 min at room temperature. The mixture was then added dropwise to the cells and the plate was gently swirled to evenly distribute the DNA. The cells were reincubated for 36 h in the continued presence of the DNA and then analysed by epifluorescence microscopy.

Hela cells were seeded at 1.5 x 10^5/2 ml of serum supplemented DMEM media into a 6 well plate and grown overnight. In an eppendorf, 1 μg DNA and 3.3 μl of Fugene 6 reagent were added to 105 μl of serum free media and after gentle mixing were incubated for 30 min at room temperature. The mixture was then

added dropwise to 2 ml of serum supplemented media in the wells and the plate was gently swirled. The cells were reincubated for 24 h in the continued presence of the DNA and then analysed under an epifluorescent microscope.

2.3.11.3 Electroporation

A protocol for electroporation was adapted from a protocol utilised in a T-cell line, Jurkat (Mehl et al., 2001). Cells were seeded at 1 x 10^7/0.5 ml of serum supplemented media. In an electroporator cuvette, 5 μg of DNA was added followed by the cell suspension. The solutions were mixed three times using a sterile glass pasteur pipette and subjected to electroporation. Cells were subsequently electroporated at 290 V and 950 μF. The cells were reincubated in a cell culture incubator for 6 h after which the cells were centrifuged at 1000 g for 1 min and resuspended in fresh media. This was followed by a 36 h incubation under cell culture conditions and subsequent analysis by epifluorescence microscopy.

2.3.12 Flow Cytometry

Flow cytometry allows simultaneous measurements of multiple parameters in individual cells moving through a fluid stream (reviewed in Steen, 1992). The largest population of cells exhibiting maximal fluorophore uptake were assumed to have typical morphology and were subsequently gated for analysis. In the current study, flow cytometry was used to quantitatively assess the uptake of fluorescently conjugated Tat and R_8 peptides at different temperatures and in the absence and presence of a number of pharmacological agents that have previously been shown to affect endocytic pathways.

2.3.12.1 Uptake of Alexa-488 Conjugated Tat and R_8

Temperature dependent uptake of 1 μM alexa-488 R_8 or 3 μM alexa-488 Tat at 4 °C or 37 °C was carried out over a period of 2 h. These cationic peptides exhibit a high amount of cell surface binding which has been shown to lead to overestimations of peptide uptake (Richard et al., 2003). Therefore, following each incubation with peptide, the cells were washed three times in PBS, incubated for 5 min at 37 °C in 0.25 % trypsin and subjected to three washes with 14 μg/ml heparin at room temperature and a further two washes in PBS. The trypsin digests

cell surface bound peptide whilst the heparin binds to the digested peptide, preventing its re-association with the cell membrane, thereby ensuring that only true uptake is quantified irrespective of surface binding. Cells were finally resuspended in 200 µl of ice cold PBS and transferred into a falcon tube for subsequent flow cytometry.

To assess the effects of endocytosis inhibitors on peptide uptake in K562 cells, 5 x 10^5 cells were pretreated with the drug for 15 min at 37 °C, followed by a 60 min incubation with either 1 µM alexa-488 R_8 or 3 µM alexa-488 Tat in the continued presence of the drug. Control cells were incubated with the respective diluent. Cells were washed and processed as described above and analysed by flow cytometry.

Peptide uptake was analysed in the FL-1 channel using the following settings:

	Voltage	Amp Gain	Mode
FSC	E-1	5.00	linear
SSC	310	2.00	linear
FL-1	370		log

2.3.13 Data Analysis

For flow cytometry experiments, cell-associated fluorescence was acquired using log amplification and expressed as the geometric mean of all the population minus the geometric mean of the autofluorescence of untreated cells. Statistical significance was calculated using a one-way analysis of variance (ANOVA) followed by Dunnetts post-hoc test. The standard deviation (SD) of the data points was calculated and the number (n) of experiments are as indicated for each experiment.

Chapter 3:

Subcellular Localisation and Biochemical Analysis of P-glycoprotein in KG1a Cells

3.1 Introduction

Since P-gp was originally described and characterised as a drug transporter in 1976 (Juliano & Ling, 1976), its structure and function have been extensively studied and has already been described in section 1.4.1. and 1.4.2. In complete contrast, its intracellular trafficking and distribution have received comparatively little attention. Progress in this field has been hampered by the lack of specific tools such as good antibodies against P-gp, which were, before the onset of green fluorescent protein (GFP) technology, essential for studying protein trafficking and distribution. Although several antibodies are commercially available for the immunodetection of P-gp, use of these antibodies for conclusive data is hampered by the problem of cross-reactivity. Figure 3.1 illustrates commonly used anti-P-gp antibodies and their respective binding sites.

The most widely used antibody for the immunodetection of P-gp is the monoclonal C219 variant, recognising the peptide sequence VVQEALDKAREGRT, derived from the nucleotide binding domain of P-gp (van den Elsen et al., 1999). However, it reacts with all isoforms of P-gp including MDR3 and sister of P-gp (Georges et al., 1990). It also exhibits an extensive cross-reactivity profile, with several cross-reactants having a molecular weight close to that of P-gp. It cross-reacts with c-erbB2 (180-185 kDa; Liu et al., 1997) and a 200 kDa protein identified as the heavy chain of myosin (Thiebaut et al., 1989). It also cross-reacts with an unknown protein of 190 kDa that is found in rat, mouse and bovine brain capillaries (Beaulieu et al., 1995; Jette et al., 1995b). Perhaps a more worrying revelation is its cross-reactivity with a protein of 170 kDa, which mediates resistance to methotrexate, in the absence of P-gp expression (Norris et al., 1989). It inhibits P-gp function by inhibiting both its ATPase activity and drug binding to its membrane spanning domains (Georges et al., 1991; Kokubu et al., 1997). Another commonly used antibody, JSB-1, recognises an intramembrane epitope close to the carboxy-terminus on the cytoplasmic surface of P-gp (Scheper et al., 1988) and this antibody has been shown to be specific to MDR1 (Schinkel et al., 1991). It does however cross-react with pyruvate carboxylase (130 kDa), an

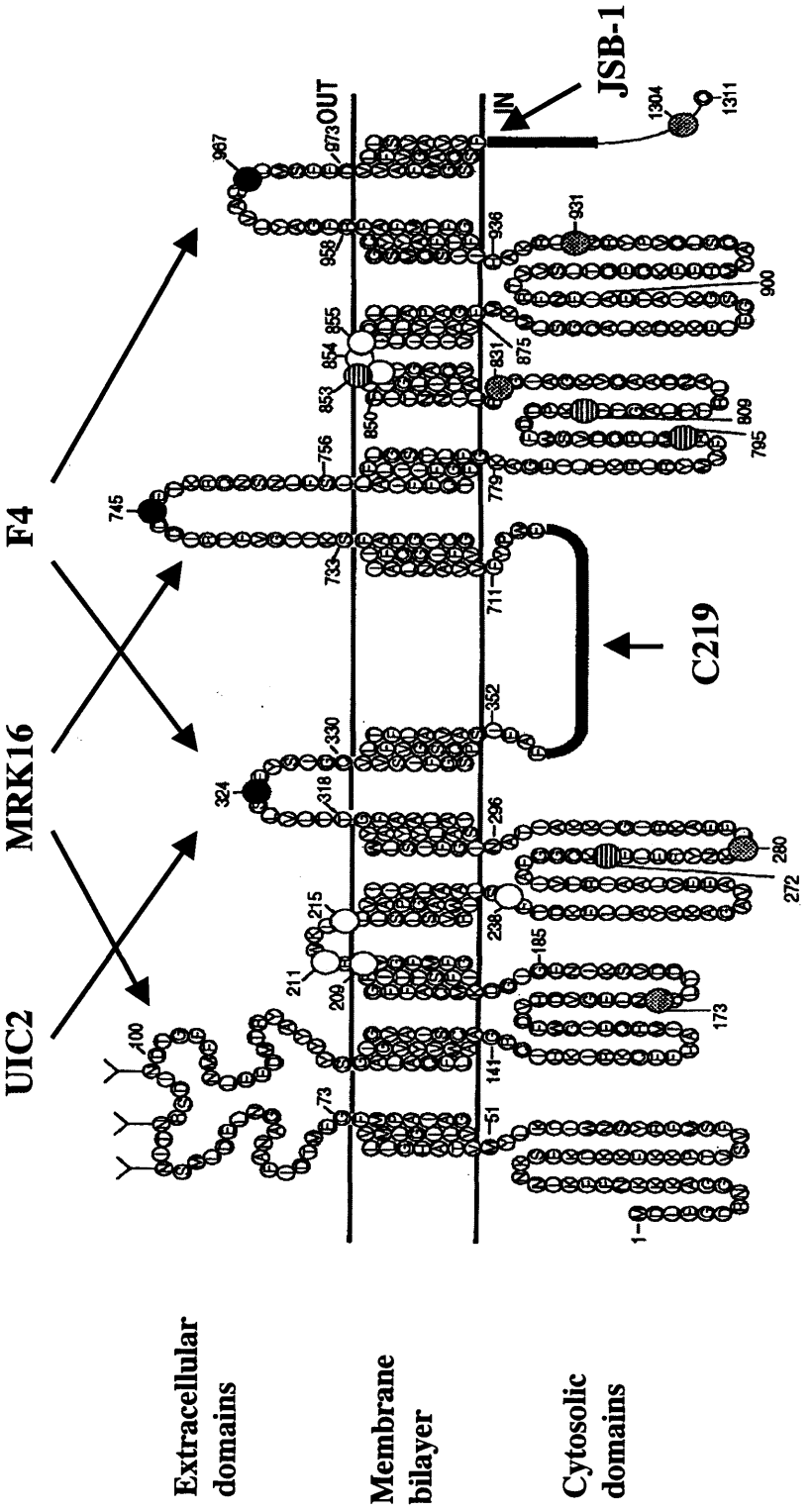

Figure 3.1. Schematic representation of the membrane topology of P-glycoprotein (Loo and Clarke, 1995), showing the antibody recognition sites.

abundant mitochondrial enzyme (Rao et al., 1995). A more recent antibody designated F4 recognises an external epitope localised in or near the third and/or sixth extracellular loops, specifically on human MDR1 (Chu et al., 1993). There are as yet no reported cross reactants for this antibody, giving it a clear advantage over the other antibodies. Other commercial antibodies include UIC2 and MRK16, which recognise external epitopes on P-gp (Hamada & Tsuruo, 1986; Mechetner & Roninson, 1992). MRK16 binds to P-gp via its first and fourth extracellular loops (Georges et al., 1993) whilst UIC2 recognises the third extracellular loop (Zhuo et al., 1999). Both have the capacity to inhibit P-gp mediated efflux (Mechetner & Roninson, 1992; Mikisch et al., 1992). Prior to the analysis of P-gp in KG1a cells, it was essential to characterise the specificity and suitability of these antibodies.

Information regarding the trafficking pathway of P-gp may be gained from the presence of targeting moieties that navigate the associated protein from the plasma membrane. Ubiquitination involves the covalent attachment of one (monoubiquitination) or multiple (polyubiquitination) ubiquitin moieties to the side chain of lysine residues on proteins. First, ubiquitin becomes activated by the formation of a high-energy thioester bond with a ubiquitin activating enzyme. Ubiquitin is then transferred to a ubiquitin conjugating enzyme, followed by conjugation to the substrate protein, which often requires a third enzyme, a ubiquitin protein ligase (described in Pickart, 2001). Ubiquitination is thought to regulate a variety of cellular processes including cell cycle control, DNA repair, antigen presentation, and the regulation of signal transduction pathways and transcription (reviewed in Hershko & Ciechanover, 1998) but is thought to function primarily as a signal for degradation in the proteasome or lysosome following endocytosis. Protein such as the epidermal growth factor receptor are ubiquitinated then directed into the internal membranes of LE/multivesicular bodies (Longva et al., 2002). Their fate is then determined and they are trafficked into the lysosome. As well as the well characterised function of ubiquitination in degradation, it is now known that it also functions simply as an internalisation signal (Shih et al., 2000).

Polyubiquitination of P-gp has been reported and this modification was

thought to regulate P-gp degradation in MDR K562 cells (Ohkawa et al., 1999). Another study in MDR MCF-7 breast cancer cells demonstrated that P-gp function and stability is regulated by constitutive ubiquitination (Zhang et al., 2004). In both studies, P-gp degradation was deemed to occur in the proteasome. The proteasome is a large multi-subunit protein complex comprising of a proteolytic active core complex consisting of a cylindrical stack of four heptamer rings which harbour the catalytic sites (reviewed in Voges et al., 1999). The pores at either end are gated by a regulatory complex attached to the cylinder (Groll et al., 2000). Both studies concluded that regulation of P-gp turnover would also provide a novel target for circumvention of P-gp mediated resistance. As well as containing ubiquitination sites, P-gp also contains a di-leucine motif, another endocytosis and degradation domain. However, this has only been implicated in the correct folding of P-gp (Loo et al., 2005) and the role of this motif in targeting P-gp for degradation is yet to be investigated. Experiments were conducted in this study to determine whether P-gp is ubiquitinated in KG1a cells.

Clues to the trafficking pathways utilised by P-gp can also be obtained from studies of the trafficking of the closely related ABC transporter, the cystic fibrosis transmembrane conductance regulator (CFTR). CFTR functions as a chloride channel at the apical surface of many epithelial cells (Denning et al., 1992) and its biosynthetic processing and intracellular trafficking has been extensively studied. This is due to the fact that a mutation in the CFTR gene results in a misfolded protein that fails to traffic to the plasma membrane and marks the onset of cystic fibrosis (Gelman & Kopito, 2002). CFTR has been shown to be constitutively internalised by clathrin-mediated endocytosis (Lukacs et al., 1997; Bradbury et al., 1999) via recognition of coat proteins by its tyrosine and di-leucine motifs; both of these are required for its internalisation (Prince et al., 1999; Hu et al., 2001). Once internalised CFTR is thought to recycle back to the cell surface either directly via the transferrin route or possibly even through the Golgi (Gentzsch et al., 2004). A large fraction of CFTR also exists within a subapical pool, from where it is translocated to the cell surface on demand (Moyer et al., 1998). Polyubiquitinated CFTR has also been characterised and this modification contributes to its

proteasomal degradation of both mature and mutated CFTR (Ward et al., 1995). Ubiquitination of CFTR was however shown to be co-translational rather than a post-translational modification.

Compared with CFTR, few studies have investigated the intracellular trafficking of P-gp from the perspective of its trafficking route(s) from the plasma membrane. Kim and co-workers utilised a human intestinal carcinoma cell line, LS174T, treated with step-wise increases in bisantrene (an anthracene derivative) over a 12-16 week period, to induce overexpression of P-gp (Kim et al., 1997). They made several observations regarding the localisation and endocytosis of P-gp; (i) 70 % of P-gp was located on the cell surface, (ii) cell surface P-gp undergoes constitutive endocytosis through a clathrin dependent pathway, and recycles to the plasma membrane through a Rab5 positive endosomal compartment. Of particular interest was the observation that the pharmacological redistribution of P-gp from the cell surface, into intracellular compartments, restored the drug sensitivity of the cell to DNR. Fu and co-workers studied P-gp trafficking in HeLa cells transfected with MDR1-EGFP and demonstrated that the protein was progressively transported from the endoplasmic reticulum to the Golgi and finally to the plasma membrane over a period of 24 h (Fu et al., 2004). Little or no intracellular accumulation of DNR was seen when P-gp-EGFP was allowed to traffic to the plasma membrane, but they showed that retention of P-gp intracellularly by inhibiting intracellular trafficking with the Golgi disrupting agent, brefeldin A and the proton ionophore, monensin, resulted in an increase in DNR accumulation. Loo and Clarke reported that preventing P-gp from reaching the cell surface following its synthesis may be used to reverse MDR. P-gp is first synthesised as a 140-150 kDa precursor in the endoplasmic reticulum, which is then converted to the mature 170 kDa P-gp, that is then trafficked to the cell surface. Their approach was to inhibit P-gp maturation and trafficking to the cell surface after its synthesis in the endoplasmic reticulum using the proteasome inhibitor MG-132 resulting in accumulation of non-functional P-gp (Loo & Clarke, 1999). This modification of P-gp traffic could sensitise resistant cells and prove to be an alternative pharmacological route to current anti-P-gp strategies.

Of note is the fact that the above studies have utilised a P-gp overexpressing system, either via transfection (Loo & Clarke, 1999; Fu et al., 2004; Loo et al., 2005) or by challenging cells over long periods with a cytotoxic drug (Kim et al., 1997; Ohkawa et al., 1999; Zhang et al., 2004). However the KG1a cell line naturally expresses high levels of P-gp although the majority of the protein lies intracellularly. This provides an excellent model to study whether this pool contributes to its status as a naturally resistant cell line. Additionally the trafficking of P-gp in this cell line may be unique such that the endocytic and or secretory pathways maintain a high level of intracellular P-gp. It is of significant interest to cell biology and drug delivery as to how the cell achieves this and for these reasons and the aforementioned, P-gp was studied in this cell line. The aim of this study was to characterise the cellular distribution and trafficking of P-gp in KG1a cells.

3.2 Methods

A protocol for detecting P-gp following electrophoresis and Western blotting was initially characterised by optimising the electrophoretic transfer of high molecular weight proteins. Different transfer buffers were tested for their ability to transfer proteins onto nitrocellulose and the composition of the three tested buffers are as follows; (1) 16.9 g glycine, 3.65 g Tris and 300 ml methanol made up to 1.5 L with dH_2O, (2) 28.5 g glycine, 6.05 g Tris, 1 g SDS and 100 ml methanol made up to 1 L with dH_2O, (3) 28.5 g glycine, 6.05 g Tris, 0.25 g SDS and 100 ml methanol made up to 1 L with dH_2O. Following electrophoretic transfer, polyacrylamide gels were stained with Coomassie Brilliant blue and the nitrocellulose sheet was stained with Ponceau S as described in sections 2.3.6 and 2.3.7. The optimal transfer buffer was used for all subsequent blots.

To detect the presence of P-gp in KG1a cells a cell lysate and membrane preparation was isolated as described in sections 2.3.3.1 and 2.3.3.2 respectively. Then 80 and 25 μg of cell lysate and 300 μg of membrane preparation were subjected to SDS-PAGE as described in section 2.3.5, followed by Western blotting using C219, JSB-1 and F4 antibodies respectively as described in section

2.3.6. The expression of caveolin-1, a caveolae associated protein, in these cells was also assessed by subjecting 25 μg of membrane preparation to Western blotting with an anti-caveolin-1 antibody.

Methods for P-gp immunoprecipitation from KG1a cell extracts were extensively characterised. The immunoprecipitation procedure was previously detailed in section 2.3.5. In order to increase the specificity of the method, two different anti-P-gp antibodies were used, one to immunoprecipitate and another for immunodetection and as the antibodies do not share common cross-reactants or epitopes, there is a greater chance that only one common protein will be recognised. Several combinations of C219, JSB-1 and F4 were tested and the final optimal conditions were determined to be F4 for the immunoprecipitation and C219 for immunodetection and these were used for all subsequent immunoprecipitations. The protocol was further optimised by varying the amount of antibody used to precipitate P-gp. Five consecutive immunoprecipitations of a KG1a cell lysate were carried out using 0.5, 1, 3, 5 and 10 μl of F4 incubated with the protein G-agarose beads. The optimal amount of antibody was determined and used for all subsequent immunoprecipitations. During immunoprecipitation, a clearing procedure was included for the removal of any cell material with a natural affinity for protein G-coated beads. To assess whether P-gp was lost during this procedure, immunoprecipitation of a membrane preparation was carried out as described in 2.3.5 and following the clearing procedure, the beads were isolated and proteins were dissociated from the beads as described. The level of P-gp immunoprecipitated from different cell extracts was also investigated following isolation of a cell lysate, whole cell lysate and membrane fraction as described in sections 2.3.3.1 and 2.3.3.2.

The membrane localisation of P-gp was investigated by determining whether P-gp was localised to detergent soluble or insoluble regions of the membrane. A method by Brown and Rose (Brown & Rose, 1992) was adopted to isolate detergent soluble and insoluble fractions from KG1a cells (described in section 2.3.3.3). Both fractions were subjected to immunoprecipitation.

To determine the ubiquitin status of P-gp, a membrane fraction was isolated and subjected to P-gp immunoprecipitation and Western blotting with either C219 or an anti-ubiquitin antibody. A control experiment was also carried out as described in section 2.3.5. To assess the effects of K^+ depletion and cellular cytosol acidification using ammonium chloride on the ubiquitin status of P-gp, cells were treated as described in section 2.3.2.1 and 2.3.2.2 respectively.

The cellular distribution of P-gp in KG1a cells was analysed by indirect immunofluorescence microscopy using a protocol that had been extensively developed during this project. F4 antibody was used to immunolabel P-gp as described in section 2.3.9.1, utilising acetone post-fixation and permeabilisation. Control experiments were performed by incubation with fluorescently conjugated secondary antibody alone. Wortmannin, a fungal metabolite isolated from *Penicillium funiculosum*, is a potent inhibitor of phosphatidylinositol-3-kinases (reviewed in Ui et al., 1995) which are key enzymes implicated in regulating signal transduction and membrane trafficking (Shpetner et al., 1996) and was used to characterise P-gp expression and distribution. A working concentration of 150 nM was determined by testing the effect of wortmannin on EEA-1 and Tf distribution. This was done by pretreating cells for 1 h with 150 nM wortmannin or its diluent (DMSO), followed by fixation and immunolabelling for EEA-1 as described in section 2.3.9.1, using Triton X-100 permeabilisation. To test the effect of wortmannin on Tf, TxR-Tf was internalised into KG1a cells as described in section 2.3.9.2.1, washed and incubated for a further 1 h in the presence of 150 nM wortmannin. Cells were then washed three times in PBS and visualised immediately under the microscope. The effect of wortmannin on P-gp distribution was assessed as described for EEA-1.

3.3 Results

3.3.1. Optimisation of the electrophoretic transfer of proteins for western blotting

Initial experiments involved the optimisation of a protocol for Western blotting and focused on the efficiency of electrophoretic transfer of proteins from gel to nitrocellulose. Three different transfer buffers of differing compositions

were tested and gel staining with Coomassie Brilliant blue solution was used to assess the transfer efficiency of high molecular weight markers. Transfer using buffer 1 was unable to mediate transfer of higher molecular weight proteins of 116-200 kDa, although there appeared to be complete transfer of the lower molecular weight proteins (Figure 3.2A). P-gp, with a molecular weight of 170-180 kDa, would not be transferred under these conditions. Therefore, 1 % SDS was added in buffer 2 and transfer was greatly enhanced as complete transfer of proteins had occured (Figure 3.2B). However Ponceau S staining of the nitrocellulose revealed that proteins had passed through the nitrocellulose membrane and could not be detected. Therefore, SDS levels were decreased to 0.25 % and it was shown that there was again efficient transfer of all proteins from the gel (Figure 3.2C) but when the nitrocellulose was stained, all proteins were still present on the membrane.

3.3.2 Detection of P-glycoprotein in KG1a cells and characterisation of anti-P-glycoprotein antibodies

Integral to all the techniques used, was the immunodetection of P-gp using commercial antibodies. However, as described above, these display extensive cross-reactivity profiles. Therefore characterisation of these antibodies via Western blotting was first carried out. Cell lysates and membrane preparations were prepared from KG1a cells and subjected to western blotting using C219 and JSB-1 (cell lysate) or F4 (membrane preparation). Blotting with C219 reveals a band at 170 kDa, the predicted molecular weight for P-gp and also a broad band at approximately 200 kDa (Figure 3.3A). Blotting with JSB-1 displayed several bands (Figure 3.3B) with approximate weights of 200, 170, 140 and 120 kDa. The 170 kDa band most likely corresponds to P-gp. Blotting with the F4 antibody produced a single band at approximately 170 kDa. No cross-reacting proteins were observed with this antibody despite loading 300 μg of protein (Figure 3.3C).

3.3.3 Optimisation of P-glycoprotein immunoprecipitation

Immunoprecipitation was utilised as a method for the purification and more

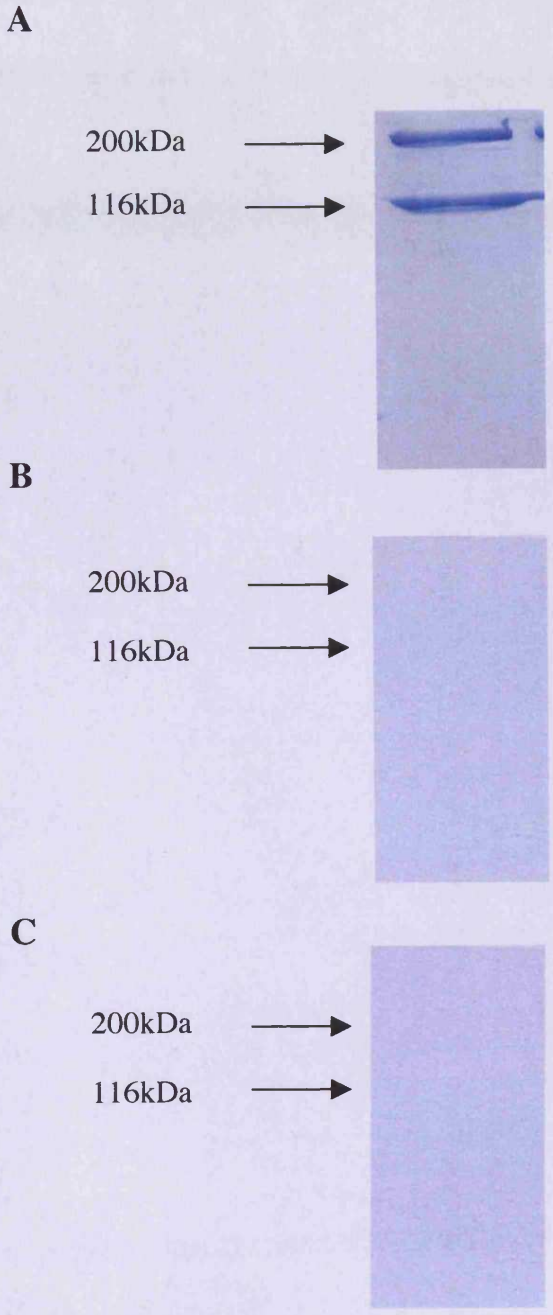

Figure 3.2. Optimisation of electrophoretic protein transfer. Broad range molecular weight markers were subjected to SDS-PAGE then electrophoretic transfer using three different transfer buffers (A, B and C). The gels were then stained with Coomassie Brilliant blue to assess the transfer efficiency. Protein standards are indicated on the left hand side.

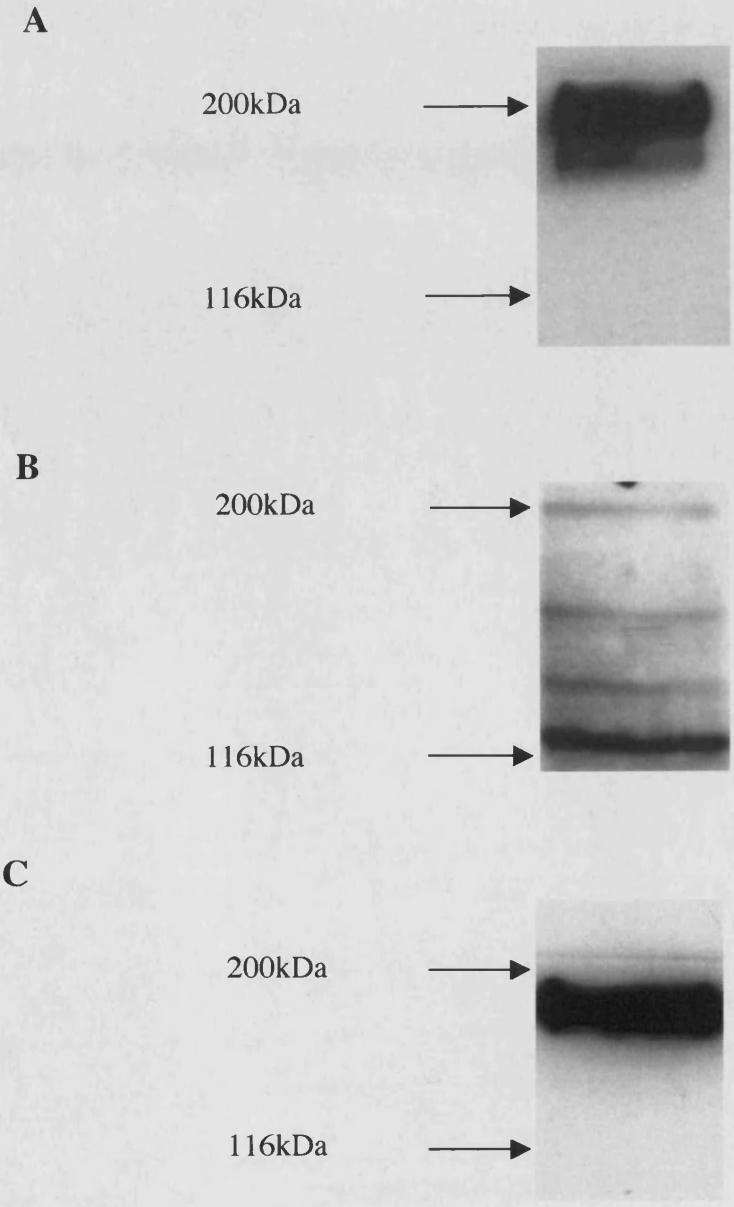

Figure 3.3. Characterisation of P-gp antibodies. Cell lysates (A and B) and a membrane preparation were prepared from KG1a cells and subjected to immunoblotting with (A) C219 (80 μg), (B) JSB-1 (25 μg) and (C) F4 (300 μg).

selective detection of P-gp from a variety of cell extracts and a protocol for P-gp immunoprecipitation was optimised in KG1a cells. A combination of different anti-P-gp antibodies were assessed and use of F4 for immunoprecipitation and C219 for immunodetection was initially found to be optimal for P-gp immunoprecipitation and was used for all subsequent immunoprecipitations. To find the optimum amount of antibody required to immunoprecipitate P-gp, five consecutive immunoprecipitations of a cell lysate were carried out after 0.5, 1, 3, 5 or 10 µl of F4 antibody was incubated with a fixed volume of beads. The results, shown in Figure 3.4, demonstrate that immunoprecipitation with 0.5 µl of F4 failed to isolate detectable levels of P-gp (lane 1). The use of 1, 3 and 5 µl of antibody resulted in a gradual increase in the intensity of the P-gp band (lanes 2-4 respectively). However, 10 µl of F4 failed to isolate any detectable levels of P-gp (lane 5). Two weak bands were consistently observed at approximately 120 and 140 kDa. Based on these results, 5 µl of F4 was used for subsequent immunoprecipitations. To investigate the possibility that P-gp is lost during the clearing procedure, immunoprecipitation was performed on a membrane fraction and the protein G-agarose beads were isolated following clearing and the proteins were isolated and subjected to Western blotting and immunodetection with C219. The results are shown in Figure 3.5. Blotting a membrane preparation prior to clearing revealed two bands at approximately 170 and 200 kDa, in addition to the lower molecular weight bands at 120, 140, 150 and 160 kDa. After clearing, it is apparent that all the protein bands detected in the membrane fraction, including P-gp, have the capacity to bind to the beads (lane 2). However, following immunoprecipitation there was an enrichment of only the two bands at 170 and 200 kDa which increase as the amount of immunoprecipitated sample loaded onto the gel is increased from 5 (lane 3) to 20 (lane 4) then 50 µl (lane 5). Two faint bands at 120 and 140 kDa were also observed with increasing intensity as the loading volume was increased.

3.3.4 Detection of P-glycoprotein in membrane fractions

Cell proteins are often compartmentalised into distinct plasma membrane

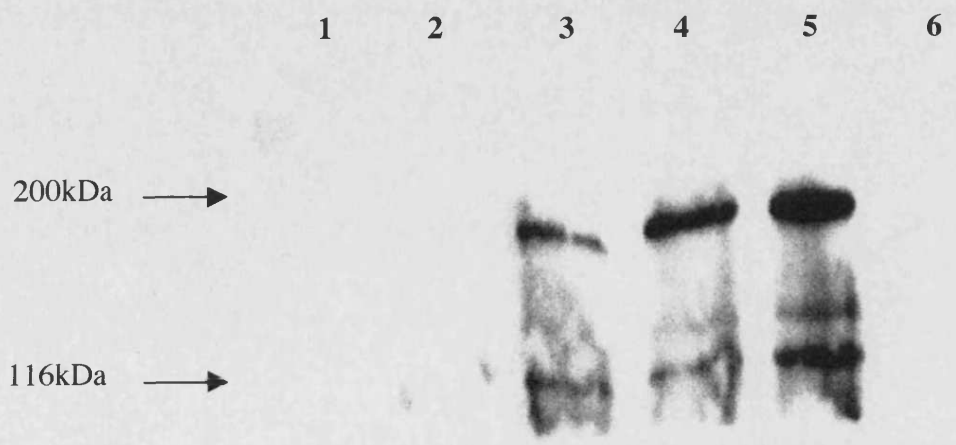

Figure 3.4. Optimisation of P-gp immunoprecipitation. A cell lysate was isolated from KG1a cells and subjected to immunoprecipitation using varying quantities of F4 antibody to precipitate P-gp. The gel was loaded with either 30 μg of lysate (lane 1) or imunoprecipitates obtained using 0.5, 1, 3, 5 and 10 μl of F4 antibody incubated with protein-G agarose beads (lanes 2-6 respectively). P-gp was then probed with the C219 antibody.

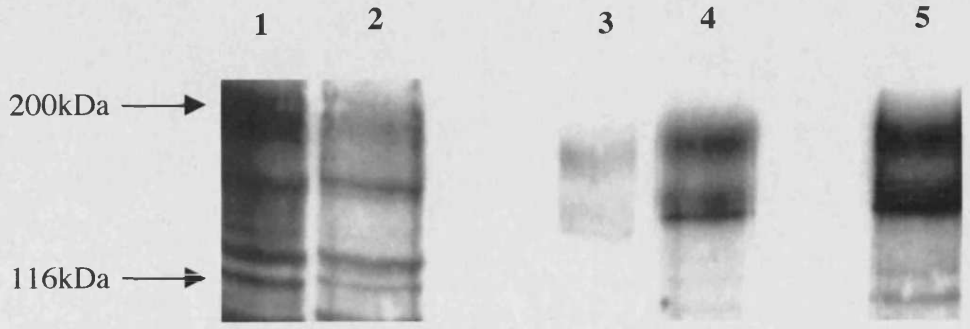

Figure 3.5. P-gp detection during immunoprecipitation. KG1a membrane preparation was isolated and 80 μg was loaded onto the gel (lane 1). Then 1 mg was subjected to immunoprecipitation. Following the preclearing, proteins were dissociated from the beads (lane 2) and after immunoprecipitation 5, 20 and 50 μl of the immunoprecipitate was loaded onto the gel (lanes 3-5 respectively). The blot was probed with C219 antibody.

regions that can be defined as either detergent (or Triton X-100) soluble or insoluble. P-gp has been reported to reside within cholesterol rich detergent insoluble regions of the membrane such as lipid rafts and caveolae (Rothnie et al., 2001). These cholesterol rich domains are characterised as being Triton X-100 insoluble. Both detergent soluble and insoluble fractions were isolated and equal amounts subjected to immunoprecipitation using the optimised protocol. P-gp was found at approximately equal amounts in both detergent soluble and insoluble membrane domains (Figure 3.6A) and weak bands were again observed in both samples at 120 and 140 kDa. The detection of P-gp in a detergent insoluble membrane domain prompted further characterisation of this fraction. Caveolae are characterised as detergent insoluble membrane domains that have been shown to be associated with P-gp (Jodoin et al., 2003). To determine whether caveolae are present in KG1a cells, a membrane preparation was blotted for caveolin-1, a caveolae associated protein. Although a band is observed at 21 kDa, the predicted molecular weight for caveolin-1, several other bands of higher molecular weight were also observed (Figure 3.6B). This possibly suggests some degree of non-specific binding of the antibody. It is therefore difficult to draw conclusions from this experiment.

3.3.5 Immunoprecipitation of P-glycoprotein from various cell extracts

P-gp was also measured in cell lysates, whole cell lysates and membrane fractions. Immunoprecipitation from the cell lysate revealed bands at 170 (corresponding to P-gp), 120 and 140 kDa (Figure 3.7A). P-gp immunoprecipitation from a whole cell lysate displayed a more intense P-gp band at 170 kDa and also a band of equal intensity at 200 kDa (Figure 3.7B). When P-gp was precipitated from the membrane fraction, a similar result was seen to the whole cell lysate with apparently equal bands at 170 and 200 kDa, although these were of a slightly lower intensity (Figure 3.7C).

3.3.6 P-glycoprotein distribution in KG1a cells

The subcellular distribution of P-gp was then determined in KG1a cells

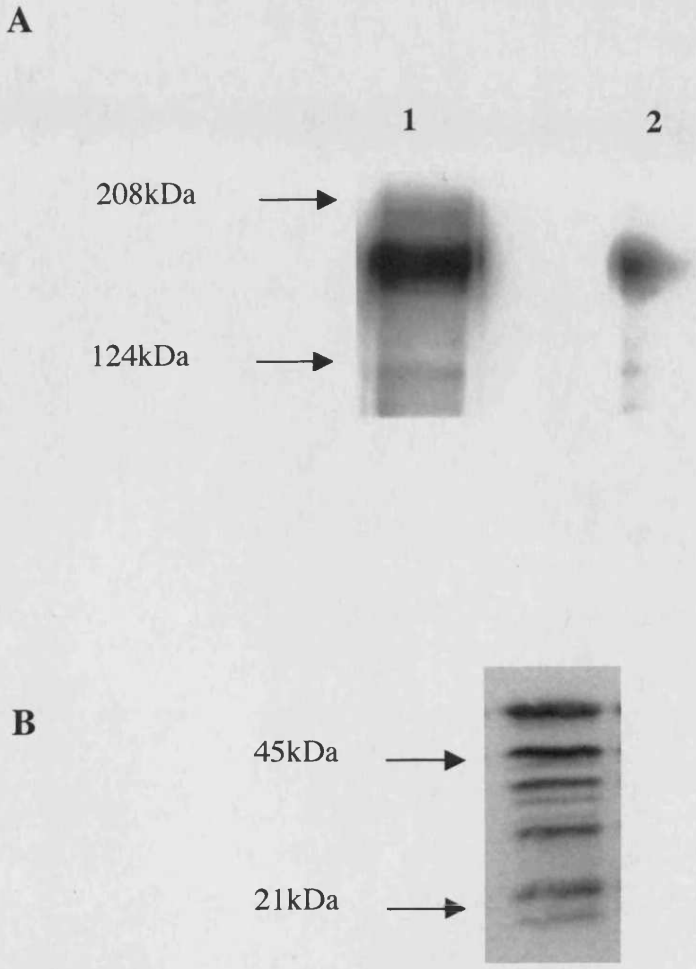

Figure 3.6. Localisation of P-gp in both detergent soluble and insoluble membrane domains. (A) P-gp was immunoprecipitated from a detergent soluble (lane 1) and insoluble (lane 2) fraction with the F4 antibody and subsequently probed with C219. (B) A membrane preparation (25 μg) was blotted with an anti-caveolin-1 antibody.

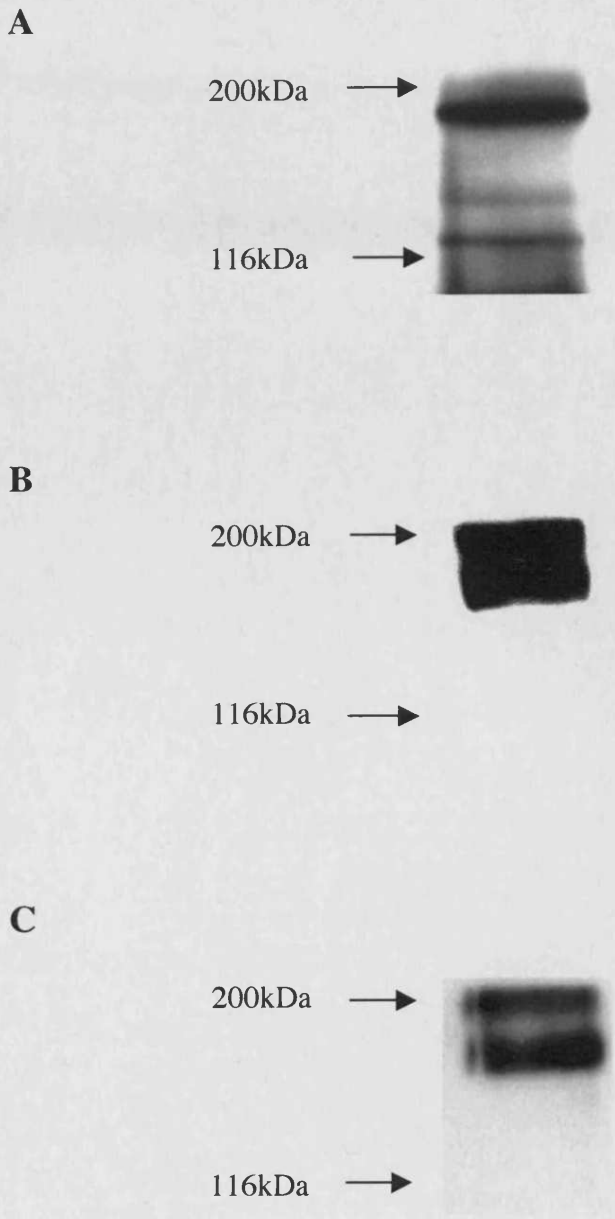

Figure 3.7. Immunoprecipitation of P-gp from a cell lysate, whole cell lysate and membrane fraction. (A) Cell lysate, (B) whole cell lysate and (C) membrane preparations were isolated and P-gp was immunoprecipitated from each fraction using F4 antibody and then immunodetected with C219.

using an optimised immunofluorescence protocol that was extensively characterised and developed during this study. Initial studies utilised an immunofluorescence protocol involving Triton X-100 permeabilisation of KG1a cells. However as no P-gp labelling was observed under these experimental conditions, acetone post-fixation and permeabilisation was adopted and proved optimal for P-gp labelling. Immunolabelling with the F4 anti-P-gp antibody revealed small vesicular structures distributed diffusely throughout the cell. Larger structures polarised to one side of the cell were also observed in a minority of cells (Figure 3.8). It was clear that there was very little plasma membrane labelling as the major signal was emanated from intracellular vesicles.

3.3.7 Effects of wortmannin on P-glycoprotein distribution in KG1a cells

To further characterise the nature and origin of the P-gp positive vesicles, the cells were treated with wortmannin. A working concentration for wortmannin was determined by testing the well known effects of wortmannin on EEA-1 labelling and endosome structure. KG1a cells were treated with wortmannin then subjected to immunolabelling with an anti-EEA-1 antibody using Triton X-100 permeabilisation. Fluorescence microscopy reveals that in the absence of wortmannin, EEA-1 labels vesicular structures located on the cell periphery (Figure 3.9A). However, this pattern of labelling was abolished by wortmannin treatment (Figure 3.9B). The loss of EEA-1 labelling in wortmannin treated cells is due to the dissociation of EEA-1, from EE membranes as a result of loss of activity of the phosphatidylinositol-3-kinase, hVP34 (Patki et al., 1997). Internalised TxR-Tf was also observed in vesicular structures, although these structures were comparatively smaller in size than EEA-1 positive structures (Figure 3.9C). Wortmannin treatment resulted in the appearance of swollen of TxR-Tf containing endocytic structures (Figure 3.9D). These structures are characteristic of wortmannin treated cells (Shpetner et al., 1996) and is thought to be due to a combination of increased internalisation and decreased recycling (Martys et al., 1996). The effect of wortmannin on P-gp distribution was then investigated and the effects on P-gp distribution were similar to those observed for Tf. The small

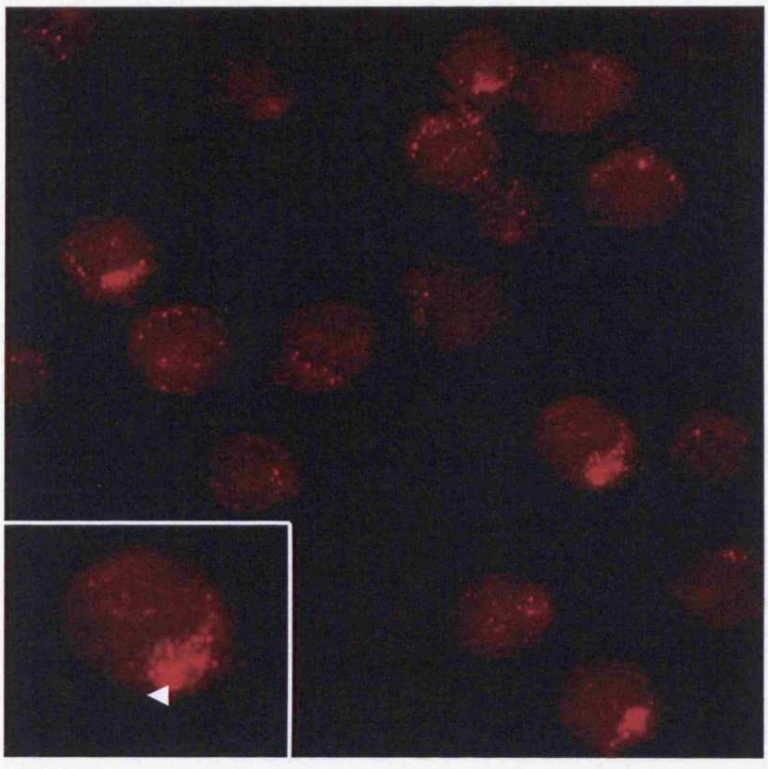

Figure 3.8. Cellular localisation of P-gp in KG1a cells. KG1a cells were fixed and immunolabelled for P-gp with F4 antibody. An enlarged cell is shown in the bottom left hand corner with an arrow showing the dense labelling of P-gp.

punctate vesicles seen in control cells (Figure 3.9E) were greatly enlarged in wortmannin treated cells (Figure 3.9F). This strongly suggests that the P-gp vesicles were of endosomal origin.

3.3.8 Assessment of the ubiquitination status of P-glycoprotein

Ubiquitination of P-gp has been reported by two independent groups (Zhang et al., 2004; Ohkawa et al., 1999). Identification of the ubiquitin status of P-gp in KG1a cells would give valuable clues as to the trafficking pathways and intracellular fate of P-gp. P-gp was immunoprecipitated from a membrane fraction and then either blotted with C219 (Figure 3.10A, lane1) or with an anti-ubiquitin antibody (Figure 3.10A, lane 2). P-gp was co-immunoprecipitated with ubiquitin as the 170 kDa P-gp band was also detected with the anti-ubiquitin antibody. The fact that the P-gp band and the ubiquitin band share the same molecular weight suggests that P-gp is not polyubiquitinated. The 200 kDa band was not detected with the ubiquitin antibody. A control experiment immunoprecipitation was carried out in the absence of F4 and blotted with the anti-ubiquitin antibody. Ubiquitin was detected in both the presence (Figure 3.10B, lane 1) and absence (Figure 3.10B, lane 2) of the F4 antibody. However, it is difficult to draw conclusive observations from this experiment alone.

3.3.9 Effects of clathrin-mediated endocytosis inhibitors on the ubiquitin status of P-glycoprotein

K^+ depletion of cells is regularly utilised to inhibit clathrin-mediated endocytosis (Larkin et al., 1983). It has also been reported that K^+ depletion inhibits the ubiquitination of the growth hormone receptor (van Kerkhof et al., 2001). To investigate whether this is also the case for P-gp, K^+ depleted cells were immunoprecipitated with F4 and blotted with an anti-ubiquitin antibody. The experiment was carried out twice and the results are shown in Figure 3.11. The first experiment reveals a clear inhibition of ubiquitination as indicated by the absence of the ubiquitin band in K^+ depleted samples (Figure 3.11A, lane 2) this band was however observed in control cells (Figure 3.11A, lane 1). Identical results were

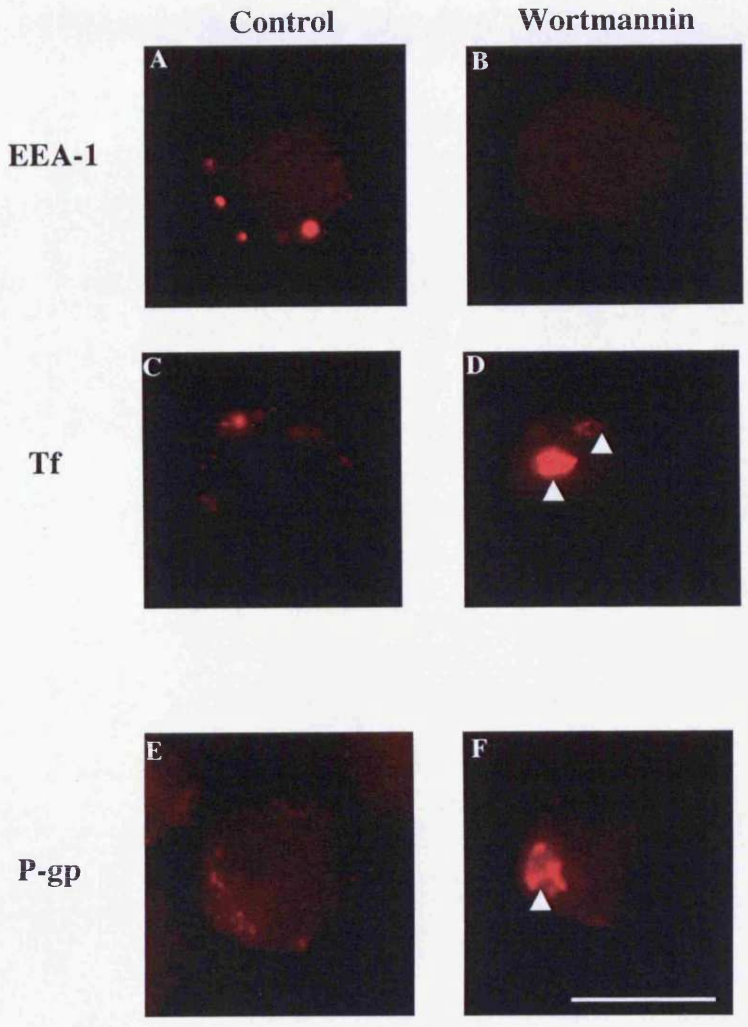

Figure 3.9. Effects of wortmannin on P-gp distribution in KG1a cells. The distribution of EEA-1 in the absence (A) or presence (B) of 150 nM wortmannin was determined by preincubating cells for 1 h with wortmannin prior to fixing and immunolabelling for EEA-1. The effect of wortmannin on Tf distribution was determined by internalising Tf for 1 h before incubating with either the diluent DMSO (C) or wortmannin (D). Cells were then treated with wortmannin as for EEA-1 with either DMSO (E) or wortmannin (F). Representative cells are shown in each case. Arrowheads indicate wortmannin induced structures. Scale bar=10 μm.

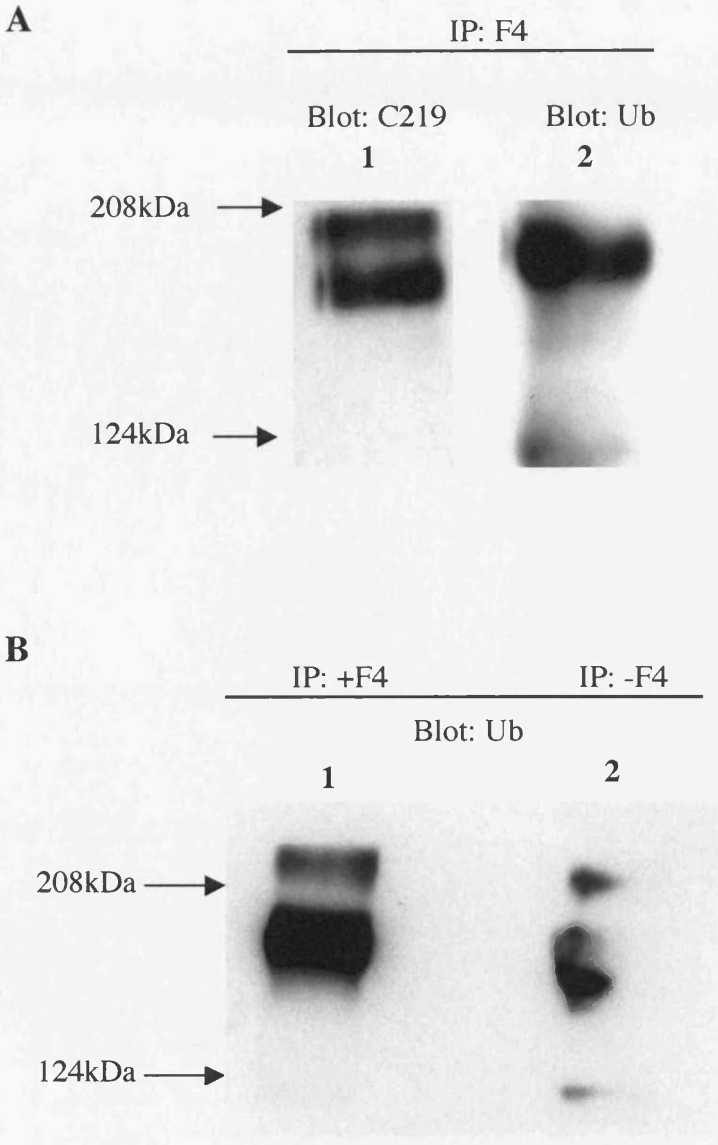

Figure 3.10. Immnuoprecipitation of ubiquitinated P-gp. (A) P-gp was immunoprecipitated (IP) from a membrane fraction using F4 antibody and the immunoprecipitate was subjected to Western blotting and probed with either C219 (lane 1) or an anti-ubiquitin antibody (Ub; lane 2). (B) Immunoprecipitation from a membrane fraction was performed either in the presence (lane 1) or absence (lane 2) of F4 antibody. Samples were then probed with an anti-ubiquitin antibody.

observed for the second experiment where again the ubiquitin band present in control cells (Figure 3.11B, lane 1) was absent from K^+ depleted samples (Figure 3.11B, lane 2). This therefore indicates that the detected ubiquitin band is sensitive to K^+ depletion. To confirm whether inhibition of clathrin mediated endocytosis can indeed inhibit the possible ubiquitination of P-gp another method, cellular cytosol acidification which is also known to inhibit clathrin-mediated endocytosis, was also used (Sandvig et al., 1987). The results revealed that the ubiquitin band was evident in control cells (Figure 3.12, lane 1), but it appeared to be reduced in treated cells (Figure 3.12, lane 2).

3.4 Discussion

The initial goals of this study were to characterise further the subcellular distribution of P-gp in KG1a cells and to identify the nature of P-gp positive organelles. Additionally attempts were made to identify whether co- or post-translational modification of this protein occurs in a way that could affect its endocytosis and intracellular fate from the plasma membrane. These were very important questions in this particular cell line as the reported lack of plasma membrane P-gp may suggest specific features of these cells with respect to P-gp dynamics.

To accomplish these objectives, it was first essential to extensively characterise and develop protocols for techniques such as western blotting, immunoprecipitation and immunofluorescence microscopy. Essential to these techniques was the use of anti-P-gp antibodies, which display extensive cross-reactivity profiles. Whilst the F4 antibody, with no reported cross-reactants, was found to be the most specific for P-gp in KG1a cells, C219 and JSB-1 both revealed bands at 200 kDa which in the case of C219, may be myosin (Thiebaut et al., 1989). However, and contrary to this, a 200 kDa band was also observed when when immunoprecipitations were performed with the F4 antibody from membrane followed by C219 detection. Thus the 200 kDa band may also be a variant of P-gp. Lower molecular weight bands at approximately 120 and 140 kDa were

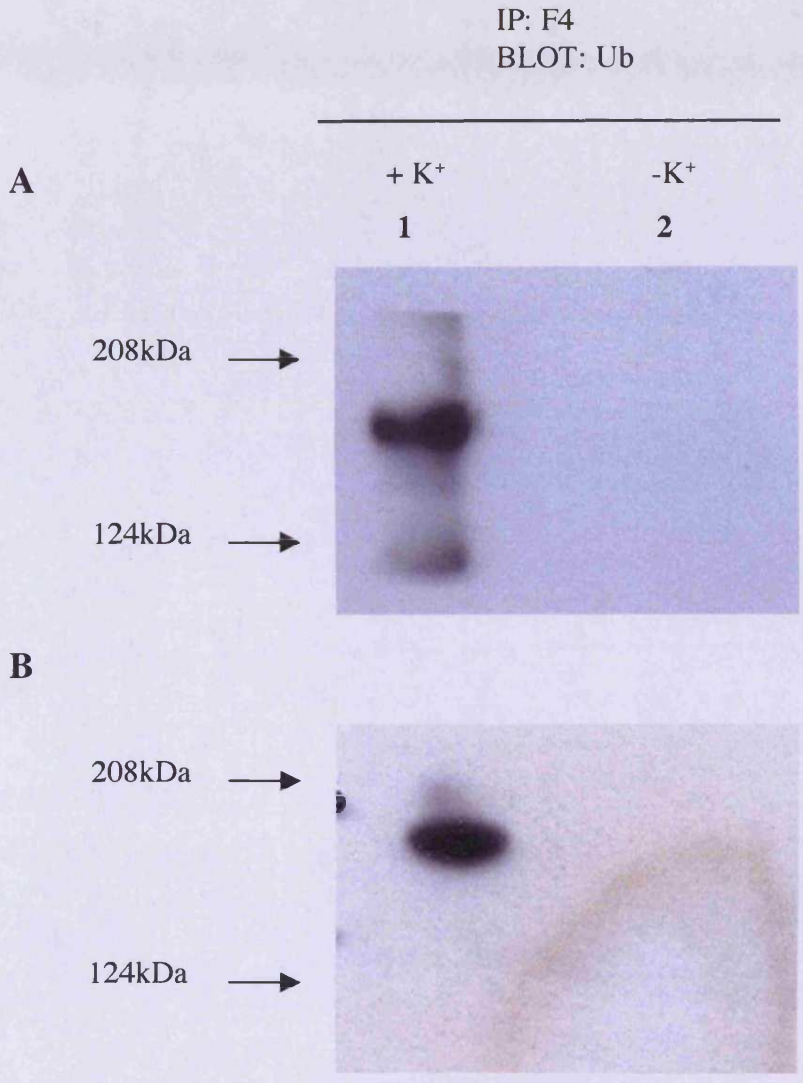

Figure 3.11. Effects of K^+ depletion on P-gp ubiquitination. Cells were either subjected to K^+ depletion (lane 2) or the appropriate control (lane 1). P-gp was then immunoprecipitated and probed for ubiquitin. The experiment was repeated twice (A and B).

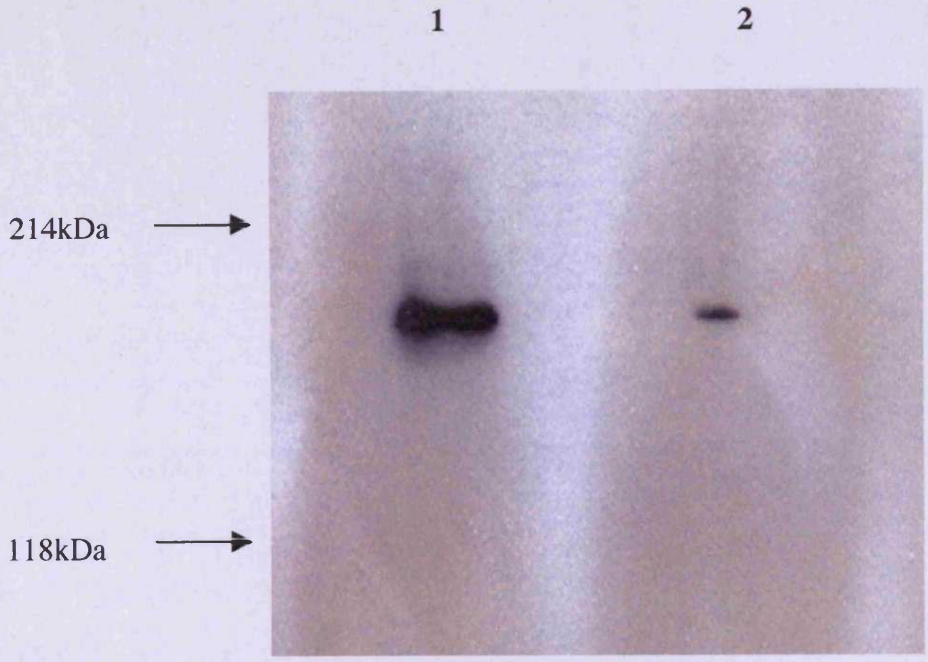

Figure 3.12. Effects of cellular cytosol acidification on P-gp ubiquitination. Cells were treated with ammonium chloride (lane 2) or the appropriate control (lane 1) and then subjected to immunoprecipitation for P-gp then probed for ubiquitin.

consistently observed on most blots. The 140 kDa band is consistent with immature, unglycosylated P-gp (Loo & Clarke, 1999), whilst the 120 kDa may be an earlier form of P-gp or possibly a degradation product. This highlights the potential pitfalls of using such antibodies not only *in vitro*, but also *ex vivo*. Liu and co-workers proposed that two different P-gp antibodies should be used for the detection of P-gp in clinical samples to avoid any false positives (Liu et al., 1997). This is ideal as the only protein common to both antibodies would be P-gp. This strategy was adopted when developing an immunoprecipitation protocol for this study, where the F4 antibody was used to immunoprecipitate and C219 for western blotting.

The cell membrane is a heterogeneous surface consisting of distinct domains that can be separated into detergent-soluble and insoluble domains. Detergent-insoluble domains are characterised as cholesterol and sphingolipid rich domains, such as lipid rafts and caveolae (Hooper, 1999). P-gp in KG1a cells was found to be associated with both detergent-soluble and insoluble domains. This heterogeneous distribution of P-gp within two distinct membrane regions has also been reported in MDR HT-29 human colon adenocarcinoma cells, where only 40 % of P-gp was localised to detergent insoluble membrane domains (Lavie et al., 1998). Several studies have revealed the dependence of P-gp function on a cholesterol rich membrane environment. A study by Troost and co-workers found that P-gp localised in detergent soluble domains by cholesterol depletion, had minimal efflux activity and its activity was only restored when P-gp was relocated to cholesterol rich domains (Troost et al., 2004). Ghetie and co-workers also reported that P-gp in lipid rafts has higher efflux activity than P-gp outside of these domains (Ghetie et al., 2004). This suggests that P-gp shuttles between at least two membrane localisations and is only active in specific membrane domains. It could also be that another factor localised to rafts may be modulating P-gp activity.

The detergent-insoluble domain may possibly be caveolae as studies have shown that P-gp bears a caveolae binding motif at its cytosolic amino-terminal region (Demeule et al., 2000; Jodoin et al., 2003). However, blood cells and blood cell lines, including these myeloid leukaemic cell lines do not usually express the

caveolae protein, caveolin-1 (Fra et al., 1994; Parolini et al., 1996). Only one study has reported the expression of caveolin-1, in a human T cell leukaemia cell line, Jurkat (Hatanaka et al., 1998). There are however no reports in KG1a cells and it was difficult to determine conclusively whether KG1a cells express caveolin-1 as several bands of higher molecular weight were observed. These may be due to non-specific binding although analysis of KG1a mRNA may resolve this issue.

As immunofluorescence microscopy had not been previously performed on KG1a and K562 cells in the laboratory, a number of methods were investigated utilising different fixation and permeabilisation protocols. An interesting observation was that cells fixed with PFA and permeabilised with Triton X-100 could be labelled for EEA-1 but not P-gp, whereas in cells that were fixed in PFA then post-fixed and permeabilised in acetone the reverse was true. Fixation can result in conformational changes in protein structure and alter antigenic profiles. These effects may vary according to the fixation method employed and so some fixatives may mask only specific antigens, hence the inability of an antibody to work with different fixation methods.

Analysis of P-gp distribution in KG1a cells revealed that P-gp was located intracellularly within small vesicles and infrequently within larger structures, with no apparent plasma or nuclear membrane labelling. These results are consistent with a study by Ferrao and co-workers who also found P-gp to be located within cytoplasmic vesicles (Ferrao et al., 2001). P-gp has been associated with several intracellular structures (described in section 1.3.2) but the true origin and identity of P-gp positive cytoplasmic vesicles in KG1a cells remains to be determined. However, wortmannin experiments provided clues that at least a fraction of these organelles are endosomes. The loss of EEA-1 labelling in wortmannin treated cells is due to the dissociation of EEA-1, from EE membranes (Patki et al., 1997) as a result of the inhibition of hVP34, a phosphatidylinositol-3-kinase involved in endocytic membrane traffic and generation of phosphatidylinositol-3-phospate. This enzyme recruits EEA-1 to endosomal membranes via the FYVE domain and so loss of hVP34 activity results in a decreased fraction of membrane bound EEA-1. P-gp positive compartments were shown to enlarge in wortmannin treated cells,

suggesting that the P-gp may reside on vesicles derived from the endocytic pathway, as wortmannin is known to induce the swelling of RE, LE and lysosomes (Martys et al., 1996; Reaves et al., 1996; Mousavi et al., 2003). It is also possible that P-gp resides within endocytic structures derived from EE which contain recycling membrane proteins that can fuse directly with the plasma membrane (Lim et al., 2001). Such endosomes may be utilised by some proteins such as P-gp, as a storage compartment (Herman et al., 1994). Dual labelling confocal microscopy using combinations of F4 with marker proteins and ligands as shown in figure 1.3 would also help pinpoint the identities of the P-gp positive organelles. Ferrao and co-workers also observed some plasma membrane labelling of P-gp as measured by FACS, however microscopy did not reveal any significant membrane labelling. It must be noted that these images were obtained from a single epifluorescent image and confocal microscopy and z-stacking will be required to investigate this further. P-gp has also been localised to nuclear membranes in MDR MCF-7 cells (Calcabrini et al., 2000) and for the same reason, we cannot rule out the possibility that this is also the case in KG1a cells, although no obvious nuclear labelling of P-gp was observed by immunofluorescence microscopy.

This intracellular P-gp may represent an intracellular pool awaiting translocation onto the cell surface in response to cytotoxic agents. One possible trigger for this translocation may be an alteration in pH (Calcabrini et al., 2000) such as that seen in MDR cells. A cytoplasmic pool of P-gp was also identified in MDR K562 cells and this was postulated to be a storage pool for maintaining a steady state level of surface P-gp (Labroille et al., 1998). In hepatocytes, an intracellular pool of P-gp also exists and this is translocated to the canalicular membrane on demand (Kipp et al., 2001).

The polyubiquitination of P-gp has been previously documented and is thought to regulate P-gp turnover (Ohkawa et al., 1999; Zhang et al., 2004). However, both studies overexpressed P-gp by culturing cells in the presence of doxorubicin and this artificial overexpression of P-gp may itself induce the ubiquitination of P-gp. In KG1a cells, a band was consistently observed after immunoprecipitating with F4 and probing with the anti-ubiquitin antibody, at the

same molecular weight for P-gp. This was indicative of monoubiquitination rather than polyubiquitination. However the data shown in Figure 3.10B revealed that the bands identified with the anti-ubiquitin antibody were not specific to the F4 antibody. However, considering that the same proteins that are immunoprecipitated also have the capacity to bind non-specifically to protein G-coated agarose beads (Figure 3.5, lane 2), we proceeded to address whether P-gp ubiquitination was regulated, as in the case for the growth hormone receptor, by endocytic events. To do this we investigated the effects of K^+ depletion and cellular cytosol acidification on ubiquitination, as these conditions have been shown to inhibit uptake via clathrin coated vesicles and ubiquitination of the growth hormone receptor (van Kerkhof et al., 2001). These conditions inhibit clathrin mediated endocytosis (Larkin et al., 1983; Sandvig et al., 1987) by depleting free cellular clathrin, thereby inhibiting clathrin lattice formation (Brown & Peterson, 1999). A clear reduction in the levels of P-gp ubiquitination were observed in K^+ depleted cells and in cells subjected to cellular cytosol acidification. This suggests that loss of free clathrin results in a reduction in the endocytic rate of P-glycoprotein and as ubiquitination is a prerequisite for endocytosis then both K^+ depletion and cytosol acidification reduced P-gp ubiquitination. Conversely as clathrin-coated vesicle formation also occurs intracellularly, it raises the possibility that P-gp is ubiquitinated intracellularly and not necessarily on the plasma membrane. These results need to be consolidated but these methods were very labour intensive, involved many steps and subsequently were difficult to reproduce. The experiments would also need to be repeated with other P-gp and ubiquitin antibodies.

In conclusion, KG1a cells support the majority of their P-gp within an intracellular compartment. The sensitivity of this compartment to wortmannin suggests that it is of endosomal origin. There was also evidence to suggest that P-gp was mono-ubiquitinated in these cells which provides valuable clues as to the possible trafficking routes of P-gp. Having studied the cellular distribution of P-gp in this chapter, the following chapter progressed to testing the functional contribution of this P-gp to MDR and whether redistribution of P-gp could be used to modulate P-gp function (Chapter 4).

Chapter 4:

Elucidation of Drug Resistance Mechanisms Operating Within KG1a and K562 Cells

4.1 Introduction

A successful therapeutic strategy should hold an appreciation of the possible resistance mechanisms that may significantly inhibit the efficacy of drugs. P-gp inhibitors are commonly employed to assess P-gp activity in cells. Although many strategies for the circumvention of P-gp are in use *in vitro* (described in section 1.5), the most commonly used P-gp inhibitors are verapamil and cyclosporin A (Figure 4.1A and 4.1B respectively). Verapamil is a calcium channel blocker commonly used in the treatment of cardiac arrhythmias and high blood pressure. It is also a competitive inhibitor of P-gp (Yusa & Tsuruo, 1989) and is thought to bind to the molecule on its fourth, sixth, tenth, eleventh and twelfth transmembrane domains (Loo & Clarke, 2001). It was initially described as a modulator of MDR in 1981 (Tsuruo et al., 1981) and aside from its inhibitory effects on P-gp mediated efflux, it has also been shown to reduce P-gp expression three-fold in two MDR human leukaemia cell lines, K562 and CEM (Muller et al., 1994). Conversely, in an *in vivo* mouse model, verapamil was shown to induce the expression of P-gp but only at the protein level (Granzotto et al., 2004). However, verapamil also has several effects on MDR, irrespective of P-gp. It interacts with the membrane, inducing membrane fluidity (Drori et al., 1995), which may result in drug leakage into the cell. It reduces the intracellular pH of MDR cells (Hamilton et al., 1993) which would aid drug retention. As well as inhibiting P-gp, it also inhibits MRP1 function by depleting cellular glutathione (Loe et al., 2000).

Cyclosporin A is a cyclic peptide of 11 amino acids and is a primary metabolite of several fungi including *Trichoderma polysporum* and *Tolypocladium inflatum*. It is also a competitive inhibitor of P-gp (Tamai & Safa, 1990), binding to its eleventh and twelfth transmembrane domains (Demeule et al., 1998). However, it also has the capacity to modulate other mechanisms of drug resistance, distinct from P-gp. As it generally inhibits ATP hydrolysis, it may potentially inhibit the function of all drug transporters (Ambudkar et al., 1999). Indeed it has been shown to be a weak resistance modifier of MRP1 (Leier et al., 1994). It induces biochemical changes in transmembrane signalling mechanisms (Damjanovich et al., 1987), which may effect the cellular response to cytotoxic stimuli. It was also shown to reduce oxidative phosphorylation and energy generation in mitochondria

A

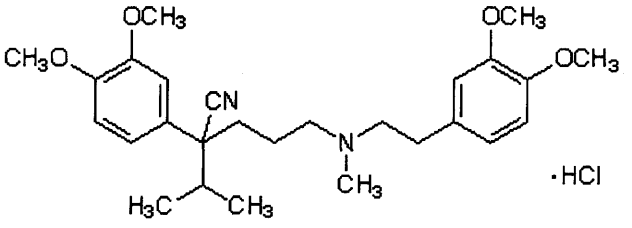

B

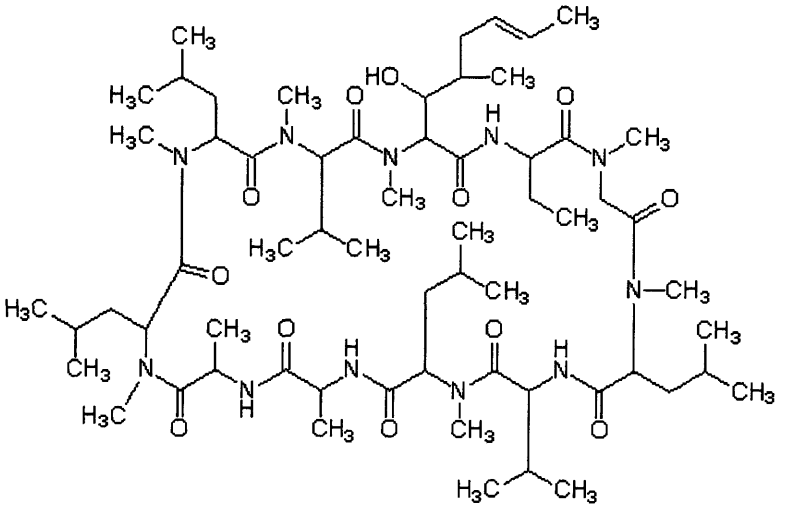

Figure 4.1. Chemical structures of (A) verapamil and (B) cyclosporin A.

(Jung et al., 1987) and also inhibits enzyme complexes involved in the electron-transport chain (Ichas et al., 1997). Like verapamil, it induces intracellular acidification (Hamilton et al., 1993) and can also induce the expression of P-gp as demonstrated in both an *in vivo* model in rats (Jette et al., 1996) and also *in vitro*, in endothelial and renal tubule cells (Hauser et al., 1998).

KG1a and K562 cells serve as useful models for the study of MDR as K562 cells do not normally express P-gp but its expression can be dramatically upregulated upon drug challenge and KG1a cells have high P-gp expression and are intrinsically resistant to several drugs. Drug resistance has previously been studied in KG1a and K562 cells, but there is huge discrepancy regarding the mean inhibitory concentration (IC_{50}) for DNR in both K562 and KG1a cells with published values differing fifty-fold and in one study in K562 cells there was no observed cytotoxicity after incubating K562 cells for 48 h in 3.5 μM DNR (Ferrao et al., 2001). Such indescrepancies are invariably due to the methods utilised for assessing cytotoxicity and also the culture and passage numbers of the cells. During the course of this study, an undergraduate student (that I supervised in part) utilised the MTT assay to calculate IC_{50} values for both cell lines after they were incubated with DNR for 24 h. IC_{50} values of 92 and 60 nM were obtained for K562 and KG1a cells respectively, which compares favourably with some studies (Lehne & Rugstad, 1998; Gong et al., 2002) but differ substantially from others (Ferrao et al., 2001; Marks et al., 1996). Drug resistance mechanisms have previously been studied in KG1a and K562 cells but the results have been difficult to interpret and there is little agreement between groups that have studied these cells in detail. Earlier in this study, P-gp in KG1a cells was shown to be predominantly intracellular, being localised to punctate cytoplasmic vesicles distributed diffusely throughout the cell (Chapter 3, Figure 3.8). This is in agreement with findings of a previous study by Ferrao and co-workers (Ferrao et al., 2001) and raises the important issue of the functionality of intracellular P-gp, which is strongly debated. A study in the colon tumour cell line, LS 174T, which express high levels of intracellular P-gp, has shown that cells are sensitive to P-gp substrates vincristine and doxorubicin (Duensing & Slate, 1994). However, this notion is rapidly changing with increasing evidence demonstrating the competence and ability of

intracellular P-gp in conferring drug resistance. Intracellular P-gp is thought to be responsible for the intrinsic drug resistance seen in colon adenocarcinomas, melanomas and leukaemias such as AML (Garbe, 1993; Schadendorf et al., 1994; Molinari et al., 1998; Meschini et al., 2000; Ferrao et al., 2001). Intracellular P-gp in KG1a cells was shown to be functional by several groups (Marks et al., 1996; Fardel et al., 1998; Ferrao et al., 2001), although there has been some confusion over the mechanism of resistance conferred by this intracellular fraction. Two mechanisms of resistance have been demonstrated in KG1a cells one of which is P-gp mediated drug efflux and the other, drug sequestration, occurs independently of P-gp in an unidentified cytoplasmic compartment (Lautier et al., 1997).

K562 cells have been shown to sequester anthracyclines within a dense unidentified perinuclear region (Ferrao et al., 2001). Another study identified this region as the lysosomal compartment in both drug resistant and sensitive cells (Loetchutinat et al., 2001), whilst another study has shown that in K562 cells, the drug is located diffusely within the nucleus and cytoplasm, whilst mitochondrial sequestration was seen in MDR K562 cells. These authors also ruled out any involvement of lysosomes and Golgi in drug sequestration (Gong et al., 2000).

The clinical importance of AML and CML and the significance of MDR to the high mortality rate associated with these leukaemias, warrants a more detailed study of drug resistance within them. This study therefore aimed to elucidate in more detail the mechanisms of resistance operating within KG1a and K562 cells. Essential for this study, was the use of a cytotoxic agent recognised as a P-gp substrate. A large number of drugs have been identified as P-gp substrates (described in section 1.4.1). The anthracyclines are a family of cytotoxic agents including doxorubicin, used for the treatment of solid tumours and DNR, mainly used for the treatment of haematological malignancies. Anthracycline antibiotics are comprised of a planar cyclic anthraquinone moiety attached to an amino sugar, with the amine group that can be ionised with an estimated p*K*a value of 7.6-8.2 (Dalmark & Storm, 1981; Figure 4.2A). At physiological pH the drug exists in equilibrium between charged and uncharged species. Initial reports suggest that they entered cells via facilitated transport because of the apparent saturation of

uptake with increasing drug concentration (Skovsgaard, 1978). However, it is now generally accepted that they enter cells via passive diffusion of the uncharged species through lipid membranes (Dalmark, 1981; Dalmark & Storm, 1981; Dalmark & Hoffmann, 1983). Their cytotoxic effects are mediated via several mechanisms including induction of free oxygen radical generation (Benchekroun et al., 1993) and enhanced apoptosis via activation of the sphingomyelin-ceramide pathway (Jaffrezou et al., 1996). Their interaction with the plasma membrane and the cytoskeleton can also contribute to their cytotoxic effects (Arancia et al., 1988; Molinari et al., 1990; reviewed in Tritton, 1991). They have also demonstrated some mitochondrial activity (Gosalvez et al., 1974) but their more accepted site of action is via DNA binding in the nucleus. Binding to DNA is thought to occur via the protonable amino group and they inhibit DNA replication, transcription and repair by intercalation into the DNA molecule (Gabbay et al., 1976). Inhibition of topoisomerase II seems to be the final stage leading to cell death as they stabilise the DNA-topoisomerase II complex, inhibiting the rejoining action of the enzyme, resulting in DNA double-strand breaks (Tewey et al., 1984; Cummings et al., 1991).

Although the anthracyclines are still commonly used in the clinic for the treatment of cancers, their clinical efficacy is significantly hindered by MDR. Numerous mechanisms of resistance against the anthracyclines have been identified and include P-gp, MRP, LRP and BCRP mediated efflux, intracellular sequestration, glutathione detoxification, decreased levels and activity of topoisomerase II and an increase in DNA repair (reviewed in Nielsen et al., 1996). DNR was chosen for this study due to its continued use in the combination therapy of leukaemias such as AML, because it is a known substrate for P-gp and finally its inherently fluorescent properties allows its cellular distribution and accumulation to be visualised and quantified within live cells, by fluorescent microscopy and flow cytometry respectively.

During the course of this study, Gong and co-workers described sequestration mechanisms in another AML cell line, HL-60 (Gong et al., 2003). In drug resistant HL-60 cells, DNR was sequestered in lysosomes but a neutral

zwitterionic dye, sulforhodamine 101 (SR101; Figure 4.2B) was found to be actively sequestered in the Golgi by MRP. This feature was unique to MDR cells as opposed to drug sensitive cells which harboured DNR and SR101 within the cytoplasmic and nuclear compartment (Gong et al., 2003). It is therefore important when trying to build a complete picture of drug resistance in cells, to analyse the relationship between the chemical structure of a drug and its susceptibility to different resistance mechanisms. Subsequently, SR101 distribution was also investigated in KG1a and K562 cells and comparisons were made with DNR. The overall aims of this study was to elucidate the drug resistance mechanisms operating in KG1a and K562 cells using the weakly basic chemotherapeutic agent, DNR and the zwitterionic dye, SR101.

4.2 Methods

To analyse DNR distribution in KG1a and K562 cells, cells were incubated with DNR as described in section 2.3.7.2.3. The effects of a number of pharmacological modulators on DNR distribution were also investigated. Verapamil (10 μg/ml) and cyclosporin A (6 μg/ml) were used to assess the effect of P-gp inhibition on DNR distribution. For this, the cells were pretreated with the drug or its diluent (dH_2O and methanol for verapamil and cyclosporin A respectively) for 15 min and then for 1 h with 2 μg/ml DNR in the continued presence of the drug. Nigericin (10 μM), a proton ionophore and bafilomycin A1 (30 nM), a vacuolar proton pump inhibitor, were used to assess whether the disruption of lysosomal pH affects DNR distribution. Both these agents neutralise endosomal pH but via different mechanisms. Nigericin neutralises lysosomal pH by mediating the exchange of H^+ for K^+ (Tartakoff, 1983) and bafilomycin A1, a macrolide antibiotic, disrupts lysosomal pH via inhibition of the vacuolar H^+ ATPase (Bowman et al., 1988; Crider et al., 1994). The cells were treated similarly to the cyclosporin A and verapamil treated cells. The diluents were methanol and ethanol for nigericin and bafilomycin A1 respectively. The sensitivity of P-gp localisation to wortmannin was previously shown in this study (Figure 3.9F) and experiments were performed to investigate whether DNR distribution was similarly affected by the drug.

A

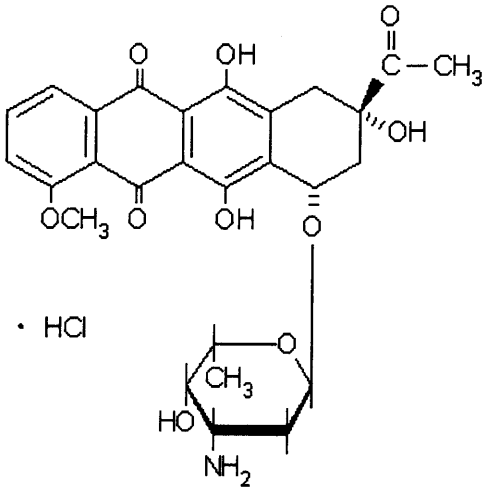

B

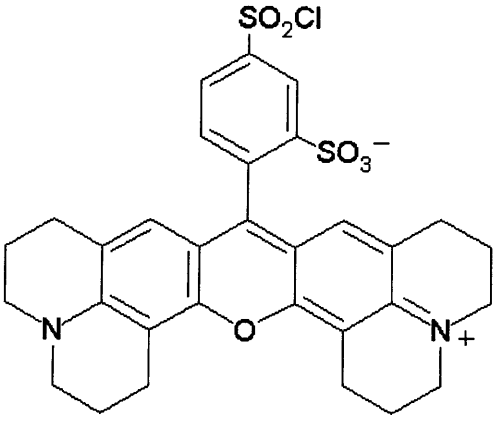

Figure 4.2. Chemical structures of (A) daunorubicin and (B) sulforhodamine 101.

Immunofluorescence microscopy was used to determine the cellular distribution of P-gp and of the cellular organelle markers EEA-1, TGN46, LAMPII and TxR-Dex. EEA-1, TGN46, P-gp and LAMPII labelling were carried out as described in section 2.3.7.1 using PFA fixation and Triton X-100 permeabilisation for EEA-1 and TGN46 and PFA fixation and acetone post-fixation and permeabilisation for P-gp and LAMPII. The effects of 5 μg/ml brefeldin A on TGN46 labelling in K562 cells and 150 nM wortmannin on P-gp labelling in KG1a cells was analysed by pretreating the cells with either the drug or appropriate diluent (DMSO and methanol for wortmannin and brefeldin A respectively) for 30 min. This was then followed by PFA fixation and immunolabelling as described in section 2.3.9.1. Brefeldin A has dramatic effects on Golgi structures resulting in a merger of the *cis-*, *medial-* and *trans*-Golgi with the endoplasmic reticulum, thus results in a more disperse Golgi labelling (Sciaky et al., 1997). The effect of brefeldin A on the Golgi is due to the inhibtion of ADP-ribosylation factor (Helms & Rothman, 1992), which prevents assembly of coat proteins such as clathrin on the Golgi (Molendijk et al., 2004).

TxR-Dex was used to label lysosomes as described in section 2.3.7.2.1. Colocalisation studies between TxR-Dex and DNR were carried out by internalising TxR-Dex as described above, then adding DNR during the last hour of TxR-Dex incubation.

To analyse SR101 distribution in KG1a and K562 cells, the compound was incubated with cells as described in section 2.3.7.2.4. The effect of P-gp inhibition on SR101 distribution in KG1a cells was analysed as described for DNR. The effect of 5 μg/ml brefeldin A on SR101 distribution in K562 cells was also analysed as described for other drugs.

The rat mdr1b-EGFP plasmid was amplified, purified and characterised as described in section 2.3.10.1, 2.3.10.2 and 2.3.10.3 respectively. Cells were then transfected with this plasmid or a control EGFP plasmid. Transfection was carried out by three different methods, lipofectamine 2000, Fugene 6 and electroporation as described in sections 2.3.11.1, 2.3.11.2 and 2.3.11.3 respectively. HeLa cells

were also transfected using Fugene 6 as described in section 2.3.11.2. To assess the functionality of P-gp in HeLa cells, cells were transfected then 24 h later, were incubated with 2 μg/ml DNR for 1 h and analysed by epifluorescence microscopy.

4.3 Results

4.3.1 DNR distribution in KG1a and K562 cells

To analyse the distribution of DNR, both cell lines were incubated with 2 μg/ml DNR for 1 h. DNR in KG1a cells was localised in cytoplasmic vesicles with very weak nuclear labelling also evident in these cells, however this is not immediately obvious from the printed images, as they do not clearly resemble what is observed under the microscope and is also partly due to the limitations of epifluorescence micrsocopy (described later in section 4.3.4; Figure 4.3A). A prominent labelling of the nuclear envelope in KG1a cells was also evident. DNR labelling in K562 cells was noticeably distinct from that of KG1a. DNR was localised to a dense perinuclear compartment. Again, very little nuclear accumulation was evident (Figure 4.3B) and prominent labelling of the nuclear envelope was again observed.

4.3.2 Analysis of the functionality of P-glycoprotein in KG1a cells

The identification of drug sequestration in both cell lines, prompted further studies to identity this compartment. KG1a and K562 cells were pretreated for 15 min with verapamil or cyclosporin A prior to the addition of DNR for 1 h in the continued presence of the drug. In contrast to control cells which displayed only weak nuclear fluorescence (Figure 4.4A), verapamil treatment induced a dramatic increase in nuclear accumulation of the drug (Figure 4.4B). Identical results were observed using cyclosporin A, where again higher fluorescence was evident in the nuclear compartment of drug treated cells (Figure 4.4D), compared to control cells (Figure 4.4C). However, neither verapamil nor cyclosporin A were able to disrupt the vesicular DNR labelling in KG1a cells, as the drug could still be observed in vesicles. To identify any potential non-specific effects of these P-gp inhibitors on MDR, the effects of verapamil and cyclosporin A on DNR distribution was investigated in K562 cells that lack P-gp (Fardel et al., 1998). Verapamil treatment

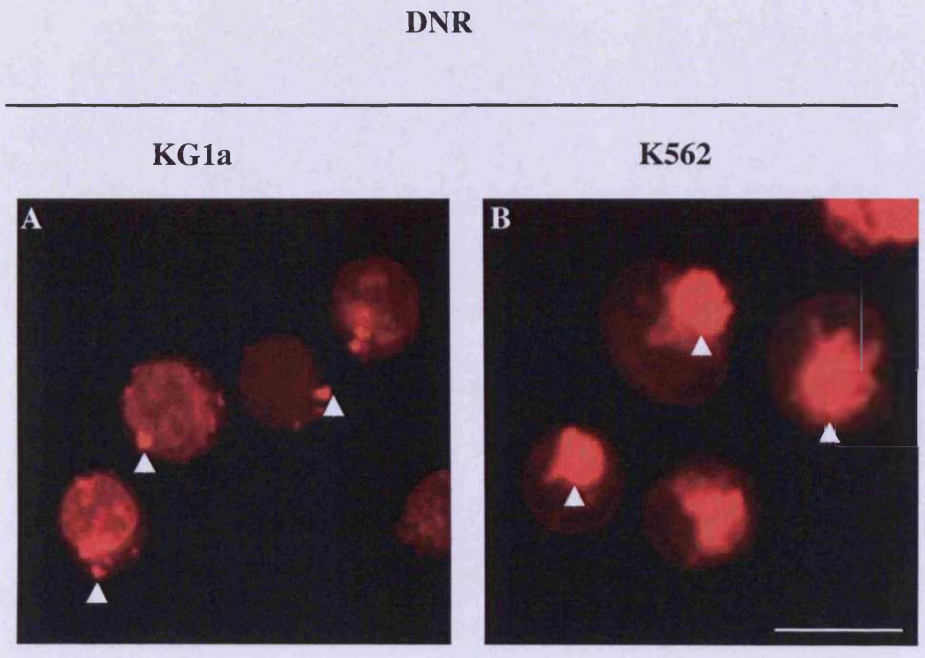

Figure 4.3. Cellular distribution of DNR in KG1a and K562 cells. KG1a (A) and K562 (B) cells were incubated with 2 μg/ml DNR for 1 h at 37 °C, then analysed by epifluorescence microscopy. Arrowheads indicate DNR positive structures. Scale bar= 10 μm.

of K562 cells also disrupted the dense perinuclear labelling of DNR observed in control cells (Figure 4.4E), resulting in diffuse cytoplasmic and nuclear localisation of the drug (Figure 4.4F). However, when the experiment was repeated with cyclosporin A, there were no observable effects on DNR distribution as it labelled a dense perinuclear compartment in both control (Figure 4.4G) and cyclosporin A treated cells (Figure 4.4H). This revealed major differences in these two cell lines with respect to both the subcellular distribution of DNR and the effects of P-gp inhibitors on DNR sequestration.

4.3.3 Comparison of the distribution of cellular organelles in KG1a and K562 cells

The inability of P-gp inhibitors to disrupt the compartmentalisation of DNR in KG1a and K562 cells, led to the possibility that sequestration in these cells is not related to P-gp activity. Lysosomes, endosomes and the Golgi have all been implicated in the sequestration of weak base drugs such as DNR (Altan et al., 1998) and the mitochondria has also been identified as a possible site of sequestration of weak base drugs (Duvvuri et al., 2004). The identity of the DNR sequestering compartment in KG1a and K562 cells was subsequently investigated. Prior to this, comparison of the subcellular distribution of predominantly endocytic organelles was performed in these cells. Despite extensive use of KG1a cells in MDR studies, there were no published reports of the distribution of subcellular structures in this cell line. This data could therefore prove useful for explaining the differential distribution of DNR that was observed. Immunolabelling with an anti-EEA-1 antibody revealed punctate structures located diffusely in both KG1a and K562 cells (Figure 4.5A and 4.5B respectively). Labelling for TGN46 was also similar in the two cell lines and was very dense and polarised (Figure 4.5C and 4.5D respectively). LAMPII labelled punctate and diffuse structures in KG1a cells (Figure 4.5E) but this was in marked contrast to the dense perinuclear labelling observed in K562 cells (Figure 4.5F). TxR-Dex chased into the lysosomes over a period of four hours displayed a similar distribution to LAMPII in both cell lines, with a punctate vesicular distribution in KG1a cells (Figure 4.5G) and dense perinuclear labelling in K562 cells (Figure 4.5H). Thus the prominent differences

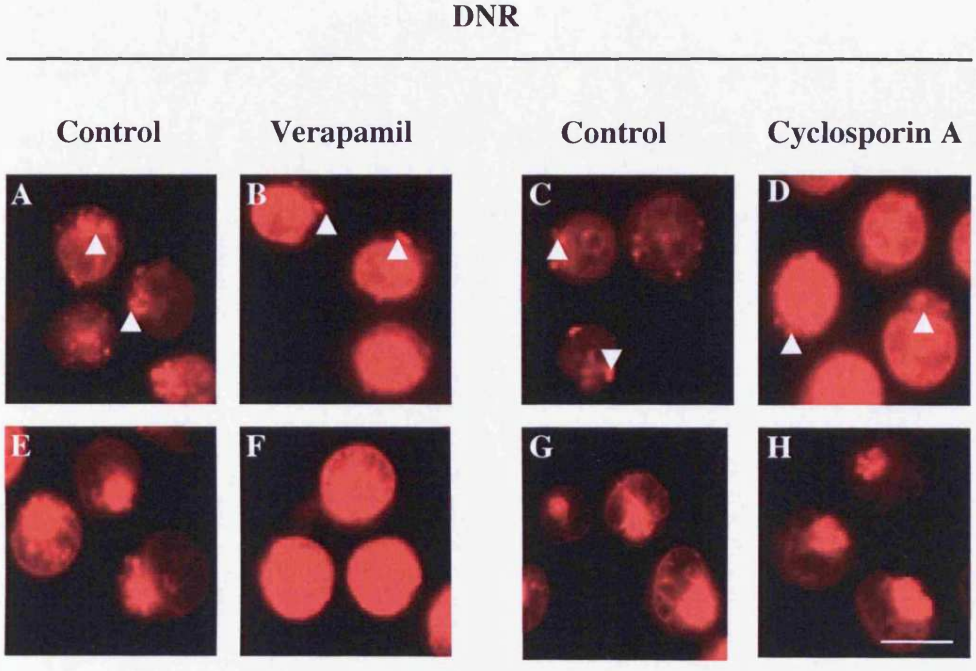

Figure 4.4. Functionality of intracellular P-gp in KG1a cells. KG1a (A-D) and K562 (E-H) cells were either incubated with DNR in the presence of PBS (A and E) or methanol (C and G) as controls for verapamil and cyclosporin A respectively or were treated with 10 μg/ml verapamil (B and F) or 6 μg/ml cyclosporin A (C and G). Arrowheads indicate the vesicular DNR structures in KG1a cells in both treated and untreated cells. Scale bar= 10 μm.

in LAMPII and TxR-Dex labelling between the two cell lines, mirrors the localisation of sequestered DNR.

4.3.4 Cellular localisation of DNR in KG1a and K562 cells

To confirm that the lysosomes were the site of DNR sequestration, cells were treated with nigericin and bafilomycin A1, both of which neutralise endosomal pH. Cells were first pretreated with either nigericin or bafilomycin A1 and then incubated for 1h with DNR in the continued presence of the drugs. Nigericin treatment of KG1a cells eliminated the vesicular DNR labelling (Figure 4.6A) and the drug was redistributed to the nucleus (Figure 4.6B). Treatment with bafilomycin A1 mirrored the effects of nigericin, and the vesicular structures observed in control cells (Figure 4.6C) were abolished, revealing the nuclear localisation of DNR (Figure 4.6D). Nigericin treatment of K562 cells disrupted the dense perinuclear DNR labelling (Figure 4.6E), resulting in cytoplasmic and nuclear localisation of the drug (Figure 4.6F). Bafilomycin A1 revealed the same effects as nigericin, and the dense perinuclear labelling of DNR (Figure 4.6G) was also relocated to the nucleus and cytoplasm (Figure 4.6H). To consolidate this evidence of the lysosomal sequestration of DNR, colocalisation studies between TxR-Dex and DNR were performed in KG1a and K562 cells using confocal microscopy. TxR-Dex was internalised for 2 h, chased into lysosomes for 4 h and cells were incubated with DNR during the last hour of the chase. As previously described, TxR-Dex labelled distinct vesicular structures, distributed diffusely throughout the KG1a cell (Figure 4.7A). DNR in these cells was, as expected, localised to diffuse vesicular structures, but bleaching of fluorescence made them difficult to visualise (Figure 4.7B). Confocal microscopy, compared to epifluorescence microscopy, showed more clearly the lack of nuclear labelling and also the prominent labelling of the nuclear envelope. There was almost complete colocalisation between DNR and TxR-Dex when images were overlayed (observed as yellow vesicles in figure 4.7C). TxR-Dex consistently labelled a dense perinuclear compartment in K562 cells (Figure 4.7D), a distribution that was closely mirrored by DNR (Figure 4.7E). As expected DNR and dextran showed a high degree of colocalisation (Figure 4.7F). Again the lack of nuclear labelling of DNR was clearly observed in cells imaged by confocal microscopy as compared to

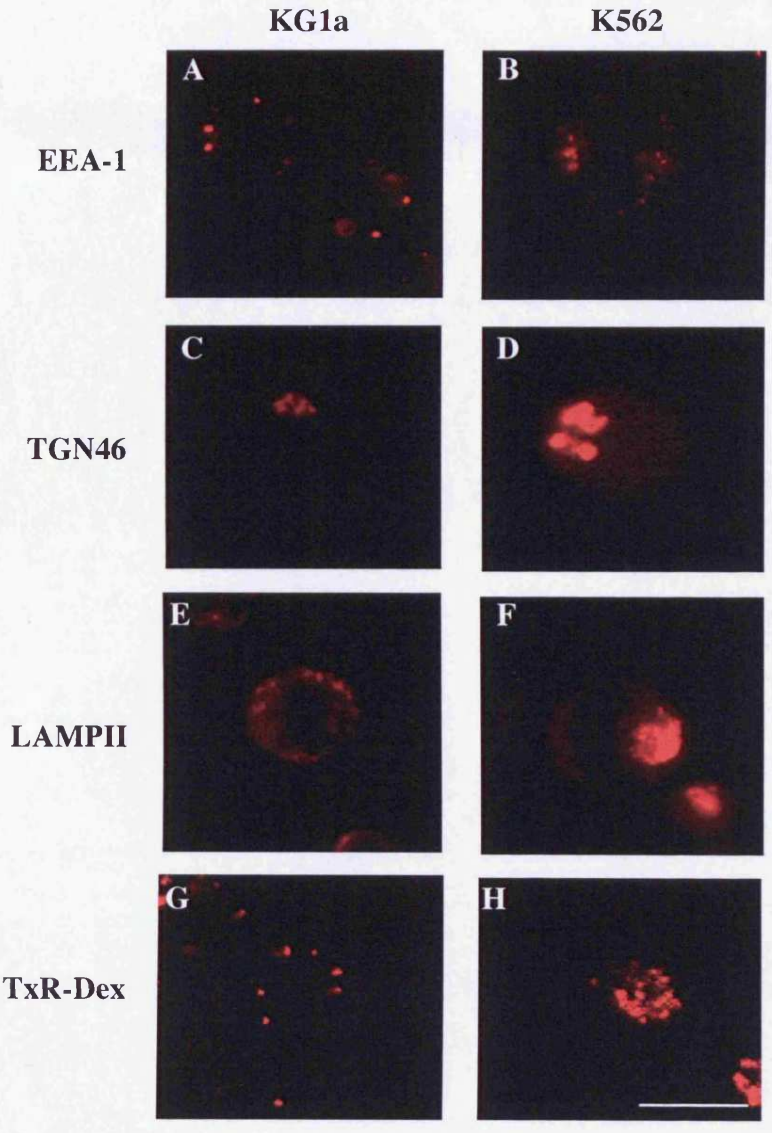

Figure 4.5. Distribution of cellular markers in KG1a and K562 cells. Cells were subjected to immunofluorescence labelling for EEA-1 (A and B), TGN46 (C and D) and LAMPII (E and F) as described in materials and methods. Txr-Dex (1 mg/ml) was internalised for 2 h then chased into lysosomes for 4 h at 37°C (G and H). Dextran loaded cells were analysed by confocal microscopy. Scale bar= 10 μm.

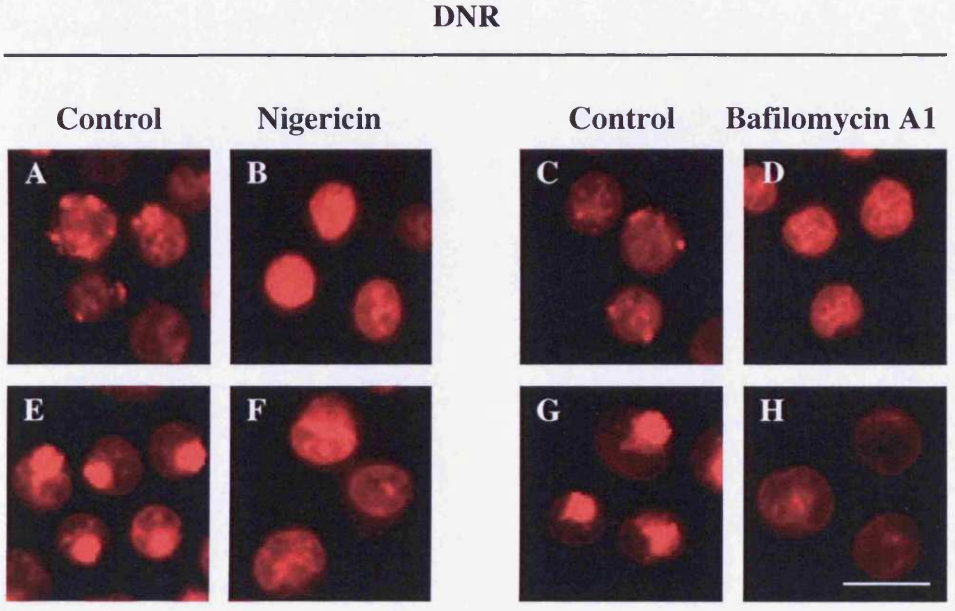

Figure 4.6. Effects of nigericin and bafilomycin A1 on DNR distribution. KG1a (A-D) and K562 (E-H) cells were either incubated with DNR in the presence of ethanol (A, E, C and G) as controls for nigericin and bafilomycin A1 or were treated with 10 μM nigericin (B and F) or 30 nM bafilomycin A1 (C and G). Scale bar= 10 μm.

epifluorescence microscopy as shown in Figure 4.3B. The prominent labelling of the nuclear envelope is also more clearly seen in the confocal image. The overlayed image showed almost complete colocalisation between DNR and TxR-Dex in these cells (Figure 4.7F). This suggests that the lysosomes are the primary site of DNR sequestration in both KG1a and K562.

4.3.5 Effect of P-glycoprotein redistribution on DNR sequestration

P-gp redistribution from the plasma membrane to intracellular compartments has been shown to influence its function and ultimately reverse MDR (Kim et al., 1997; Loo & Clarke, 1999; Fu et al., 2004). As wortmannin was previously found to influence P-gp distribution (Figure 3.7F), the effects of this redistribution on P-gp function and ultimately DNR localisation, was investigated. Cells were treated with wortmannin then immunolabelled with the F4 antibody. As previously shown (Chapter 3, Figure 3.9F), wortmannin treatment caused a redistribution of P-gp from small punctate structures (Figure 4.8A) to an enlarged structure polarised to one side of the cell (Figure 4.8B). The effect of wortmannin on DNR distribution was then assessed. As consistently observed, DNR in control cells was localised to cytoplasmic vesicles distributed diffusely throughout the cell (Figure 4.8C) but in the presence of this drug, the DNR labelled vesicles appeared to be clustered and polarised to one side of the cell (Figure 4.8D). In many cases the labelling pattern mirrored that of DNR in untreated K562 cells. However, there was no apparent increase in the nuclear localisation of DNR in the presence of wortmannin, suggesting that neither the relocalisation P-gp or DNR sequestering structures had an effect on the nuclear localisation of the drug.

4.3.6 SR101 distribution in KG1a and K562 cells

The cellular localisation of the zwitterionic fluorescent dye, SR101, was assessed by direct fluorescence microscopy. KG1a and K562 cells were incubated with 5 μg/ml of SR101 for 1 h. In KG1a cells, SR101 labelled the entire cell, however in the majority of cells, distinct vesicular staining was also evident (Figure 4.9A), suggestive of some degree of compartmentalisation. This observation prompted a further incubation of the SR101 loaded cells for 1 h in the absence of SR101, to determine whether the cells were further able to sequester the

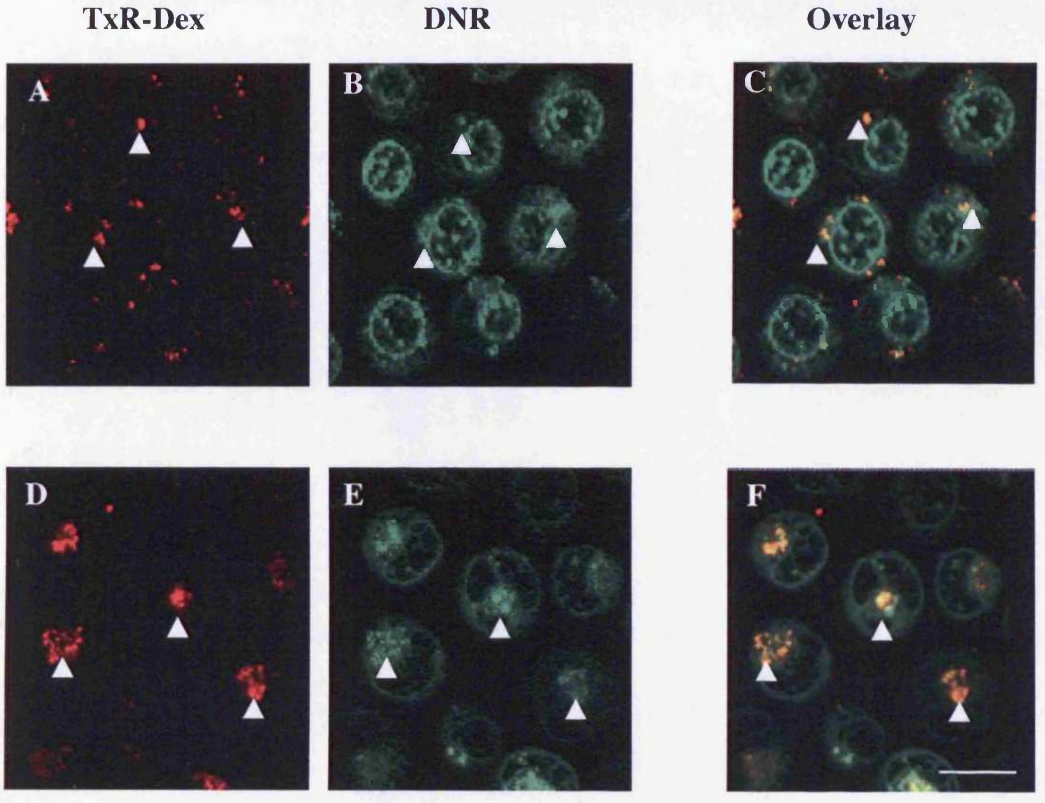

Figure 4.7. Colocalisation studies between DNR and TxR-Dex in KG1a and K562 cells. KG1a (A-C) and K562 cells (D-F) cells were incubated with 1 mg/ml TxR-Dex for 2 h followed by a 4 h chase into lysosomes (A and D). DNR (2 μg/ml) was incubated with cells in the final 1 h of incubation (B and E). Cells were washed and analysed by confocal microscopy. DNR and TxR-Dex images were overlapped to assess colocalisation (Cand F). Arrowheads indicate the colocalised structures in both cell lines. Scale bar= 10 μm.

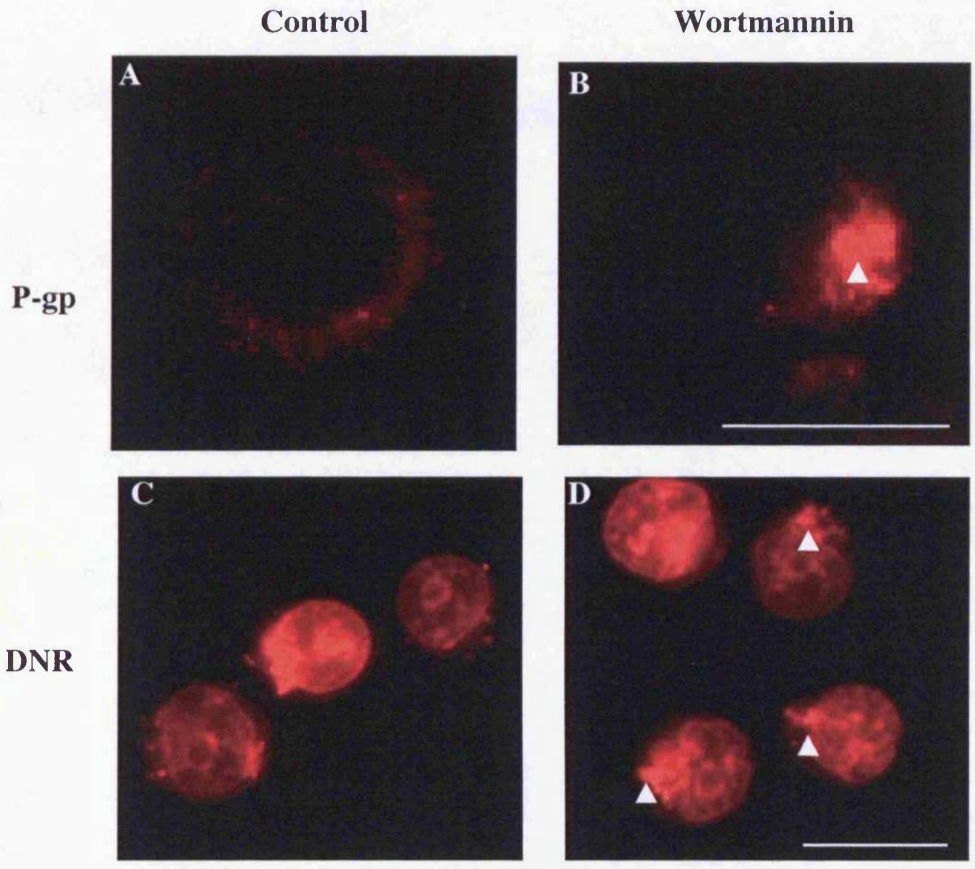

Figure 4.8. Effect of wortmannin on DNR distribution. KG1a cells were immunolabelled for P-gp either in the absence (A) or presence (B) of 150 nM wortmannin. DNR (2 μg/ml) was incubated with KG1a cells either in the absence (C) or presence (D) of wortmannin. Arrowheads indicate the wortmannin induced structures. Scale bar= 10 μm.

dye. Following this additional 1 h incubation, it was evident that there was complete sequestration of SR101 within vesicular structures (Figure 4.9B). Identical observations were seen when these experiments were performed in K562 cells where an initial diffuse cellular labelling was observed (Figure 4.9C) but the final sequestration locality of the dye was perinuclear and very similar to DNR labelling patterns (Figure 4.9D).

4.3.7 Cellular localisation of SR101 in KG1a cells

To determine whether SR101 sequestration is influenced by P-gp activity, KG1a cells were pretreated with verapamil and cyclosporin A for 15 min and then incubated for 1 h in the presence of SR101, followed by a final 1 h incubation in the absence of the dye. SR101 was located within cytoplasmic vesicular structures in untreated cells (Figure 4.10A) but this vesicular labelling was disrupted following verapamil treatment and cells displayed diffuse cytoplasmic and nuclear labelling (Figure 4.10B). These effects were mirrored by cyclosporin A, where the vesicular labelling seen in untreated cells (Figure 4.10C) was also disrupted in the presence of the drug revealing complete cytoplasmic and nuclear labelling (Figure 4.10D). This strongly implicates the involvement of P-gp in SR101 sequestration in these organelles.

4.3.8 Cellular localisation of SR101 in K562 cells

SR101 sequestration within Golgi compartments was demonstrated in MDR HL60 cells by epifluorescence microscopy (Gong et al., 2003). As the Golgi also locates to a perinuclear region in K562 cells, experiments were performed to determine whether the SR101 labelling in K562 cells was also in the Golgi. For this, SR101 loaded cells were treated with the Golgi disrupting agent brefeldin A. It was however important to determine whether brefeldin A was having the typical effects in K562 cells at the concentration previously used in other cell lines. Therefore, cells were treated with brefeldin A, then immunolabelled with an anti-TGN46 antibody. As previously shown in Figure 4.5D, TGN46 is localised to a dense and polarised region in the cell (Figure 4.11A). Treatment with brefeldin A resulted in more dispersed and vesicular TGN46 labelling (Figure 4.11B), a characteristic effect of brefeldin A induced Golgi fragmentation (Sciaky et al.,

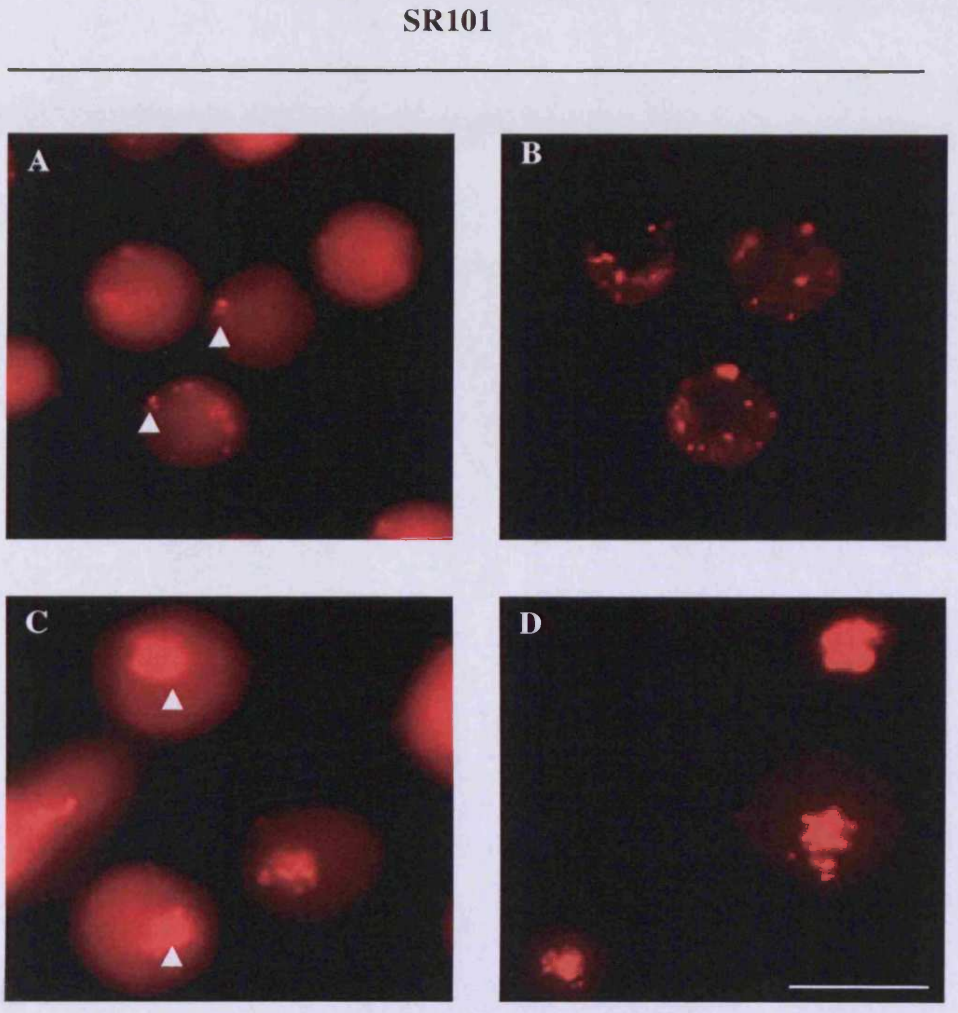

Figure 4.9. SR101 distribution in KG1a and K562 cells. KG1a (A and B) and K562 (c and D) cells were incubated with 5 μM SR101 for 1 h at 37 °C, washed and either analysed immediately (A and C) or incubated for a further 1 h in the absence of SR101 (B and D). Arrowheads indicate compartmentalisation of the drug. Scale bar= 10 μm.

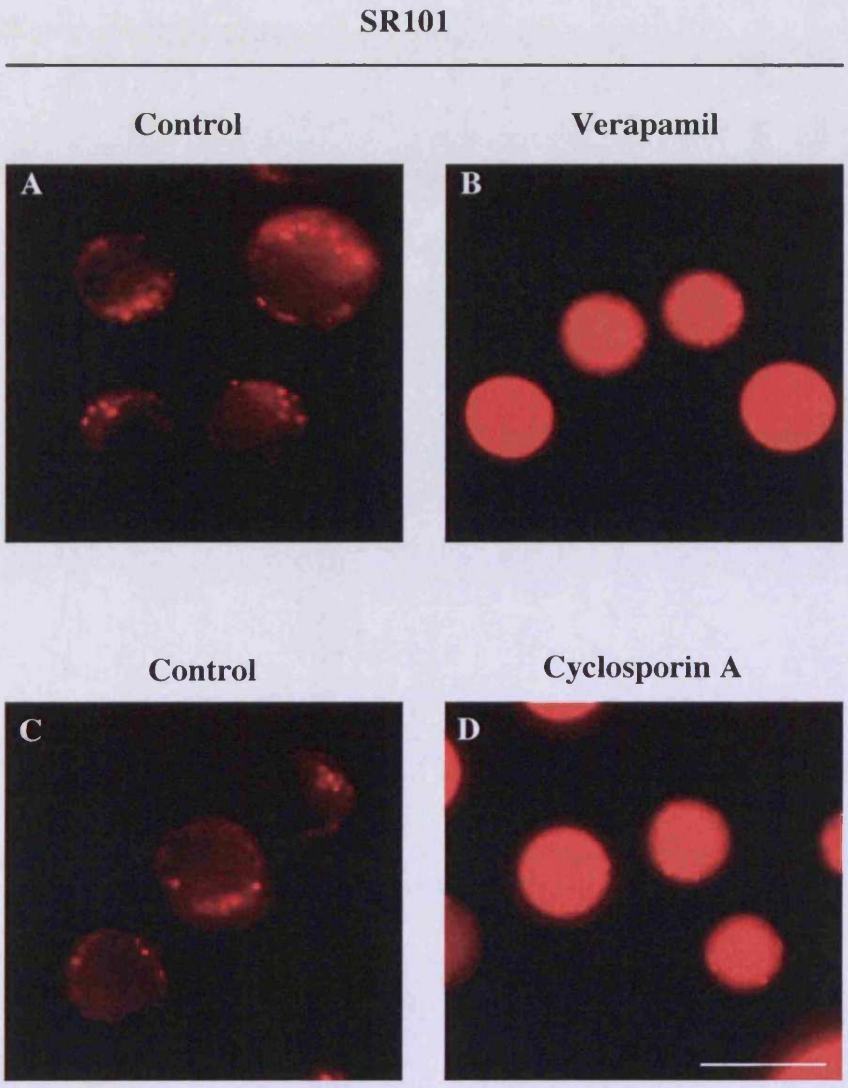

Figure 4.10. Effects of verapamil and cyclosporin A on SR101 distribution in KG1a cells. KG1a cells were incubated with 5 μM SR101 with either PBS (A) or methanol (C) as control for verapamil and cyclosporin A respectively, or were treated with 10 μg/ml verapamil (B) or 6 μg/ml cyclosporin A (D). Scale bar= 10 μm.

1997). As the protein is dissipated by the drug, the labelling was also less intense than that observed in untreated cells. To assess the effects of brefeldin A on SR101 distribution, K562 cells were subsequently pretreated with brefeldin A for 15 min, then for 1 h in the presence of SR101 and a further 1 h after the removal of the SR101. The dense SR101 fluorescence in untreated cells (Figure 4.11C) was dissipated in a similar manner as the TGN46 (Figure 4.11D). Diffuse cytoplasmic labelling, synonymous to that observed following the initial SR101 incubation, was also evident in brefeldin A treated cells.

4.3.9 Characterisation of rat mdr1b-EGFP plasmid

The cells utilised in this study have either undetectable (K562) or high (KG1a) intrinsic P-gp expression and as shown in this study, have fundamental differences in their sensitivities to P-gp inhibitors. Experiments were then designed to investigate whether immediate upregulation of P-gp via plasmid tranfection would in any way change their characteristics with respect to the sequestration of DNR. To assess the effect of P-gp overexpression on drug accumulation or distribution, a rat mdr1b-EGFP was used for transfection studies. The plasmid was initially amplified, purified and characterised by restriction enzyme digestion. The plasmid map showing the targeted restriction sites is illustrated in Figure 4.12A. The plasmid was subjected to either single digests with NotI, EcoRI and BamHI to linearise the plasmid, or a double digest with NotI and EcoR1 to separate mdr1b-EGFP from the vector. The results are shown in figure 4.12B and show the undigested plasmid with an expected molecular weight of approximately 8.6 kb (lane 1). Single digestion with NotI revealed two fragments, at approximately 4 kb and 4.6 kb (lane 2). This is consistent with the presence of two NotI sites. Single digests with EcoRI and BamHI revealed single bands at 8.6 kb (lanes 3 and 4 respectively). A double digest with NotI and EcoRI produced two fragments at the correct size for mdr1b-EGFP (4.7 kb) and the remaining vector (3.9 kb; lane 5).

4.3.10 Transfection of KG1a and K562 cells by electroporation with rat mdr1b-EGFP plasmid

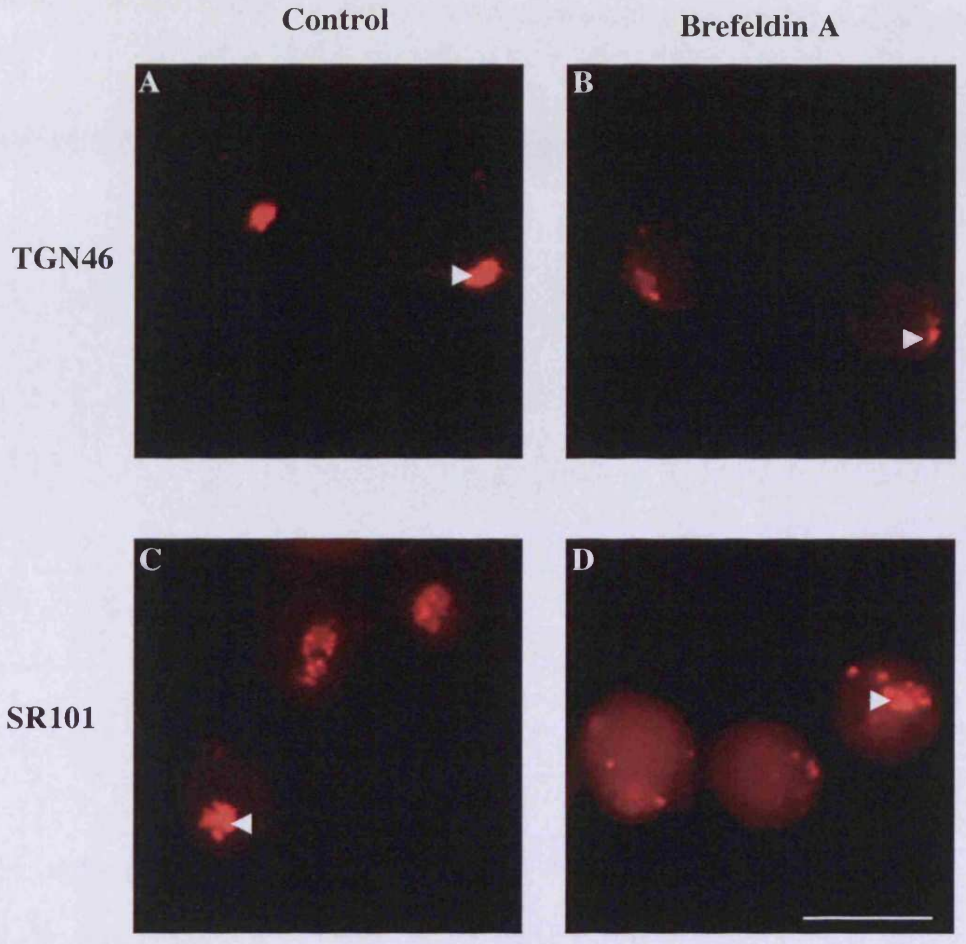

Figure 4.11. Effects of brefeldin A on SR101 distribution in K562 cells. K562 cells were immunolabelled for TGN46 either in the absence (A) or presence (B) of 5 μg/ml brefeldin A. SR101 was incubated with K562 cells either in the absence (C) or presence (D) of brefeldin A as described in materials and methods. Arrowheads indicate the differences in TGN46 and SR101 labelling following treatment with brefeldin A. Scale bar= 10 μm.

KG1a and K562 cells were initially transfected with the rat mdr1b-EGFP by electroporation. A protocol was first optimised using different cell densities and concentrations of plasmid. Initial protocols for electroporation resulted in approximately 90 % cell death, as assessed by trypan blue staining. By omitting penicillin/streptomycin from the media during transfection, toxicity was dramatically reduced. At 36 h post-transfection mdr1b-EGFP positive cells were observed but the transfection efficiency was never higher than 1 %. However the method also allowed analysis of subcellular localisation of this protein and in KG1a cells there was significant plasma membrane labelling with additional strong labelling in a perinuclear region that based on earlier TGN46 labelling, corresponds to the Golgi (Figure 4.13A). Plasma membrane labeling was also observed in K562 cells but the perinuclear labelling was not so apparent (Figure 4.13B).

4.3.11 Transfection of KG1a and K562 cells by Fugene 6 and Lipofectamine with rat mdr1b-EGFP plasmid

The low transfection efficiency achieved with electroporation prompted further experiments with alternative methods of transfection and for this, lipid based transfection reagents, Lipofectamine 2000 and Fugene 6. Lipofectamine 2000 proved ineffective in both cell lines despite using a wide variety of DNA/lipid ratios and incubation conditions. Fugene 6 was only effective in K562 cells albeit with a very low transfection efficiency compared to those achieved for electroporation. Mdr1b-EGFP in K562 cells labelled the plasma membrane and prominent labelling of a perinuclear compartment was also observed (Figure 4.14A). However, these cells also displayed very large membrane protrusions that often were larger than the diameter of the cell. Of particular interest is that the membrane protrusions also appear to be labelled with mdr1b-EGFP. To determine whether this phenomenon is a product of mdr1b-EGFP overexpression or a result of Fugene 6 tranfection, a plasmid encoding EGFP alone was then transfected into K562 cells. The same membrane protrusions were also observed in cells transfected with the EGFP plasmid alone but in these cells, the EGFP was located throughout the cytoplasm of the cell with prominent fluorescence in the nuclear compartment (Figure 4.14B). Of particular interest is the observed EGFP

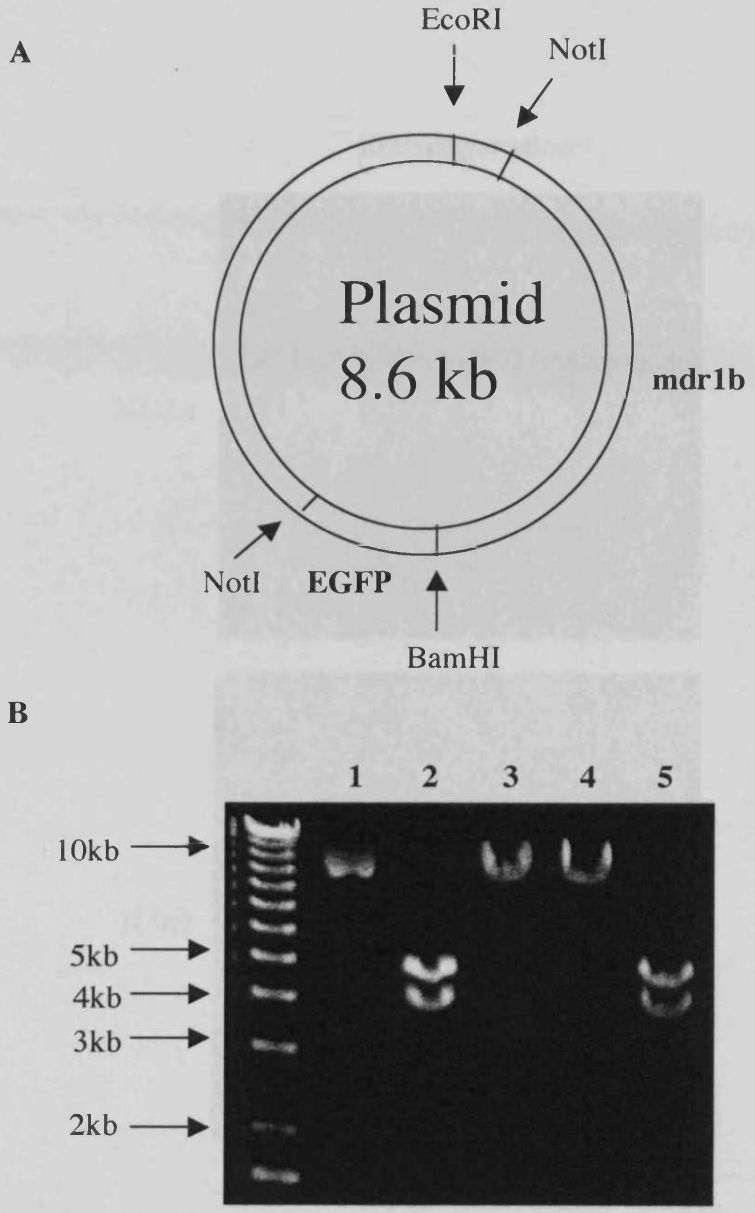

Figure 4.12. Characterisation of the rat mdr1b-EGFP plasmid. (A) plasmid map showing te restriction sites surrounding mdr1b-EGFP. (B) Rat mdr1b-EGFP plasmid was either left uncut (lane 1) or treated with the restriction enzymes NotI (lane 2), EcoRI (lane 3), BamHI (lane 4) and NotI and EcoRI in a double digest (lane 5). All samples were run on a 0.6 % agarose gel and photographed on a polaroid gel imaging system. Kb markers are indicated on the left hand side of the gel.

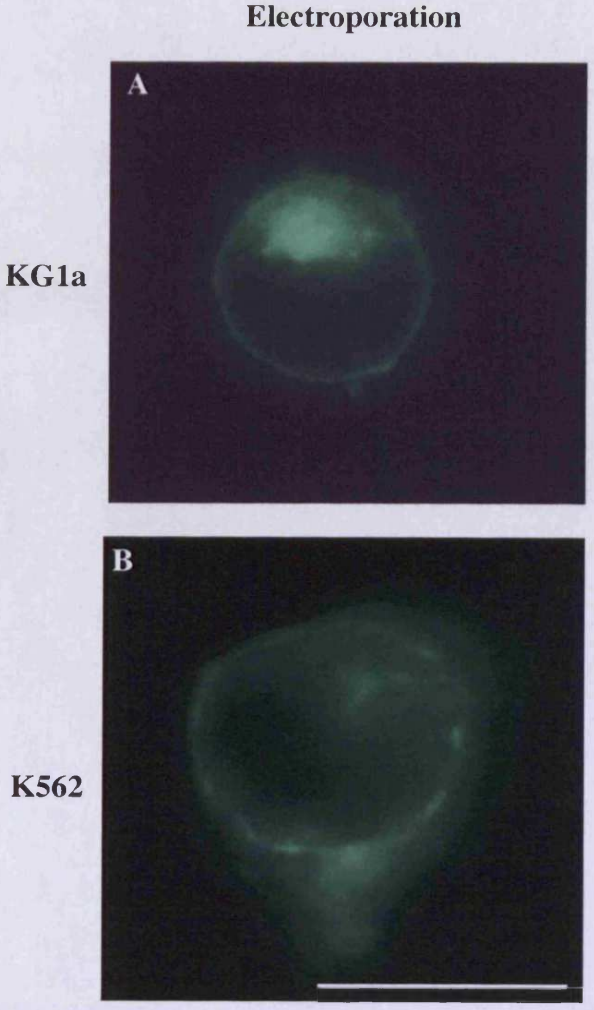

Figure 4.13. Electroporation of KG1a and K562 cells with the rat mdr1b-EGFP. KG1a (A) and K562 (B) cells were subjected to electroporation with 5 μg mdr1b-EGFP plasmid. Cells were analysed 36 h following transfection. Scale bar= 10 μm.

fluorescence within the confines of this membrane protrusion, showing that this is an extension of the cell cytoplasmic compartment. This phenotype is therefore associated with Fugene 6 mediated transfection rather than P-gp overexpression. These effects halted further experiments with this transfection reagent in these cells.

4.3.12 Transfection of HeLa cells with rat mdr1b-EGFP

Studies have shown that transfection of cell lines such as the human ovary carcinoma cell line (Hela) with MDR-1 confers a resistant phenotype (Fu et al., 2004). Despite the fact that transfection studies in leukaemia cells with this plasmid were unsuccessful, further experiments were performed to investigate whether rat mdr1b was functional in a human cancer cell line, Hela. Hela cells were transfected with Fugene 6 and 24 h following transfection, cells were incubated for 1 h with DNR and visualised by epifluorescence microscopy. Transfection efficiency was much higher in these cells (approximately 20 %) compared with leukaemia cells. The fluorescent protein was localised to the plasma membrane suggesting that traffic of the rat variant is unhindered in the human cell line (Figure 4.15A). There was also significantly less DNR in these transfected cells and this is the most obvious in Figure 4.15B. The apparent green label of the cell shown by the arrowhead in Figure 4.15A is due to bleeding of DNR fluorescence into the green channel and this is showing that there is no plasma membrane green fluorescence in this cell. It is apparent in Figure 4.15C that only cells with plasma membrane labelling of mdr1b effectively exclude DNR from the nucleus. This highlights the problems of using this microscope with DNR that has a broad fluorescence spectra.

4.4 Discussion

In this study we investigated drug sequestration mechanisms operating in KG1a and K562 cells using DNR and SR101. As described earlier in sections 1.7.1 and 1.7.2, both cell lines have generated much conflicting data regarding their MDR phenotype. The observation that KG1a support the majority of their P-gp within intracellular compartments raised the important issue of whether this P-gp

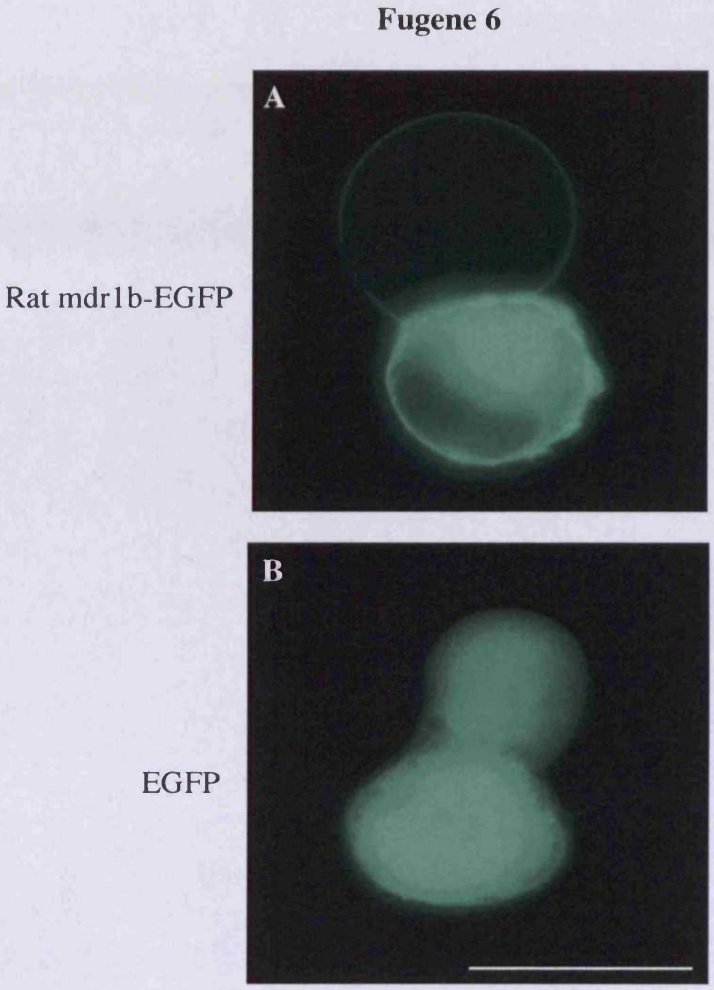

Figure 4.14. Fugene 6 transfection of K562 cells with rat mdr1b-EGFP. K562 cells were transfected using Fugene 6 with either 1 μg mdr1b-EGFP plasmid (A) or 1 μg EGFP plasmid (B). Cells were analysed 36 h following transfection. Scale bar= 10 μm.

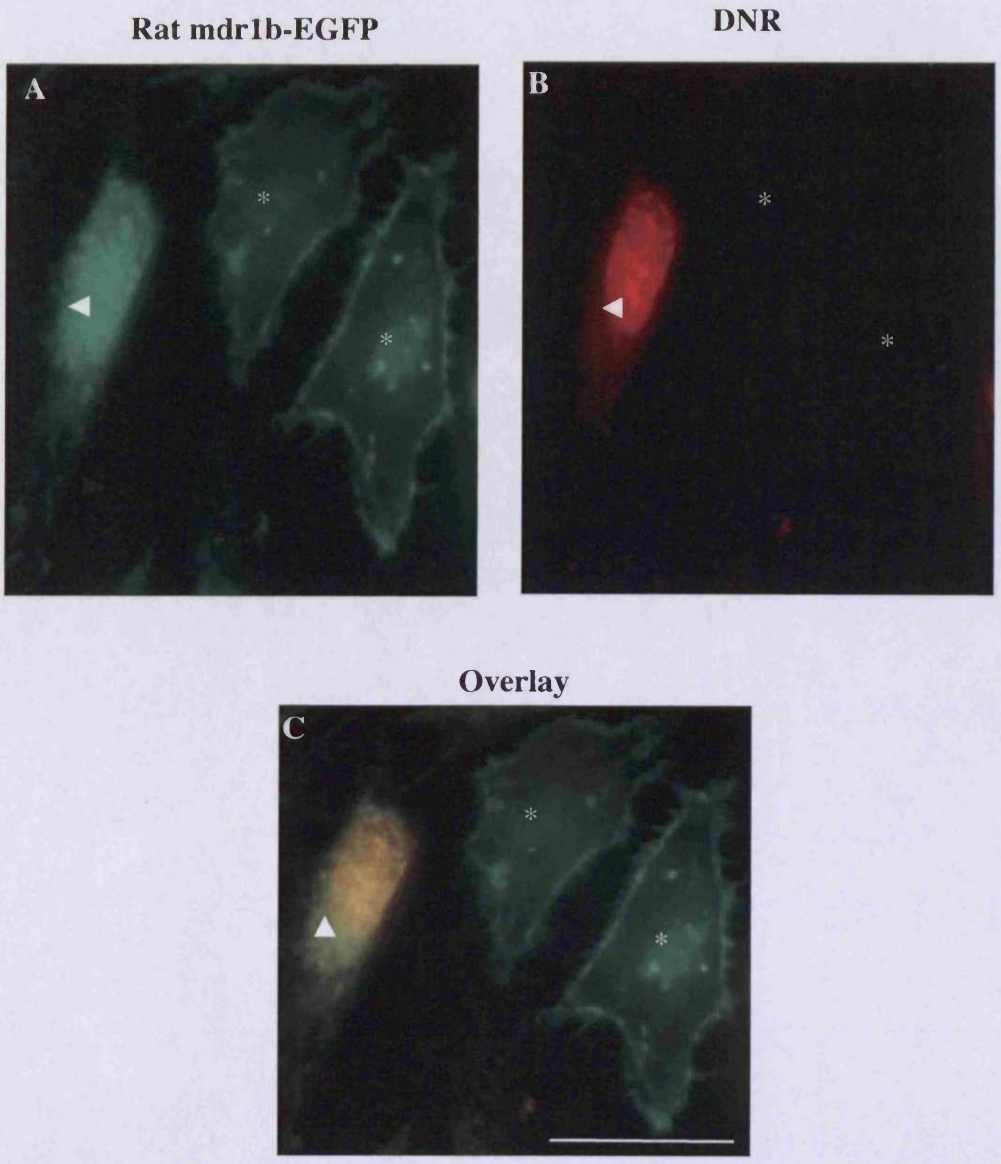

Figure 4.15. Fugene 6 transfection of Hela cells with rat mdr1b-EGFP. Hela cells were subjected to Fugene 6 transfection with 1 μg mdr1b-EGFP plasmid (A). After 24 h, DNR (2 μg/ml) was incubated with transfected cells for 1 h (B). The mdr1b-EGFP and DNR images were then overlayed (C). Arrowhead indicates the bleed through of fluorescence from DNR into the green channel and the asterisk highlights the transfected cells which lack DNR accumulation. Scale bar= 10 μm.

fraction is competent in mediating drug resistance in KG1a cells. Studies with verapamil and cyclosporin A point towards functional intracellular P-gp in these cells, as they both induced the nuclear accumulation of DNR. Functional intracellular P-gp has been previously demonstrated in KG1a cells (Marks et al., 1996; Lautier et al., 1997; Fardel et al., 1998; Ferrao et al., 2001). As both verapamil and cyclosporin A have multiple effects on drug resistance, irrespective of P-gp, we tested their effects on DNR distribution in K562 cells, which lack P-gp expression. Only verapamil appeared to disrupt the perinuclear labelling in K562 cells and an apparent increase in cellular levels of DNR were also observed, although FACS analysis is needed to verify this. This effect may be due to verapamil-mediated reduction in intracellular pH which aids drug accumulation (Hamilton et al., 1993).

Treatment of KG1a cells with wortmannin led to a similar redistribution of both P-gp and DNR. However, this does not necessarily imply that these are located within the same compartment as the effects of wortmannin are widespread and several endocytic structures such as RE, LE and lysosomes may be affected (Martys et al., 1996; Reaves et al., 1996; Mousavi et al., 2003). Despite the redistribution of P-gp by wortmannin, there was no apparent effects on its function. A likely explanation is that the redistribution of P-gp positive vesicles occurred in these cells from an intracellular pool with little contribution from the plasma membrane. Wortmannin is more likely to have bigger effects in other cell lines that support the majority of P-gp on the plasma membrane.

In this study, DNR was shown to be sequestered in lysosomal structures in KG1a cells and very little nuclear associated drug was observed. Substantial evidence that these DNR harbouring organelles were lysosomes came from studies with nigericin and bafilomycin A1 and from the confocal observations of the colocalisation of DNR with dextran. DNR sequestration appeared to be independent of P-gp as neither verapamil or cyclosporin A disrupted the observed vesicular localisation of DNR. In agreement with our findings, Lautier and co-workers were also unable to disrupt this labelling with another P-gp inhibitor PSC833 or verapamil. However in contrast to our results, they failed to see any

effects with nigericin (Lautier et al., 1997). Ferrao and co-workers also found DNR to be sequestered within vesicular structures in KG1a cells, although they attributed this to P-gp mediated sequestration, having shown that they could disrupt this labelling by treating cells with cyclosporin A and verapamil (Ferrao et al., 2001). To our knowledge this is the first time that the DNR sequestering compartment in KG1a cells has been identified as the lysosomes both directly via colocalisation studies and indirectly by the use of pharmacological agents.

Drug sequestration also occurred in K562 cells although DNR distribution was markedly different in these cells compared to KG1a cells and DNR was localised to a dense perinuclear compartment in contrast to the vesicular labelling observed in KG1a cells. This compartment was also identified as lysosomes. The lysosomal accumulation of DNR in K562 cells has been reported previously. Slapak and co-workers identified lysosomal sequestration after they selectively modulated thew dynamics of cellular compartments with pharmacological agents. They found that chloroquine selectively enlarged both the lysosomal and DNR sequestering compartment, but had no effect on the mitochondrial compartment and from this concluded that the drug was sequestered in lysosomes (Slapak et al., 1992). In agreement with this, Loetchutinat and co-workers demonstrated colocalisation between DNR and lysotracker blue probe using confocal microscopy (Loetchutinat et al., 2001). However, a more recent study by Gong and co-workers contradicts these studies as they reported diffuse cytosolic and nuclear labelling of DNR in K562 cells; they also claimed that DNR was sequestered in mitochondria of MDR K562 cells (Gong et al., 2000).

The contribution of drug sequestration to drug resistance in K562 cells has been strongly debated. Loetchutinat and co-workers found that lysosomal sequestration alone cannot account for drug resistance as both the sensitive and resistant cell lines appear to display lysosomal sequestration (Loetchutinat et al., 2001). This is not unique to K562 cells as only drug sensitive uterine sarcoma cells sequester drugs whereas no sequestration is observed in drug resistant cells (Wang et al., 2000). However, this is not a universal phenomenon, as a redistribution of drugs from the nucleus and cytoplasm and into endocytic structures is often

observed in MDR cells (Gervasoni et al., 1991; Rutherford & Willingham, 1993; Hurwitz et al., 1997; Altan et al., 1998; Bour-Dill et al., 2000; Gong et al., 2003). In HL-60 leukaemia cells, very little vesicular DNR was observed and the drug was strongly localised to the nucleus. However, significant lysosomal sequestration was observed in the resistant cell line and the authors go on to show that this is due to pH alterations (Gong et al., 2003). The intralysosomal pH of sensitive cells was 6.44 but was 5.17 in resistant cells. This strongly suggests that the orchestration and control of endocytic pathways are affected during attainment towards a MDR status. It also points to fundamental differences in these cells with respect to the activity of the sensitive cell lines to sequester DNR.

Using studies with DNR, endocytic probes and antibodies against endocytic organelles, this study showed that the arrangement of late endosomes and lysosomes were very different between KG1a and K562 cells. This may point to their differing haemopoietic lineages or their mutated genes. A change from vesicular lysosomal labelling (as observed in KG1a cells) to a dense perinuclear compartment (as observed in K562 cells) may also be a product of differing cytosolic pH between these cells. When the cytoplasmic pH increases, as is often seen in MDR cells, there is an alteration in the lysosome morphology, from vesicular structures to dense perinuclear compartment (Heuser, 1989). This alteration in lysosome morphology has been observed between drug sensitive U937 cells and their MDR counterpart U-A10 (Hurwitz et al., 1997). Interestingly in these cells lysosomal sequestration contributes a great deal to drug sequestration, despite cell surface expression of P-gp. It may be that this lysosomal configuration is optimal for drug sequestration or it may reflect an expansion in the quantity and size of the lysosomes often seen in MDR cells (Ouar et al., 2003).

The intense labelling of the nuclear membrane with DNR was consistently observed in both cell lines and raises the possibility that a permeability barrier exists for this drug on the nuclear envelope. Although in the previous chapter no nuclear labelling of P-gp was evident but this may be due to the limitations of epifluorescence microscopy as confocal microscopy clearly showed this phenomenon. P-gp expression on nuclear membranes has been shown in MDR

MCF-7 cells where it is believed to be active in drug exclusion from the nucleus (Calcabrini et al., 2000). Conversely, the nuclear envelope may itself sequester DNR from its target site. One study has shown that nuclear transport of cells in suspension is greatly reduced when compared to that of flattened adherent cells (Feldherr & Akin, 1993), and this may explain the inability of DNR to cross the nuclear membrane in these cells.

During the course of this study, Gong and co-workers claim to have identified for the first time the existence of two distinct mechanisms of sequestration in MDR HL-60 cells. They observed that DNR accumulated in lysosomes whereas SR101 accumulated in the Golgi via MRP mediated transport (Gong et al., 2003). However, these studies were performed using epifluorescence micrsocopy and as this study shows in figure 4.15, great care must be taken in the interpretation of data. It was only by using confocal microscopy and sequential scanning that this thesis was able to clearly show colocalisation of DNR with dextran in lysosomes (Figure 4.7). This present study also identified differential sequestration of DNR and SR101 in KG1a and K562 cells and revealed differences in SR101 sequestration between KG1a and K562 cells. DNR was sequestered in lysosomes in both cells lines but in KG1a cells SR101 localised into vesicular structures and this labelling was sensitive to P-gp inhibitors. K562 cells appeared to sequester SR101 within a brefeldin A sensitive compartment (presumably the Golgi) and Gong and co-workers also reported the Golgi localisation of SR101 in resistant HL-60 cells. However, they attributed this localisation to MRP whose expression was dramatically increased compared with drug sensitive cells. As K562 cells have been shown to be deficient in both P-gp and MRP (Fardel et al., 1998), it is unlikely that MRP mediates these effects. Thus this Golgi localisation may be a passive process, but if this was the case, then SR101 should also accumulate in the Golgi of KG1a cells yet this was not observed. It may therefore be that the transporter function of P-gp is a more powerful determinant of SR101 localisation. This demonstrates that KG1a and K562 cells also have the capacity to sequester drugs by different mechanisms leading to their localisation in distinct organelles.

Challenging cells with drugs for extended periods of time results in the generation of MDR cells that often express increased levels of P-gp. However, MDR is a multifaceted phenomenon and the expression of many proteins may be affected during progression to MDR status. Alternatively, the contribution of P-gp to MDR could also be studied if cell lines could be generated that transiently over-express MDR-1. Tagging a fluorescent protein to the drug transporter would then allow easy analysis of both expression levels and localisation by direct fluorescent microscopy. It would also allow comparison of DNR uptake between transfected and untransfected cells. In KG1a cells it was also of interest to ascertain whether expression of P-gp beyond the high endogenous levels would maintain the high intracellular/plasma membrane localisation ratio that is characteristic of this cell line.

Rat MDR-1-EGFP vector was utilised for these studies but despite employing a number of transfection methods and many different parameters within each method, it was not possible to achieve levels of transfection higher than 1 %. The refractory nature of these cells to physical and chemical methods of transfection has previously been reported and only by using viral vectors could transfection efficiency be increased (Roddie et al., 2000). The results with Fugene 6 were very unexpected, however the use of the empty EGFP vector quickly demonstrated that this was a methodological rather than a P-gp phenomenon. Electroporation has however been successfully employed to transfect blood cells (Toneguzzo & Keating, 1986; Van Tendeloo et al., 2000; Li et al., 2001; Wu et al., 2001), although this method also resulted in low transfection efficiencies. The refractory nature of these cells may be due to their primitive haemopoietic status or it maybe that suspension cells do not maintain good contact with the DNA complex (Marit et al., 2000).

The transient transfection studies did allow, for the first time, analysis of the subcellular localisation of this protein in leukaemia cells. Interestingly in both cell lines, the protein was extensively localised to the plasma membrane suggesting that in KG1a cells, the traffic mechanisms exist for delivering P-gp to this location. It would be interesting to observe whether upregulation of P-gp expression by drug

challenge also results in significant plasma membrane labelling. Of note also was the fact that the rat variant was trafficked to the plasma membrane; this suggests that the signals and machinery for traffic from the endoplasmic reticulum to the plasma membrane are retained within species. Owing to the low transfection efficiencies further attempts to determine the uptake and distribution characteristics of DNR and SR101 in these cells was not persued. However, DNR uptake was assessed when Hela cells were transfected with the same plasmid. Despite the photobleeding problems that were encountered with DNR it was clear that rat MDR-1 was trafficked to the plasma membrane of these cells and more importantly it was functional in this human cell line. There are however issues over using this rat P-gp variant for drug studies as there may be differences between the MDR profiles and substrate specificities between species and ideally the human variant should be used (Tang-Wai et al., 1995).

In conclusion, this study has identified two mechanisms of drug resistance operating in KG1a cells; P-gp-mediated drug exclusion from the nucleus and possibly even drug sequestration within verapamil and cyclosporin A sensitive vesicles and within lysosomes, which occurs irrespective of P-gp. In K562 cells, drug sequestration alone, within lysosomes and the Golgi, appears to be effective at preventing nulear accumulation of the drug. However, the redistribution of P-gp in KG1a cells using wortmannin failed to produce a noticeable increase in the nuclear accumulation of DNR. The study then focused on the cellular uptake and intracellular fate of PTD to evaluate their potential as resistance modulators in these cells.

Chapter 5:

Evaluation of the Mechanism of Uptake of Protein Transduction Domains

5.1 Introduction

Several strategies have been developed to attempt circumvention of P-gp mediated resistance (described in section 1.5). However, these strategies have had fairly limited success in the clinic. Much effort is still devoted towards achieving effective inhibition of P-gp. An alternative strategy is to deliver a therapeutic agent into a cell using the cells endocytic pathway. This macromolecular approach is less likely to be affected by P-gp and other drug transporters. However, biological barriers such as the plasma and endosomal membranes, pose major hurdles to this drug delivery strategy and there has been extensive searching for molecules that may act as vectors to overcome these hurdles. Endogenous ligands for plasma membrane receptors such as Tf, can be used to overcome this but their use is constrained by the fact that they remain inside the endocytic pathway throughout their traffic inside the cell and so cannot be used to deliver an agent into the cytosol. PTDs represent a group of peptides that have received widespread interest in drug delivery research. They are characterised as being highly cationic and several reports suggest that they are able to enhance the uptake of small and large molecules that are either associated with them via ionic interactions or are covalently bound. Another important feature of these peptides is their ability to overcome drug resistance. Mazel and co-workers showed that doxorubicin conjugated to SynB1, which is derived from the antimicrobial peptide protegrin 1 and penetratin, were able to overcome drug resistance *in vitro* in MDR K562 cells (Mazel et al., 2001). A separate study showed that Tat Peptide and a Tat-GFP conjugate were efficiently taken up by primary haematopoietic cells including $CD34^+$ variants (Lea et al., 2003). These peptides may therefore prove valuable in diseases such as AML and CML.

Two PTD were utilised in this study, Tat and R_8. Tat protein is a ribonucleic acid binding protein that regulates transcription and is essential for the replication of HIV-1. Exogenous Tat has the capacity to enter the cell and localise to the nuclear compartment where it mediates its function. The Tat peptide sequence is comprised of many arginine residues and it was found that deletion of a single arginine impaired uptake severely and so arginine was shown to be essential for translocation (Wender et al., 2000). Therefore various homopolymers

of arginines were investigated for their potential to transduce their cargo. Futaki and co-workers studied the relationship between the number of arginines and transduction efficiency and found that R_8, an octamer of arginines, displayed optimal transduction efficiency (Futaki et al., 2001) and this was also adopted for this study.

Initial studies towards the understanding of mechanisms of PTD uptake commonly adopted the use of both pharmacological modulators and low temperatures to inhibit various mechanisms of endocytosis. Vives and co-workers reported no difference in cellular uptake of Tat when inhibitors of caveolae and non-coated vesicle endocytosis were used (Vives et al., 1997). Suzuki and co-workers demonstrated the inability of inhibitors of macropinocytosis and caveolae dependent endocytosis, to effect the uptake of the PTD Rev, Tat and R_8 (Suzuki et al., 2002). Derossi and co-workers ruled out endocytosis as an uptake mechanism of penetratin, as uptake was unaffected at 4 °C (Derossi et al., 1996). In agreement with this, Futaki and co-workers also demonstrated that uptake of Rev was temperature insensitive (Futaki et al., 2001). There was therefore a general concensus from these initial studies that PTD exploit a non-endocytic mechanism of uptake. This mechanism may correspond to one of the transduction mechanisms described in section 1.8.1. Indeed, Derossi and co-workers proposed that the inverted micelle model may be accountable for penetratin uptake (Derossi et al., 1996). Following internalisation, nuclear localisation of PTD and full length protein alike was also consistently observed either by fluorescence microscopy (Elliott & O'Hare, 1997; Futaki et al., 2001; Suzuki et al., 2002) or by quantification of radiolabelled protein in isolated nuclei (Frankel & Pabo, 1988).

However, many of the previous studies on the mechanisms of uptake and intracellular fate of PTD were invalidated following the revelation by Richard and co-workers, who demonstrated that flow cytometry could not be used to evaluate cellular uptake without first treating the cells with a proteinase such as trypsin (Richard et al., 2003). They revealed that a majority of the peptide that was quantified by flow cytometry was bound to the plasma membrane, thus flow cytometry overestimated the amount of peptide internalised by cells. The data also

explained in part why there were so many reports of efficient peptide uptake when cells and PTD were co-incubated at 4 °C. This study and another also demonstrated that VP22 and other PTD were localised to the nuclei in fixed cells but were localised in vesicles by microscopy in the absence of any fixative (Lundberg & Johansson, 2002).

In light of these revelations, there was a major reevaluation of the mechanism of uptake and cellular localisation of PTD. As pharmacological inhibitors of endocytosis inhibit peptide uptake and and cell localised peptides are often observed in vesicles, there is now a general concensus that endocytosis is a major contributing factor to internalisation of PTD (reviewed in Vives, 2003). However the exact endocytic mechanism appears to differ considerably between studies. Drin and co-workers investigated SynB and penetratin uptake in K562 cells and reported temperature sensitive uptake by fluid phase endocytosis (Drin et al., 2003). Nakase and co-workers found that R_8 is taken up by macropinocytosis in HeLa cells (Nakase et al., 2004). In agreement, Kaplan and co-workers also demonstrated the macropinocytic uptake of Tat in namalwa cells (Kaplan et al., 2005). Two studies have described the internalisation of Tat via caveolae in a HeLa derived cell line, HL3T1, and CHO cells (Ferrari et al., 2003; Fittipaldi et al., 2003). Whilst other studies reported Tat protein and peptide internalisation by clathrin-mediated endocytosis (Vendeville et al., 2004; Richard et al., 2005).

There is however very little information regarding the nature of the endocytic structures that contain PTD following endocytic capture. Less still is known about the intracellular fate of these molecules. Vendeville and co-workers localised the Tat protein to LE by co-localisation studies with the mannose-6-phosphate receptor in Jurkat cells (Vendeville et al., 2004). Richard and co-workers identified Tat in acidic cellular compartments in HeLa cells (Richard et al., 2005). Conversely, Fischer and co-workers reported the Golgi localisation of Tat in HeLa cells as shown by co-localisation studies with the Golgi marker ceramide (Fischer et al., 2004). Several studies have also shown co-localisation between PTD and Tf in HeLa cells (Potocky et al., 2003; Richard et al., 2003) and fibroblasts (Ross et al., 2004). In the absence of fixing, PTD have still been shown

to localise to the cytoplasm and nucleus. Two studies have also shown the nuclear localisation of R_7 (Mitchell et al., 2000) and Tat protein (Vandeville et al., 2004) in Jurkat cells, irrespective of fixing. Despite the inclusion of a trypsinisation step, Thoren and co-workers also demonstrated uptake of various PTD at 4 °C and their nuclear localisation in unfixed V79 cells (Thoren et al., 2003). Thus several questions remain unanswered regarding the cellular dynamics of these peptides.

Fluorescent conjugates of Tat and R_8 were investigated. The peptides were synthesized in the laboratory of Professor Shiroh Futaki and this group has extensively studied and compared a number of PTD including Tat, penetratin and synthetic peptides containing various numbers of arginine residues (R_4-R_{16}). The aims of this study was to investigate the uptake and cellular dynamics of Tat and R_8.

5.2 Methods

Quantification of cellular uptake of 3 μM alexa-488-Tat and 1 μM alexa-488-R_8 at 4 and 37°C was carried out in K562 cells as described in section 2.3.12.2. Cell-associated fluorescence was measured at 0, 5, 15, 30, 60 and 120 min by flow cytometry as described in section 2.3.12.2.

To examine the effect of endocytosis inhibitors on peptide uptake, K562 cells were treated with 150 nM wortmannin, 10 μM EIPA, 10 μM nocodazole, 50 μM cytochalasin D as described in section 2.3.12.1. The effects of 5 and 10 mM methyl-β-cyclodextrin on Tat and R_8 uptake were also investigated by pretreating cells with the drug for 30 min, leaving cells to recover for 30 min, followed by a 1 h incubation with the peptide in the absence of the drug. Due to the instability of wortmannin in cell media, wortmannin treated cells were centrifuged after 30 min of peptide incubation and resuspended in fresh drug and peptide. Control cells were incubated with the respective diluent (DMSO for wortmannin, nocodazole and cytochalasin D, methanol for EIPA and dH_2O for methyl-β-cyclodextrin). All the drugs used have been shown to affect endocytosis at the concentrations used in this study. EIPA and cytochalasin D (an inhibitor of actin polymerisation) are inhibitors of macropinocytosis (Zhuang et al., 1984; Sampath & Pollard, 1991).

Wortmannin is an inhibitor of macropinocytosis and fluid phase endocytosis (Clague et al., 1995; Araki et al., 1996). Nocodazole, an inhibitor of microtubule polymerisation, has been shown to cause a 20 % reduction of endocytosis of transferrin in K562 cells (Jin & Snider, 1993). Methyl-β-cyclodextrin extracts cholesterol from the cell membrane and has been shown to inhibit clathrin and caveolae mediated internalisation (Rodal et al., 1999; Thomsen et al., 2002) and macropinocytosis (Grimmer et al., 2002). Cells were then analysed by flow cytometry as described in section 2.3.12.1.

To determine the cellular localisation of 3 μM alexa-488-Tat and TxR-R_8, cells were treated with the peptides as described in section 2.3.9.2.6. The effect of 150 nM wortmannin on the distribution of 3 μM alexa-488-Tat and TxR-R_8 in KG1a cells and 3 μM alexa-488-Tat and 1 μM alexa-488-R_8 in K562 cells, was analysed by pretreating the cells for 15 min with wortmannin and then incubating with the peptide in the continued presence of the drug for a further 1 h. Cells were analysed by epifluorescence microscopy and representative examples are shown in each case.

To investigate the effect of temperature on peptide distribution, cells were treated as described in section 2.3.9.2.6 then analysed by epifluorescence microscopy.

5.3 Results

5.3.1 Distribution of alexa-488 Tat and TxR-R_8 in KG1a and K562 cells

Initially, the distribution of alexa-488-Tat and TxR-R_8 was assessed in KG1a and K562 cells. Both cell lines were treated with 3 μM of peptides for 1 h at 37 °C. In KG1a cells both Tat and R_8 were localised in small diffuse cytoplasmic vesicles (Figure 5.1A and B respectively). In K562 cells both peptides were enriched to vesicles in a dense perinuclear compartment (Figure 5.1C and D respectively. Interestingly, the profiles for R_8 and Tat mirrored those for DNR labelling in both cells. No apparent nuclear or cytosolic labelling was observed for either peptide in both cell lines.

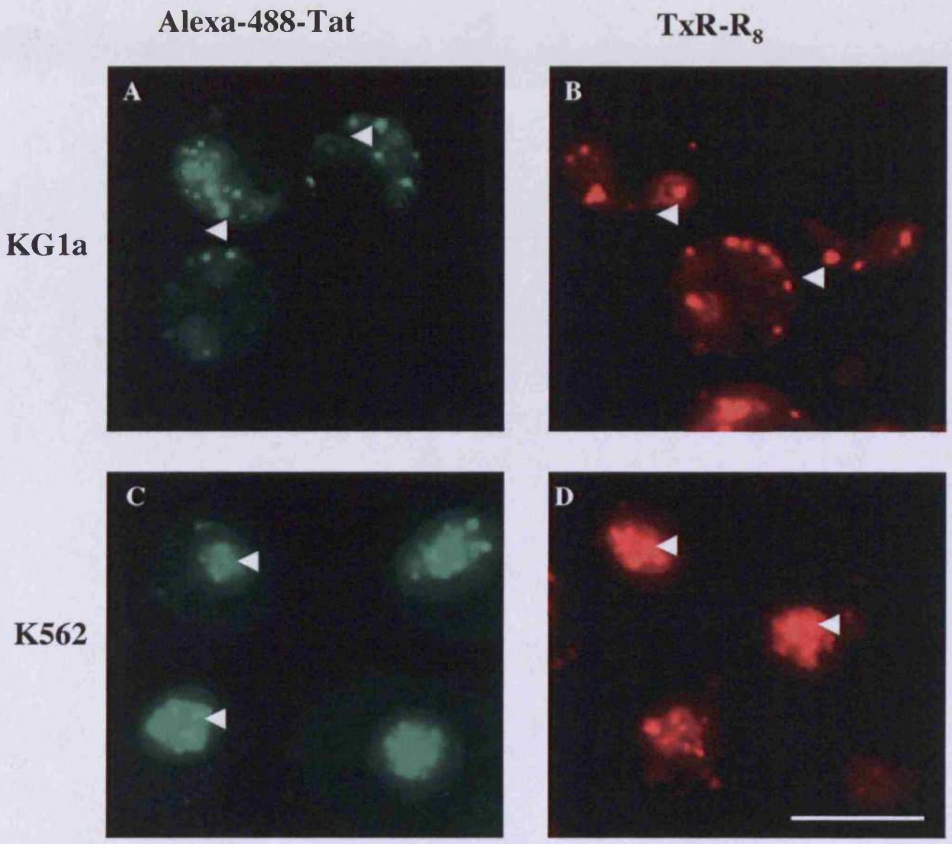

Figure 5.1. Distribution of alexa-488 Tat and TxR-R_8 in KG1a and K562 cells. KG1a (A and B) and K562 (C and D) cells were incubated with alexa-488-Tat (A and C) or TxR-R_8 (B and D) for 1 h at 37 °C. Arrowheads indicate the peptide labelled structures. Scale bar= 10 μm.

5.3.2 Time dependent uptake of alexa-488-Tat and -R_8 in KG1a and K562 cells

Flow cytometry was used to assess uptake of these peptides at various time points up to 2 h. Trypsin treatment of peptide loaded cells, followed by heparin washes were incorporated into the protocol to remove surface bound peptide. KG1a and K562 cells were incubated with either 3 μM alexa-488-Tat or 1 μM alexa-488-R_8 for 0-120 min, incubated with trypsin and washed with heparin then analysed by flow cytometry. The results in Figure 5.2A show that in KG1a cells there was a rapid increase in cell uptake of both peptides but whilst R_8 uptake had plateaued by 30 min, Tat uptake did not plateau even after 120 min. In K562 cells (Figure 5.2B), uptake was initially much slower for both peptides when compared to KG1a cells and then continued at approximately this rate up to 2 h. There was less of a peptide effect with these cells as comparable levels of peptides were observed at the final time point.

5.3.3 Effect of temperature on uptake of alexa-488-Tat and -R_8 in KG1a and K562 cells

The effect of temperature on peptide uptake was then investigated by treating cells with 3 μM alexa-488-Tat or 1 μM alexa-488-R_8 at either 4 or 37 °C for 1 h prior to processing for flow cytometry. The results are expressed as histogram plots of fluorescence intensity (x-axis) versus number of cells (y-axis) in Figure 5.3. At 5 min in KG1a cells, there was appreciable uptake of both Tat (Figure 5.3A, black line) and R_8 (Figure 5.3C, black line) at 37 °C, although Tat uptake displayed considerable heterogeneity, with a small population of cells taking up much higher levels of Tat. At 4 °C a large population of KG1a cells incubated with Tat displayed only background levels of fluorescence, however, a small population of cells had taken up much higher levels of fluorescence, which in some cells is comparable to that at 37 °C (Figure 5.3A, grey line). A similar pattern was observed with R_8, with some cells displaying only background levels of fluorescence, whilst the fluorescence levels in other cells exceeded that at 37 °C (Figure 5.3C, grey line). At 1 h, there was an increase in fluorescence of both Tat and R_8 at 37 °C, although a greater fluorescence shift was observed for Tat (Figure 5.3B, black line) when compared to R_8 (Figure 5.3D, black line). Surprisingly, a similar increase in fluorescence was also evident at 4 °C and though there was

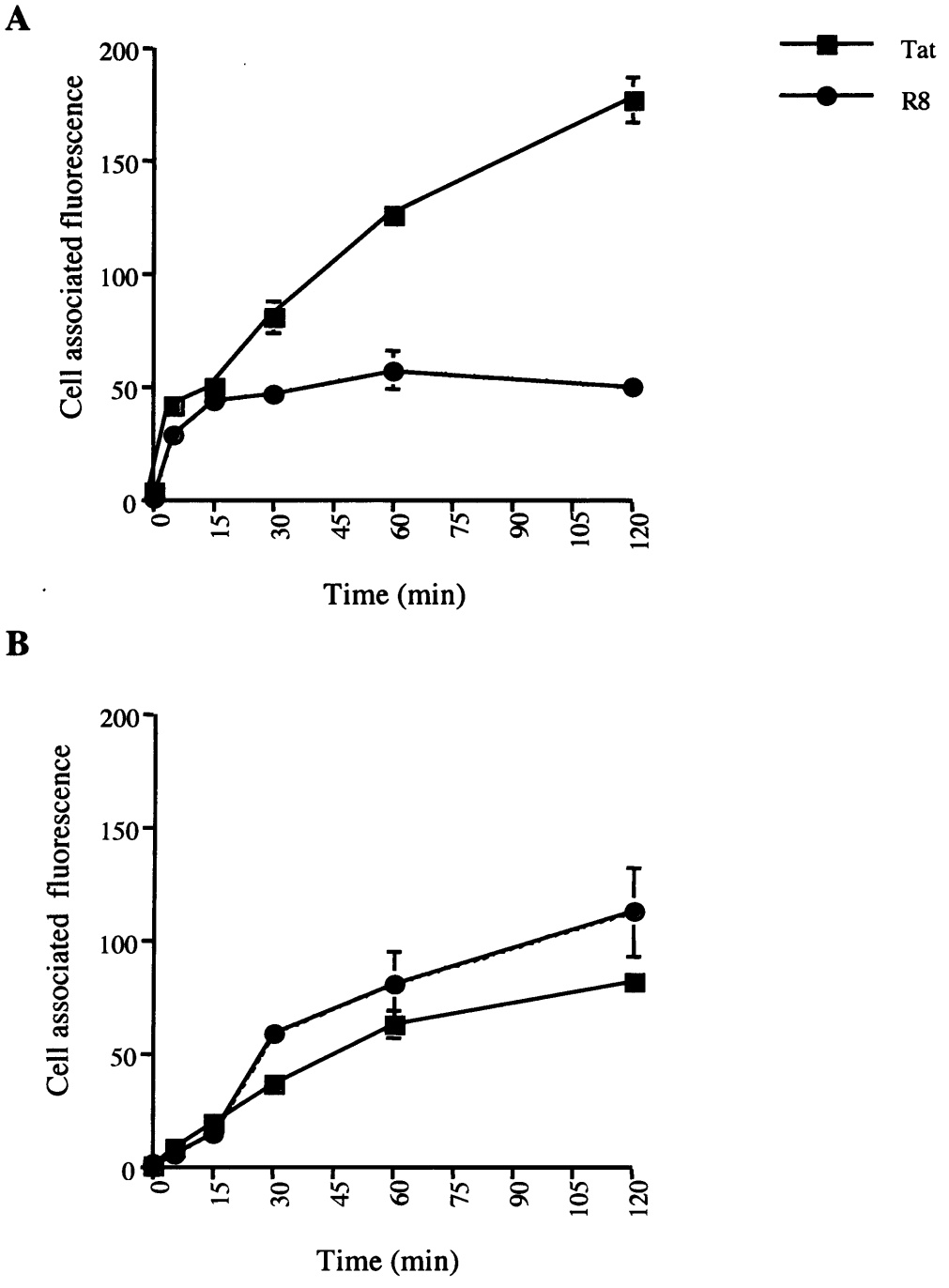

Figure 5.2. Time dependent uptake of alexa-488 Tat and $-R_8$ in KG1a and K562 cells. KG1a (A) and K562 (B) cells were incubated with alexa-488 Tat (squares) and $-R_8$ (circles) for 2 h at 37 °C. Cells were washed with trypsin and heparin then analysed by FACS. Each point is the mean ±SD of three experiments. For each point, the mean fluorescence intensity of cells alone was substracted from the fluorescence of cells incubated with the peptide.

considerable heterogeneity, with some cells displaying background levels of fluorescence, a large population of cells has fluorescence values that exceeded those incubated at 37 °C (Figure 5.3B and D respectively, grey lines).

Very different profiles were observed in K562 cells. There was again considerable uptake of Tat and R_8 at 37 °C after 5 min (Figure 5.3E and G respectively, black lines), but at lower levels than that observed in KG1a cells under the same conditions. At 4 °C, heterogeneity was again evident for Tat and R_8 (Figure 5.3E and G respectively, grey line), with some cells displaying only background fluorescence whilst others, although a minority, had fluorescence comparable to that observed at 37 °C (Figure 5.3E and G respectively, grey lines). At 1 h, there was a further increase in fluorescence at 37 °C for Tat (Figure 5.3F, black line) and R_8 (Figure 5.3H, black line), although unlike KG1a cells, there was higher uptake of R_8 compared to Tat. At 4 °C, there did not seem to be an appreciable shift in fluorescence of Tat or R_8 compared to that seen at 5 min (Figure 5.3F and H respectively, grey lines).

5.3.4 Effect of temperature on alexa-488-Tat and TxR-R_8 distribution in KG1a and K562 cells

The unexpected observation of significant peptide uptake at 4 °C, especially in KG1a cells, prompted further investigation using fluorescence microscopy. Cells were incubated with 3 μM alexa-488-Tat or TxR-R_8 for 1 h at either 4, 16 or 37 °C. Analysis of peptide distribution at 16 °C was chosen as this temperature allows uptake from the plasma membrane but inhibits delivery from EE to LE and lysosomes (van Dam & Stoorvogel, 2002) and these experiments may therefore give clues as to the possible localisation of the peptides. At 4 °C in KG1a cells, diffuse labelling of both Tat and R_8 was observed (Figure 5.4A and D respectively), although some labelling of the plasma membrane was also seen with R_8. At 16 °C, the same diffuse labelling is observed but with higher intensity for both Tat and R_8 (Figure 5.4B and E respectively) although no vesicular labelling was apparent at this temperature. Owing to the limitations of epifluorescence microscopy, it is difficult to determine whether the diffuse labelling seen for both peptides at 4 and

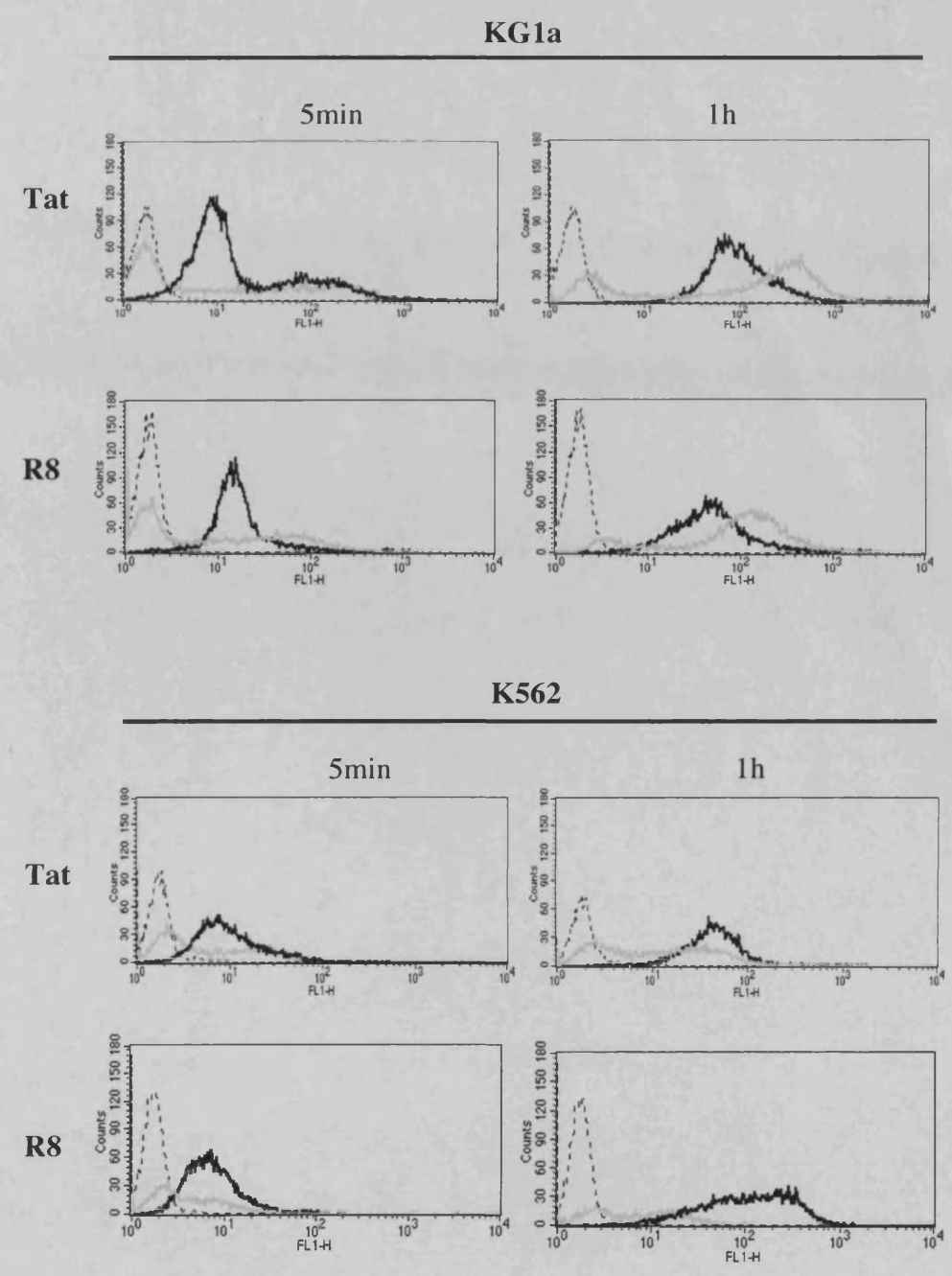

Figure 5.3. Temperature dependent uptake of alexa-488 Tat and $-R_8$ in KG1a and K562 cells. KG1a (A-D) and K562 cells (E-H) were incubated for 5 min (A, C, E and G) or 60 min (E, D, F and H) with Tat (A, B, E and F) or R_8 (C, D, G and H) at either 4 °C (grey line) or 37 °C (black line). Background fluorescence was indicated by the dotted line.

16 °C represents the plasma membrane or whether any is localised to the cytosol. At 37 °C, as expected, vesicular labelling of Tat and R_8 was observed (Figure 5.4C and F respectively). At 4 °C in K562 cells, diffuse labelling was again observed for Tat, with some cells also showing bright spots of fluorescence on the cell surface (Figure 5.4G). Distinct plasma membrane labelling with R_8 was observed, in addition to diffuse labelling (Figure 5.4J). At 16 °C, more intense diffuse labelling was observed for both Tat and R_8 but again no vesicular labelling was seen (Figure 5.4H and K respectively). At 37 °C, there was distinct labelling of a dense perinuclear compartment for both Tat and R_8 (Figure 5.4I and L respectively).

5.3.5 Effect of EIPA, nocodazole, wortmannin, cytochalasin D and methyl-β-cyclodextrin on alexa-488-Tat and -R_8 uptake in K562 cells

To gain further information about the mechanism of uptake of alexa-488-Tat and -R_8, K562 cells were pretreated with the endocytosis inhibitors EIPA, nocodazole, wortmannin, cytochalasin D or methyl-β-cyclodextrin and then incubated with either 3 μM alexa-488-Tat (Figure 5.5A) or 1 μM alexa-488-R_8 (Figure 5.5B). EIPA caused a small but significant decrease in Tat uptake of 18 % whilst nocodazole and wortmannin caused a greater decrease of approximately 29 and 40 % respectively. However, the biggest reduction in Tat uptake was observed following treatment with cytochalasin D, where there was almost 80 % reduction in uptake. Treatment of cells with methyl-β-cyclodextrin under the experimental conditions used in this study resulted in significant cell death as identified by trypan blue exclusion, following trypsin treatment and so the effects of this drug could not be tested. EIPA did not inhibit R_8 uptake to any significant effect, whilst nocodazole and wortmannin caused approximately 33 % and 55 % reduction in uptake respectively. Again, cytochalasin D had the greatest inhibitory effect on R_8 uptake, and almost 83 % reduction was observed. To explain the big reduction in uptake of peptides in K562 cells, the effect of cytochalasin D on peptide uptake was subsequently analysed within the lab by a colleague using fluorescence microscopy. It was shown that under the experimental conditions used, selective cell death of cells loaded with larger amounts of peptide had occurred. When cytochalasin D treated cells were visualised immediately after incubation with

the peptide, there was great heterogeneity in peptide loading with many cells displaying strong intracellular fluorescence, whilst others displayed much weaker fluorescence. Following the washing procedure, the cells with high peptide uptake were no longer observed, whilst only cells with weak peptide labelling were seen, hence the apparent large reduction in uptake.

5.3.6 Effect of wortmannin on the distribution of alexa-488-Tat and -R_8 or TxR-R_8 in KG1a and K562 cells

The effect of wortmannin on Tat and R_8 distribution was then examined to assess whether the peptide positive structures were sensitive to this drug. Cells were pretreated with wortmannin, then incubated with 3 μM alexa-488-Tat or 1 μM alexa-488-R_8 for K562 cells or 3 μM alexa-488-Tat and TxR-R_8 for KG1a cells, in the continued presence of wortmannin. In untreated KG1a cells, R_8 was localised to diffuse vesicular structures (Figure 5.6A) whilst in wortmannin treated cells, the peptides were mislocalised from small vesicles to large vacuole like structures (Figure 5.6B). Similarly, Tat in untreated cells, was also localised to diffuse vesicular structures (Figure 5.6D) and was redistributed to enlarged structures in wortmannin treated cells (Figure 5.6E). However, wortmannin had minimal effects on Tat or R_8 distribution in K562 cells as both R_8 and Tat were still localised to a dense perinuclear region in both control (Figure 5.6G and J respectively) and in wortmannin treated cells (Figure 5.6H and K respectively). As the perinuclear staining is so intense in these cells it was difficult to observe any subtle wortmannin effects. Bright field images for KG1a (Figure 5.6C and F) and K562 cells (Figure 5.6I and L) were taken to reveal the magnitude of the swollen vacuole with respect to the dimensions of the cell.

5.4 Discussion

This study aimed to characterise the mechanism of cellular uptake and intracellular localisation of Tat and R_8, in KG1a and K562 cells. Uptake of Tat and R_8 into cells occurs via ionic interactions between the cationic peptides and negatively charged cell surface moieties such as heparan sulphate proteoglycans that are expressed on most cell types (Tyagi et al., 2001; Suzuki et al., 2002; Console et al., 2003). One study has consequently shown that in cells defective for

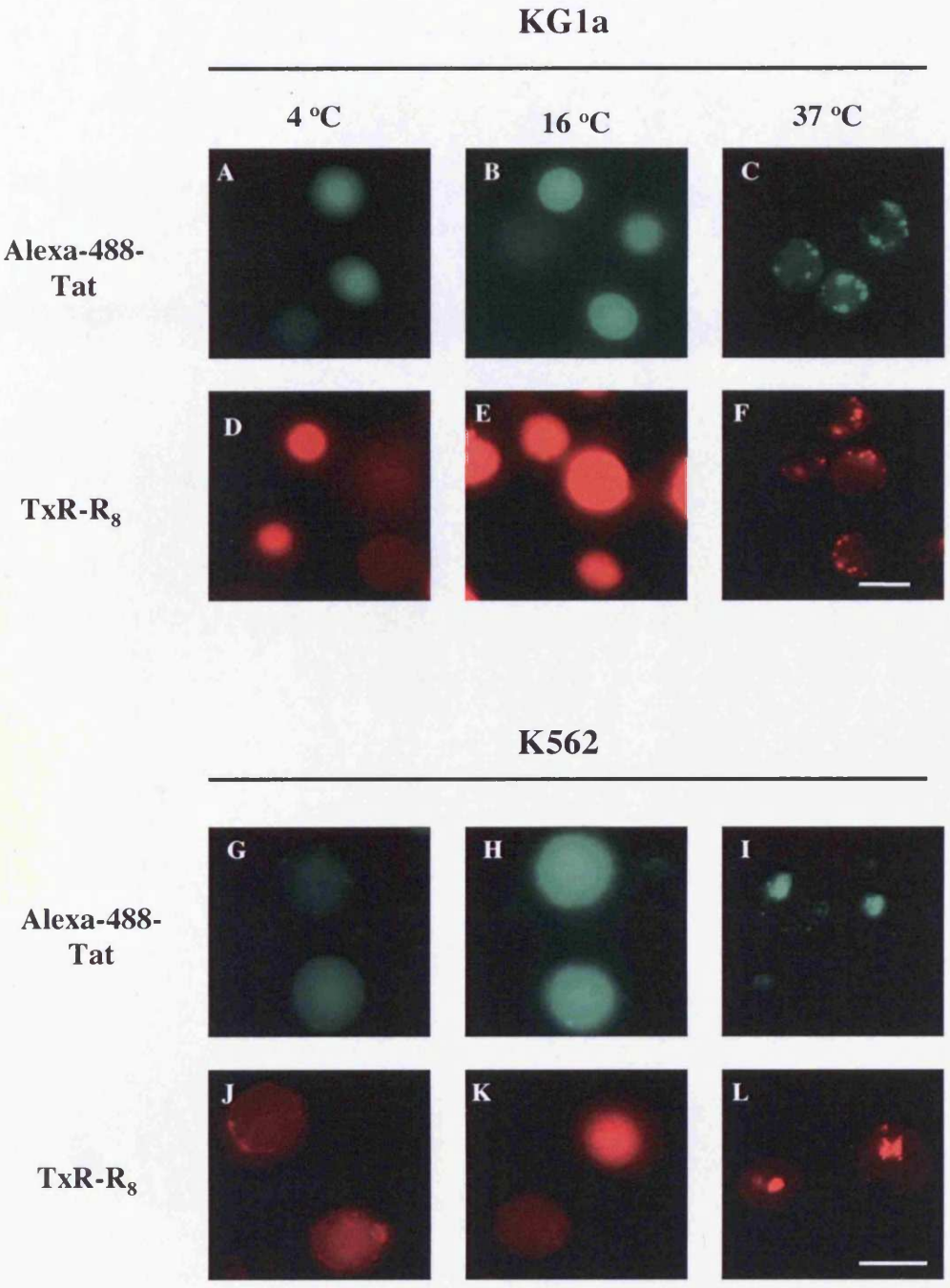

Figure 5.4. Temperature effects the distribution of alexa-488 Tat and TxR-R_8 in KG1a and K562 cells. KG1a (A-F) and K562 (G-L) were incuabted for 1 h with either alexa-488 Tat (A-C and G-I) or TxR-R_8 (D-F and J-L) for 1 h at either 4 (A, D, G and J), 16 (B, E, H and K) or 37 °C (C, F, I and L).

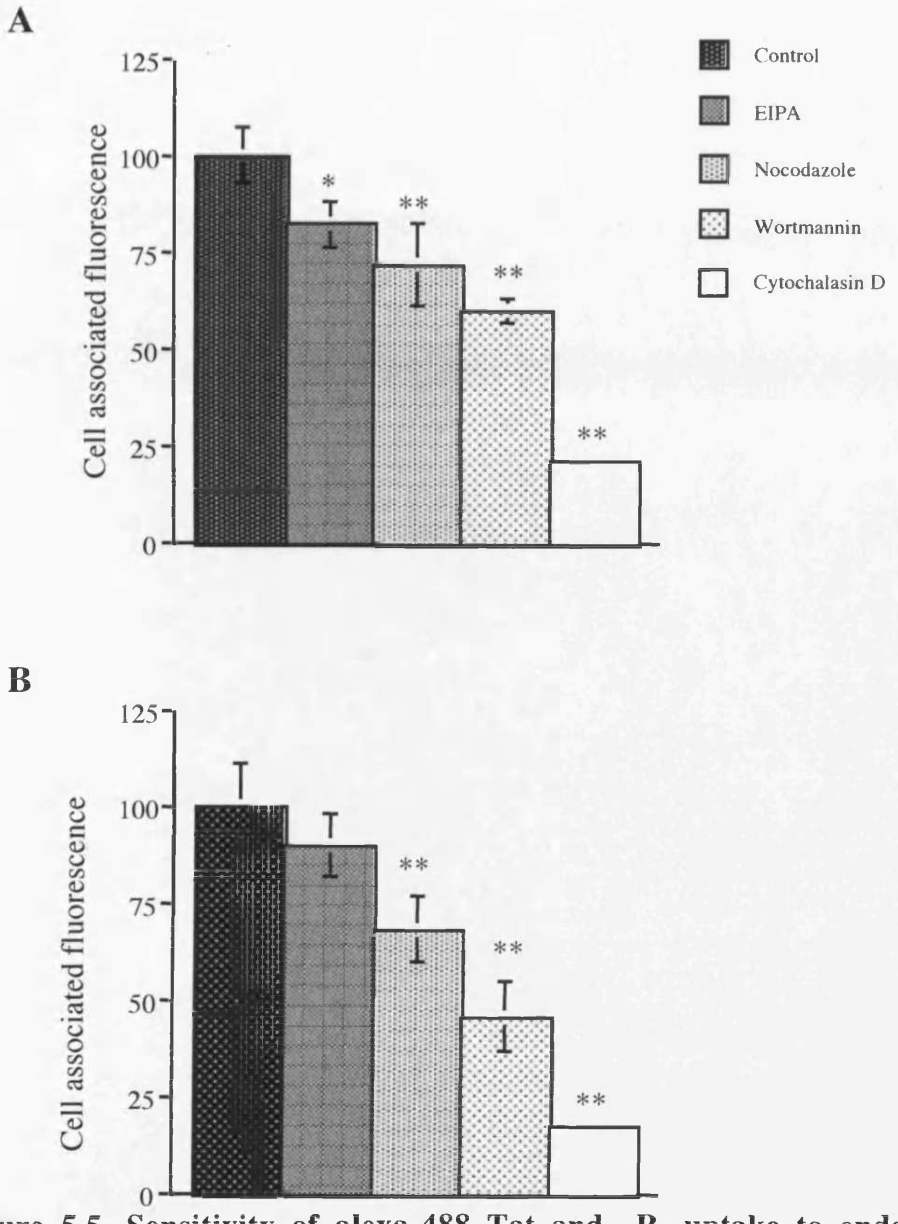

Figure 5.5. Sensitivity of alexa-488 Tat and $-R_8$ uptake to endocytosis modulators. The effects of 10 μM EIPA, 10 μM nocodazole, 150 nM wortmannin and 50 μM cytochalasin D on the accumulation of alexa-488 Tat (A) and R_8 (B) was determined by FACS analysis as described in materials and methods. Each bar is the mean±SD of five experiments. For each point, the mean fluorescence intensity of untreated cells was subtracted from fluorescence obtained with the peptide. Statistical analysis was performed by ANOVA followed by Dunnettes post test, * $p<0.05$ and ** $p<0.01$.

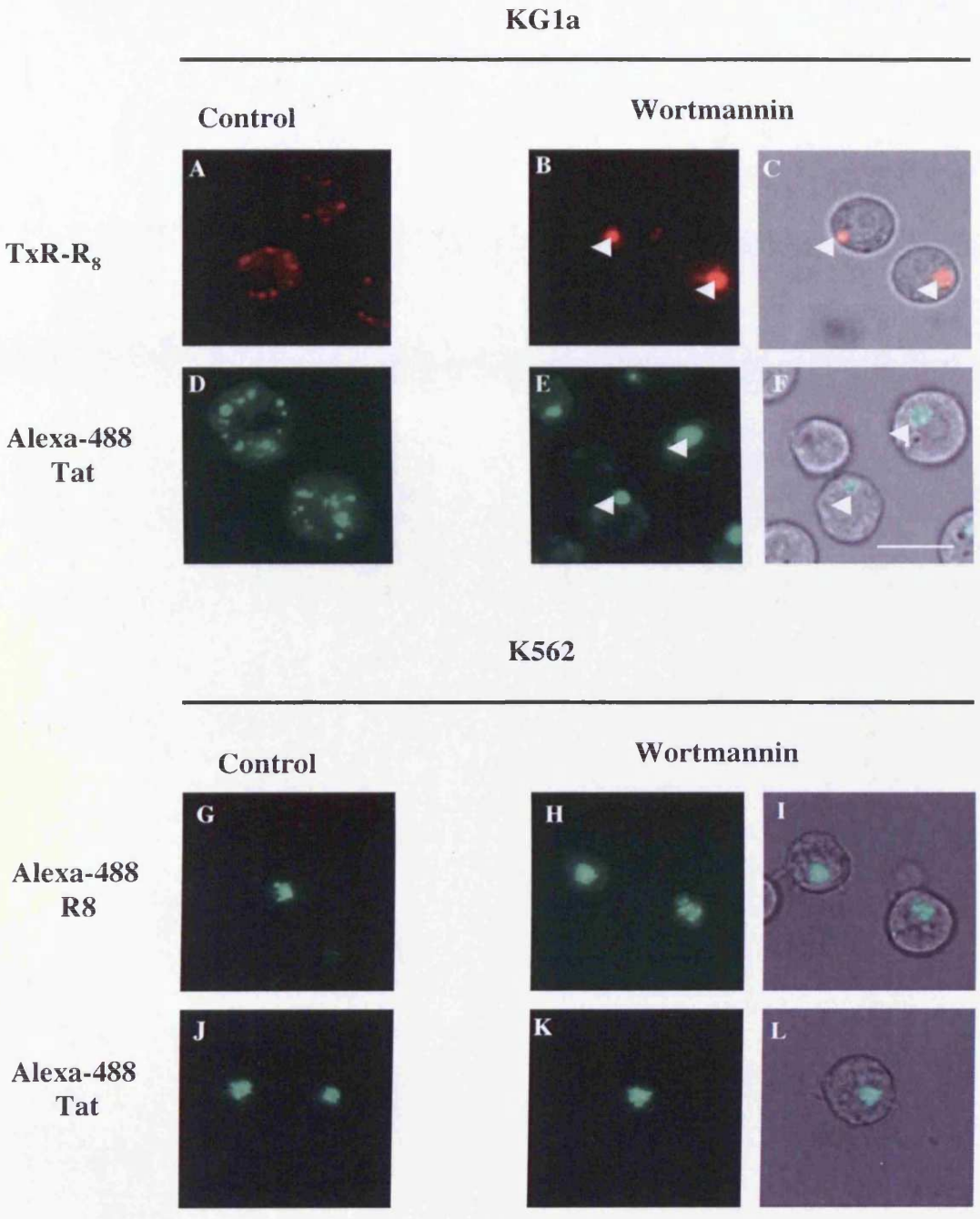

Figure 5.6. Effect of wortmannin on alexa-488 Tat and TxR-R_8 distribution in KG1a and K562 cells. KG1a (A-F) and K562 (G-L) cells were incubated either with 3 μM TxR-R_8 (A-C), 3 μM alexa-488 Tat (D-F and J-L) or 1 μM alexa-488 R_8 (G-I) in the absence or presence of 150 nM wortmannin as detailed above. Phase contrast pictures were taken of wortmannin treated KG1a (C and F) and K562 (I and L) cells to reveal the confines of the cell. Arrowheads indicate the wortmannin induced structures in KG1a cells. Sclae bar= 10 μm.

glycosaminoglycan synthesis, there is a dramatic reduction in the uptake of Tat and penetratin (Console et al., 2003). K562 cells, have also been shown to express low levels of proteoglycans (Stellrecht et al., 1993), but seemed very able to internalise both peptides in a time and temperature dependent manner. Glycosaminoglycans may therefore be essential for uptake of peptides in some cells but not in others (Silhol et al., 2002). R_8, despite being used at three-fold lower concentrations, was taken up more efficiently than Tat in K562 cells whilst higher uptake of R_8 compared with Tat was previously reported by Futaki and coworkers (Futaki et al., 2001). The high internalisation efficiency of polyarginine chains is attributed to their guanidium group which strongly interacts with anionic moieties exposed at the cell surface thereby facilitating membrane transduction (Rothbard et al., 2002). In KG1a cells, Tat was internalised with higher efficiency than R_8 and this may reflect the difference in concentrations used for Tat and R_8. These studies all point to the fact that there is a great deal of variation in uptake of these peptides in different cell lines.

PTD have been reported to enter cells via caveolae dependent endocytosis (Ferrari et al., 2003), clathrin dependent endocytosis (Vendeville et al., 2004), fluid phase endocytosis (Drin et al., 2003) and macropinocytosis (Nakase et al., 2004; Kaplan et al., 2005). In agreement with a role for endocytosis, one study argued against direct diffusion, due to the inability of Tat and penetratin to cross mitochondrial membranes, and implicated transporter mediated uptake into cells (Ross et al., 2004). Conversely, as the peptides are known to interact strongly with the plasma membrane, they may be taken up constitutively with bulk membrane whenever the cell undergoes an endocytic event. Various endocytic inhibitors were tested for their effect on peptide uptake and although the effect of wortmannin, nocodazole and cytochalasin D were comparable for both peptides, EIPA only caused a significant reduction in Tat uptake. However, as the effect of EIPA on peptide uptake was quite small, it suggests that macropinocytosis may not be the primary mode of internalisation for these peptides. In a separate study, approximately 70 % of R_8 uptake was insensitive to amiloride thus suggesting that macropinocytosis is not the sole entry mechanism for these peptides (Nakase et al., 2004). Significant inhibition of Tat and R_8 uptake by wortmannin and cytochalasin

D also pointed towards macropinocytosis as an uptake mechanism in K562 cells, as both drugs also inhibit macropinocytosis (Sampath & Pollard, 1991; Araki et al., 1996). Wortmannin has also been shown to inhibit fluid phase uptake (Clague et al., 1995) and cytochalasin D, which inhibits actin polymerisation, may potentially effect all mechanisms of cellular internalisation (reviewed in Engqvist-Goldstein & Drubin, 2003). Drin and coworkers, showed that cytochalasin D had no effect on the uptake of SynB and penetratin in K562 cells (Drin et al., 2003). When cytochalasin D treated cells were subsequently analysed under the microscope by a colleague, they were shown to be permeable to trypan blue thus it may be that the observed effects of this drug was due to loss of cell viability rather than a specific inhibition of uptake. Nocodazole was shown to induce a 20% reduction in endocytosis in K562 cells of the TfR (Jin & Snider, 1993). This appears to be similar to the observed reduction in Tat and R_8 uptake in these cells which was observed to be around 30%. This suggests a minimal requirement for microtubules in this event. This data strongly implicates an endocytic mechanism of uptake in these cells. It will be interesting to determine whether incubation of K562 cells with nocodazole and cytochalasin D affects delivery of the peptides to late endocytic structures that we hypothesise to be the terminal organelle stations. In conclusion, it seems likely that a cell may utilise several endocytic uptake mechanisms to internalise these peptides. This argues against a specific receptor and for a great deal of heterogeneity between cell lines depending on their function and the efficiency of uptake via specific pathways.

Both KG1a and K562 cells exhibited peptide-associated fluorescence at 4 °C and in some KG1a cells, this was often higher than that observed at 37 °C. We cannot rule out the possibility that some peptide remains inaccessible to trypsin and heparin or that the cell surface associated peptide is internalised following the brief 37 °C incubation with trypsin. Alternatively, temperature insensitive or non-endocytic uptake could have taken place and the current study cannot refute this. The existence of two distinct mechanisms of uptake was identified in previous studies by Thoren and co-workers who identified an endocytic mechanism of uptake for penetratin in PC12 cells and also a non-endocytic mechanism of uptake of R_7 in the same cell line (Thoren et al., 2003). Mitchell and co-workers showed

that oligoarginines were taken up by metabolic sensitive but temperature insensitive mechanism in live cells and this also suggests a non-endocytic mechanism may still take place (Mitchell et al., 2000). Zaro and Shen found that the majority of Tat was preferentially transduced to the cytosolic compartment rather than endocytosed into vesicles (Zaro & Shen, 2003).

The distribution of Tat and R_8 at 4 °C appears very diffuse and the lack of vesicular or nuclear labelling indicates that the peptide is unlikely to be intracellular and is more likely to be associated with the cell surface. Interestingly, at 16 °C, a similar pattern of fluorescence is observed but with higher intensity. It is difficult, without confocal microscopy, to conclude that there is uptake of peptide even at 16 °C. Again the lack of prominent vesicular and nuclear labelling most likely indicates that the peptide is still bound to the cell surface. It will now be interesting to repeat these experiments with cells depleted of ATP. This approach has also been shown to significantly inhibit uptake at 37 °C (Richard et al., 2003, 2005). However, all the studies have been confined to 37 °C experiments and it would be interesting to see what effect ATP depletion has on cell associated fluorescence at 4 °C and 37 °C in these cells.

Wortmannin resulted in a redistribution of the Tat and R_8 into enlarged structures in KG1a cells, these were more pronounced than the earlier described DNR structures that were also observed after treating the cells with this drug. This observation, coupled with the similarities between peptide and LE/lysosomal and DNR labelling in KG1a and K562 cells all strongly implicate lysosomes as being the sequestration site for both Tat and R_8 in the two cell lines. The distribution of Tat and R_8 in K562 cells appears to be the same as that observed by Drin and co-workers for another PTD, SynB (Drin et al., 2003). They speculated that the SynB positive perinuclear compartment observed in K562 cells was consistent with LE/lysosomes in these cells. In another blood cell line, Vendeville and co-workers also observed the colocalisation of Tat protein with LAMP proteins, implicating LE as the site of Tat accumulation. (Vendeville et al., 2004). Another study has also demonstrated the localisation of Tat in an acidic compartment in HeLa cells, although they do not expand on the identity of this compartment (Richard et al.,

2005). Console and coworkers also reported the partial colocalisation of penetratin with lysosomes in CHO cells (Console et al., 2003).

The endosomal uptake of these peptides may in fact be an important feature of their function. As they progress through the endocytic pathway, the pH becomes more acidic and this acidity is essential for PTD and full length Tat protein translocation out of endosomes and into the cytosol and nucleus (Potocky et al., 2003; Fischer et al., 2004; Vendeville et al., 2004). Similar experiments that were performed with dextran and DNR in this thesis should prove whether PTD traffic to lysosomes. In the likely event that this is true, then it may be argued that their usefulness for drug delivery may be limited as their associated cargo may be sensitive to the hostile lysosome environment. However, it must be remembered that only a small fraction of the peptide may require to be translocated to the cytosol and/or nucleus to mediate a physiological effect on the cell. This may also be the case for the full length Tat protein as there is no evidence that it effects endosome dynamics and morphology and there is, as previously noted, substantial evidence for it being trafficked to late endocytic structures.

In conclusion, PTD in KG1a and K562 cells are internalised via a predominantly endocytic mechanism although a non-endocytic mechanism may also be implicated to a lesser extent as the endocytosis inhibitors used and lower temperatures failed to completely abolish peptide uptake. The cellular localisation of PTD shows similarities with LE/lysosomal markers and DNR which implicates this compartment as the preferred location for these PTD.

Chapter 6:

General Discussion

6.1 General Discussion

Since P-gp was first identified as a mediator of MDR in 1975 (Juliano & Ling, 1976), an extensive substrate list has been compiled for this transporter, demonstrating the far-reaching effects of P-gp mediated drug resistance alone. It is almost easy to forget that hundreds of other resistance mechanisms exist and undoubtedly many more are yet to be discovered. However, despite the endless effort and enthusiasm devoted to studying this phenomenon over the past 60 years, surprisingly this is not reflected in our current ability to circumvent drug resistance in the clinic. This has inspired the foundations of this project and highlights its importance and clinical relevance. This study focused on the resistance mechanisms operating within human cell line models of AML and CML, where fatalities often proceed the onset of drug resistance. The initial aims of this project was therefore to elucidate the mechanisms of resistance that operate within these cells, then progress to testing novel concepts for the circumvention of P-gp mediated resistance.

Although studies on drug resistance have been carried out in these cells, they have yielded conflicting observations. This appears to be a common feature in many studies devoted to the elucidation of drug resistance mechanisms and many possible reasons for this have arisen. One study has shown that different batches of FBS in culture media may alter drug sensitivity of the cell, yielding different cytotoxicity data from the same cell line, in the same laboratory (Ferrand et al., 1996). In P-gp expressing cells, P-gp is thought to effect MTT assays, which are commonly used to assess drug sensitivity (Vellonen et al., 2004). The use of non-specific pharmacological tools such as antibodies (C219 and JSB-1) and drugs such as the commonly used resistance modulators (verapamil and cyclosporin A) may also lead to false observations. This was demonstrated in this study where verapamil disrupted DNR accumulation in the P-gp negative K562 cells. Although verapamil and cyclosporin A were used in this study to assess the functionality of P-gp, we were confident that the effect of cyclosporin A was specific for P-gp inhibition, based on the inability of cyclosporin A to disrupt the perinuclear DNR labelling in K562 cells and the vesicular DNR labelling in KG1a cells. Anti-P-gp

antibodies used in this study were primarily characterised by Western blotting to determine their specificity and suitability for immunofluorescence microscopy, the validity of which heavily depends on antibody specificity. Taking these issues into consideration, meant that much emphasis was placed on the characterisation and optimisation of the techniques used.

During the biochemical analysis of P-gp, the detection of a 200 kDa band following immunoprecipitation with F4 and blotting with C219, led us to believe that P-gp may be modified in such a way, yielding a protein of higher molecular weight. This led us to investigate the possibility that P-gp may be ubiquitinated in KG1a cells. P-gp ubiquitination has been shown previously in two independent studies (Ohkawa et al., 1999; Zhang et al., 2004). However both studies utilised a P-gp overexpressing system, where high expression levels may influence P-gp ubiquitination and degradation. In KG1a cells, our identification of P-gp ubiquitination, which is sensitive to endocytosis inhibition, suggests that ubiquitin has a constitutive role in governing P-gp endocytosis and trafficking. As ubiquitination is primarily associated with degradation this would provide an ideal target for the manipulation of P-gp turnover and possibly trafficking, although this was not addressed during this project.

The ubiquitination status of P-gp may help to explain an important observation regarding the behaviour of P-gp in KG1a cells. Consistent with previous observations, we showed that KG1a cells support the majority of their P-gp within intracellular vesicles. Mono-ubiquitination has been shown to serve as an endocytosis motif, directing the internalisation of the associated protein (Shih et al., 2000). This raises the possibility that the ubiquitin motif associated with P-gp serves to maintain the intracellular localisation of P-gp. It is possible that ubiquitin causes the rapid cycling of P-gp between this intracellular compartment and the cell surface, conferring a steady state intracellular localisation of P-gp. The inhibition of P-gp ubiquitination under conditions which inhibit clathrin mediated endocytosis can be used to support the hypothesis that ubiquitination is utilised as an internalisation motif, possibly via the clathrin route.

The nature and identity of this intracellular P-gp, despite being reported (Ferrao et al., 2001), had not previously been investigated. However, we took the first steps in identifying this compartment as being endocytic in nature owing to its sensitivity to wortmannin treatment. This also supports the hypothesis that intracellular P-gp in these cells is derived from the plasma membrane. This predominantly intracellular localisation of P-gp in these cells raised the important question of whether this P-gp was indeed functional. The notion that cell surface P-gp is more effective at mediating drug resistance compared to intracellular P-gp is indeed more logical as preventing drug entry into the cell would be more effective than developing mechanisms to circumvent the effects of the drug once it is inside the cell. Studies with commonly used P-gp inhibitors suggests that this P-gp is functional in these cells and serves a cytoprotective role. Its cytoprotective role in such immature cells is valuable as these are common precursors for a diverse range of blood cells. Conversely, P-gp may serve a more physiological role in maintaining the stem cell like characteristics of KG1a cells as P-gp is known to be an inhibitor of differentiation. Indeed, immature cells express the differentiation marker CD34, which in turn is used as a marker for P-gp expression (Campos et al., 1992). P-gp is therefore expected to pose a bigger problem in leukaemias arising from such immature cells as demonstrated in AML where AML-M0, derived from CD34 positive immature blood cells, often represents the most drug resistant and fatal subtype of AML (Visser & van Bekkum, 1990).

Attempts were made to overexpress P-gp in both KG1a and K562 cells via transfection with rat mdr1b-EGFP plasmid. Transfection of these cells proved very difficult, meaning that we were unable to address this. However we showed that rat P-gp was successfully synthesised and trafficked to the cell surface in our human cell lines, KG1a, K562 and Hela. This finding raised an important point regarding P-gp distribution in KG1a cells. If cells are capable of directing P-gp to the cell surface what is the advantage of synthesising and retaining it, in a functional state, within intracellular compartments? It would have been interesting to challenge the cells with DNR for prolonged periods and determine whether this P-gp is translocated to the cell surface in response to the cytotxic agent. However, to achieve a stable phenotype when challenging cells with a cytotoxic agent requires

steady increases in drug dose over a year period and this would not have been feasible during this project. Also attempts to obtain a KG1a/200 cell line which has been challenged with doxorubicin were unsuccessful. As we were unable to test the functionality of P-gp in these cells, we used Hela cells to achieve higher transfection efficiencies. Rat P-gp was also synthesised and trafficked to the cell surface where it effectively excluded DNR from the cell.

Although studies have addressed resistance mechanisms in KG1a cells, we were the first to show that drug sequestration occurs in lysosomal compartment in KG1a cells, irrespective of P-gp. This is in contrast to the findings of Ferrao and co-workers who attributed drug sequestration in KG1a cells to P-gp (Ferrao et al., 2001). This discrepancy was particularly surprising since both observations were based on identical experiments utilising verapamil and cyclosporin A. Lysosomal sequestration was ruled out in KG1a cells in another study, which failed to show any effect of nigericin on DNR sequestration (Lautier et al., 1997). However, we identified lysosomal sequestration by three different methods. Initially, we identified differences between the late endocytic compartments in KG1a and K562 cells and correlated these to differences between DNR distribution. We also used pharmacological modulators of endosomal pH (nigericin and bafilomycin A1) and demonstrated the disruption of DNR sequestration in KG1a cells in the presence of these agents. Finally we performed colocalisation studies with dextran, which was used to label the lysosomal compartment in a pulse-chase experiment. Such discrepancies are common amongst stduies on drug resistance and Den Boer and co-workers demonstrated possible reasons for such variation when evaluating P-gp expression in acute lymphoblastic leukaemia specimens. They examined the effects of different fixation methods, day to day variation in staining and variation in reports by different observers. They revealed 30 % variation when samples were stained with antibodies on different days, or when different observers interpreted the results (Den Boer et al., 1997).

Although lysosomal sequestration is a common feature of many weak base drugs, some drugs do not fit into this category. Therefore different resistance mechanisms may be needed for different drugs. During this project, Gong and

coworkers revealed the differential sequestration of the weakly basic DNR and the neutral SR101 in the lysosomes and Golgi respectively in HL60 cells (Gong et al., 2003). We also investigated the ability of KG1a and K562 cells to differentially sequester SR101. We found that not only was DNR and SR101 differentially sequestered in each cell line, but we also identified differences in SR101 sequestration between KG1a and K562 cells. SR101 was localised to the Golgi in K562 cells and in P-gp positive vesicles in KG1a cells, as demonstrated by their respective sensitivities to brefeldin A and verapamil and cyclosporin A. This highlights the need for a multifactorial drug resistance phenotype capable of dealing with a diversity of cytotoxic agents. SR101 may accumulate in the Golgi by default, but being a P-gp substrate, P-gp may ultimately decide its intracellular fate in KG1a cells. This diverse multifactorial nature of drug resistance reflects not only the complexity of the phenotype, but the importance of such studies which aim to clarify mechanisms implicated in a disease states. Although ideally this study should be done in clinical samples, these were not readily available and any available samples were contaminated with many blood cell types. It would however, be important to directly compare drug sequestration and P-gp expression between *ex vivo* and *in vitro* models.

Having identified and clarified some of the mechanisms of resistance operating in these cells, the project progressed to testing novel hypothesis for the circumvention of drug resistance. These cells provided the ideal model for testing possible resistance modulators as they display multiple mechanisms of resistance and the nuclear accumulation of DNR can be readily visualised by fluorescence microscopy when P-gp function or drug sequestration is disrupted. Several different strategies for P-gp inhibition have already been investigated both *in vitro* and *in vivo*, however, many of these have disadvantages that limit their clinical efficiency. Pharmacological modulation is not always effective as pretreatment of cells with certain P-gp inhibitors can often induce the expression of P-gp (Schuetz et al., 1996; Granzotto et al., 2004). P-gp inhibition may also select for the expression of other mechanisms of resistance. This has been demonstrated both *in vitro,* where sa 180 cells pretreated with verapamil increased their resistance level two-fold, and also *in vivo,* where verapamil pretreatment of mice bearing the

leukaemia P388 resulted in a decrease in their life span from 21 days to 16.4 days (Donenko et al., 1991). Resistance in both cases occurs independently of P-gp. Antibodies such as MRK16 and UIC2 may be problematic due to the problem of immunogenicity and their inability to target solid tumours. Antisense oligonucleotides are susceptible to degradation and can be recycled so they can effect more than one target gene and induce antisense unrelated effects. Furthermore high concentrations are required to inhibit gene expression. Clearly a gap still exists in the search for an effective P-gp inhibitor.

Initially we tested whether the redistribution of P-gp may modulate P-gp function and hence circumvent drug resistance, the redistribution of P-gp in response to wortmannin treatment gave the ideal opportunity to test this hypothesis. However, as there was no increase in nuclear accumulation of DNR it would seem that this strategy may be confined to a redistribution of P-gp from the cell surface to an intracellular compartment (Kim et al., 1997). An alternative strategy may therefore involve the inhibition of P-gp translocation onto the cell surface. Our transfected Hela cells may be an appropriate model to test this in the future as not only are they capable of trafficking functional P-gp to the cell surface, but high transfection efficiencies can be achieved allowing further experimental analysis.

We then turned our attention to PTD which have shown to be effective at bypassing P-gp (Mazel et al., 2001). PTD may prove to be doubly effective against drug resistance as they not only have the potential to bypass transporter mediated resistance but may potentially allow DNR to escape sequestration by allowing its translocation across lysosomal membranes, thereby facilitating its nuclear accumulation. This potential to act on multiple mechanisms of resistance makes them a revolutionary strategy against drug resistance. This project only addressed the mechanisms of uptake of Tat and R_8 with preliminary characterisation of their cellular localisation, the two aspects which are still strongly debated. The cationic nature of these peptides makes them particularly susceptible to binding not only to the cell surface but also to artificial surfaces, making microscopy work very difficult. Our cell lines proved ideal for such studies as there appeared to be

minimal surface binding of these peptides. We found a predominantly endocytic mechanism of uptake for these peptides and their cellular distribution in KG1a and K562 cells was synonymous to that observed for LE/lysosomal and DNR labelling thus strongly implicating LE/lysosomal localisation. Indeed, dual labelling of these peptides with dextran, as performed by my supervisor, Dr. Arwyn Jones revealed that the observed labelling was indeed lysosomal. The results of this study have now been submitted for publication in the Journal of Biological Chemistry. Although unfortunately there was insufficient time to extend this study to investigating the cellular fate of DNR-PTD conjugates and whether these would indeed help to increase cell cytotoxicity in these cells.

References

References

Abraham, E. H., Prat, A. G., Gerweck, L., Seneveratne, T., Arceci, R. J., Kramer, R., Guidotti, G. & Cantiello, H. F. (1993). The multidrug resistance (mdr1) gene product functions as an ATP channel. *Proc. Natl. Acad. Sci. USA.* **90**:312-316.

Advani, R., Saba, H. I., Tallman, M. S., Rowe, J. M., Wiernik, P. H., Ramek, J., Dugan, K., Lum, B., Villena, J., Davis, E., Paietta, E., Litchman, M., Sikic, B. I. & Greenberg, P. L. (1999). Treatment of refractory and relapsed acute myelogenous leukemia with combination chemotherapy plus the multidrug resistance modulator PSC 833 (Valspodar). *Blood.* **93**:787-795.

Akiyama, S., Shiraishi, N., Kuratomi, Y., Nakagawa, M. & Kuwano, M. (1986). Circumvention of multiple-drug resistance in human cancer cells by thioridazine, trifluoperazine, and chlorpromazine. *J. Natl. Cancer Inst.* **76**:839-844.

Altan, N., Chen, Y., Schindler, M. & Simon, S. M. (1998). Defective acidification in human breast tumor cells and implications for chemotherapy. *J. Exp. Med.* **187**:1583-1589.

Amarante-Mendes, G. P., Naekyung Kim, C., Liu, L., Huang, Y., Perkins, C. L., Green, D. R. & Bhalla, K. (1998). Bcr-Abl exterts its antiapoptotic effect against diverse apoptotic stimuli through blockage of mitochondrial release of cytochrome C and activation of caspase-3. *Blood.* **91**:1700-1705.

Ambudkar, S. V., Dey, S., Hrycyna, C. A., Ramachandra, M., Pastan, I. & Gottesman, M. M. (1999). Biochemical, cellular, and pharmacological aspects of the multidrug transporter. *Annu. Rev. Pharmacol. Toxicol.* **39**:361-398.

Andersson, L. C., Jokinen, M. & Gahmberg, C. G. (1979b). Induction of erythroid differentiation in the human leukaemia cell line K562. *Nature.* **278**:364-365.

Andersson, L. C., Nilsson, K. & Gahmberg, C. G. (1979a). K562-a human erythroleukemic cell line. *Int. J. Cancer.* **23**:143-147.

Araki, N., Johnson, M. T. & Swanson, J. A. (1996). A role for phosphoinositide 3-kinase in the completion of macropinocytosis and phagocytosis by macrophages. *J. Cell Biol.* **135**:1249-1260.

Arancia, G., Molinari, A., Calcabrini, A., Meschini, S. & Cianfriglia, M. (2001). Intracellular P-glycoprotein in multidrug resistant tumor cells. *Ital. J. Anat. Embryol.* **106**:59-68.

Arancia, G., Molinari, A., Crateri, P., Calcabrini, A., Silvestri, L. & Isacchi, G. (1988). Adraimaycin-plasma membrane interaction in human erythrocytes. *Eur. J. Cell Biol.* **47**:379-387.

Astriab-Fischer, A., Sergueev, D., Fisher, M., Shaw, B. R. & Juliano, R. L. (2002). Conjugates of antisense oligonucleotides with the Tat and antennapedia cell-penetrating peptides: effects on cellular uptake, binding to target sequences, and biologic actions. *Pharm. Res.* **19**: 744-754.

Baer, M. R., George, S. L., Dodge, R. K., O'Loughlin, K. L., Minderman, H., Caligiuri, M. A., Anastasi, J., Powell, B. L., Kolitz, J. E., Schiffer, C. A., Bloomfield, C. D. & Larsen, R. A. (2002). Phase 3 study of the multidrug resistance modulator PSC833 in previously untreated patients 60 years of age and older with acute myeloid leukemia: Cancer and Leukemia Group B Study 9720. *Blood.* **100**:1224-1232.

Bailly, J. D., Skladanowski, A., Bettaieb, A., Mansat, V., Larsen, A. K. & Laurent, G. (1997). Natural resistance of acute myeloid leukemia cell lines to mitoxantrone is associated with lack of apoptosis. *Leukemia.* **11**:1523-1532.

Baldini, N., Scotlandi, K., Serra, M., Shikita, T., Zini, N., Ognibene, A., Santi, S., Ferracini, R & Maraldi, N. M. (1995). Nuclear immunolocalization of P-

glycoprotein in multidrug-resistant cell lines showing similar mechanisms of doxorubicin distribution. *Eur. J. Cell Biol.* **68**:226-239.

Beaulieu, E., Demeule, M., Pouliot, J. F., Averill-Bates, D. A., Murphy, G. F. & Beliveau, R. (1995). P-glycoprotein of blood brain barrier: cross-reactivity of Mab C219 with a 190 kDa protein in bovine and rat isolated brain capillaries. *Biochim. Biophys. Acta.* **1233**:27-32.

Begley, D. J. (2004a). Delivery of therapeutic agents to the central nervous system: the problems and the possibilities. *Pharmacol. Ther.* **104**:29-45.

Begley, D. J. (2004b). ABC transporters and the blood-brain barrier. *Curr. Pharm. Des.* **10**:1295-1312.

Bekaii-Saab, T. S., Perloff, M. D., Weemhoff, J. L., Greenblatt, D. J. & von Moltke, L. L. (2004). Interactions of tamoxifen, N-desmethyltamoxifen and 4-hydroxytamoxifen with P-glycoprotein and CYP3A. *Biopharm. Drug Dispos.* **25**:283-289.

Benchekroun, M. N., Sinha, B. K. & Robert, J. (1993). Doxorubicin-induced oxygen free radical formation in sensitive and doxorubicin-resistant variants of rat glioblastoma cell lines. *FEBS Lett.* **326**:302-305.

Bennett, J. M., Catovsky, D., Daniel, M. T., Flandrin, G., Galton, D. A., Gralnick, H. R. & Sultan, C. (1985). Proposed revised criteria for the classification of acute myeloid leukemia. A report of the French-American-British Cooperative Group. *Ann. Intern. Med.* **103**:620-625.

Bertram, J., Palfner, K., Killian, M., Brysch, W., Schlingensiepen, K. H., Hiddemann, W. & Kneba, M. (1995). Reversal of multiple drug resistance in vitro by phosphorothioate oligonucleotides and ribozymes. *Anticancer Drugs.* **6**:124-134.

Bezombes, C., Maestre, N., Laurent, G., Levade, T., Bettaieb, A. & Jaffrezou, J. P. (1998). Restoration of TNF-alpha-induced ceramide generation and apoptosis in resistant human leukemia KG1a cells by the P-glycoprotein blocker PSC833. *FASEB J.* **12**:101-109.

Bhatia, R., Verfaillie, C. M., Miller, J. S. & McGlave, P. B. (1997). Autologous transplantation therapy for chronic myelogenous leukemia. *Blood.* **89**:2623-2634.

Boesch, D., Gaveriaux, C., Jachez, B., Pourtier-Manzanedo, A., Bollinger, P. & Loor, F. (1991). In vivo circumvention of P-glycoprotein-mediated multidrug resistance of tumor cells with SDZ PSC 833. *Cancer Res.* **51**:4226-4233.

Boonstra, R., Timmer-Bosscha, H., van Echten-Arends, J., van der Kolk, D. M., van den Berg, A., de Jong, B., Tew, K. D., Poppema, S. & de Vries, E. G. (2004). Mitoxantrone resistance in a small cell lung cancer cell line is associated with ABCA2 upregulation. *Br. J. Cancer.* **90**:2411-2417.

Borg, A. G., Burgess, R., Green, L. M., Scheper, R. J. & Liu Yin, J. A. (2000). P-glycoprotein and multidrug resistance-associated protein, but not lung resistance protein, lower the intracellular daunorubicin accumulation in acute myeloid leukaemic cells. *Br. J. Haematol.* **108**:48-54.

Bour-Dill, C., Gramain, M. P., Merlin, J. L., Marchal, S. & Guillemin, F. (2000). Determination of intracellular organelles implicated in daunorubicin cytoplasmic sequestration in multidrug-resistant MCF-7 cells using fluorescence microscopy image analysis. *Cytometry.* **39**:16-25.

Bowman, E. J., Siebers, A. & Altendorf, K. (1988). Bafilomycins: a class of inhibitors of membrane ATPases from microorganisms, animal cells, and plant cells. *Proc. Natl. Acad. Sci. USA.* **85**:7972-7976.

Bradbury, N. A., Clark, J. A., Watkins, S. C., Widnell, C. C., Smith, H. S. 4th. & Bridges, R. J. (1999). Characterization of the internalization pathways for the

cystic fibrosis transmembrane conductance regulator. *Am. J. Physiol.* **276**:L659-668.

Bradford, M. M. (1976). A rapid and sensitive method for the quantitation of microgram quantities of protein utilizing the principle of protein-dye binding. *Anal. Biochem.* **72**:248-54.

Brangi, M., Litman, T., Ciotti, M., Nishiyama, K., Kohlhagen, G., Takimoto, C., Robey, R., Pommier, Y., Fojo, T. & Bates, S. E. (1999). Camptothecin resistance: role of the ATP-binding cassette (ABC), mitoxantrone-resistance half-transporter (MXR), and potential for glucuronidation in MXR-expressing cells. *Cancer Res.* **59**:5938-5946.

Breuninger, L. M., Paul, S., Gaughan, K., Miki, T., Chan, A., Aaronson, S. A. & Kruh, G. D. (1995). Expression of multidrug resistance-associated protein in NIH/3T3 cells confers multidrug resistance associated with increased drug efflux and altered intracellular drug distribution. *Cancer Res.* **55**:5342-5347.

Breier, A., Barancik, M., Stefankova, Z., Uhrik, B. & Tribulova, N. (1994). Effect of pentoxifylline on P-glycoprotein mediated vincristine resistance of L1210 mouse leukemic cell line. *Neoplasma.* **41**:297-303.

Brown, C. M. & Peterson, N. O. (1999). Free clathrin triskelions are required for the stability of clathrin-associated adaptor protein (AP-2) coated pit nucleation sites. *Biochem. Cell Biol.* **77**:439-448.

Brown, D. A. & Rose, J. K. (1992). Sorting of GPI-anchored proteins to glycolipid-enriched membrane subdomains during transport to the apical cell surface. *Cell.* **68**:533-544.

Cain, C. C., Sipe, D. M. & Murphy, R. F. (1989). Regulation of endocytic pH by the Na+,K+-ATPase in living cells. *Proc. Natl. Acad. Sci. USA.* **86**:544-548.

Calcabrini, A., Meschini, S., Stringaro, A., Cianfriglia, M., Arancia, G. & Molinari, A. (2000). Detection of P-glycoprotein in the nuclear envelope of multidrug resistant cells. *Histochem. J.* **32**:599-606.

Campos, L., Guyotat, D., Archimbaud, E., Calmard-Oriol, P., Tsuruo, T., Troncy, J., Treille, D. & Fiere, D. (1992). Clinical significance of multidrug resistance P-glycoprotein expression on acute nonlymphoblastic leukemia cells at diagnosis. *Blood.* **79**:473-476.

Campos, L., Rouault, J. P., Sabido, O., Oriol, P., Roubi, N., Vasselon, C., Archimbaud, E., Maguad, J. P. & Guyotat, D. (1993). High expression of bcl-2 protein in acute myeloid leukaemia cells is associated with poor response to chemotherapy. *Blood.* **81**:3091-3096.

Cao, G., Pei, W., Ge, H., Liang, O., Luo, Y., Sharp, F. R., Lu, A., Ran, R., Graham, S. H. & Chen, J. (2002). In vivo delivery of a Bcl-xL fusion protein containing the TAT protein tranduction domain protects against ischemic brain injury and neuronal apoptosis. *J. Neurosci.* **22**:5423-5431.

Carter, A., Dann, E. J., Katz, T., Shechter, Y., Oliven, A., Regev, R., Eytan, E., Rowe, J. M. & Eytan, G. D. (2001). Cells from chronic myelogenous leukaemia patients at presentation exhibit multidrug resistance not mediated by either MDR1 or MRP1. *Br. J. Haematol.* **114**:581-590.

Chambers, T. C., Pohl, J., Raynor, R. L. & Kuo, J. F. (1993). Identification of specific sites in human P-glycoprotein phosphorylated by protein kinase C. *J. Biol. Chem.* **268**:4592-4595.

Chen, A. Y., Yu, C., Potmesil, M., Wall, M. E., Wani, M. C. & Liu, L. F. (1991). Camptothecin overcomes MDR1-mediated resistance in human KB carcinoma cells. *Cancer Res.* **51**:6039-6044.

Chen, C. J., Chin, J. E., Ueda, K., Clark, D. P., Pastan, I., Gottesman, M. M. & Roninson, I. B. (1986). Internal duplication and homolgy with bacterial transport proteins in the mdr1 (P-glycoprotein) gene from multidrug-resistant human cells. *Cell.* **47**:381-389.

Chen, Y. N., Sharma, S. K., Ramsey, T. M., Jiang, L., Martin, M. S., Baker, K., Adams, P. D., Bair, K. W. & Kaelin, W. G. Jr. (1999). Selective killing of transformed cells by cyclin/cyclin-dependent kinase 2 antagonists. *Proc. Natl. Acad. Sci. USA.* **96**:4325-4329

Childs, S., Yeh, R. L., Hui, D. & Ling, V. (1998). Taxol resistance mediated by transfection of the liver-specific sister gene of P-glycoprotein. *Cancer Res.* **58**:4160-4167.

Chin, J. E., Soffir, R., Noonan, K. E., Choi, K. & Roninson, I. B. (1989). Structure and expression of the human MDR (P-glycoprotein) gene family. *Mol. Cell Biol.* **9**:3808-3820.

Christoforidis, S., McBride, H. M., Burgoyne, R. D. & Zerial, M. (1999). The Rab5 effector EEA1 is a core component of endosome docking. *Nature.* **397**:621-625.

Chu, T. M., Kawinski, E. & Lin, T. H. (1993). Characterization of a new monoclonal antibody F4 detecting cell surface epitope and P-glycoprotein in drug-resistant human tumor cell lines. *Hybridoma.* **12**:417-429.

Chu, T. M., Lin, T. H. & Kawinski, E. (1994). Detection of soluble P-glycoprotein in culture media and extracellular fluids. *Biochem. Biophys. Res. Commun.* **203**:506-512.

Ciechanover, A., Schwartz, A. L., Dautry-Varsat, A. & Lodish, H. F. (1983). Kinetics of internalization and recycling of transferrin and the transferrin receptor in a human hepatoma cell line. *J. Biol. Chem.* **258**:9681-9689.

Clague, M., Thorpe, C. & Jones, A. T. (1995). Phosphatidylinositol 3-kinase regulation of fluid phase endocytosis. *FEBS Lett.* **367**:272-274.

Cole, S. P., Bhardwaj, G., Gerlach, J. H., Mackie, J. E., Grant, C. E., Almquist, K. C., Stewart, A. J., Kurz, E. U., Duncan, A. M. & Deeley, R. G. (1992). Overexpression of a transporter gene in a multidrug-resistant human lung cancer cell line. *Science.* **258**:1650-1654.

Cole, S. P., Sparks, K. E., Fraser, K., Loe, D. W., Grant, C. E., Wilson, G. M. & Deeley, R. G. (1994). Pharmacological characterization of multidrug resistant MRP-transfected human tumor cells. *Cancer Res.* **54**:5902-5910.

Collett, A., Higgs, N. B., Sims, E., Rowland, M. & Warhurst, G. (1999). Modulation of the permeability of H2 receptor antagonists cimetidine and ranitidine by P-glycoprotein in rat intestine and the human colonic cell line Caco-2. *J. Pharmacol. Exp. Ther.* **288**:171-178.

Colvin, O. M., Friedman, H. S., Gamcsik, M. P., Fenselau, C. & Hilton, J. (1993). Role of glutathione in cellular resistance to alkylating agents. *Adv. Enzyme Regul.* **33**:19-26.

Conner, S. D. & Schmid, S. L. (2003). Regulated portals of entry into the cell. *Nature.* **422**:37-44.

Console, S., Marty, C., Garcia-Echeverria, C., Schwendener, R. & Ballmer-Hofer, K. (2003). Antennapedia and HIV transactivator of transcription (TAT) "protein transduction domains" promote endocytosis of high molecular weight cargo upon binding to cell surface glycosaminoglycans. *J. Biol. Chem.* **278**:35109-35114.

Cremona, O. (2001). Live stripping of clathrin-coated vesicles. *Dev. Cell.* **1**:592-594.

Crider, B. P., Xie, X. S. & Stone, D. K. (1994). Bafilomycin inhibits proton flow through the H+ channel of vacuolar proton pumps. *J. Biol. Chem.* **269**:17379-

Cuervo, A. M. & Dice, J. F. (1996). A receptor for the selective uptake and degradation of proteins by lysosomes. *Science.* **273**:501-503.

Cummings, J., Anderson, L., Willmont, N. & Smyth, J. F. (1991). The molecular pharmacology of doxorubicin in vivo. *Eur. J. Cancer.* **27**:532-535.

Dale, I. L., Tuffley, W., Callaghan, R., Holmes, J. A., Martin, K., Luscombe, M., Mistry, P., Ryder, H., Stewart, A. J., Charlton, P., Twentyman, P. R. & Bevan, P. (1998). Reversal of P-glycoprotein-mediated multidrug resistance by XR9051, a novel diketopiperazine derivative. *Br. J. Cancer.* **78**:885-892.

Dalmark, M. (1981). Characteristics of doxorubicin transport in human red blood cells. *Scand. J. Clin. Lab. Invest.* **41**:633-639.

Dalmark, M. & Hoffmann, E. K. (1983). Doxorubicin (Adriamycin) transport in Ehrlich ascites tumour cells: comparison with transport in human red blood cells. *Scand. J. Clin. Lab. Invest.* **43**:241-248.

Dalmark, M. & Storm, H. H. (1981). A Fickian diffusion transport process with features of transport catalysis. Doxorubicin transport in human red blood cells. *J. Gen. Physiol.* **78**:349-364.

Damjanovich, S., Aszalos, A., Mulhern, S. A., Szollosi, J., Balazs, M., Tron, L. & Fulwyler, M. J. (1987). Cyclosporin depolarizes human lymphocytes: earliest observed effect on cell metabolism. *Eur. J. Immunol.* **17**:763-768.

Dano, K. (1973). Active outward transport of daunomycin in resistant Ehrlich ascites tumor cells. *Biochim. Biophys. Acta.* **323**:466-483.

Dantzig, A. H., Shepard, R. L., Cao, J., Law, K. L., Ehlhardt, W. J., Baugham, T. M., Bumol, T. F. & Starling, J. J. (1996). Reversal of P-glycoprotein-mediated multidrug resistance by a potent cyclopropyldibenzosuberane modulator LY335979. *Cancer Res.* **56**:4171-4179.

Dean, M., Rzhetsky, A. & Allikmets, R. (2001). The human ATP-binding cassette (ABC) transporter superfamily. *Genome Res.* **11**:1156-1166.

de Graaf, D., Sharma, R. C., Mechetner, E. B., Schimke, R. T. & Roninson, I. B. (1996). P-glycoprotein confers methotrexate resistance in 3T6 cells with deficient carrier-mediated methotrexate uptake. *Proc. Natl. Acad. Sci. USA.* **93**:1238-1242.

de Lange, E. C., Marchand. S., van den Berg, D., van der Sandt, I. C., de Boer, A. G., Delon, A., Bouquet, S. & Couet, W. (2000). In vitro and in vivo investigations on fluoroquinolones; effects of the P-glycoprotein efflux transporter on brain distribution of sparfloxacin. *Eur. J. Pharm. Sci.* **12**:85-93.

Demeule, M., Jodoin, J., Gingras, D. & Beliveau, R. (2000). P-glycoprotein is localized in caveolae in resistant cells and in brain capillaries. *FEBS Lett.* **466**:219-224.

Demeule, M., Laplante, A., Murphy, G. F., Wenger, R. M. & Beliveau, R. (1998). Identification of the cyclosporin-binding site in P-glycoprotein. *Biochemistry.* **37**:18110-18118.

Den Boer, M. L., Zwaan, C. M., Pieters, R., Kazemier, K. M., Rottier, M. M., Flens, M. J., Scheper, R. J. & Veerman, A. J. (1997). Optimal immunocytochemical and flow cytometric detection of P-gp, MRP and LRP in childhood acute lymphoblastic leukemia. *Leukemia.* **11**:1078-1085.

Denning, G. M., Ostedgaard, L. S., Cheng, S. H., Smith, A. E. & Welsh, M. J. (1992). Localization of cystic fibrosis transmembrane conductance regulator in chloride secretory epithelia. *J. Clin. Invest.* **89**:339-349.

Derossi, D., Calvet, S., Trembleau, A., Brunissen, A., Chassaing, G. & Prochiantz, A. (1996). Cell internalization of the third helix of the Antennapedia homeodomain is receptor-independent. *J. Biol. Chem.* **271**:18188-18193.

Derossi, D., Joliot, A. H., Chassaing, G. & Prochiantz, A. (1994). The third helix of the Antennapedia homeodomain translocates through biological membranes. *J. Biol. Chem.* **269**:10444-10450.

de Thornel, A., Bettaieb, A., Jean, C., Laurent, G. & Quillet-Mary, A. (2001). Role of protein kinase C zeta isoform in Fas resistance of immature myeloid KG1a leukemic cells. *Blood.* **98**:3770-3777.

Dietrich, J., Kastrup, J., Nielsen, B. L., Odum, N. & Geisler, C. (1997). Regulation and function of the CD3 gamma DxxxLL motif: a binding site for adaptor protein-1 and adaptor protein-2 in vitro. *J. Cell Biol.* **138**:271-281.

Dinndorf, P. A., Andrews, R. G., Benjamin, D., Ridgway, D., Wolff, L. & Bernstein, I. D. (1986). Expression of normal myeloid-associated antigens by acute leukemia cells. *Blood.* **67**:1048-1053.

Donenko, F. V., Efferth, T., Mattern, J., Moroz, L. V. & Volm, M. (1991). Resistance to doxorubicin in tumor cells in vitro and in vivo after pretreatment with verapamil. *Chemotherapy.* **37**:57-61.

Dorr, R., Karanes, C., Spier, C., Grogan, T., Greer, J., Moore, J., Weinberger, B., Schiller, G., Pearce, T., Litchman, M., Dalton, W., Roe, D. & List, A. F. (2001). Phase I/II study of the P-glycoprotein modulator PSC833 in patients with acute myeloid leukemia. *J. Clin. Oncol.* **19**:1589-1599.

Doyle, L. A., Yang, W., Abruzzo, L. V., Krogmann, T., Gao, Y., Rishi, A. K. & Ross, D. D. (1998). A multidrug resistance transporter from human MCF-7 breast cancer cells. *Pro. Natl. Acad. Sci. USA.* **95**:15665-15670.

Drin, G., Cottin, S., Blanc, E., Rees, A. R. & Temsamani, J. (2003). Studies on the internalization mechanism of cationic cell-penetrating peptides. *J. Biol. Chem.* **278**:31192-31201.

Drori, S., Eytan, G. D. & Assaraf, Y. G. (1995). Potentiation of anticancer-drug cytotoxicity by mutlidrug-resistance chemosensitizers involves alterations in membrane fluidity leading to increased membrane permeability. *Eur. J. Biochem.* **228**:1020-1029.

Druker, B. J., Talpaz, M., Resta, D. J., Peng, B., Buchdunger, E., Ford, J. M., Lydon, N. B., Kantarjian, H., Capdeville, R., Ohno-Jones, S. & Sawyers, C. L. (2001). Efficacy and safety of a specific inhibitor of the BCR-ABL tyrosine kinase in chronic myeloid leukemia. *N. Engl. J. Med.* **344**:1031-1037.

Duensing, T. D. & Slate, D. L. (1994). Intracellular expression of P-glycoprotein in a human colon tumor cell line. *Anticancer Res.* **14**:13-20.

Duvvuri, M., Gong, Y., Chatterji, D. & Krise, J. P. (2004). Weak base permeability characteristics influence the intracellular sequestration site in the multidrug-resistant human leukemic cell line HL-60. *J. Biol. Chem.* **279**:32367-32372.

Eguchi, Y., Shimizu, S. & Tsujimoto, Y. (1997). Intracellular ATP levels determine cell death fate by apoptosis or necrosis. *Cancer Res.* **57**:1835-1840.

Elliott, G. & O'Hare, P. (1997). Intercellular trafficking and protein delivery by a herpesvirus structural protein. *Cell.* **88**:223-233.

Elmquist, A., Lindgren, M., Bartfai, T. & Langel, U. (2001). VE-cadherin-derived cell penetrating peptide, pVEC, with carrier functions. *Exp. Cell Res.* **269**:237-244.

Engqvist-Goldstein, A. E. & Drubin, D. G. (2003). Actin assembly: from yeast to mammals. *Annu. Rev. Cell Dev. Biol.* **19**:287-332.

Faderl, S., Talpaz, M., Estrov, Z., O'Brien, S., Kurzrock, R. & Kantarjian, H. M. (1999). The biology of chronic myeloid leukemia. *N. Engl. J. Med.* **341**:164-172.

Falguieres, T., Mallard, F., Baron, C., Hanau, D., Lingwood, C., Goud, B., Salamero, J. & Johannes, L. (2001). Targeting of Shiga toxin B-subunit to retrograde transport route in association with detergent resistant membranes. *Mol. Biol. Cell.* **12**:2453-2468.

Fardel, O., Payen, L., Courtois, A., Drenou, B., Fauchet, R. & Rault, B. (1998). Differential expression and activity of P-glycoprotein and multidrug resistance-associated protein in CD34-positive KG1a leukemic cells. *Int. J. Oncol.* **12**:315-319.

Feldherr, C. M. & Akin, D. (1993). Regulation of nuclear transport in proliferating and quiescent cells. *Exp. Cell Res.* **205**:179-186.

Ferrand, V. L., Chauvet, M. M., Dell'Amico, M. H., Tsuruo, T., Hirn, M. H. & Bourdeaux, M. J. (1996). MDR-related properties of K562 cells grown in two different culture media. *Anticancer Res.* **16**:3653-3658.

Ferrao, P., Sincock, P., Cole, S. & Ashman, L. (2001). Intracellular P-gp contributes to functional drug efflux and resistance in acute myeloid leukaemia. *Leuk. Res.* **25**:395-405.

Ferrari, A., Pellegrini, V., Arcangeli, C., Fittipaldi, A., Giacca, M. & Beltram, F. (2003). Caveolae-mediated internalization of extracellular HIV-1 tat fusion proteins visualized in real time. *Mol. Ther.* **8**: 284-294.

Filipits, M., Pohl, G., Stranzl, T., Suchomel, R. W., Scheper, R. J., Jager, U., Geissler, K., Lechner, K. & Pirker, R. (1998). Expression of the lung resistance protein predicts poor outcome in de novo acute myeloid leukemia. *Blood.* **91**:1508-1513.

Filipits, M., Suchomel, R. W., Lechner, K. & Pirker, R. (1997b). Immunocytochemical detection of the multidrug resistance-associated protein and P-glycoprotein in acute myeloid leukemia: impact of antibodies, sample source and disease status. *Leukemia.* **11**:1073-1077.

Filipits, M., Suchomel, R. W., Zochbauer, S., Brunner, R., Lechner, K. & Pirker, R. (1997a). Multidrug resistance-associated protein in acute myeloid leukemia: No impact on treatment outcome. *Clin. Cancer Res.* **3**:1419-1425.

Fischer, R., Kohler, K., Fotin-Mleczek, M. & Brock, R. (2004). A stepwise dissection of the intracellular fate of cationic cell-penetrating peptides. *J. Biol. Chem.* **279**:12625-12635.

Fitgerald, D. J., Willingham, M. C., Cardarelli, C. O., Hamada, H., Tsuruo, T., Gottesman, M. M. & Pastan, I. (1987). A monoclonal antibody-Pseudomonas toxin conjugate that specifically kills multidrug-resistant cells. *Proc. Natl. Acad. Sci. USA.* **84**:4288-4292.

Fittipaldi, A., Ferrari, A., Zoppe, M., Arcangeli, C., Pellegrini, V., Beltram, F. & Giacca, M. (2003). Cell membrane lipid rafts mediate caveolar endocytosis of HIV-1 Tat fusion proteins. *J. Biol. Chem.* **278**:34141-34149.

Florea, B. I., van der Sandt, I. C., Schreir, S. M., Kooiman, K., Deryckere, K., de Boer, A. G., Junginger, H. E. & Borchard, G. (2001). Evidence of P-glycoprotein mediated apical to basolateral transport of flunisolide in human broncho-tracheal epithelial cells (Calu-3). *Br. J. Pharmacol.* **134**:1555-1563.

Ford, J. M., Prozialeck, W. C. & Hait, W. N. (1989). Structural features determining activity of phenothiazines and related drugs for inhibition of cell growth and reversal of multidrug resistance. *Mol. Pharmacol.* **35**:105-115.

Fra, A. M., Williamson, E., Simons, K. & Parton, R. G. (1994). Detergent-insoluble glycolipid microdomains in lymphocytes in the absence of caveolae. *J. Biol. Chem.* **269**:30745-30748.

Frankel, A. D. & Pabo, C. O. (1988). Cellular uptake of the tat protein from human immunodeficiency virus. *Cell.* **55**:1189-1193.

Fu, D., Bebawy, M., Kable, E. P. & Roufogalis, B. D. (2004). Dynamic and intracellular trafficking of P-glycoprotein-EGFP fusion protein: Implications in multidrug resistance in cancer. *Int. J. Cancer.* **109**:174-181.

Futaki, S., Ishikawa, T., Niwa, M., Kitagawa, K. & Yagami, T. (1997). Embodying a stable α-helical protein structure through efficient chemical ligation via thioether formation. *Bioorg. Med. Chem.* **5**:1883-1891.

Futaki, S., Suzuki, T., Ohashi, W., Yagami, T., Tanaka, S., Ueda, K. & Sugiura, Y. (2001). Arginine-rich peptides. An abundant source of membrane-permeable peptides having potential as carriers for intracellular protein delivery. *J. Biol. Chem.* **276**:5836-5840.

Futter, C. E., Pearse, A., Hewlett, L. J. & Hopkins, C. R. (1996). Multivesicular endosomes containing internalized EGF-EGF receptor complexes mature and then fuse directly with lysosomes. *J. Cell Biol.* **132**:1011-1023.

Gabbay, E. J., Grier, D., Fingerle, R. E., Reimer, R., Levy, R., Pearce, S. W. & Wilson, W. D. (1976). Interaction specificity of the anthracyclines with deoxyribonucleic acid. *Biochemistry.* **15**:2062-2070.

Gagescu, R., Demaurex, N., Parton, R. G., Hunziker, W., Huber, L. A. & Gruenberg, J. (2000). The recycling endosome of Madin-Darby canine kidney cells is a mildly acidic compartment rich in raft components. *Mol. Biol. Cell.* **11**:2775-2791.

Gale, R. P. & Canaani, E. (1984). An 8-kilobase abl RNA transcript in chronic myelogenous leukemia. *Proc. Natl. Acad. Sci. USA.* **81**:5648-5652.

Garbe, C. (1993). Chemotherapy and chemoimmunotherapy in disseminated malignant melanoma. *Melanoma Res.* **3**:291-299.

Gazit, E., Lee, W. J., Brey, P. T. & Shai, Y. (1994). Mode of action of the antibacterial ceropin B2: a spectrofluorometric study. *Biochemistry.* **33**:10681-10692

Gelman, M. S. & Kopito, R. R. (2002). Rescuing protein conformation: prospects for pharmacological therapy in cystic fibrosis. *J. Clin. Invest.* **110**:1591-1597.

Gentzsch, M., Chang, X. B., Cui, L., Wu, Y., Ozols, V. V., Choudhury, A., Pagano, R. E. & Riordan, J. R. (2004). Endocytic trafficking routes of wild type and DeltaF508 cystic fibrosis transmembrane conductance regulator. *Mol. Biol. Cell.* **15**:2684-2696.

Georges, E., Bradley, G., Gariepy, J. & Ling, V. (1990). Detection of P-glycoprotein isoforms by gene-specific monoclonal antibodies. *Proc. Natl. Acad. Sci. USA.* **87**:152-156.

Georges, E., Tsuruo, T. & Ling, V. (1993). Topology of P-glycoprotein as determined by epitope mapping of MRK-16 monoclonal antibody. *J. Biol. Chem.* **268**:1792-1798.

Georges, E., Zhang, J. T. & Ling, V. (1991). Modulation of ATP and drug binding by monoclonal antibodies against P-glycoprotein. *J. Cell Physiol.* **148**:479-484.

Gerlach, J. H., Endicott, J. A., Juranka, P. F., Henderson, G., Sarangi, F., Deuchars, K. L. & Ling, V. (1986). Homolgy between P-glycoprotein and a bacterial haemolysin transport protein suggests a model for multidrug resistance. *Nature.* **324**:485-489.

Gervasoni, J. E. Jr., Fields, S. Z., Krishna, S., Baker, M. A., Rosado, M., Thuraisamy, K., Hindenburg, A. A. & Taub, R. N. (1991). Subcellular distribution of daunorubicin in P-glycoprotein-positive and –negative drug-resistant cell lines using laser-assisted confocal microscopy. *Cancer Res.* **51**:4955-4963.

Ghetie, M. A., Marches, R., Kufert, S. & Vitetta, E. S. (2004). An anti-CD19 antibody inhibits the interaction between P-glycoprotein (P-gp) and CD19, causes P-gp to translocate out of lipid rafts, and chemosensitizes a multidrug-resistant (MDR) lymphoma cell line. *Blood.* **104**:178-183.

Ghosh, R. N., Mallet, W. G., Soe, T.T., McGraw, T. E. & Maxfield, F. R. (1998). An endocytosed TGN38 chimeric protein is delivered to the TGN after trafficking through the endocytic recycling compartment in CHO cells. *J. Cell Biol.* **142**:923-936.

Giles, F. J., Kantarjian, H. M., Cortes, J., Thomas, D. A., Talpaz, M., Manshouri, T. & Albitar, M. (1999). Multidrug resistance protein expression in chronic myeloid leukemia: associations and significance. *Cancer.* **86**:805-813.

Glickman, J., Croen, K., Kelly, S. & Al-Awqati, Q. (1983). Golgi membranes contain an electrogenic H+ pump in parallel to a chloride conductance. *J. Cell Biol.* **97**:1303-1308.

Goldman, J. M. (2000). Tyrosine-kinase inhibition in treatment of chronic myeloid leukaemia. *Lancet.* **355**:1031-1032.

Gong, Y., Duvvuri, M. & Krise, J. P. (2003). Separate roles for the Golgi apparatus and lysosomes in the sequestration of drugs in the multi-drug resistant human leukemic cell line HL-60. *J. Biol. Chem.* **278**:50234-50239.

Gong, Y., Wang, Y., Chen, F., Han, J., Miao, J., Shao, N., Fang, Z. & Ou Yang, R. (2000). Identification of the subcellular localization of daunorubicin in multidrug-resistant K562 cell line. *Leuk. Res.* **24**:769-774.

Gosalvez, M., Blanco, M., Hunter, J., Miko, M. & Chance, B. (1974). Effects of anticancer agents on the respiration of isolated mitochondria and tumor cells. *Eur. J. Cancer.* **10**:567-574.

Gottlieb, R. A., Nordberg, J., Skowronski, E. & Baboir, B. M. (1996). Apoptosis induced in Jurkat cells by several agents is preceded by intracellular acidification. *Proc. Natl. Acad. Sci. USA.* **93**:654-658.

Granzotto, M., Drigo, I., Candussio, L., Rosati, A., Bartoli, F., Giraldi, T. & Decorti, G. (2004). Rifampicin and verapamil induce the expression of P-glycoprotein in vivo in Ehrlich ascites tumor cells. *Cancer Lett.* **205**:107-115.

Green, M. & Loewenstein, P. M. (1988). Autonomous functional domains of chemically synthesized human immunodeficiency virus tat trans-activator protein. *Cell.* **55**:1179-1188.

Green, S. A. & Kelly, R. B. (1992). Low density lipoprotein receptor and cation-independent mannose 6-phosphate receptor are transported from the cell surface to the Golgi apparatus at equal rates in PC12 cells. *J. Cell Biol.* **117**:47-55.

Greenberger, L. M., Williams, S. S. & Horwitz, S. B. (1987). Biosynthesis of heterogeneous forms of multidrug resistance-associated glycoproteins. *J. Biol. Chem.* **262**:13685-13689.

Griffiths, G., Back, R. & Marsh, M. (1989). A quantitative analysis of the endocytic pathway in baby hamster kidney cells. *J. Cell Biol.* **109**:2703-2720.

Griffiths, G., Hoflack, B., Simons, K., Mellman, I. & Kornfeld, S. (1988). The mannose 6-phosphate receptor and the biogenesis of lysosomes. *Cell.* **52**:329-341.

Grimmer, S., van Deurs, B. & Sandvig, K. (2002). Membrane ruffling and macropinocytosis in A431 cells require cholesterol. *J. Cell Sci.* **115**:2953-2962.

Groll, M., Bajorek, M., Kohler, A., Moroder, L., Rubin, D. M., Huber, R., Glickman, M. H. & Finley, D. (2000). A gated channel into the proteasome core particle. *Nat. Struct. Biol.* **7**:1062-1067.

Gros, P., Croop, J. & Housmann, D. (1986). Mammalian multidrug resistance gene: complete cDNA sequence indicates strong homology to bacterial transport proteins. *Cell.* **47**:371-380.

Gruenberg, J., Griffiths, G. & Howell, K. E. (1989). Characterization of the early endosome and putative endocytic carrier vesicles in vivo and with an assay of vesicle fusion in vitro. *J. Cell Biol.* **108**:1301-1316.

Guelen, L., Paterson, H., Gaken, J., Meyers, M., Farzaneh, F. & Tavassoli, M. (2004). TAT-apoptotin is efficiently delivered and induces apoptosis in cancer cells. *Oncogene.* **23**:1153-1165.

Hamada, H. & Tsuruo, T. (1986). Functional role for the 170- to 180-kDa glycoprotein specific to drug-resistant tumor cells as revealed by monoclonal antibodies. *Proc. Natl. Acad. Sci. USA.* **83**:7785-7789.

Hamann, P. R., Hinman, L. M., Hollander, I., Beyer, C. F., Lindh, D., Holcomb, R., Hallett, W., Tsou, H. R., Upeslacis, J., Shochat, D., Mountain, A., Flowers, D. A. & Bernstein, I. (2002). Gemtuzumab ozogamicin, a potent and selective anti-CD33 antibody- calicheamicin conjugate for treatment of acute myeloid leukemia. *Bioconjug. Chem.* **13**:47-58.

Hamilton, G., Cosentini, E. P., Teleky, B., Koperna, T., Zacheri, J., Riegler, M., Feil, W., Schiessel, R. & Wenzi, E. (1993). The multidrug-resistance modifiers

verapamil, cyclosporine A and tamoxifen induce an intracellular acidification in colon carcinoma cell lines in vitro. *Anticancer Res.* **13**:2059-2064.

Harding, C., Heuser, J. & Stahl, P. (1983). Receptor-mediated endocytosis of transferrin and recycling of the transferrin receptor in rat reticulocytes. *J. Cell Biol.* **97**:329-339.

Hatanaka, M., Maeda, T., Ikemoto, T., Mori, H., Seya, T. & Shimizu, A. (1998). Expression of caveolin-1 in human T cell leukemia cell lines. *Biochem. Biophys. Res. Commun.* **253**:382-387.

Hauser, I. A., Koziolek, M., Hopfer, U. & Thevenod, F. (1998). Therapeutic concentrations of cyclosporine A, but not FK506, increase P-glycoprotein expression in endothelial and renal tubule cells. *Kidney Int.* **54**:1139-1149.

Helms, J. B. & Rothman, J. E. (1992). Inhibition by brefeldin A of a Golgi membrane enzyme that catalyses exchange of guanine nucleotide bound to ARF. *Nature.* **360**:352-354.

Herman, G. A., Bonzelius, F., Cieutat, A. M. & Kelly, R. B. (1994). A distinct class of intracellular storage vesicles, identified by expression of the glucose transporter GLUT4. *Proc. Natl. Acad. Sci. USA.* **91**:12750-12754.

Hershko, A. & Ciechanover, A. (1998). The ubiquitin system. *Annu. Rev. Biochem.* **67**:425-479.

Herweijer, H., Sonneveld, P., Baas, F. & Nooter, K. (1990). Expression of mdr1 and mdr3 multidrug-resistance genes in human acute and chronic myeloid leukemias and association with stimulation of drug accumulation by cyclosporine. *J. Natl. Cancer Inst.* **82**:1133-1140.

Heuser, J. (1989). Changes in lysosome shape and distribution correlated with changes in cytoplasmic pH. *J. Cell Biol.* **108**:855-864.

Higgins, C. F., Callaghan, R., Linton, K. J., Rosenberg, M. F. & Ford, R. C. (1997). Structure of the multidrug resistance P-glycoprotein. *Semin. Cancer Biol.* **8**:135-142.

Higgins, C. F. & Gottesman, M. M. (1992). Is the multidrug transporter a flippase? *Trends Biochem. Sci.* **17**:18-21.

Hirose, M., Hosoi, E., Hamano, S. & Jalili, A. (2003). Multidrug resistance in hematological malignancy. *J. Med. Invest.* **50**:126-135.

Hoffman, M. M. & Roepe, P. D. (1997). Analysis of ion transport perturbations caused by hu MDR 1 protein overexpression. *Biochemistry.* **36**:11153-11168.

Hoki, Y., Fujimori, A. & Pommier, Y. (1997). Differential cytotoxicity of clinically important camptothecin derivatives in P-glycoprotein-overexpressing cell lines. *Cancer Chemother. Pharmacol.* **40**:433-438.

Homolya, L., Varadi, A. & Sarkadi, B. (2003). Multidrug resistance-associated proteins: Export pumps for conjugates with glutathione, glucuronate or sulfate. *Biofactors.* **17**:103-114.

Hooper, N. M. (1999). Detergent-insoluble glycosphingolipid/cholesterol-rich membrane domains, lipid rafts and caveolae (review). *Mol. Membr. Biol.* **16**:145-156.

Hu, W., Howard, M. & Lukacs, G. L. (2001). Multiple endocytic signals in the C-terminal tail of the cystic fibrosis transmembrane conductance regulator. *Biochem. J.* **354**:561-572.

Huang, F., Khvorova, A., Marshall, W. & Sorkin, A. (2004). Analysis of clathrin-mediated endocytosis of epidermal growth factor receptor by RNA interference. *J. Biol. Chem.* **279**:16657-16661.

Hunault, M., Zhou, D., Delmer, A., Ramond, S., Viguie, F., Cadiou, M., Perrot, J. Y., Levy, V., Rio, B., Cymbalista, F., Zittoun, R. & Marie, J. P. (1997). Multidrug resistance gene expression in acute myeloid leukemia: major prognosis significance for in vivo drug resistance to induction treatment. *Ann. Hematol.* **74**:65-71.

Hunter, J., Jepson, M. A., Tsuruo, T., Simmons, N. L. & Hirst, B. H. (1993). Functional expression of P-glycoprotein in apical membranes of human intestinal Caco-2 cells. Kinetics of vinblastine secretion and interaction with modulators. *J. Biol. Chem.* **268**:14991-14997.

Hurwitz, S. J., Terashima, M., Mizunuma, N. & Slapak, C. A. (1997). Vesicular anthracycline accumulation in doxorubicin-selected U937 cells: participation of lysosomes. *Blood.* **89**:3745-3754.

Hyafil, F., Vergely, C., Du Vignaud, P. & Grand-Perret, T. (1993). In vitro and in vivo reversal of multidrug resistance by GF120918, an acridonecarboxamide derivative. *Cancer Res.* **53**:4595-4602.

Ichas, F., Jouaville, L. S. & Mazat, J. P. (1997). Mitochondria are excitable organelles capable of generating and conveying electrical and calcium signals. *Cell.* **89**:1145-1153.

Ikonen, E. (2001). Roles of lipid rafts in membrane transport. *Curr. Opin. Cell Biol.* **13**:470-477.

Illmer, T., Schaich, M., Platzbecker, U., Freiberg-Richter, J., Oelschlagel, U., von Bonin, M., Pursche, S., Bergemann, T., Ehninger, G. & Schleyer, E. (2004). P-glycoprotein-mediated drug efflux is a resistance mechanism of chronic myelogenous leukemia cells to treatment with imatinib mesylate. *Leukemia.* **18**:401-408.

Izquierdo, M. A., Neefjes, J. J., Mathari, A. E., Flens, M. J., Scheffer, G. L. & Scheper, R. J. (1996b). Overexpression of the ABC transporter TAP in multidrug-resistant human cancer cell lines. *Br. J. Cancer.* **74**:1961-1967.

Izquierdo, M. A., Scheffer, G. L., Flens, M. J., Schroeijers, A. B., van der Valk, P. & Scheper, R. J. (1996a). Major vault protein LRP-related multidrug resistance. *Eur. J. Cancer.* **32A**:979-984.

Jaffrezou, J. P., Levade, T., Bettaieb, A., Andrieu, N., Bezombes, C., Maestre, N., Vermeesch, S., Rousse, A. & Laurent, G. (1996). Daunorubicin-induced apoptosis: triggering of ceramide generation through sphingomyelin hydrolysis. *EMBO J.* **15**:2417-2424.

Jaroszewski, J. W., Kaplan, O., Syi, J. L., Sehested, M., Faustino, P. J. & Cohen, J. S. (1990). Concerning antisense inhibition of the multiple drug resistance gene. *Cancer Commun.* **2**:287-294.

Jette, L., Beaulieu, E., Leclerc, J. M. & Beliveau, R. (1996). Cyclosporin A treatment induces overexpression of P-glycoprotein in the kidney and other tissues. *Am. J. Physiol.* **270**:F756-F765.

Jette, L., Murphy, G. F., Leclerc, J. M. & Beliveau, R. (1995a). Interaction of drugs with P-glycoprotein in brain capillaries. *Biochem. Pharmacol.* **50**:1701-1709.

Jette, L., Pouliot, J. F., Murphy, G. F. & Beliveau, R. (1995b). Isoform I (mdr3) is the major form of P-glycoprotein expressed in mouse brain capillaries. Evidence for cross-reactivity of antibody C219 with an unrelated protein. *Biochem. J.* **305**:761-766.

Jin, M. & Snider, M. D. (1993). Role of microtubules in transferrin receptor transport from the cell surface to endosomes and the Golgi complex. *J. Biol. Chem.* **268**:18390-18397.

Jodoin, J., Demeule, M., Fenart, L., Cecchelli, R., Farmer, S., Linton, K. J., Higgins, C. F. & Beliveau, R. (2003). P-glycoprotein in blood-brain barrier endothelial cells: interaction and oligomerization with caveolins. *J. Neurochem.* **87**:1010-1023.

Johannes, L. & Lamaze, C. (2002). Clathrin-dependent or not: is it still the question? *Traffic.* **3**:443-451.

Johnstone, R. W., Cretney, E. & Smyth, M. J. (1999). Pglycoprotein protects leukemia cells against caspase-dependent, but not caspase-independent, cell death. *Blood.* **93**:1075-1085.

Johnstone, R. W., Ruefli, A. A. & Smyth, M. J. (2000). Multiple physiological functions for the multidrug transporter P-glycoprotein? *Trends Biochem. Sci.* **25**:1-6.

Joliot, A., Pernelle, C., Deagostini-Bazin, H. & Prochiantz, A. (1991). Antennapedia homeobox peptide regulates neural morphogenesis. *Proc. Natl. Acad. Sci. USA.* **88**:1864-1868

Juliano, R. L. & Ling, V. (1976). A surface glycoprotein modulating drug permeability in Chinese hamster ovary cell mutants. *Biochim. Biophys. Acta.* **455**:152-162.

Jung, K., Reinholdt, C. & Scholz, D. (1987). Inhibitory effect of cyclosporine on the respiratory efficiency of isolated human kidney mitochondria. *Transplantation.* **43**:162-163.

Kaplan, I. M., Wadia, J. S. & Dowdy, S. F. (2005). Cationic TAT peptide transduction domain enters cells by macropinocytosis. *J. Control. Release.* **102**:247-253.

Karlsson, J., Kuo, S. M., Ziemniak, J. & Artursson, P. (1993). Transport of celiprolol across human intestinal epithelial (Caco-2) cells: mediation of secretion by multiple transporters including P-glycoprotein. *Br. J. Pharmacol.* **110**:1009-1016.

Kartner, N., Riordan, J. R. & Ling, V. (1983). Cell surface P-glycoprotein associated with multidrug resistance in mammalian cell lines. *Science.* **221**:1285-1288.

Kelley, S. L., Basu, A., Teicher, B. A., Hacker, M. P., Hamer, D. H. & Lazo, J. S. (1988). Overexpression of the metallothionein confers resistance to anticancer drugs. *Science.* **241**:1813-1815.

Kessel, D., Botterill, V. & Wodlinsky, I. (1968). Uptake and retention of daunomycin by mouse leukemic cells as factors in drug response. *Cancer Res.* **28**:938-941.

Kiehntopf, M., Brach, M. A., Licht, T., Petschauer, S., Karawajew, L., Kirschning, C. & Hermann, F. (1994). Ribozyme-mediated cleavage of the MDR-1 transcript restores chemosensitivity in previously resistant cancer cells. *EMBO J.* **13**:4645-4652.

Kim, H., Barroso, M., Samanta, R., Greenberger, L. & Sztul, E. (1997). Experimentally induced changes in the endocytic traffic of P-glycoprotein alter drug resistance of cancer cells. *Am. J. Physiol.* **273**:C687-C702.

Kipp, H., Pichetshote, N. & Arias, I. M. (2001). Transporters on demand: intrahepatic pools of canalicular ATP binding cassette transporters in rat liver. *J. Biol. Chem.* **276**:7218-7224.

Kitazono, M., Sumizawa, T., Takebayashi, Y., Chen, Z. S., Furukawa, T., Nagayama, S., Tani, A., Takao, S., Aikou, T. & Akiyama, S. (1999). Multidrug

resistance and the lung resistance-related protein in human colon carcinoma SW-620 cells. *J. Natl. Cancer Inst.* **91**:1647-1653.

Koeffler, H. P., Billing, R., Lusis, A. J., Sparkes, R. & Golde, D. W. (1980). An undifferentiated variant derived from the human acute myelogenous leukemia cell line (KG-1). *Blood.* **56**:265-273.

Kokubu, N., Cohen, D. & Watanabe, T. (1997). Functional modulation of ATPase of P-glycoprotein by C219, a monoclonal antibody against P-glycoprotein. *Biochem. Biophys. Res. Commun.* **230**:398-401.

Kruijtzer, C. M., Beijnen, J. H., Rosing, H., ten Bokkel Huinink, W. W., Schot, M., Jewell, R. C., Paul, E. M. & Schellens, J. H. (2002). Increased oral bioavailability of topotecan in combination with the breast cancer resistance protein and P-glycoprotein inhibitor GF120918. *J. Clin. Oncol.* **20**:2943-2950.

Kuwazuru, Y., Yoshimura, A., Hanada, S., Ichikawa, M., Saito, T., Uozumi, K., Utsunomiya, A., Arima, T. & Akiyama, S. (1990). Expression of the multidrug transporter, P-glycoprotein, in chronic myelogenous leukaemia cells in blast crisis. *Br. J. Haematol.* **74**:24-29.

Labroille, G., Belloc, F., Bilhou-Nabera, C., Bonnefille, S., Bascans, E., Boisseau, M. R., Bernard, P. & Lacombe, F. (1998). Cytometric study of intracellular P-gp expression and reversal of drug resistance. *Cytometry.* **32**:86-94.

Laing, N. M., Belinsky, M. G., Kruh, G. D., Bell, D. W., Boyd, J. T., Barone, L., Testa, J. R. & Tew, K. D. (1998). Amplification of the ATP-binding cassette 2 transporter gene is functionally linked with enhanced efflux of estramustine in ovarian carcinoma cells. *Cancer Res.* **58**:1332-1337.

Lampidis, T. J., Castello, C., del Giglio, A., Pressman, B. C., Viallet, P., Trevorrow, K. W., Valet, G. K., Tapiero, H. & Savaraj, N. (1989). Relevance of

the chemical charge of rhodamine dyes to multiple drug resistance. *Biochem. Pharmacol.* **38**:4267-4271.

Lampidis, T. J., Kolonias, D., Podona, T., Israel, M., Safa, A. R., Lothstein, L., Savaraj, N., Tapiero, H. & Priebe, W. (1997). Circumvention of P-GP MDR as a function of anthracycline lipophilicity and charge. *Biochemistry.* **36**:2679-2685.

Larkin, J. M., Brown, M. S., Goldstein, J. L. & Anderson, R. G. (1983). Depletion of intracellular potassium arrests coated pit formation and receptor-mediated endocytosis in fibroblasts. *Cell.* **33**:273-285.

Lautier, D., Bailly, J. D., Demur, C., Herbert, J. M., Bousquet, C. & Laurent, G. (1997). Altered intracellular distribution of daunorubicin in immature acute myeloid leukemia cells. *Int. J. Cancer.* **71**:292-299.

Lavie, Y., Fiucci, G. & Liscovitch, M. (1998). Up-regulation of caveolae and caveolar constituents in multidrug-resistant cancer cells. *J. Biol. Chem.* **273**:32380-32383.

Lavie, Y. & Liscovitch, M. (2000). Changes in lipid and protein constituents of rafts and caveolae in multidrug resistant cancer cells and their functional consequences. *Glycoconj. J.* **17**:253-259.

Lea, N. C., Buggins, A. G., Orr, S. J., Mufti, G. J. & Thomas, N. S. (2003). High efficiency protein transduction of quiescent and proliferating primary hematopoietic cells. *J. Biochem. Biophys. Methods.* **55**:251-258.

Lee, C. G., Gottesman, M. M., Cararelli, C. O., Ramachandra, M., Jeang, K. T., Ambudkar, S. V., Pastan, I. & Dey, S. (1998). HIV-1 protease inhibitors are substrates for the MDR1 multidrug transporter. *Biochemistry.* **37**:3594-3601.

Legler, D. F., Doucey, M. A., Schneider, P., Chapatte, L., Bender, F. C. & Bron, C. (2005). Differential insertion of GPI-anchored GFPs into lipid rafts of live cells. *FASEB J.* **19**:73-75.

Legrand, O., Zittoun, R. & Marie, J. P. (1999). Role of MRP1 in multidrug resistance in acute myeloid leukemia. *Leukemia.* **13**:578-584.

Lehne, G. & Rugstad, H. E. (1998). Cytotoxic effect of the cyclosporin PSC 833 in multidrug-resistant leukaemia cells with increased expression of P-glycoprotein. *Br. J. Cancer.* **78**:593-600.

Leier, I., Jedlitschky, G., Buccholz, U., Cole, S. P., Deeley, R. G. & Keppler, D. (1994). The MRP gene encodes an ATP-dependent export pump for leukotriene C4 and structurally related conjugates. *J. Biol. Chem.* **269**:27807-27810.

Leith, C. P. (1998). Multidrug resistance in leukemia. *Curr. Opin. Hematol.* **5**:287-291.

Leith, C. P., Kopecky, K. J., Chen, I. M., Eijdems, L., Slovak, M. L., McConnell, T. S., Head, D. R., Weick, J., Grever, M. R., Appelbaum, F. R. & Willman, C. L. (1999). Frequency and clinical significance of the expression of the multidrug resistance proteins MDR1/P-glycoprotein, MRP1, and LRP in acute myeloid leukemia: a Southwest Oncology Group Study. *Blood.* **94**:1086-1099.

Lewin, M., Carlesso, N., Tung, C. H., Tang, X. W., Cory, D., Scadden, D. T. & Weissleder, R. (2000). Tat peptide-derivatized magnetic nanoparticles allow in vivo tracking and recovery of progenitor cells. *Nat. Biotechnol.* **18**:410-414.

Li, A. P., Kaminski, D. L. & Rasmussen, A. (1995). Substrates of human hepatic cytochrome P450 3A4. *Toxicology.* **104**:1-8.

Li, L. H., McCarthy, P. & Hui, S. W. (2001). High-efficiency electrotransfection of human primary hematopoietic stem cells. *FASEB J.* **15**:586-588.

Lim, S. N., Bonzelius, F., Low, S. H., Wille, H., Weimbs, T. & Herman, G. A. (2001). Identification of discrete classes of endosome-derived small vesicles as a major cellular pool for recycling membrane proteins. *Mol. Biol. Cell.* **12**:981-995.

Lin Yin, J. A., Wheatley, K., Rees, J. K., Burnett, A. K; UK MRC Adult Leukemia Working Party. (2001). Comparison of 'sequential' versus 'standard' chemotherapy as re-induction treatment, with or without cyclosporine, in refractory/relapsed acute myeloid leukaemia (AML): results of the UK Medical Research Council AML-R trial. *Br. J. Haematol.* **113**:713-726.

Liscovitch, M. & Lavie, Y. (2000). Multidrug resistance: a role for cholesterol efflux pathways? *Trends Biochem. Sci.* **25**:530-534.

Liscovitch, M. & Lavie, Y. (2002). Cancer multidrug resistance: A review of recent drug discovery research. *IDrugs.* **5**:349-355.

List, A. F., Kopecky, K. J., Willman, C. L., Head, D. R., Persons, D. L., Slovak, M. L., Dorr, R., Karanes, C., Hynes, H. E., Doroshow, J. H., Shurafa, M. & Appelbaum, F. R. (2001). Benefit of cyclosporine modulation of drug resistance in patients with poor-risk acute myeloid leukemia: a Southwest Oncology Group study. *Blood.* **98**:3212-3220.

List, A. F., Kopecky, K. J., Willman, C. L., Head, D. R., Slovak, M. L., Douer, D., Dakhil, S. R. & Appelbaum, F. R. (2002). Cyclosporine inhibition of P-glycoprotein in chronic myeloid leukemia blast phase. *Blood.* **100**:1910-1912.

List, A. F., Spier, C., Greer, J., Wolff, S., Hutter, J., Dorr, R., Salmon, S., Futscher, B., Baier, M. & Dalton, W. (1993). Phase I/II trial of cyclosporine as a chemotherapy-resistance modifier in acute leukemia *J. Clin. Oncol.* **11**:1652-1660.

List, A. F., Spier, C. G., Grogan, T. M., Johnson, C., Roe, D. J., Greer, J. P., Wolff, S. N., Broxterman, H. J., Scheffer, G. L., Scheper, R. J. & Dalton, W. S. (1996).

Overexpression of the major vault transporter protein lung-resistance protein predicts treatment outcome in acute myeloid leukemia. *Blood.* **87**:2464-2469.

Liu, B., Sun, D., Xia, W., Hung, M. C. & Yu, D. (1997). Cross-reactivity of C219 anti-p170(mdr-1) antibody with p185(c-erbB2) in breast cancer cells: cautions on evaluating p170(mdr-1). *J. Natl. Cancer Inst.* **89**:1524-1529.

Liu, L. F., Liu, C. C. & Alberts, B. M. (1980). Type II DNA topoisomerases: enzymes that can unknot a topologically knotted DNA molecule via a reversible double-strand break. *Cell.* **19**:697-707.

Liu, Y. Y., Han, T. Y., Giuliano, A. E. & Cabot, M. C. (2001). Ceramide glycosylation potentiates cellular multidrug resistance. *FASEB J.* **15**:719-730.

Liu, Y. Y., Han, T. Y., Giuliano, A. E. & Cabot, M. C. (1999). Expression of glucosylceramide synthase, converting ceramide to glucosylceramide, confers adriamycin resistance in human breast cancer cells. *J. Biol. Chem.* **274**:1140-1146.

Loe, D. W., Deeley, R. G. & Cole, S. P. (2000). Verapamil stimulates glutathione transport by the 190-kDa multidrug resistance protein 1 (MRP1). *J. Pharmacol. Exp. Ther.* **293**:530-538.

Loetchutinat, C., Priebe, W. & Garnier-Suillerot, A. (2001). Drug sequestration in cytoplasmic organelles does not contribute to the diminished sensitivity of anthracyclines in multidrug resistant K562 cells. *Eur. J. Biochem.* **268**:4459-4467.

Longhurst, T. J., O'Neill, G. M., Harvie, R. M. & Davey, R. A. (1996). The anthracycline resistance-associated (ara) gene, a novel gene associated with multidrug resistance in human leukaemia cell line. *Br. J.Cancer.* **74**:1331-1335.

Longva, K. E., Blystad, F. D., Stang, E., Larsen, A. M., Johannessen, L. E. & Madshus, I. H. (2002). Ubiquitination and proteasomal activity is required for

transport of the EGF receptor to inner membranes of multivesicular bodies. *J. Cell Biol.* **156**:843-854.

Loo, T. W., Bartlett, M. C. & Clarke, D. M. (2005). The dileucine motif at the COOH terminus of human multidrug resistance P-glycoprotein is important for folding but not activity. *J. Biol. Chem.* **280**:2522-2528.

Loo, T. W. & Clarke, D. M. (1995). Membrane topology of a cysteine less mutant of human P-glycoprotein. *J. Biol. Chem.* **270**:843-848.

Loo, T. W. & Clarke, D. M. (1999). The human multidrug resistance P-glycoprotein is inactive when its maturation is inhibited: potential for a role in cancer chemotherapy. *FASEB. J.* **13**:1724-1732.

Loo, T. W. & Clarke, D. M. (2001). Defining the drug-binding site in the human multidrug resistance P-glycoprotein using a methanethiosulfonate analog of verapamil, MTS-verapamil. *J. Biol. Chem.* **276**:14972-14979.

Lowe, S. W., Ruley, H. E., Jacks, T. & Housman, D. E. (1993). p53-dependent apoptosis modulates the cytotoxicity of anticancer agents. *Cell.* **74**:957-967.

Lozzio, C. B. & Lozzio, B. B. (1975). Human chronic myelogenous leukemia cell-line with positive Philadelphia chromosome. *Blood.* **45**:321-334.

Lozzio, B. B., Lozzio, C. B., Bamberger, E. G. & Feliu, A. S. (1981). A multipotential leukemia cell line (K-562) of human origin. *Proc. Soc. Exp. Biol. Med.* **166**:546-550.

Lukacs, G. L., Segal, G., Kartner, N., Grinstein, S. & Zhang, F. (1997). Constitutive internalization of cystic fibrosis transmembrane conductance regulator occurs via clathrin-dependent endocytosis and is regulated by protein phosphorylation. *Biochem. J.* **328**:353-361.

Lundberg, M. & Johansson, M. (2002). Positively charged DNA-binding proteins cause apparent cell membrane translocation. *Biochem. Biophys. Res. Commun.* **291**:367-371.

Lundberg, P. & Langel, U. (2003). A brief introduction to cell penetrating peptides. *J. Mol. Recognit.* **16**:227-233.

Luzio, J. P., Rous, B. A., Bright, N. A., Pryor, P. R., Mullock, B. M. & Piper, R. C. (2000). Lysosome-endosome fusion and lysosome biogenesis. *J. Cell Sci.* **113**:1515-1524.

Mallard, F., Antony, C., Tenza, D., Salamero, J., Goud, B. & Johannes, L. (1998). Direct pathways from early/recycling endosomes to the Golgi apparatus revealed through the study of shiga toxin B-fragment transport. *J. Cell Biol.* **143**:973-990.

Marie, J. P., Huet, S., Faussat, A. M., Perrot, J. Y., Chevillard, S., Barbu, V., Bayle, C., Boutonnat, J., Calvo, F., Campos-Guyotat, L., Colosetti, P., Cazin, J. L., de Cremoux, P., Delvincourt, C., Demur, C., Drenou, B., Fenneteau, O., Feuillard, J., Garnier-Suillerot, A., Genne, P., Gorisse, M. C., Gosselin, P., Jouault, H., Lacave, R. & Robert, J. (1997). Multicentric evaluation of the MDR phenotype in leukemia. French Network of the Drug Resistance Intergroup, and Drug Resistance Network of Assistance Publique-Hopitaux de Paris. *Leukemia.* **11**:1086-1094.

Marie, J. P., Zittoun, R. & Sikic, B. I. (1991). Multidrug resistance (*mdr*1) gene expression in adult acute leukemias: correlations with treatment outcome and in vitro drug sensitivity. *Blood.* **78**:586-592.

Marit, G., Cao, Y., Froussard, P., Ripoche, J., Dupouy, M., Elandaloussi, A., Lacombe, F., Mahon, F. X., Keller, H., Pla, M., Reiffers, J. & Theze, J. (2000). Increased liposome-mediated gene transfer into hematopoietic cells grown in adhesion to stromal or fibroblast cell line monolayers. *Eur. J. Haematol.* **64**:22-31.

Marks, D. C., Su, G. M., Davey, R. A. & Davey, M. W. (1996). Extended multidrug resistance in haemopoietic cells. *Br. J. Haematol.* **95**:587-595.

Martys, J. L., Wjasow, C., Gangi, D. M., Kielian, M. C., McGraw, T. E. & Backer, J. M. (1996). Wortmannin-sensitive trafficking pathways in Chinese hamster ovary cells. Differential effects on endocytosis and lysosomal sorting. *J. Biol. Chem.* **271**:10953-10962.

Matsuo, K., Kohno, K., Takano, H., Sato, S., Kiue, A. & Kuwano, M. (1990). Reduction of drug accumulation and DNA topoisomerase II activity in acquired teniposide-resistant human cancer KB cell lines. *Cancer Res.* **50**:5819-5824.

Matsuzaki, J., Yamamoto, C., Miyama, T., Takanaga, H., Matsuo, H., Ishizuka, H., Kawahara, Y., Kuwano, M., Naito, M., Tsuruo, T. & Sawada, Y. (1999a). Contribution of P-glycoprotein to bunitrolol efflux across blood-brain barrier. *Biopharm. Drug Dispos.* **20**:85-90.

Matsuzaki, K., Sugishita, K. & Miyajima, K. (1999b). Interactions of an antimicrobial peptide, magainin 2, with lipopolysaccharide-containing liposomes as a model for outer membranes of gram-negative bacteria. *FEBS Lett.* **449**:221-224.

Mauxion, F., Le Borgne, R., Munier-Lehmann, H. & Hoflack, B. (1996). A casein kinase II phosphorylation site in the cytoplasmic domain of the cation-dependent mannose 6-phosphate receptor determines the high affinity interaction of the AP-1 Golgi assembly proteins with membranes. *J. Biol. Chem.* **271**:2171-2178.

Mayor, S., Presley, J. F. & Maxfield, F. R. (1993). Sorting of membrane components from endosomes and subsequent recycling to the cell surface occurs by a bulk flow process. *J. Cell Biol.* **121**:1257-1269.

Mayor, S., Sabharanjak, S. & Maxfield, F. R. (1998). Cholesterol-dependent retention of GPI-anchored proteins in endosomes. *EMBO J.* **17**:4626-4638.

Mazel, M., Clair, P., Rouselle, C., Vidal, P., Scherrmann, J. M., Mathieu, D. & Temsamani, J. (2001). Doxorubicin-peptide conjugates overcome multidrug resistance. *Anticancer drugs.* **12**:107-116.

McGahon, A., Bissonnette, R., Schmitt, M., Cotter, K. M., Green, D. R. & Cotter, T. G. (1994). BCR-ABL maintains resistance of chronic myelogenous leukemia cells to apoptotic cell death. *Blood.* **83**:1179-1187.

Mechetner, E. B. & Roninson, I. B. (1992). Efficient inhibition of P-glycoprotein-mediated multidrug resistance with a monoclonal antibody. *Proc. Natl. Acad. Sci. USA.* **89**:5824-5828.

Mehl, A. M., Jones, M., Rowe, M. & Brennan, P. (2001). Characterization of a CD40-dominant inhibitory receptor mutant. *J. Immunol.* **167**:6388-6393.

Mellman, I. & Steinman, R. M. (2001). Dendritic cells: specialized and regulated antigen processing machines. *Cell.* **106**:255-258.

Meschini, S., Calcabrini, A., Monti, E., Del Bufalo, D., Stringaro, A., Dolfini, E. & Arancia, G. (2000). Intracellular P-glycoprotein expression is associated with the intrinsic multidrug resistance phenotype in human colon adenocarcinoma cells. *Int. J. Cancer.* **87**:615-628.

Meschini, S., Marra, M., Calcabrini, A., Monti, E., Gariboldi, M., Dolfini, E. & Arancia, G. (2002). Role of the lung resistance-related protein (LRP) in the drug sensitivity of cultured tumor cells. *Toxicol. In Vitro.* **16**:389-398.

Mikisch, G. H., Pai, L. H., Gottesman, M. M. & Pastan, I. (1992). Monoclonal antibody MRK16 reverses the multidrug resistance of multidrug-resistant transgenic mice. *Cancer Res.* **52**:4427-4432.

Mitchell, D. J., Kim, D. T., Steinman, L., Fathman, C. G. & Rothbard, J. B. (2000). Polyarginine enters cells more efficiently than other polycationic homopolymers. *J. Pept. Res.* **56**:318-325.

Miyashita, T., Krajewski, S., Krajewska, M., Wang, H. G., Lin, H. K., Liebermann, D. A., Hoffman, B. & Reed, J. C. (1994). Tumor suppressor p53 is a regulator of bcl-2 and bax gene expression in vitro and in vivo. *Oncogene.* **9**:1799-1805.

Molendijk, A. J., Ruperti, B. & Palme, K. (2004). Small GTPases in vesicle trafficking. *Curr. Opin. Plant Biol.* 7:694-700.

Molinari, A., Calcabrini, A., Crateri, P. & Arancia, G. (1990). Interaction of anthracyclinic antibiotics with cytoskeletal components of cultured carcinoma cells (CG5). *Exp. Mol. Pathol.* **53**:11-33.

Molinari, A., Calcabrini, A., Meschini, S., Stringaro, A., Del Bufalo, D., Cianfriglia, M. & Arancia, G. (1998). Detection of P-glycoprotein in the Golgi apparatus of drug-untreated human melanoma cells. *Int. J. Cancer.* **75**:885-893.

Molinari, A., Cianfriglia, M., Meschini, S., Calcabrini, A. & Arancia, G. (1994). P-glycoprotein expression in the Golgi apparatus of multidrug-resistant cells. *Int. J. Cancer.* **59**:789-795.

Morris, M. C., Vidal, P., Chaloin, L., Heitz, F. & Divita, G. (1997). A new peptide vector for efficient delivery of oligonucleotides into mammalian cells. *Nucleic Acids Res.* **25**:2730-2736.

Mousavi, S. A., Brech, A., Berg, T. & Kjeken, R. (2003). Phosphoinositide 3-kinase regulates maturation of lysosomes in rat hepatocytes. *Biochem. J.* **372**:861-869.

Moyer, B. D., Loffing, J., Schwiebert, E. M., Loffing-Cueni, D., Halpin, P. A., Karlson, K. H., Ismailov, I. I., Guggino, W. B., Langford, G. M. & Stanton, B. A. (1998). Membrane trafficking of the cystic fibrosis gene product, cystic fibrosis transmembrane conductance regulator, tagged with green fluorescent protein in madin-darby canine kidney cells. *J. Biol. Chem.* **273**:21759-21768.

Mubashar, M., Harrington, K. J., Chaudhary, K. S., Lalani, el-N., Stamp, G. W. & Peters, A. M. (2004). Differential effects of toremifene on doxorubicin, vinblastine and Tc-99m-sestamibi in P-glycoprotein-expressing breast and head and neck cancer cell lines. *Acta. Oncol.* **43**:443-452.

Mulder, H. S., Dekker, H., Pinedo, H. M. & Lankelma, J. (1995). The P-glycoprotein-mediated relative decrease in cytosolic free drug concentration is similar for several anthracyclines with varying lipophilicity. *Biochem. Pharmacol.* **50**:967-974.

Muller, C., Bailly, J. D., Goubin, F., Laredo, J., Jaffrezou, J. P., Bordier, C. & Laurent, G. (1994). Verapamil decreases P-glycoprotein expression in multidrug-resistant human leukemic cell lines. *Int. J. Cancer.* **56**:749-754.

Murakami, T., Shibuya, I., Ise, T., Chen, Z. S., Akiyama, S., Nakagawa, M., Izumi, H., Nakamura, T., Matsuo, K., Yamada, Y. & Kohno, K. (2001). Elevated expression of vacuolar proton pump genes and cellular PH in cisplatin resistance. *Int. J. Cancer.* **93**:869-874.

Nagahara, H., Vocero-Akbani, A. M., Snyder, E. L., Ho, A., Latham, D. G., Lissy, N. A., Becker-Hapak, M., Ezhevsky, S. A. & Dowdy, S. F. (1998). Transduction of full-length TAT fusion proteins into mammalian cells: TAT-p27Kip1 induces cell migration. *Nat. Med.* **4**:1449-1452

Nakase, I., Niwa, M., Takeuchi, T., Sonomura, K., Kawabata, N., Koike, Y., Takehashi, M., Tanaka, S., Ueda, K., Simpson, J. C., Jones, A. T., Sugiura, Y. &

Futaki, S. (2004). Cellular uptake of arginine-rich peptides: roles for macropinocytosis and actin rearrangement. *Mol. Ther.* **10**:1011-1022.

Neefjes, J. J., Momburg, F. & Hammerling, G. J. (1993). Selective and ATP-dependent translocation of peptides by the MHC-encoded transporter. *Science.* **261**:769-771.

Newman, M. J., Rodarte, J. C., Benbatoul, K. D., Romano, S. J., Zhang, C., Krane, S., Moran, E. J., Uyeda, R. T., Dixon, R., Guns, E. S. & Mayer, L. D. (2000). Discovery and characterization of OC144-093, a novel inhibitor of P-glycoprotein-mediated multidrug resistance. *Cancer Res.* **60**:2964-2972.

Nichols, B. J. (2002). A distinct class of endosome mediates clathrin-independent endocytosis to the Golgi complex. *Nat. Cell Biol.* **4**:374-378.

Nichols, B. J., Kenworthy, A. K., Polishchuk, R. S., Lodge, R., Roberts, T. H., Hirschberg, K., Phair, R. D. & Lippincott-Schwartz, J. (2001). Rapid cycling of lipid raft markers between the cell surface and Golgi complex. *J. Cell Biol.* **153**:529-541.

Nielsen, D., Maare, C. & Skovsgaard, T. (1996). Cellular resistance to anthracyclines. *Gen. Pharmacol.* **27**:251-255.

Niwa, K., Tanaka, R., Murase, H., Ishikawa, T., Fujita, H., Himeno, M. & Tanaka, Y. (2003). Two lysosomal membrane proteins, LGP85 and LGP107, are delivered to late endosomes/lysosomes through different intracellular routes after exiting from the trans-Golgi network. *Biochem. Biophys. Res. Commun.* **301**:833-840.

Norris, M. D., Haber, M., King, M. & Davey, R. A. (1989). Atypical multidrug resistance in CCRF-CEM cells selected for high level methotrexate resistance: reactivity to monoclonal antibody C219 in the absence of P-glycoprotein expression. *Biochem. Biophys. Res. Commun.* **165**:1435-1441.

Oehlke, J., Scheller, A., Wiesner, B., Krause, E., Beyermann, M., Klauschenz, E., Melzig, M. & Bienert, M. (1998). Cellular uptake of an alpha-helical amphipathic model peptide with the potential to deliver polar compounds into the cell interior non-endocytically. *Biochim, Biophys, Acta.* **1414**:127-139.

Ohkawa, K., Asakura, T., Takada, K., Sawai, T., Hashizume, Y., Okawa, Y. & Yanaihara, N. (1999). Calpain inhibitor causes accumulation of ubiquitinated P-glycoprotein at the cell surface: possible role of calpain in P-glycoprotein turnover. *Int. J. Oncol.* **15**:677-686.

Ohno, H., Stewart, J., Fournier, M. C., Bosshart, H., Rhee, I., Miyatake, S., Saito, T., Gallusser, A., Kirchhausen, T. & Bonifacino, J. S. (1995). Interaction of tyrosine-based sorting signals with clathrin-associated proteins. *Science.* **269**:1872-1875.

Ouar, Z., Bens, M., Vignes, C., Paulais, M., Pringel, C., Fleury, J., Cluzeaud, F., Lacave, R. & Vandewalle, A. (2003). Inhibitors of vacuolar H+-ATPase impair the preferential accumulation of daunomycin in lysosomes and reverse the resistance to anthracyclines in drug-resistant renal epithelial cells. *Biochem. J.* **370**:185-193.

Paietta, E. (1997). Classical mutlidrug resistance in acute myeloid leukaemia. *Med. Oncol.* **14**:53-60.

Pallis, M. & Russell, N. (2000). P-glycoprotein plays a drug-efflux-independent role in augmenting cell survival in acute myeloblastic leukemia and is associated with modulation of a sphingomyelin-ceramide apoptotic pathway. *Blood.* **95**:2897-2904.

Parolini, I., Sargiacomo, M., Lisanti, M. P. & Peschle, C. (1996). Signal transduction and glycophosphatidylinositol-linked proteins (lyn, lck, CD4, CD45, G proteins, and CD55) selectively localize in Triton-insoluble plasma membrane domains of human leukemic cell lines and normal granulocytes. *Blood.* **87**:3783-3794.

Patki, V., Virbasius, J., Lane, W. S., Toh, B. H., Shpetner, H. S. & Corvera, S. (1997). Identification of an early endosomal protein regulated by phosphatidylinositol 3-kinase. *Proc. Natl. Acad. Sci. USA.* **94**:7326-7330.

Paulis-Magnus, C., Murdter, T., Godel, A., Mettang, T., Eichelbaum, M., Klotz, U. & Fromm, M. F. (2001). P-glycoprotein-mediated transport of digoxin, alpha-methyldigoxin and beta-acetyldigoxin. *Naunyn Schmiedebergs Arch. Pharmacol.* **363**:337-343.

Paulis-Magnus, C., von Richter, O., Burk, O., Zeigler, A., Mettang, T., Eichelbaum, M. & Fromm, M. F. (2000). Characterization of the major metabolites of verapamil as substrates and inhibitors of P-glycoprotein. *J. Pharmacol. Exp. Ther.* **293**:376-382.

Pawagi, A. B., Wang, J., Silverman, M., Reithmeier, R. A. & Deber, C. M. (1994). Transmembrane aromatic amino acid distribution in P-glycoprotein. A functional role in broad substrate specificity. *J. Mol. Biol.* **235**:554-564.

Pelkmans, L., Burli, T., Zerial, M. & Helenius, A. (2004). Caveolin-stabilized membrane domains as multifunctional transport and sorting devices in endocytic membrane traffic. *Cell.* **118**:767-780.

Pelkmans, L. & Helenius, A. (2002). Endocytosis via caveolae. *Traffic.* **3**:311-320.

Pelkmans, L., Kartenbeck, J. & Helenius, A. (2001). Caveolar endocytosis of simian virus 40 reveals a new two-step vesicular-transport pathway to the ER. *Nat. Cell Biol.* **3**:473-483.

Pickart, C. M. (2001). Mechainisms underlying ubiquitination. *Annu. Rev. Biochem.* **70**:503-533.

Piper, R. C. & Luzio, J. P. (2001). Late endosomes: sorting and partitioning in multivesicular bodies. *Traffic.* **2**:612-621.

Pirker, R., FitzGerald, D. J., Raschack, M., Frank, Z., Willingham, M. C. & Pastan, I. (1989). Enhancement of the activity of immunotoxins by analogues of verapamil. *Cancer Res.* **49**:4791-4795.

Pirker, R., Keilhauer, G., Raschack, M., Lechner, C. & Ludwig, H. (1990). Reversal of multi-drug resistance in human KB cell lines by structural analogs of verapamil. *Int. J. Cancer.* **45**:916-919.

Pooga, M., Hallbrink, M., Zorko, M. & Langel, U. (1998b). Cell penetration by transportan. *FASEB J.* **12**:67-77.

Pooga, M., Soomets, U., Hallbrink, M., Valkna, A., Saar, K., Rezaei, K., Kahl, U., Hao, J. X., Xu, X. J., Wiesenfeld-Hallin, Z., Hokfelt, T., Bartfai, T. & Langel, U. (1998a). Cell penetrating PNA constructs regulate galanin receptor levels and modify pain transmission in vivo. *Nat, Biotechnol.* **16**:857-861.

Potocky, T. B., Menon, A. K. & Gellman, S. H. (2003). Cytoplasmic and nuclear delivery of a TAT-derived peptide and a beta-peptide after endocytic uptake into Hela cells. *J. Biol. Chem.* **278**:50188-50194.

Prescott, A. R., Lucocq, J. M., James, J., Lister, J. M. & Ponnambalam, S. (1997). Distinct compartmentalization of TGN46 and beta 1,4-galactosyltransferase in Hela cells. *Eur. J. Cell Biol.* **72**:238-246.

Prince, L. S., Peter, K., Hatton, S. R., Zaliauskiene, L., Cotlin, L. F., Clancy, J. P., Marchase, R. B. & Collawn, J. F. (1999). Efficient endocytosis of the cystic fibrosis transmembrane conductance regulator requires a tyrosine-based signal. *J. Biol. Chem.* **274**:3602-3609.

Prokocimer, M. & Rotter, V. (1994). Structure and function of p53 in normal cells and their aberrations in cancer cells: projection on the hematologic cell lineages. *Blood.* **84**:2391-2411.

Pryor, P. R., Mullock, B. M., Bright, N. A., Gray, S. R. & Luzio, J. P. (2000). The role of intaorganellar Ca(2+) in late endosome-lysosome heterotypic fusion and in the reformation of lysosomes from hybrid organelles. *J. Cell Biol.* **149**:1053-1062.

Puri, V., Watanabe, R., Singh, R. D., Dominguez, M., Brown, J. C., Wheatley, C. L., Marks, D. L. & Pagano, R. E. (2001). Clathrin-dependent and –independent internalization of plasma membrane sphingolipids initiates two Golgi targeting pathways. *J. Cell Biol.* **154**:535-548.

Qian, X. D. & Beck, W. T. (1990). Progesterone photoaffinity labels P-glycoprotein in multidrug-resistant human leukemic lymphoblasts. *J. Biol. Chem.* **265**:18753-18756.

Rajagopal, A. & Simon, S. M. (2003). Subcellular localization and activity of multidrug resistance proteins. *Mol. Biol. Cell.* **14**:3389-3399.

Rao, V. V., Anthony, D. C. & Piwnica-Worms, D. (1995). Multidrug resistance P-glycoprotein monoclonal antibody JSB-1 crossreacts with pyruvate carboxylase. *J. Histochem. Cytochem.* **43**:1187-1192.

Raviv, Y., Pollard, H. B., Bruggemann, E. P., Pastan, I. & Gottesman, M. M. (1990). Photosensitized labeling of a functional multidrug transporter in living drug-resistant tumor cells. *J. Biol. Chem.* **265**:3975-3980.

Reaves, B. J., Bright, N. A., Mullock, B. M. & Luzio, J. P. (1996). The effect of wortmannin on the localization of lysosomal type I integral membrane glycoproteins suggests a role for phosphoinositide 3-kinase activity in regulating membrane traffic late in the endocytic pathway. *J. Cell Sci.* **109**:749-762.

Reed, J. C. (1995). Regulation of apoptosis by bcl-2 family proteins and its role in cancer and chemoresistance. *Curr. Opin. Oncol.* 7:541-546.

Relling, M. V. (1996). Are the major effects of P-glycoprotein modulators due to altered pharmacokinetics of anticancer drugs?. *Ther. Drug Monit.***18**:350-356.

Relling, M. V., Nemec, J., Schuetz, E. G., Schuetz, J. D., Gonzalez, F. J. & Korzekwa, K. R. (1994). *O*-Demethylation of epipodophyllotoxins is catalyzed by human cytochrome P450 3A4. *Mol. Pharmacol.* **45**:352-358.

Richard, J. P., Melikov, K., Brooks, H., Prevot, P., Lebleu, B. & Chernomordik, L. V. (2005). Cellular uptake of unconjugated TAT peptide involves clathrin-dependent endocytosis and heparan sulfate receptors. *J. Biol. Chem.* **280**:15300-15306.

Richard, J. P., Melikov, K., Vives, E., Ramos, C., Verbeure, B., Gait, M. J., Chernomordik, L. V. & Lebleu, B. (2003). Cell-penetrating peptides. A reevaluation of the mechanism of cellular uptake. *J. Biol. Chem.* **278**:585-590.

Ridley, A. J. (2001). Rho proteins: linking signaling with membrane trafficking. *Traffic.* **2**:303-310.

Rivoltini, L., Colombo, M. P., Supino, R., Ballinari, D., Tsuruo, T. & Parmiani, G. (1990). Modulation of multidrug resistance by verapamil or mdr1 anti-sense oligodeoxynucleotide does not change the high susceptibility to lymphokine-activated killers in mdr-resistant human carcinoma (LoVo) line. *Int. J. Cancer.* **46**:727-732.

Robinson, L. J., Roberts, W. K., Ling, T. T., Lamming, D., Sternberg, S. S. & Roepe, P. D. (1997). Human MDR1 protein overexpression delays the apoptotic cascade in Chinese hamster ovary fibroblasts. *Biochemistry.* **36**:11169-11178.

Rodal, S. K., Skretting, G., Garred, O., Vilhardt, F., van Deurs, B. & Sandvig, K. (1999). Extraction of cholesterol with methyl-beta-cyclodextrin perturbs formation of clathrin-coated endocytic vesicles. *Mol. Biol. Cell.* **10**:961-974.

Roddie, P. H., Paterson, T. & Turner, M. L. (2000). Gene transfer to primary acute myeloid leukaemia blasts and myeloid leukaemia cell lines. *Cytokines Cell Mol. Ther.* **6**:127-134.

Roepe, P. D. (1995). The role of the MDR protein in altered drug translocation across tumor cell membranes. *Biochim. Biophys. Acta.* **1241**:385-405

Romsicki, Y. & Sharom, F. J. (2001). Phospholipid flippase activity of the reconstituted P-glycoprotein multidrug transporter. *Biochemistry.* **40**: 6937-6947.

Ross, M. F., Filipovska, A., Smith, R. A., Gait, M. J. & Murphy, M. P. (2004). Cell-penetrating peptides do not cross mitochondrial membranes even when conjugated to a lipophilic cation: evidence against direct passage through phospholipid bilayers. *Biochem. J.* **383**:457-468.

Rothbard, J. B., Garlington, S., Lin, Q., Kirschberg, T., Kreider, E., McGrane, P. L., Wender, P. A. & Khavari, P. A. (2000). Conjugation of arginine oligomers to cyclosporin A facilitates topical delivery and inhibition of inflammation. *Nat. Med.* **6**:1253-1257.

Rothbard, J. B., Kreider, E., Van Deusen, C. L., Wright, L., Wylie, B. L. & Wender, P. A. (2002). Arginine-rich molecular transporters for drug delivery: role of backbone spacing in cellular uptake. *J. Med. Chem.* **45**:3612-3618.

Rothberg, K. G., Heuser, J. E., Donzell, W. C., Ying, Y. S., Glenney, J. R. & Anderson, R. G. (1992). Caveolin, a protein component of caveolae membrane coats. *Cell.* **68**:673-682.

Rothnie, A., Theron, D., Soceneantu, L., Martin, C., Traikia, M., Berridge, G., Higgins, C. F., Devaux, P. F. & Callaghan, R. (2001). The importance of cholesterol in maintenance of P-glycoprotein activity and its membrane perturbing influence. *Eur. Biophys. J.* **30**:430-442.

Rottenberg, H. (1979). The measurement of membrane potential and deltapH in cells, organelles, and vesicles. *Methods Enzymol.* **55**:547-569.

Rouselle, C., Clair, P., Lefauconnier, J. M., Kaczorek, M., Scherrmann, J. M. & Temsamani, J. (2000). New advances in the transport of doxorubicin through the blood-brain barrier by a peptide vector mediated strategy. *Mol. pharmacol.* **57**:679-686

Rouselle, C., Clair, P., Smirnova, M., Kolesnikov, Y., Pasternak, G. W., Gac-Breton, S., Rees, A. R., Scherrmann, J. N. & Temsamani, J. (2003). Improved brain uptake and pharmacological activity of dalargin using a peptide-vector-mediated strategy. *J. Pharmacol. Exp. Ther.* **306**:371-376.

Rouselle, C., Clair, P., Temsamani, J. & Scherrmann, J. M. (2002). Improved brain delivery of benzylpenicillin with a peptide-vector-mediated strategy. *J. Drug Target.* **10**: 309-315.

Rowley, J. D. (1973). A new consistent chromosomal abnormality in chronic myelogenous leukemia identified by quinacrine fluorescence and Giemsa staining. *Nature.* **243**:290-293.

Ruetz, S. & Gros, P. (1994). Phosphatidylcholine translocase: a physiological role for the mdr2 gene. *Cell.* **77**:1071-1081.

Rutherford, T. R., Clegg, J. B. & Weatherall, D. J. (1979). K562 human leukemic cells synthesise embryonic haemoglobin in response to haemin. *Nature.* **280**:164-165.

Rutledge, E. A., Mikoryak, C. A. & Draper, R. K. (1991). Turnover of the transferrin receptor is not influenced by removing most of the extracellular domain. *J. Biol. Chem.* **266**:21125-21130.

Saeki, T., Ueda, K., Tanigawara, Y., Hori, R. & Komano, T. (1993). Human P-glycoproteins transports cyclosporin A and FK506. *J. Biol. Chem.* **268**:6077-6080.

Sai, Y., Nies, A. T. & Arias, I. M. (1999). Bile acid secretion and direct targeting of *mdr1*-green fluorescent protein from Golgi to the canalicular membrane in polarized WIF-B cells. *J. Cell Sci.* **112**:4535-4545.

Sampath, P. & Pollard, T. D. (1991). Effects of cytochalasin, phalloidin, and pH on the elongation of actin filaments. *Biochemistry.* **30**:1973-1980.

Sandvig, K., Olsnes, S., Peterson, O. W. & van Deurs, B. (1987). Acidification of the cytosol inhibits endocytosis from coated pits. *J. Cell Biol.* **105**:679-689.

Sargent, J. M., Williamson, C. J., Maliepaard, M., Elgie, A. W., Scheper, R. J. & Taylor, C. G. (2001). Breast cancer resistance protein expression and resistance to daunorubicin in blast cells from patients with acute myeloid leukaemia. *Br. J. Haematol.* **115**:257-262.

Savage, D. G. & Antman, K. H. (2002). Imatinib mesylate-a new oral targeted therapy. *N. Engl. J. Med.* **346**:683-693.

Sawyers, C. L. (1999). Chronic myeloid leukemia. *N. Engl. J. Med.* **340**: 1330-1340.

Sawyers, C. L., Hochhaus, A., Feldman, E., Goldman, J. M., Miller, C. B., Ottmann, O. G., Schiffer, C. A., Talpaz, M., Guilhot, F., Deininger, M. W., Fischer, T., O'Brien, S. G., Stone, R. M., Gambacorti-Passerini, C. B., Russell, N. H., Reiffers, J. J., Shea, T. C., Chapuis, B., Coutre, S., Tura, S., Morra, E., Larson, R. A., Saven, A., Peschel, C., Gratwohl, A., Mandelli, F., Ben-Am, M., Gathmann,

I., Capdeville, R., Paquette, R. L. & Druker, B. J. (2002). Imatinib induces hematologic and cytogenetic responses in patients with chronic myelogenous leukemia in myeloid blast crisis: results of a phase II study. *Blood.* **99**:3530-3539.

Schadendorf, D., Worm, M., Algermissen, B., Kohlmus, C. M. & Czarnetzki, B. M. (1994). Chemosensitivity testing of human malignant melanoma. A retrospective analysis of clinical response and in vitro drug sensitivity. *Cancer.* **73**:103-108.

Schapiro, F. B. & Grinstein, S. (2000). Determinants of the pH of the Golgi complex. *J. Biol. Chem.* **275**:21025-21032.

Scheper, R. J., Broxterman, H. J., Scheffer, G. L., Kaaijk, P., Dalton, W. S., van Heijningen, T. H., van Kalken, C. K., Slovak, M. L., de Vries, E. G., van der Valk, P., Meijer, C. J. L. M. & Pinedo, H. M. (1993). Overexpression of a M(r) 110,000 vesicular protein in non-P-glycoprotein-mediated multidrug resistance. *Cancer Res.* **53**:1475-1479.

Scheper, R. J., Bulte, J. W., Brakkee, J. G., Quak, J. J., van der Schoot, E., Balm, A. J., Meijer, C. J., Broxterman, H. J., Kuiper, C. M. & Lankelma, J. (1988). Monoclonal antibody JSB-1 detects a highly conserved epitope on the P-glycoprotein associated with multi-drug resistance. *Int. J. Cancer.* **42**:389-394.

Schinkel, A. H., Roelofs, E. M. & Borst, P. (1991). Characterization of the human MDR3 P-glycoprotein and its recognition by P-glycoprotein-specific monoclonal antibodies. *Cancer Res.* **51**:2628-2635.

Schinkel, A. H., Wagenaar, E., Mol, C. A. & van Deemter, L. (1996). P-glycoprotein in the blood-brain barrier of mice influences the bain penetration and pharmacological activity of many drugs. *J. Clin. Invest.* **97**:2517-2524.

Schinkel, A. H., Wagenaar, E., van Deemter, L., Mol, C. A. & Borst, P. (1995). Absence of the mdr1a P-glycoprotein in mice affects tissue distribution and

pharmacokinetics of dexamethasone, digoxin, and cyclosporin A. *J. Clin. Invest.* **96**:1698-1705.

Schmid, S. L. (1997). Clathrin-coated vesicle formation and protein sorting: an integrated process. *Annu. Rev. Biochem.* **66**:5-548.

Schuetz, E. G., Beck, W. T. & Schuetz, J. D. (1996). Modulators and substrates of P-glycoprotein and cytochrome P4503A coordinately up-regulate these proteins in human colon carcinoma cells. *Mol. Pharmacol.* **49**:311-318.

Schuetz, E. G., Yasuda, K., Arimori, K. & Schuetz, J. D. (1998). Human MDR1 and mouse mdr1a P-glycoprotein alter the cellular retention and disposition of erythromycin but not of retinoic acid or benzo(a)pyrene. *Arch. Biochem. Biophys.* **350**:340-347.

Schuurhuis, G. J., Broxterman, H. J., van der Hoeven, J. J., Pinedo, H. M. & Lankelma, J. (1987). Potentiation of doxorubicin cytotoxicity by the calcium antagonist bepridil in anthracycline-resistant and -sensitive cell lines. A comparison with verapamil. *Cancer Chemother. Pharmacol.* **20**:285-290.

Sciaky, N., Presley, J., Smith, C., Zaal, K. J., Cole, N., Moreira, J. E., Terasaki, M., Siggia, E. & Lippincott-Schwartz, J. (1997). Golgi tubule traffic and the effects of brefeldin A visualized in living cells. *J. Cell Biol.* **139**:1137-1155.

Sehested, M., Skovsgaard, T., van Deurs, B. & Winther-Nielsen, H. (1987). Increase in non-specific adsorptive endocytosis in anthracycline- and vinca alkaloid-resistant Ehrlich ascites tumor cell lines. *J. Natl. Cancer Inst.* **78**:171-179.

Seidel, A., Hasmann, M., Loser, R., Bunge, A., Schaefer, B., Herzig, I., Steidtmann, K. & Dietel, M. (1995). Intracellular localization, vesicular accumulation and kinetics of daunoruicin in sensitive and mutlidrug-resistant gastric carcinoma EPG85-257 cells. *Virchows Arch.* **426**: 249-256.

Sheff, D., Pelletier, L., O'Connell, C. B., Warren, G. & Mellman, I. (2002). Transferrin receptor recycling in the absence of perinuclear recycling endosomes. *J. Cell Biol.* **156**:797-804.

Shibagaki, N. & Udey, M. C. (2002). Dendritic cells transduced with protein antigens induce cytotoxic lymphocytes and elicit antitumor immunity. *J. Immunol.* **168**:2393-2401

Shih, S. C., Sloper-Mould, K. E. & Hicke, L. (2000). Monoubiquitin carries a novel internalization signal that is appended to activated receptors. *EMBO J.* **19**:187-198.

Shpetner, H., Joly, M., Hartley, D. & Corvera, S. (1996). Potential sites of PI-3 kinase function in the endocytic pathway revealed by the PI-3 kinase inhibitor, wortmannin. *J. Cell Biol.* **132**:595-605.

Silhol, M., Tyagi, M., Giacca, M., Lebleu, B. & Vives, E. (2002). Different mechanisms for cellular internalization of the HIV-1 Tat-derived cell penetrating peptide and recombinant proteins fused to Tat. *Eur. J. Biochem.* **269**:494-501.

Simons, K. & Toomre, D. (2000). Lipid rafts and signal transduction. *Nat. Rev. Mol. Cell Biol.* **1**:31-39.

Simon, S. M., Roy, D. & Schindler, M. (1994). Intracellular pH and the control of multidrug resistance. *Proc. Natl. Acad. Sci. USA.* **91**:1128-1132.

Skovsgaard, T. (1978). Carrier-mediated transport of daunorubicin, adriamycin, and rubidazone in Ehrlich ascites tumour cells. *Biochem. Pharmacol.* **27**:1221-1227.

Slapak, C. A., Lecerf, J-M., Daniel, J. C. & Levy, S. B. (1992). Energy-dependent accumulation of daunorubicin into subcellular compartments of human leukemia cells and cytoplasts. *J. Biol. Chem.* **267**:10638-10644.

Smetsers, T. F., Skorski, T., van de Locht, L. T., Wessels, H. M., Pennings, A. H., de Witte, T., Calabretta, B. & Mensink, E. J. (1994). Antisense BCR-ABL oligonuleotides induce apoptosis in the Philadelphia chromosome-positive cell line BV173. *Leukemia.* **8**:129-140.

Smit, J. J., Schinkel, A. H., Oude Elferink, R. P., Groen, A. K., Wagenaar, E., van Deemter, L., Mol, C. A., Ottenhoff, R., van der Lugt, N. M., van Roon, M. A., van der Walk, M. A., Offerhaus, G. J., Berns, A. J. & Borst, P. (1993). Homozygous disruption of the murine mdr2 P-glycoprotein gene leads to a complete absence of phospholipid from bile and to liver disease. *Cell.* **75**:451-462.

Smith, A. J., van Helvoort, A., van Meer, G., Szabo, K., Welker, E., Szakacs, G., Varadi, A., Sarkadi, B. & Borst, P. (2000). MDR3 P-glycoprotein, a phosphatidylcholine translocase, transports several cytotoxic drugs and directly interacts with drugs as judged by interference with nucleotide trapping. *J. Biol. Chem.* **275**:23530-23539.

Smith, R. A., Porteous, C. M., Gane, A. M. & Murphy, M. P. (2003). Delivery of bioactive molecules to mitochondria in vivo. *Proc. Natl. Acad. Sci. USA.* **100**:5407-5412.

Solary, E., Witz, B., Caillot, D., Moreau, P., Desablens, B., Cahn, J. Y., Sadoun, A., Pignon, B., Berthou, C., Maloisel, F., Guyotat, D., Casassus, P., Ifrah, N., Lamy, Y., Audhuy, B., Colombat, P. & Harousseau, J. L. (1996). Combination of quinine as a potential reversing agent with mitoxantrone and cytarabine for the treatment of acute leukemias: a randomized multicenter study. *Blood.* **88**:1198-1205.

Sowa, G., Pypaert, M. & Sessa, W. C. (2001). Distinction between signaling mechanisms in lipid rafts vs caveolae. *Proc. Natl. Acad. Sci. USA.* **98**:14072-14077.

Sparreboom, A., van Asperen, J., Mayer, U., Schinkel, A. H., Smit, J. W., Meijer, D. K., Borst, P., Nooijen, W. J., Beijnen, J. H. & van Tellingen, O. (1997). Limited oral bioavailability and active epithelial excretion of paclitaxel (Taxol) caused by P-glycoprotein in the intestine. *Proc. Natl. Acad. Sci. USA.* **94**:2031-2035.

Stavrovskaya, A., Turkina, A., Sedyakhina, N., Stromskaya, T., Zabotina, T., Khoroshko, N. & Baryshnikov, A. (1998). Prognostic value of P-glycoprotein and leukocyte differentiation antigens in chronic myeloid leukemia. *Leuk. Lymphoma.* **28**:469-482.

Steen, H. B. (1992). Noise, sensitivity and resolution of flow cytometers. *Cytometry.* **13**:822-830.

Stellrecht, C. M., Frazier, G., Selvanayagam, C., Chao, L. Y., Lee, A. & Saunders, G. F. (1993). Transcriptional regulation of a hematopoietic proteoglycan core protein gene during hematopoiesis. *J. Biol. Chem.* **268**:4078-4084.

Stenmark, H., Aasland, R., Toh, B. H. & D'Arrigo, A. (1996). Endosomal localization of the autoantigen EEA1 is mediated by a zinc-binding FYVE finger. *J. Biol. Chem.* **271**:24048-24054.

Stone, R. M., O'Donnell, M. R. & Sekeres, M. A. (2004). Acute myeloid leukemia. *Hematology (Am Soc Hematol Educ Program).* 98-117.

Stuppia, L., Calabrese, G., Peila, R., Guanciali-Franchi, P., Morizio, E., Spadano, A. & Palka, G. (1997). p53 loss and point mutations are asscoaited with suppression of apoptosis and progression of CML into myeloid blastic crisis. *Cancer Genet. Cytogenet.* **98**:28-35.

Subtil, A., Hemar, A. & Dautry-Varsat, A. (1994). Rapid endocytosis of interleukin 2 receptors when clathrin-coated pit endocytosis is inhibited. *J. Cell Sci.* **107**:3461-3468.

Sutherland, J. A., Turner, A. R., Mannoni, P., McGann, L. E. & Turc, J. M. (1986). Differentiation of K562 leukemia cells along erythroid, macrophage, and megakaryocyte lineages. *J. Biol. Response Mod.* **5**:250-262.

Suzuki, T., Futaki, S., Niwa, M., Tanaka, S., Ueda, K. & Sugiura, Y. (2002). Possible existence of common internalization mechanisms among arginine-rich peptides. *J. Biol. Chem.* **277**:2437-2443.

Takebayashi, Y., Akiyama, S., Natsugoe, S., Hokita, S., Niwa, K., Kitazono, M., Sumizawa, T., Tani, A., Furukawa, T. & Aikou, T. (1998). The expression of multidrug resistance protein in human gastrointestinal tract carcinomas. *Cancer.* **82**:661-666.

Takeshima, K., Chikushi, A., Lee, K. K., Yonehara, S. & Matsuzaki, K. (2003). Translocation of analogues of the antimicrobial peptides magainin and buforin across human cell membranes. *J. Biol. Chem.* **278**:1310-1315.

Tamai, I. & Safa, A. R. (1990). Competitive interaction of cyclosporins with the Vinca alkaloid-binding site of P-glycoprotein in multidrug-resistant cells. *J. Biol. Chem.* **265**:16509-16513.

Tan, K. B., Mattern, M. R., Eng, W. K., McCabe, F. L. & Johnson, R. K. (1989). Nonproductive rearrangement of DNA topoisomerase I and II genes: correlation with resistance to topoisomerase inhibitors. *J. Natl. Cancer Inst.* **81**:1732-1735.

Tang-Wai, D. F., Kajiji, S., DiCapua, F., de Graaf, D., Roninson, I. B. & Gros, P. (1995). Human (MDR1) and mouse (mdr1, mdr3) P-glycoproteins can be distinguished by their respective drug resistance profiles and sensitivity to modulators. *Biochemistry.* **34**:32-39.

Tartakoff, A. M. (1983). Perturbation of vesicular traffic with the carboxylic ionophore monensin. *Cell.* **32**:1026-1028.

te Boekhorst, P. A., de Leeuw, K., Schoester, M., Wittebol, S., Nooter, K., Hagemeijer, A., Lowenberg, B. & Sonneveld, P. (1993). Predominance of functional multidrug resistance (MDR-1) phenotype in CD34+ acute myeloid leukemia cells. *Blood.* **82**:3157-3162.

Tewey, K. M., Rowe, T. C., Yang, L., Halligan, B. D. & Liu, L. F. (1984). Adriamycin-induced DNA damage mediated by mammalian DNA topoisomerase II. *Science.* **226**:466-468.

Thiebaut, F., Currier, S. J., Whitaker, J., Haugland, R. F., Gottesman, M. M., Pastan, I. & Willingham, M. C. (1990). Activity of the multidrug transporter results in alkalinization of the cytosol: measurements of cytosolic pH by microinjection of a pH-sensitive dye. *J. Histochem. Cytochem.* **38**:685-690.

Thiebaut, F., Tsuruo, T., Hamada, H., Gottesman, M. M., Pastan, I. & Willingham, M. C. (1989). Immunohistochemical localization in normal tissues of different epitopes in the multidrug transport protein P170: evidence for localization in brain capillaries and crossreactivity of one antibody with a muscle protein. *J. Histochem. Cytochem.* **37**:159-164.

Thomsen, P., Roepstorff, K., Stahlhut, M. & van Deurs, B. (2002). Caveolae are highly immobile plasma membrane microdomains, which are not involved in constitutive endocytic trafficking. *Mol. Biol. Cell.* **13**:238-250.

Thoren, P. E., Persson, D., Isakson, P., Goksor, M., Onfelt, A. & Norden, B. (2003). Uptake of analogs of penetratin, Tat(48-60) and oligoarginine in live cells. *Biochem. Biophys. Res. Commun.* **307**:100-107.

Toneguzzo, F. & Keating, A. (1986). Stable expression of selectable genes introduced into human hematopoietic stem cells by electric field-mediated DNA transfer. *Proc. Natl. Acad. Sci. USA.* **83**:3496-3499.

Torchilin, V. P., Rammohan, R., Weissig, V. & Levchenko, T. S. (2001). TAT peptide on the surface of liposomes affords their efficient intracellular delivery even at low temperature and in the presence of metabolic inhibitors. *Proc. Natl. Acad. Sci. USA.* **98**:8786-8791.

Townsend, D. M. & Tew, K. D. (2003). The role of glutathione-S-transferase in anti-cancer drug resistance. *Oncogene.* **22**:7369-7375.

Tritton, T. R. (1991). Cell surface actions of adriamycin. *Pharmacol. Ther.* **49**:293-309.

Troost, J., Lindenmaier, H., Haefeli, W. E. & Weiss, J. (2004). Modulation of cellular cholesterol alters P-glycoprotein activity in multidrug-resistant cells. *Mol. Pharmacol.* **66**:1332-1339.

Tsuruoka, S., Sugimoto, K. I., Fujimura, A., Imai, M., Asano, Y. & Muto, S. (2001). P-glycoprotein-mediated drug secretion in mouse proximal tubule perfused in vitro. *J. Am. Soc. Nephrol.* **12**:177-181.

Tsuruo, T., Iida, H., Tsukagoshi, S. & Sakurai, Y. (1983). Potentiation of vincristine and Adriamycin effects in human hematopoietic tumor cell lines by calcium antagonists and calmodulin inhibitors. *Cancer Res.* **43**:2267-2272.

Tsuruo, T., Iida, H., Tsukagoshi, S. & Sakurai, Y. (1981). Overcoming of vincristine resistance in P388 leukemia in vivo and in vitro through enhanced cytotoxicity of vincristine and vinblastine by verapamil. *Cancer Res.* **41**:1967-1972.

Tung, C. H., Mueller, S. & Weissleder, R. (2002). Novel branching membrane translocational peptide as gene delivery factor. *Bioorg. Med. Chem.* **10**:3609-3614.

Turzanski, J., Grundy, M., Shang, S., Russell, N. & Pallis, M. (2005). P-glycoprotein is implicated in the inhibition of ceramide-induced apoptosis in TF-1

acute myeloid leukemia cells by modulation of the glucosylceramide synthase pathway. *Exp. Hematol.* **33**:62-72.

Twentyman, P. R. (1988). Modifictaion of cytotoxic drug resistance by non-immuno-suppressive cyclosporins. *Br. J. Cancer.* **57**:254-258.

Tyagi, M., Rusnati, M., Presta, M. & Giacca, M. (2001). Internalization of HIV-1 tat requires cell surface heparan sulfate proteoglycans. *J. Biol. Chem.* **276**:3254-3261.

Ui, M., Okada, T., Hazeki, K. & Hazeki, O. (1995). Wortmannin as a unique probe for an intracellular signalling protein, phosphoinositide 3-kinase. *Trends Biochem. Sci.* **20**:303-307.

Van Dam, E. M. & Stoorvogel, W. (2002). Dynamin-dependent transferrin receptor recycling by endosome-derived clathrin-coated vesicles. *Mol. Biol. Cell.* **13**:169-182.

van den Elsen, J. M., Kuntz, D. A., Hoedemaeker, F. J. & Rose, D. R. (1999). Antibody C219 recognizes an alpha-helical epitope on P-glycoprotein. *Proc. Natl. Acad. Sci. USA.* **96**:13679-13684.

van den Heuvel-Eibrink, M. M., Wiemer, E. A., Prins, A., Meijerink, J. P., Vossebeld, P. J., van der Holt, B., Pieters, R. & Sonneveld, P. (2002). Increased expression of the breast cancer resistance protein (BCRP) in relapsed or refractory acute myeloid leukemia (AML). *Leukemia.* **16**:833-839.

van Helvoort, A., Smith, A. J., Sprong, H., Fritzsche, I., Schinkel, A. H., Borst, P. & van Meer, G. (1996). MDR1 P-glycoprotein is a lipid translocase of broad specificity, while MDR3 P-glycoprotein specifically translocates phosphatidylcholine. *Cell.* **87**:507-517.

van Kerkhof, P., Sachse, M., Klumperman, J. & Strous, G. J. (2001). Growth hormone receptor ubiquitination coincides with recruitment to clathrin-coated membrane domains. *J. Biol. Chem.* **276**:3778-3784.

Van Tendeloo, V. F., Willems, R., Ponsaerts, P., Lenjou, M., Nijs, G., Vanhove, M., Muylaert, P., Van Cauwelaert, P., Van Broeckhoven, C., Van Bockstaele, D. R. & Berneman, Z. N. (2000). High-level transgene expression in primary human T lymphocytes and adult bone marrow CD34+ cells via electroporation-mediated gene delivery. *Gene Ther.* **7**:1431-1437.

Vasanthakumar, G. & Ahmed, N. K. (1989). Modulation of drug resistance in a daunorubicin resistant subline with oligonucleoside methylphosphonates. *Cancer Commun.* **1**:225-232.

Vellonen, K-S, Honkakoski, P. & Urtti, A. (2004). Substrates and inhibitors of efflux proteins interfere with the MTT assay in cells and may lead to underestimation of drug toxicity. *Eur. J. Pharm. Sci.* **23**:181-188.

Vendeville, A., Rayne, F., Bonhoure, A., Bettache, N., Montcourrier, P. & Beaumelle, B. (2004). HIV-1 Tat enters T cells using coated pits before translocating from acidified endosomes and eliciting biological responses. *Mol. Biol. Cell.* **15**:2347-2360.

Visser, J. W. M. & van Bekkum, D. W. (1990). Purification of pluripotent hematopoietic stem cells: past and present. *Exp. Haematol.* **18**:248-256.

Vives, E. (2003). Cellular uptake of the Tat peptide: an endocytosis mechanism following ionic interactions. *J. Mol. Recognit.* **16**:265-271.

Vives, E., Brodin, P. & Lebleu, B. (1997). A truncated HIV-1 Tat protein basic domain rapidly translocates through the plasma membrane and accumulates in the cell nucleus. *J. Biol. Chem.* **272**:16010-16017.

Vocero-Akbani, A. M., Heyden, N. V., Lissy, N. A., Ratner, L. & Dowdy, S. F. (1999). Killing HIV-infected cells by transduction with an HIV protease-activated caspase-3 protein. *Nat. Med.* **5**:29-33.

Voges, D., Zwickl, P. & Baumeister, W. (1999). The 26S proteasome: a molecular machine designed for controlled proteolysis. *Annu. Rev. Biochem.* **68**:1015-1068.

Wandel, C., Kim, R. B., Guengerich, F. P. & Wood, A. J. (2000). Mibefradil is a P-glycoprotein substrate and a potent inhibitor of both P-glycoprotein and CYP3A in vitro. *Drug Metab. Dispos.* **28**:895-898.

Wang, E., Lee, M. D. & Dunn, K. W. (2000). Lysosomal accumulation of drugs in drug-sensitive MES-SA but not multidrug-resistant MES-SA/Dx5 uterine sarcoma cells. *J. Cell Physiol.* **184**:263-274.

Ward, C. L., Omura, S. & Kopito, R. R. (1995). Degradation of CFTR by the ubiquitin-proteasome pathway. *Cell.* **83**:121-127.

Warren, L., Jardillier, J. C. & Ordentlich, P. (1991). Secretion of lysosomal enzymes by drug-sensitive and multiple drug-resistant cells. *Cancer Res.* **51**:1996-2001.

Warren, L., Malarska, A. & Jardillier, J. C. (1995). The structure of P-glycoprotein and the secretion of lysosomal enzymes in multidrug-resistant cells. *Cancer Chemother. Pharmacol.* **35**:267-269.

Weisberg, E. & Griffin, J. D. (2000). Mechanisms of resistance to the ABL tyrosine kinase inhibitor STI571 in BCR/ABL-transformed hematopoietic cell lines. *Blood.* **95**:3498-3505.

Weisz, O. A. (2003). Organelle acidification and disease. *Traffic.* **4**:57-64.

Wender, P. A., Mitchell, D. J., Pattabiraman, K., Pelkey, E. T., Steinman, L. & Rothbard, J. B. (2000). The design, synthesis, and evaluation of molecules that enable or enhance cellular uptake: peptoid molecular transporters. *Proc. Natl. Acad. Sci. USA.* **97**:13003-13008.

Wielinga, P. R., Westerhoff, H. V. & Lankelma, J. (2000). The relative importance of passive and P-glycoprotein mediated anthracycline efflux from multidrug-resistant cells. *Eur. J. Biochem.* **267**:649-657.

Willingham, M. C., Richert, N. D., Cornwell, M. M., Tsuruo, T., Hamada, H., Gottesman, M. M. & Pastan, I. H. (1987). Immunocytochemical localization of P170 at the plasma membrane of multidrug-resistant human cells. *J. Histochem. Cytochem.* **35**:1451-1456.

Wils, P., Phung-Ba, V., Warnery, A., Lechardeur, D., Raeissi, S., Hidalgo, I. J. & Scherman, D. (1994). Polarized transport of docetaxel and vinblastine mediated by P-glycoprotein in human intestinal epithelial cell monolayers. *Biochem. Pharmacol.* **48**:1528-1530.

Wilson, W. H., Bates, S. E., Fojo, A., Bryant, G., Zhan, Z., Regis, J., Wittes, R. E., Jaffe, E. S., Steinberg, S. M. & Herdt, J. (1995). Controlled trial of dexverapamil, a modulator of multidrug resistance, in lymphomas refractory to EPOCH chemotherapy. *J. Clin. Oncol.* **13**:1995-2004.

Wu, M. H., Smith, S. L. & Dolan, M. E. (2001). High efficiency electroporation of human umbilical cord blood CD34+ hematopoietic precursor cells. *Stem Cells.* **19**:492-499.

Wu, X., Whitfield, L. R. & Stewart, B. H. (2000). Atorvastatin transport in the Caco-2 cell model: contributions of P-glycoprotein and the proton-monocarboxylic acid co-transporter. *Pharm. Res.* **17**:209-215.

Wyman, T. B., Nicol, F., Zelphati, O., Scaria, P. V., Plank, C. & Szoka, F. C. Jr. (1997). Design, synthesis, and characterization of a cationic peptide that binds to nucleic acids and permeabilizes bilayers. *Biochemistry.* **36**:3008-3017.

Yahanda, A. M., Alder, K. M., Fisher, G. A., Brophy, N. A., Halsey, J., Hardy, R. I., Gosland, M. P., Lum, B. L. & Sikic, B. I. (1992). Phase I trial of etoposide with cyclosporine as a modulator of multidrug resistance. *J. Clin. Oncol.* **10**:1624-1634.

Yoh, K., Ishii, G., Yokose, T., Minegishi, Y., Tsuta, K., Goto, K., Nishiwaki, Y., Kodama, T., Suga, M. & Ochiai, A. (2004). Breast cancer resistance protein impacts clinical outcome in platinum-based chemotherapy for advanced non-small cell lung cancer. *Clin. Cancer Res.* **10**:1691-1697.

Yusa, K. & Tsuruo, T. (1989). Reversal mechanism of multidrug resistance by verapamil: direct binding of verapamil to P-glycoprotein on specific sites and transport of verapamil outward across the plasma membrane of K562/ADM cells. *Cancer. Res.* **49**:5002-5006.

Zaliauskiene, L., Kang, S., Brouillette, C. G., Lebowitz, J., Arani, R. B. & Collawn, J. F. (2000). Down-regulation of cell surface receptors is modulated by polar residues within the transmembrane domain. *Mol. Biol. Cell.* **11**:2643-2655.

Zaman, G. J., Flens, M. J., van Leusden, M. R., de Haas, M., Mulder, H. S., Lankelma, J., Pinedo, H. M., Scheper, R. J., Baas, F., Broxterman, H. J. & Borst, P. (1994). The human multidrug resistance-associated protein MRP is a plasma membrane drug-efflux pump. *Proc. Natl. Acad. Sci. USA.* **91**:8822-8826.

Zaro, J. L. & Shen, W. C. (2003). Quantitive comparison of membrane tansduction and endocytosis of oligopeptides. *Biochem. Biophys. Res. Commun.* **307**:241-247.

Zhang, Z., Wu, J. Y., Hait, W. N. & Yang, J. M. (2004). Regulation of the stability of P-glycoprotein by ubiquitination. *Mol. Pharmacol.* **66**:395-403.

Zhou-Pan, X. R., Seree, E., Zhou, X. J., Placidi, M., Maurel, P., Barra, Y. & Rahmani, R. (1993). Involvement of human liver cytochrome P450 3A in vinblastine metabolism: drug interactions. *Cancer Res.* **53**:5121-5126.

Zhuang, Y., Cragoe, E. J. Jr. Shaikewitz, T., Glaser, L. & Cassel, D. (1984). Characterization of potent Na+/H+ exchange inhibitors from the amiloride series in A431

Zhuo, Y., Gottesman, M. M. & Pastan, I. (1999). The extracellular loop between TM5 and TM6 of P-glycoprotein is required for reactivity with monoclonal antibody UIC2. *Arch. Biochem. Biophys.* **367**:74-80.

Appendix I

Abstracts

Al-Taei, S & Jones, A. T. British Pharmaceutical Conference 2004: Unravelling the spatial distribution of daunorubicin within human leukaemic cells displaying differential drug distribution and sensitivity. J. Pharm. Pharmacol. September Suppl. (2004), p11.

Al-Taei, S & Jones, A. T. European Life Science Organisation 2004 Conference: Comparative analysis of the dynamics of endocytic pathways in leukaemia cells. Proceedings of ELSO (2004), p64.

Al-Taei, S & Jones, A. T. Speaking of Science Conference Graduate Centre: Characterisation of the membrane trafficking of P-glycoprotein: establishing a model for the screening of novel P-glycoprotein inhibitors (2004).

Al-Taei, S & Jones, A. T. Postgraduate Research Day, Cardiff University: Identification of differences in drug resistance mechanisms in two leukaemic cell lines (2004).

Al-Taei, S & Jones, A. T. 6th International Symposium on Polymer Therapeutics: Characterisation of the membrane trafficking of P-glycoprotein: establishing a model for the screening of potential P-glycoprotein inhibitors. Proceedings of 6th International Symposium on Polymer Therapeutics (2003), p72.

Al-Taei, S & Jones, A. T. Postgraduate Research Day, Cardiff University: Evidence for P-glycoprotein ubiquitination in leukaemia cells (2003).

Manuscripts

Submitted

Al-Taei, S., Penning, N. A., Simpson, J. C., Futaki, S., Takeuchu, T., Nakase, I. & Jones, A. T. (2005). Protein transduction domains HIV-Tat and octaarginine are trafficked by endocytosis to late endosomes and lysosomes. *Submitted to Molecular Therapy.*

In preparation

Al-Taei, S. & Jones, A. T. (2005). Investigation of the mechanisms of resistance operating in cell line models of AML and CML.